TEXTE
108/2021

Bioaccumulation of ionic compounds - Deriving of alternative screening criteria from experimental studies

Final Report

Für Mensch & Umwelt

Umwelt Bundesamt

TEXTE 108/2021

Ressortforschungsplan of the Federal Ministry for the
Environment, Nature Conservation and Nuclear Safety

Project No. (FKZ) 3717 67 402 0
Report No. (UBA-FB) FB000468/ENG

Bioaccumulation of ionic compounds - Deriving of alternative screening criteria from experimental studies

Final Report

by

Prof. Dr. Christian Schlechtriem (Project director), Dr. Ina Ebersbach,
Dr. Carolin Müller, Sebastian Kühr
Fraunhofer Institute for Molecular Biology and Applied Ecology (Fraunhofer IME),
Division Applied Ecology, Schmallenberg (Germany)

Prof. Dr. Kai-Uwe Goss
Helmholtz-Zentrum für Umweltforschung – UFZ, Department Analytische Chemie,
Leipzig (Germany)

Prof. Dr. Stefan Trapp, Fabio Polesel
Technical University of Denmark, Department of Environmental Engineering,
Kgs. Lyngby (Denmark)

On behalf of the German Environment Agency

Impressum

Publisher
Umweltbundesamt
Wörlitzer Platz 1
06844 Dessau-Roßlau
Tel: +49 340-2103-0
Fax: +49 340-2103-2285
buergerservice@uba.de
Internet: www.umweltbundesamt.de

/umweltbundesamt.de
/umweltbundesamt

Report performed by:
Fraunhofer IME
Auf dem Aberg 1
57392 Schmallenberg
Germany

Report completed in:
December 2020

Edited by:
Section IV 2.3 Chemicals
Dr. Juliane Ackermann

Publication as pdf:
http://www.umweltbundesamt.de/publikationen

ISSN 1862-4804

Dessau-Roßlau, July 2021

Kurzbeschreibung

Das Ziel der vorliegenden Studie war es, die Bioakkumulation vollständig ionisierter Verbindungen experimentell zu bestimmen und Screening-Parameter zu identifizieren, die auf ein hohes Bioakkumulationspotential von ionisierbaren organischen Chemikalien (IOCs) hinweisen können. Drei Fütterungsstudien mit Regenbogenforellen (*Oncorhynchus mykiss*) wurden gemäß OECD TG 305 durchgeführt. Die Trennung von Leber, Magen-Darm-Trakt (GIT) und Schlachtkörper ermöglichte eine weitere Aufklärung der Gewebeverteilung der einzelnen Testsubstanzen. Die ausgewählten Chemikalien wiesen Eigenschaften auf, die sie für eine hohe Bioakkumulation verdächtig machten, und umfassten zwei Kationen (Tetrabutylphosphonium-bromid (TBP), Trimethyloctadecylammoniumchlorid (TMOA)) und vier Anionen (Benzotriazol, Tecloftalam, Pentachlorphenol (PCP), MEE-Phosphonat). Die höchsten Verteilungsfaktoren wurden für die GIT gefunden, gefolgt von der Leber. Keine der getesteten IOCs zeigte jedoch ein ausgeprägtes Biomagnifikationspotential, da die kinetischen Biomagnifikationsfaktoren (BMF_k) zwischen 0,001 und 0,05 g / g lagen (Median 0,009 g / g). Die getesteten Kationen zeigten mit Ausnahme von Tecloftalam eine geringere Assimilationseffizienz (α) (siehe OECD TG 305) als die Anionen. Im Gegensatz dazu zeigten die getesteten Anionen eine erheblich schnellere Depurationsrate (Halbwertszeit weniger als 0,5 Tage) als die Kationen (Halbwertszeit von etwa 5 Tagen). Zwanzig mögliche Screening-Parameter für das Biomagnifikationspotential ionisierter Verbindungen wurden mit verfügbaren Schätzwerkzeugen (ACD / i-Lab und COSMOmic) berechnet und mit BMF-Daten aus dieser Studie und aus der Literatur korreliert. Der COSMOmic $K_{Fisch\ /\ Wasser}$ zeigte die höchste Korrelation zum gemessenen BMF, während die meisten anderen Deskriptoren nicht signifikant korrelierten. Das vermutete Bioakkumulationspotential der sechs IOC nach Aufnahme über die Nahrung konnte in den Fütterungsstudien mit Regenbogenforellen nicht bestätigt werden. Keiner der mehr als zwanzig Screening-Parameter zeigte eine besonders hohe Korrelation mit den Testergebnissen oder den aus der Literatur gesammelten BMF-Werten. Insgesamt kann aus dem Screening geschlossen werden, dass die Ionisierung einer Chemikalie die Tendenz zur Bioakkumulation im Vergleich zu nichtionisierten Chemikalien verringert. Eine schnelle Depuration scheint ein Hauptgrund für die beobachtete geringe Biomagnifikation ionischer Verbindungen, insbesondere der Anionen, zu sein. Aufgrund des schnellen Metabolismus oder der Konjugation geladener Verbindungen kann es zu einer schnellen Depuration kommen. Zukünftige Studien sollten diese Hypothese überprüfen.

Abstract

The goal of the present study was to experimentally determine the bioaccumulation of fully ionized compounds and to identify screening parameters that can indicate high bioaccumulation potential of ionic organic chemicals (IOCs). Three feeding studies with rainbow trout (*Oncorhynchus mykiss*) were carried out according to OECD TG 305. Separation of liver, gastrointestinal tract (GIT) and carcass allowed to further elucidate the tissue distribution of the individual test substances. The chemicals chosen had characteristics that made them suspect for high bioaccumulation, and included two cations (Tetrabutylphosphonium bromide (TBP), Trimethyloctadecyl ammonium chloride (TMOA)) and four anions (Benzotriazol, Tecloftalam, Pentachlorophenol (PCP), MEE-Phosphonate). Data on the dietary biomagnification of IOCs (strong acids) were also collected from published literature. The highest distribution factors were found for the GIT, followed by liver. However, none of the tested IOCs showed a distinct biomagnification potential, as kinetic biomagnification factors (BMF_k) ranged between 0.001 and 0.05 g/g (median 0.009 g/g). Cations showed lower assimilation efficiency (α) than anions, except for Tecloftalam. In contrast, anions showed a considerably faster depuration rate (half-life less than 0.5 d) compared to cations (half-life of around 5 d). Twenty potential screening parameters for BMF were calculated with available estimation tools (ACD/i-Lab and COSMOmic)

and correlated to BMF data from this study and from literature. The COSMOmic $K_{fish/water}$ showed the highest correlation to measured BMF, while most other descriptors were insignificantly correlated. The suspected dietary bioaccumulation potential of the six IOCs could not be confirmed in the feeding studies with rainbow trout. None of the more than twenty screening parameters showed particularly high correlation to the test results nor to the BMF values collected from literature. Overall, it can be concluded from the screening that ionization lowers the tendency of a chemical to bioaccumulate, compared to non-ionized chemicals. Fast depuration seems to be a major reason for the observed low biomagnification of ionic compounds, in particular anions. Fast depuration may happen due to rapid metabolism or conjugation of charged compounds, and future studies should test this hypothesis.

Inhaltsverzeichnis

Abbildungsverzeichnis

Tabellenverzeichnis

Abbreviations

α	Chemical absorption efficiency
BCF	Bioaccumulation factor
BMF	Biomagnification factor
BMF_k	Kinetic biomagnification factor
BMF_{kg}	Growth-corrected kinetic biomagnification factor
BMF_{kgL}	Growth and Lipid-corrected kinetic biomagnification factor
BMF_{SS}	Steady state BCF
ECHA	European Chemicals Agency
FCR	Feed conversion ratio
GIT	Gastrointestinal tract
I	Specific fish feeding rate
IOC	Ionic organic compound
k_2	Depuration rate
K_{BSA}	Distribution coefficient to bovine serum albumin
$K_{fish/water}$	Distribution coefficient between fish and water
K_{HSA}	Distribution coefficient between human serum albumin and water
$K_{lip/water}$	Distribution coefficient between lipids and water
K_{MP}	Distribution coefficient to muscle protein
log D_{ow}	Logarithmic octanol/water distribution coefficient, pH dependent
log K_{HSA}	Logarithmic human serum albumin/water distribution coefficient
log K_{lipw}	Logarithmic liposome/water partition coefficient
log K_{ow}	Logarithmic octanol/water distribution coefficient
PBT	Persistent, bioaccumulating and toxic
PLA	Parallel line analysis
PSA	Polar surface area
QM	Quantum mechanical calculations
RSD	Relative standard deviation
SD	Standard deviation
TEER	Trans-epithal resistance
TPSA	Topological polar surface area
UBA	Umweltbundesamt
vPvB	Very persistent and very bioaccumulating

Zusammenfassung

Die Identifizierung und wirksame Regulierung persistenter, bioakkumulierender und toxischer bzw. sehr persistenter und sehr bioakkumulierender Stoffe (PBT-/vPvB-Stoffe) ist notwendig, um ein hohes Schutzniveau für Mensch und Umwelt zu gewährleisten. Die Beurteilung von Stoffen hinsichtlich ihres Potentials zur Anreicherung in Organismen (Bioakkumulation) ist hierbei ein entscheidendes Kriterium. Das Bioakkumulationspotential eines Stoffes wird derzeit hauptsächlich durch den OECD Test 305 (Bioakkumulationstest mit aquatischer Exposition oder Exposition über die Nahrung) an Fischen ermittelt. Zur Einschätzung des Bioakkumulationspotentials ist ein experimentell ermittelter Biokonzentrationsfaktor (BCF) von > 2 000 (Einordnung als Stoff mit PBT-Eigenschaften) oder > 5 000 (Einordnung als Stoff mit vPvB-Eigenschaften) maßgeblich. Allen experimentellen Studien zur Ermittlung des Bioakkumulationspotentials sind ein hoher Bedarf an Versuchstieren sowie ein großer zeitlicher und finanzieller Aufwand gemein. Zur Vermeidung unnötiger Bioakkumulationsstudien werden stoffintrinsische Eigenschaften herangezogen, welche sich aus der Molekülstruktur berechnen lassen oder experimentell einfach zu bestimmen sind und ein Screening des Bioakkumulationspotentials ermöglichen. Insbesondere der Verteilungskoeffizient Octanol-Wasser (log K_{ow}) wird dazu üblicherweise verwendet. Hierbei dient Octanol als Modell für Speicherlipide. So wird angenommen, dass ein Stoff mit einem log K_{ow} > 4.5 potentiell bioakkumulierend ist. Ein Stoff mit einem log K_{ow} < 3 wird hingegen nur als gering bioakkumulierend eingeschätzt, gemäß der REACH-Verordnung kann folglich auf einen Bioakkumulationstest verzichtet werden.

Das Konzept zur Bewertung des Bioakkumulationspotentials von Stoffen wurde für neutrale organische hydrophobe Stoffe entwickelt. Viele organische Stoffe liegen unter umweltrelevanten Bedingungen jedoch teilweise oder komplett ionisiert vor (Franco et al., 2010). Die Ladung ionischer Molekül hat einen starken Einfluss auf die physikalisch-chemischen Eigenschaften dieser Stoffe, weshalb sie ein anderes Umweltverhalten als neutrale organische Stoffe zeigen. In den Leitfäden der REACH-Verordnung (R.11, R.7b) wird darauf hingewiesen, dass ionische organische Chemikalien (IOCs) bei der Bewertung des Bioakkumulationspotentials gesondert behandelt werden müssen (pH-Abhängigkeit des log K_{ow} bzw. des log D_{ow}). Als Beispiele werden Sulfonate, Carboxylate, Hydroxyle oder Amine genannt. Als Bewertungsansatz wird die Korrektur des K_{ow} mittels des neutralen Anteils (Multiplikation mit dem Faktor f_N) vorgeschlagen. Dies impliziert, dass die ionische Spezies im Wasser verbleibt und an keinen Sorptionsprozessen beteiligt ist. Viele experimentelle Daten belegen mittlerweile allerdings, dass dies nicht zutrifft (Bittermann et al., 2014). Eine Datenauswertung von Meylan et al. (1999) zeigt, dass große organische Reste einen Einfluss auf die Akkumulation haben. Ebenso befördert auch eine Verteilung der Ladung über eine größere Oberfläche die Hydrophobie der Ionen. Zusätzliche Effekte, wie z.B. die Ionenfalle und die Bindung von Ionen an Zellmembranen und Proteine machen die Abschätzung der Akkumulation von IOCs komplexer (Fu et al., 2009).

Der log K_{ow} hat für die Abschätzung des Bioakkumulationspotentials von IOCs keine Aussagekraft. Octanol ist als isotrope Phase zur Untersuchung der Anreicherung von IOCs ungeeignet, da sich ionische Stoffe vorwiegend in anisotropen Phasen wie Membranlipiden anreichern (Armitage et al., 2013). Außerdem zeigen Studien, dass der log D_{ow} die Sorption ionischer Spezies um mehrere Größenordnungen unterschätzt (Smejtek und Wang, 1993; Escher und Schwarzenbach, 1996). Daher ist der log K_{ow} generell ein ungeeigneter Ansatz für die Bewertung der Bioakkumulation von IOCs. Ein alternatives Screening-Kriterium zum log K_{ow} oder log D_{ow} ist in der Regulation jedoch momentan nicht etabliert.

Eine Auswertung der Datenverfügbarkeit aus den REACH Registrierungen mit einer Jahresproduktion ab 1 000 Tonnen zeigte, dass in 18 % der Fälle keine Bioakkumulationstests vorliegen, da der registrierte Stoff ionisch oder hydrolytisch instabil ist (REACH Compliance: Auswertung der Datenverfügbarkeit aus den REACH Registrierungen FKZ 3714 67 420 0). Dabei blieb offen, inwieweit die Auslassung einer Bioakkumulationsbewertung gerechtfertigt war. Aufgrund des Fehlens von geeigneten Screeningtools wurden diese bei QSAR-basierten Massenscreenings nach potentiellen PBT-Stoffen aus der Gesamtzahl der unter REACH registrierten Stoffe IOCs bisher ausgelassen. Aufgrund der schwachen Datenlage ist unklar, ob IOCs generell hinsichtlich ihres Bioakkumulationspotentials entlastet werden können und ob das Screening der neutralen Spezies ausreicht, um alle PBT-/vPvB-Stoffe zu identifizieren.

In der Literatur sind mehrere Studien zu finden, welche sich mit der Bioakkumulation (aquatische Exposition) von IOCs beschäftigen (Fu et al., 2009; Rendal et al., 2011; Anskjær et al., 2013). Verschiedene aquatische Organismen werden betrachtet. Die Doktorarbeit von Rendal (2013) gibt z. B. einen guten Überblick über die pH-abhängige Bioakkumulation und Toxizität von schwachen organischen Elektrolyten. Ob eine organische Spezies in neutraler oder ionischer Form vorliegt, wird über den pH-Wert bestimmt und hängt von dem pK_a-Wert der Säure oder Base ab. Generell steigen die Bioakkumulation und die Toxizität mit steigendem Anteil der neutralen Spezies, da diese lipophiler sind. Ionische Spezies bioakkumulieren bevorzugt in Membranen und an Proteinen (Armitage et al., 2013). Die Bioakkumulation und die Toxizität der neutralen Spezies scheinen generell höher als die der ionischen Spezies. Gemäß Armitage et al. (2017) ist für Stoffe mit einem neutralen Anteil ab 10 % dieser für die Bioakkumulation ausschlaggebend.

Der log K_{lipw} ist der Liposom/Wasser Verteilungskoeffizient und ein mögliches Screening-Kriterium für das Bioakkumulationspotential von IOCs. In mehreren Studien werden Liposomen bestehend aus Phosphatidylcholin als geeignetes künstliches Modell für Membranen beschrieben (Escher und Schwarzenbach, 1996; Ottiger und Wunderli-Allenspach, 1997; Yamamoto und Liljestrand, 2004). Einige Studien vergleichen den log K_{lipw} mit dem log D_{ow} für IOCs (Smejtek und Wang, 1993; Escher und Schwarzenbach, 1996; siehe auch Fu et al., 2009) und zeigen, dass der log D_{ow} die Sorption ionischer Spezies an Biomembranen um mehrere Größenordnungen unterschätzt.

Nakamura et al. (2008) vergleichen den log K_{lipw} mit experimentellen BCF-Werten für ein ionisierbares Arzneimittel (Fluoxetin). Müller et al. (1999) sowie van der Heijden und Jonker (2009) vergleichen den log K_{lipw} mit dem BCF einiger neutraler Stoffe. Alle drei Studien können die Bioakkumulation anhand des log K_{lipw} relativ gut vorhersagen. Trotz der wenigen direkten experimentellen Vergleiche zwischen log K_{lipw} und BCF kann anhand von Vergleichen zwischen dem log K_{lipw} und dem log K_{ow} und verschiedener Modellierungen davon ausgegangen werden, dass sich der log K_{lipw} für die Vorhersage der Bioakkumulation von IOCs besser eignet als der log K_{ow} (oder auch der log D_{ow}). Der log K_{lipw} in Verbindung mit weiteren Verteilungskoeffizienten (z.B. dem Protein-Wasser Verteilungskoeffizient) könnte auch in Modellen und als Screening-Kriterium für die Bioakkumulation von IOCs Verwendung finden (Endo et al., 2011; Armitage et al., 2013). Mit COSMOmic-Modellen kann der log K_{lipw} gut modelliert werden (Bittermann et al., 2016). In der regulatorischen Praxis ist dieser Ansatz jedoch noch sehr aufwendig und für ein Massenscreening weniger geeignet, da die quantenchemischen Rechnungen bei größeren Molekülen sehr zeitintensiv sind. Allerdings könnten diese Rechnungen alternativ auf einem niedrigeren Niveau durchgeführt werden, das zwar weniger präzise Aussagen zulässt, aber auch weniger rechenaufwändig ist.

Palm et al. (1996) konnten nachweisen, dass die polare Oberfläche (Polar Surface Area, PSA) von basischen Molekülen (Betablocker) signifikant mit der beobachteten Adsorption in häufig

verwendeten in vitro Modellsystemen (wie z.B. Caco-2 oder Ileum der Ratte) korreliert. Die Topologische Polare Surface Area (TPSA) kann mit breit verfügbaren Tools abgeschätzt werden (z.B. ACD/i-Lab) und wird bereits im „Drugdesign“ als Prädiktor der oralen Bioverfügbarkeit eingesetzt (Ertl, 2008). TPSA könnte zusammen mit anderen Parametern als Screening-Parameter für das Bioakkumulationspotential verwendet werden.

In einem aktuellen Review von Armitage et al. (2017) über das Bioakkumulationspotential von IOCs wird ein gestuftes Vorgehen vorgeschlagen. Die neutrale Spezies wird als Worst-Case für die Bioakkumulation angenommen und daher wird ein Stoff entlastet, falls die neutrale Spezies kein Bioakkumulationspotential auf Screening-Ebene (log K_{ow}) aufweist. Falls hingegen die neutrale Spezies ein Bioakkumulationspotential aufweist, soll anhand aktueller Modelle eine Verfeinerung der Bewertung, unter Berücksichtigung der ionischen Spezies und der Biotransformation, vorgenommen werden.

Aufgrund der geringeren Membranpermeabilität von IOCs und des andererseits hohen Trans-Epithalen-Widerstandes (TEER) der Kiemen im Vergleich zum TEER des Magen-Darm-Traktes und der damit einhergehenden größeren Durchlässigkeit des Magen-Darm-Trakts (GIT) wird vermutet, dass IOCs über den GIT besser aufgenommen werden. Ein entscheidender Unterschied der beiden Aufnahmepfade ist auch die längere Verweildauer im Magen-Darm-Trakt. Studien zeigen, dass neutrale Stoffe eine konstante Aufnahmeeffizienz über einen größeren K_{OW}-Bereich haben (Kelly et al., 2004; O'Connor et al., 2013). Die in der Arbeit von Arnot und Quinn (2015) untersuchten Daten aus Fischfütterungsstudien zeigen, dass IOCs nicht entscheidend geringer aufgenommen werden als neutrale Verbindungen mit ähnlichen Eigenschaften. Armitage et al. (2017) diskutieren hingegen, dass der ionische Anteil eines IOCs keinen entscheidenden Einfluss auf die Aufnahme über den GIT hat. Bei all diesen Überlegungen wird allerdings die Bedeutung des parazellulären Transportes während der Aufnahme außer Acht gelassen.

Hierauf aufbauend können die Ziele dieses Projekts wie folgt benannt werden:

Es sollte überprüft werden, inwieweit IOCs hinsichtlich ihres Bioakkumulationspotentials eine Gefahr darstellen können, und ob auch für IOCs mit log D < 3 eine potentielle Gefahr bezüglich der Anreicherung in Organismen (Bioakkumulation) besteht. Gleichzeitig sollte untersucht werden, ob IOCs mit einem log K_{lipw} > 4 ein hohes Bioakkumulationspotential haben können (B/vB nach REACH, Annex XIII) und inwieweit die Bioakkumulationsbewertung auf Basis des neutralen Moleküls durchgeführt werden kann. Bereits vorhandene Ansätze wie z.B. das Bewertungskonzept von Armitage et al. (2017) sowie die Ansätze von Meylan et al. (1999) und Fu et al. (2009) sollten hinsichtlich ihrer Eignung überprüft werden.

Anhand verschiedener Screeningparameter [log D, log K_{lipw}, Oberflächenladung (COSMOmic, TPSA), Struktur und andere] sollten repräsentative Stoffe ausgewählt werden, die basierend auf den Screeningparametern potentiell bioakkumulierend sind. Da die bisherigen Ansätze sich auf neutrale Stoffe konzentrieren, sollten insbesondere IOCs, welche unter umweltrelevanten Bedingungen zu > 90 % ionisch oder permanent ionisch vorliegen, Gegenstand des Forschungsvorhabens sein. Die Eignung der Screeningparameter und die Vorhersage der Bioakkumulation von IOCs sollte experimentell anhand von Fischfütterungsstudien nach OECD 305 (OECD, 2012) geprüft werden.

Das Projekt lässt sich in seinen Abläufen in mehrere Arbeitspakete unterteilen:

Arbeitspaket 1:

In der Literatur wird für die Abschätzung des Bioakkumulationspotentials von IOCs häufig der log K_{lipw} und der log D angegeben. Weitere mögliche Screeningparameter sollten in diesem Arbeitspaket ermittelt und ausgewählt werden.

Die Verteilungskoeffizienten Membran/Wasser und Protein/Wasser wären aus mechanistischer Sicht die erste Wahl für ein solches Screening. Allerdings haben die vorhandenen Modelle zur Vorhersage der Protein/Wasser Verteilung von Ionen einen so begrenzten Anwendungsbereich, dass sie für ein Screening praktisch nicht in Frage kommen (Linden et al., 2017). Alternativ wurde daher untersucht, inwiefern sich einfache Hydrophobizitätsparameter für Ionen aus ihrer molekularen Struktur berechnen lassen, die ebenfalls mit den gesuchten Proteinsorptionskoeffizienten korrelieren. Diese empirischen Ansätze können z.B. über die Beschreibung der maximalen Ladungsdichte an der Molekülоberfläche oder die Molekülfläche, die eine gewisse Ladungsdichte überschreitet, parametrisiert werden. Solche empirischen Ansätze werden für Anionen und Kationen getrennt durchgeführt, da bereits bekannt ist, dass Anionen und Kationen mit exakt gleicher Größe, Gestalt und van-der-Waals-Wechselwirkungen trotzdem sehr unterschiedlich sorbieren (Bittermann et al., 2014). Für die Vorhersage der Membran/Wasser-Verteilung der Ionen wurde COSMOmic verwendet.

Die Screeningparameter sollten, falls möglich, mit vorhandenen BCF oder BMF-Werten von IOCs geprüft werden, um deren Eignung abzuschätzen.

Arnot und Quinn (2015) haben die Ergebnisse (BMF-Werte) von 400 Fütterungsstudien mit Fischen zusammengestellt. Davon sind 7 % (28) der Substanzen Stoffe, die im Darm teils oder ganz ionisiert vorliegen, wie Pentachlorphenol, perfluorierte Stoffe und Medikamente. Ergebnisse von Fischfütterungsstudien mit Antibiotika wurden im EU-Projekt PHARMAS zusammengestellt und lagen zur weiteren Auswertung vor (Trapp und Legind, 2011). Im EU-Projekt OSIRIS wurden BCF-Daten zu ionischen Stoffen gesammelt. Eine Studie mit einem Teil dieser BCF-Daten, bestehend aus 73 Säuren und 65 Basen, wurde in Fu et al. (2009) veröffentlicht. In ihrem Review zur Bioakkumulation ionisch vorliegender organischer Substanzen konzentrierten sich Rendal et al. (2011) auf Studien, in denen die Biokonzentration beim Fisch (oder Toxizität) bei wechselndem pH gemessen wurde. Dazu liegen unter anderem Daten aus Studien mit Goldfischen und Guppies vor. Es wurde ein Datensatz zu BMF- und BCF-Werten zusammengestellt, der ausreichend Ergebnisse zu ionisierbaren und/oder geladenen Stoffen enthält, um die Eignung verschiedener Screening-Parameter mit den gesammelten Datensätzen zu prüfen. Zu den ausgewählten Datensätzen wurden die genannten Stoffparameter ermittelt (aus der Literatur oder abgeschätzt). Zusätzlich wurde die Literatur (auch die medizinische Literatur) nach weiteren Parametern durchsucht, die für BCF und BMF relevant sein könnten. Um die Vorhersagekraft möglicher Screening-Parameter für BMF- und BCF-Werte ionischer Stoffe zu evaluieren, wurden anschließend verschiedene statistische Verfahren eingesetzt, inklusive Korrelationsanalyse aber auch nicht-parametrische und multivariate Verfahren.

Arbeitspaket 2:

Die in Arbeitspaket 1 ermittelten Screeningparameter wurden in einem zweiten Arbeitsschritt zur Auswahl von Stoffen herangezogen, welche in Biomagnifikationsstudien getestet wurden. Somit war sichergestellt, dass BCF- und BMF-Werte und damit Daten zum Bioakkumulationspotenzial der Stoffe bekannt waren.

Basierend auf den bereits bestehenden Erfahrungen wurde festgelegt, dass mindestens eine quartäre Ammoniumverbindung dabei sein sollte. Diese Verbindungen sind permanent (also pH

unabhängig) geladen und vergleichsweise hydrophob. Zudem sollten auch permanente Anionen untersucht werden. Permanente Ionen werden wegen ihrer schlechten Membranpermeabilität vermutlich ein anderes Akkumulationsverhalten zeigen als andere Ionen. Da diese Ionen über den parazellulären Weg in den Blutkreislauf gelangen können, sind sie aber nicht von vornherein uninteressant. Ionische Tenside wurden als ebenfalls interessant für die Betrachtung befunden, da hier wegen der Grenzflächenaktivität ein ganz anderes Sorptionsverhalten auftreten kann als bei anderen Ionen.

Arbeitspaket 3:

Anhand der Überlegungen wurden folgende 6 Verbindungen ausgewählt:

Kationen:

1. Tetrabutylphosphoniumbromid (TBP)
2. Trimethyloctadecylammoniumchlorid (TMOA)

Anionen:

3. Tecloftalam
4. Pentachlorphenol
5. Mono-2-ethylhexyl(2-Ethylhexyl)Phosphonat (MEE-Phosphonat)
6. Benzotriazol

Aufgrund des damaligen Kenntnisstands wurde vermutet, dass die Aufnahme dieser Stoffe über den GIT größer als über die Kiemen ist. Entsprechend wurden drei Fütterungsstudien gemäß Richtlinie OECD 305 mit je zwei der ausgewählten Stoffe durchgeführt. Für Proben der Biomagnifikationsstudien wurde eine organspezifische Analyse durchgeführt.

Die drei Fütterungsstudien wurden im FhG-IME mit je zwei ionisierenden organischen (nicht radioaktiv markierten) Substanzen durchgeführt, um die Biomagnifikationsfaktoren (BMF) der einzelnen Substanzen auf Basis der Richtlinie OECD 305 zu bestimmen. Alle Biomagnifikationsstudien wurden mit Regenbogenforellen (*Oncorhynchus mykiss*) durchgeführt. Die mit den ionisierenden organischen Substanzen angereicherten Testfuttermittel wurden im FhG-IME auf Basis etablierter Protokolle (Goeritz et al., 2013) hergestellt. Die Testkonzentrationen wurden im Rahmen von Vortests überprüft, um eine spätere Beeinträchtigung der Versuchstiere durch toxische Effekte zu vermeiden.

Die im Verlauf der Fütterungsstudien aus dem Versuchstank entnommenen Tiere wurden nach der Schlachtung in unterschiedliche Organfraktionen separiert (Leber, Magen und Darm, Karkasse), um eine organspezifische Analyse zu ermöglichen. Die im Rahmen der Fütterungsstudien gewonnenen Futtermittel und Gewebeproben wurden im FhG-IME auf den Gehalt an Testsubstanzen untersucht. Die für die Analytik der einzelnen Substanzen erforderlichen Methoden wurden vor Ort entwickelt.

Das Biomagnifikationspotential der Testsubstanzen im Fisch wurde dabei aus der Kinetik der Auf- und Abnahme der einzelnen Substanzen im Gewebe bestimmt. Neben den Biomagnifikationsfaktoren konnten für die einzelnen Testsubstanzen Gewebeverteilungsfaktoren berechnet werden, welche leichte Unterschiede zwischen den Geweben bezüglich der Anreicherung der einzelnen ionischen Stoffe verdeutlichen.

Die gewählte Anreicherungsmethode für die Herstellung der experimentellen Futtermittel führt zu stabilen Konzentrationen der getesteten IOCs während der Exposition. Mit Ausnahme der anionischen IOCs Tecloftalam und Phosphonat wurde durch das Detektieren quantifizierbarer Konzentrationen der entsprechenden Verbindungen in den Karkassen und Lebern auch die Bioverfügbarkeit der IOCs über den GIT nachgewiesen.

Eine Biomagnifikation konnte jedoch für keine der IOCs nachgewiesen werden, zumal der höchste BMF_k bzw. BMF_{kg} für den gesamten Fisch bei 0,0404 bzw. 0,0463 g/g (TMOA) lag. Generell zeigten sich das Gewebe des GIT und der Leber als die am stärksten belasteten Gewebe, was sich durch den Ort der Aufnahme und den Weg des Transports im Blut über die Pfortader (Vena Porta) vom GIT zur Leber erklären lässt.

Summary

The identification and effective regulation of persistent, bioaccumulating and toxic (PBT) or very persistent and very bioaccumulating substances (vPvB substances) is necessary to ensure a high level of protection for humans and environment. The assessment of substances with regard to their potential for accumulation in organisms (bioaccumulation) is a crucial criterion. The bioaccumulation potential of a substance is currently mainly determined by the OECD TG 305 fish flow-through test. A bioconcentration factor (BCF) is experimentally determined , which allows to identify substances having a BCF >2000 or >5000 being classified as substances having "B" or "vB" properties, respectively. All experimental studies to determine the bioaccumulation potential have a high need of experimental animals and commonly require a large expenditure of time and money. In order to avoid unnecessary bioaccumulation studies, substance-specific properties are used, which can be calculated from the molecular structure or are easy to determine experimentally and allow a prediction of the bioaccumulation potential of a chemical compound. The octanol/water distribution coefficient (log K_{ow}) is commonly used for screening purposes. Here, octanol serves as a model for storage lipids. It is assumed that a substance with a log K_{ow} > 4.5 is potentially bioaccumulative. A substance with a log K_{ow} < 3, on the other hand, is only rated as slightly bioaccumulating, and according to the REACH Regulation, a bioaccumulation test can thus be waived.

The concept for evaluating the bioaccumulation potential of substances was developed for neutral organic hydrophobic substances. However, many organic substances are partially or completely ionized under environmentally relevant conditions (Franco et al., 2010). The charge of ionic molecules has a strong influence on the physicochemical properties of these substances leading to a different environmental behavior compared to neutral organic substances. The REACH guideline (R.11, R.7b) indicate that ionic organic chemicals (IOCs) must be treated separately when assessing their bioaccumulation potential (pH dependence of the log K_{ow} or log D_{ow}). Examples for IOCs are sulfonates, carboxylates, hydroxyls or amines. The correction of the log K_{ow} considering the neutral portion of an IOC (multiplication by the factor f_N) is suggested to enable bioaccumulation assessment. This implies that the ionic species remains in the water and is not involved in any sorption processes. However, experimental data indicate that this is not the case (Bittermann et al., 2014). A data analysis by Meylan et al. (1999) shows that large organic residues have an influence on the accumulation of IOCs. The distribution of the charge over a larger surface of the ions also promotes their hydrophobicity. Additional effects, such as the ion trap effect or the binding of ions to cell membranes and proteins make the estimation of the accumulation of IOCs more complex (Fu et al., 2009).

The log K_{ow} is not suitable to estimate the bioaccumulation potential of IOCs because octanol is an isotropic phase but IOCs accumulate predominantly in anisotropic phases such as membrane lipids (Armitage et al., 2013). Studies also show that the log D_{ow} underestimates the sorption of ionic species by several orders of magnitude (Smejtek and Wang, 1993; Escher and Schwarzenbach, 1996). However, an alternative screening criterion to log K_{ow} or log D_{ow} is currently not established in the regulation.

An evaluation of the data available from REACH registrations of compounds with an annual production of 1,000 tons or more showed that in 18 % of the cases no bioaccumulation tests were carried out because the registered substances were considered to be ionically or hydrolytically unstable (REACH compliance: evaluation of the data availability from the REACH registrations FKZ 3714 67 420 0). However, whether the omission of a bioaccumulation assessment was justified remained open. Due to the lack of suitable screening tools, IOCs have so far been omitted from comprehensive QSAR-based screening approaches for potential PBT

substances and it remains unclear whether IOCs can generally be considered as non-bioaccumulative in terms of their bioaccumulation potential and whether the screening of the neutral species is sufficient to identify all PBT/vPvB substances.

There are several studies in the literature that deal with the bioaccumulation (aquatic exposure) of IOCs (Fu et al., 2009; Rendal et al., 2011; Anskjær et al., 2013). Different aquatic organisms were used as test species. The doctoral thesis by Rendal (2013) gives an overview of the pH-dependent bioaccumulation and toxicity of weak organic electrolytes. Whether an organic species is in neutral or ionic form depends on the pH value of the test medium as well as on the pK_a value of the acid or base. In general, bioaccumulation and toxicity of IOCs increase with the proportion of the neutral species, as these are more lipophilic. Ionic species bioaccumulate preferably in membranes and on proteins (Armitage et al., 2013). The bioaccumulation and toxicity of the neutral species generally appear to be higher than for the ionic species. According to Armitage et al. (2017), the neutral fraction is crucial for bioaccumulation when it is 10 % or more.

The log K_{lipw} is the liposome-water partition coefficient and a possible screening criterion for the bioaccumulation potential of IOCs. Several studies have described liposomes consisting of phosphatidylcholine as a suitable artificial model for membranes (Escher and Schwarzenbach, 1996; Ottiger and Wunderli-Allenspach, 1997; Yamamoto and Liljestrand, 2004). Some studies compare the log K_{lipw} with the log D_{ow} for IOCs (Smejtek and Wang, 1993; Escher and Schwarzenbach, 1996; see also Fu et al., 2009) and show that the log D_{ow} underestimates the sorption of ionic species by several orders of magnitude. Nakamura et al. (2008) compare the log K_{lipw} with the experimental BCF of the ionizable drug fluoxetine. Müller et al. (1999) and van der Heijden and Jonker (2009) compare the log K_{lipw} with the BCF of further neutral substances. In all three studies bioaccumulation was well predicted using the log K_{lipw}. The comparison of experimentally derived log K_{lipw} and BCF values, and further comparisons between the log K_{lipw} and the log K_{ow} indicate that the log K_{lipw} is more suitable for predicting the bioaccumulation of IOCs than the log K_{ow} (or also the log D_{ow}). The log K_{lipw} in combination with further distribution coefficients (e.g. the protein-water distribution coefficient) could also be used in models and as a screening criterion for the bioaccumulation of IOCs (Endo et al., 2011; Armitage et al., 2013). The log K_{lipw} can be derived with COSMOmic models (Bittermann et al., 2016). In regulatory practice, however, this approach is still very complex and less suitable for mass screening because the quantum chemical calculations are very time-consuming for larger molecules. However, calculations could alternatively be carried out with reduced complexity but still allow sound statements.

Palm et al. (1996) were able to demonstrate that the polar surface area (PSA) of basic molecules (beta blockers) correlated significantly with the observed adsorption in frequently used in vitro model systems (such as Caco-2 or ileum of the rat). The topological polar surface area (TPSA) can be estimated using widely available tools (e.g. ACD/i-Lab) and is already used in drug design as a predictor of oral bioavailability (Ertl, 2008). TPSA, along with other parameters, could be used as a screening parameter for the bioaccumulation potential.

In a recent review by Armitage et al. (2017) on the bioaccumulation potential of IOCs, a graded approach is proposed. The neutral species is assumed to be the “worst case” regarding the bioaccumulation potential of an IOC and therefore a substance is considered to be non-bioaccumulative, if the neutral species has no bioaccumulation potential at the screening level (log K_{ow}). If, on the other hand, the neutral species has a bioaccumulation potential, the assessment should be refined based on current models, taking into account the ionic species and its potential to be biotransformed.

Due to the lower membrane permeability of IOCs, the high trans-epithal resistance (TEER) of the gills compared to the TEER of the gastrointestinal tract (GIT) and the associated greater permeability of the gastrointestinal tract, it is assumed that the absorption of IOCs via the GIT is the preferred pathway. A crucial difference between the two absorption paths is the longer remaining in the GIT. Neutral substances have a constant absorption efficiency over a large range of K_{ow} (Kelly et al., 2004; O'Connor et al., 2013). However, data from fish feeding studies examined by Arnot and Quinn (2015) show that IOCs may have a similar ingestion compared to neutral compounds with similar properties. In all of these considerations, however, the importance of paracellular transport for the uptake is neglected.

Based on this, the goals of this project were as follows: a) Investigate to which extent IOCs should be of concern with respect to bioaccumulation potential, and whether IOCs with log D < 3 are of potential concern for accumulation in organisms (bioaccumulation), b) Investigate whether IOCs with a log K_{lipw} > 4 can have a high bioaccumulation potential (B/vB according to REACH regulation; Annex XIII) and to what extent the bioaccumulation assessment can be carried out on the basis of the neutral molecule, c) Existing approaches as described by Armitage et al. (2017), Meylan et al. (1999) and Fu et al. (2009) were tested for their suitability, and d) using different screening parameters [log D, log K_{lipw}, surface charge (COSMOmic, TPSA), structure and others], representative substances were selected that are potentially bioaccumulative based on the screening parameters. The focus of the research project was on compounds being > 90 % ionic or permanently ionic under environmentally relevant conditions. Finally, the suitability of the screening parameters to predict the bioaccumulation potential of IOCs in fish was tested experimentally using fish feeding studies according to OECD 305 (OECD, 2012).

The project was divided into three work packages:

Work package 1:

In the literature, the bioaccumulation potential of IOCs is often estimated as the log K_{lipw} and log D. Further possible screening parameters were to be determined and selected in this work package. From a mechanistic point of view, the membrane/water and protein/water partition coefficients would be the first choice for such a screening approach. However, the available models for predicting the protein/water distribution of ions have such a limited applicability domain that they are not suitable for screening (Linden et al., 2017). Therefore, it was investigated to what extent simple hydrophobicity parameters for ions can be calculated from their molecular structure, which also correlates with the protein sorption coefficients. These empirical approaches can be further parameterized considering the maximum charge density on the molecular surface or the molecular area that exceeds a certain charge density. Such approaches are carried out separately for anions and cations because it is already known that anions and cations with exactly the same size, shape and van-der-Waals interactions sorb very differently (Bittermann et al., 2014). COSMOmic was used to predict the membrane/water distribution of the ions.

If possible, the screening parameters were checked with existing BCF or BMF values derived for IOCs in order to assess their suitability. Arnot and Quinn (2015) have compiled the results (BMF values) of 400 feeding studies with fish. Seven percent (28) of these substances are partially or fully ionized in the intestine, such as Pentachlorophenol, perfluorinated substances and pharmaceuticals. The results of fish feeding studies with antibiotics were compiled in the EU project PHARMAS and are available for further evaluation (Trapp and Legind, 2011). BCF data on ionic substances were collected in the EU project OSIRIS. A study with some of these BCF data, consisting of 73 acids and 65 bases, was published by Fu et al. (2009). In their review on

the bioaccumulation of IOCs, Rendal et al. (2011) focused on the bioconcentration (or toxicity) at varying pH in fish, including goldfish and guppies. A data set on BMF and BCF values was compiled, which contains sufficient data on ionizable and / or charged substances to test the suitability of various screening parameters. The specified substance parameters were determined for the selected data sets (from the literature or estimated). In addition, the literature (including the medical literature) was reviewed for other parameters that could be relevant for the prediction of BCF and BMF values. Various statistical methods including correlation analysis, but also non-parametric and multivariate methods, were afterwards used to evaluate the power of the selected screening parameters to predict the biomagnification and bioconcentration potential of ionic substances.

Work package 2:

The screening parameters determined in work package 1 were used in step 2 to select substances that were finally tested in biomagnification studies as part of work package 3. In this way it was ensured that substances were selected for which information on the bioaccumulation potential were already available.

Based on previous experience, it was decided that at least one quaternary ammonium compound should be included in the set of test compounds. These compounds are permanently (i.e. pH independent) charged and comparatively hydrophobic. In addition, permanent anions should also be examined. Permanent ions will presumably show a different accumulation behavior from other ions due to their poor membrane permeability. Since these ions can get into the circulation system via the paracellular pathway, they are of high interest for this study. Ionic surfactants were also found to be of interest because, due to their interfacial activity, a completely different sorption behavior can occur in comparison to other ions.

Work package 3:

Based on these considerations, the following 6 compounds (IOCs) were selected for further testing:

Cations:

1. Tetrabutylphosphonium bromide (TBP)

2. Trimethyloctadecylammonium chloride (TMOA)

Anions:

3. Tecloftalam

4. Pentachlorophenol

5. Mono-2-ethylhexyl (2-ethylhexyl) phosphonate (MEE Phosphonate)

6. Benzotriazol

Based on the current state of knowledge, it was assumed that the absorption of the substances via the GIT is larger than via the gills. Accordingly, three feeding studies were carried out according to OECD TG 305, each with two of the selected substances. An organ-specific analysis was carried out for samples collected during the biomagnification studies. The three feeding studies were carried out in the experimental facility of FhG-IME with non-radioactive labeled substances in order to determine the biomagnification factors (BMF) of the individual substances. All biomagnification studies were carried out with rainbow trout (*Oncorhynchus mykiss*). The experimental diets were enriched with the ionizing organic substances following

established protocols (Goeritz et al., 2013). The test concentrations were tested during preliminary experiments in order to avoid later impairment of the test animals by toxic effects.

The animals collected in the course of the feeding studies were dissected into different tissue fractions (liver, stomach and intestine, carcass) in order to enable an organ-specific analysis. The feed and tissue samples were examined for the content of the different test substances. Methods required for the analysis of the individual substances were developed.

The biomagnification potential of the test substances in fish was determined from the elimination and uptake kinetics of the individual substances in the tissue. In addition to the biomagnification factors, tissue distribution factors were calculated for each test substance, to illustrate differences in tissue concentrations between the tissues.

The experimental diets contained homogenous and stable concentrations of the tested IOCs allowing a constant exposure of the test animals. With the exception of the anionic IOCs Tecloftalam and Phosphonate, quantifiable concentrations of the tested compounds could be measured in the carcasses and livers demonstrating the bioavailability of the IOCs via the GIT.

However, biomagnification (BMF > 1) could not be demonstrated for any of the IOCs, with the highest BMF_k or BMF_{kg} for TMOA with 0.0404 or 0.0463 g/g, respectively. In general, the highest tissue concentrations were measured in GIT and liver samples, which can be explained by the transfer of the ingested IOCs by blood (proteins) via the vena porta from the GIT to the liver.

1 Determining and selection of screening parameters for the determination of the bioaccumulation potential

1.1 Introduction

There is no generally accepted approach to estimate the bioaccumulation potential of organic ions (Treu et al., 2015) – despite the fact that the regulation of organic ions is a prevailing challenge (Franco et al., 2010). Ionogenic organic chemicals comprise very diverse structures and chemical classes such as surfactants, pharmaceuticals, some classes of pesticides, poly- or perfluorinated acids (Franco et al., 2010) as well as ionic liquids (Thuy Pham et al., 2010). The use of a single and easy to determine threshold value (such as the logarithmic octanol/water partition coefficient value), which is applied for neutral chemicals by regulation authorities (Endo et al., 2013), will not suffice as a standard criterion to identify the bioaccumulation potential of charged chemicals (Treu et al., 2015). Previous work focused on the description of uptake and elimination rates (including metabolism) to describe the bioaccumulation potential of organic ions, aiming at a holistic picture (Armitage et al., 2013). While we agree that physiologically based pharmacokinetic modelling is highly needed, we consider the underlying physicochemical parameters, especially the equilibrium sorption coefficients to the different relevant phases, as a major uncertainty in our current knowledge. In previous works both, sorption to proteins as well as sorption to membrane lipids was estimated for organic ions via the respective octanol/water partition coefficient (Armitage et al., 2013). In our own work we have recently shown that this is not appropriate (Bittermann et al., 2016). In this work we therefore develop mechanistic and semi empirical models to predict such equilibrium sorption coefficients. These can then be used to screen the bioaccumulation potential of organic ions in a first tier approach that still neglects any biotransformation or other kinetics and can thus be seen as a worst case scenario. Here, we use the newly developed predictive tools to provide such a screening of chemicals for their bioconcentration potential in fish and based on a depiction of the major sorption matrices. Analogous to the pharmacokinetic literature (Poulin and Theil, 2000; Rodgers and Rowland, 2006; Schmitt, 2008; Endo et al., 2013), we assume the following sorption matrices in organisms to be the most relevant for organic ions: membrane lipid, muscle protein (which is our proxy for structural protein), serum albumin (which is our proxy for plasma proteins in fish) and water. For organic ions, we assume that the sorption capacity of storage lipid (fat) can be neglected. Ions partition into octanol, which is a pretty good proxy for storage lipid (Endo et al., 2013), only marginally as ion pairs (Escher and Schwarzenbach, 1996; Escher and Sigg, 2004).

While our general approach is straight forward and not new (Endo et al., 2013) and has been applied by us before for a few selected ionizable chemicals with available experimental data (Goss et al., 2018), the challenge lies in providing all the different partition coefficients required for a broad screening. For the neutral species of ionizable chemicals the usage of poly parameter free energy relationships (pp-LFERs) is an appropriate way to obtain these data as shown in a review (Endo and Goss, 2014). In general, pp-LFERs are capable of describing the equilibrium partitioning of neutral organic chemicals between a multitude of biologically relevant matrices and water as well as technical partitioning systems and water. Unfortunately, the applicability of pp-LFERs for ionic organic chemicals is still in its infancy and of rather empirical nature, limited to few chemical classes (Abraham and Acree, 2016; Bittermann et al., 2016; Henneberger et al., 2016a). Thus, we investigate here to which extend required partition coefficients can be estimated with the help of the commercial software COSMOthermX (Klamt, 1995), which is the only predictive tool that cannot only handle neutral species but that is principally able to

provide meaningful predictions for the partitioning of organic ions (Bittermann et al., 2016). COSMOtherm is based on quantum mechanical (QM) calculations and fundamental fluid phase thermodynamics (namely the conductor like screening model for real solvents, COSMO-RS) (Klamt and Schüürmann, 1993; Klamt, 1995) which operates with only very general fitting parameters. The COSMO-RS implementation within COSMOtherm is principally applicable to both neutral chemicals as well as ions (Klamt, 2016). For ions, it has particularly been shown to be a good model for the description of the membrane/water partition coefficient (Bittermann et al., 2014) and for ionic liquid properties (Diedenhofen and Klamt, 2010).

Out of the four sorption matrices, only the membrane and water are well-defined and are thus directly describable within COSMOtherm (Klamt et al., 2008; Bittermann et al., 2014). The other two important sorption matrices are structural proteins and plasma proteins. About 10 % of the whole body mass of vertebrates is made of structural proteins, which themselves consist to about 50 % of muscle proteins (e.g. actin and myosin), while the other half is mostly keratin and collagen (Henneberger et al., 2016a). In the case of blood plasma the composition of the sorbing matrix varies in different organisms and the contributions of specific proteins are not always clear, thus we used albumin, which is expected to dominate anionic sorption in human blood, as a proxy for the plasma proteins. Hence, for structural proteins and albumin, the only chance to grasp the major characteristics of the respective sorption matrices with COSMOtherm is via fitting experimental partition coefficients of organic ions to so-called sigma moments via a multiple linear regression (MLR). The sigma moments are an output of the quantum chemical COSMO calculation for molecules and account for the solutes interaction properties. Calibrating MLR models based on sigma moments with experimental equilibrium partitioning data works well for neutral chemicals as has been shown for a big variety of liquid-liquid partitioning systems (personal communication, COSMOlogic) and is conducted in exact analogy to the pp-LFER approach, as outlined in detail below. We tested this approach both for the partitioning of organic ions between plasma protein and water and structural protein and water.

The major aims of this work were twofold: first, to develop reliable predictive sorption models, for neutral and ionic chemicals in order to describe the bioaccumulation potential of organic ions and ionizable chemicals (without metabolism); second to identify potentially bioaccumulative compounds by applying our models to a set of almost 2000 organic ions or ionizable chemicals. For the first aim we developed MLRs based on sigma moments describing the sorption to structural proteins and albumin (for neutral and monovalent ionic chemicals, respectively). For our second aim, we combined these MLRs with the pp-LFER models for neutral species and COSMOmic for neutral and ionic chemicals and applied it to almost 2000 chemicals. The results of this work were published as Bittermann et al., 2018.

1.2 Materials and Methods for the development of a sorption model

1.2.1 Materials for the development of a sorption model

1.2.1.1 Temperature dependence of sorption coefficients

The experimental sorption data for phospholipid membranes are available for temperatures between 20 to 37 °C. The sorption differences within this temperature range are negligible, as long as the membrane is in its natural liquid crystalline state (Endo et al., 2011). The data for structural and muscle proteins and albumin had been measured at 37 °C because they originally aimed to describe sorption capacities in humans. Although the modeled fish has a temperature between 13 and 17 °C (OECD, 2008), we expect only little influence of the temperature dependence of the sorption coefficients and regard this as one of the minor uncertainties of our model.

1.2.1.2 Sorption to structural (muscle) proteins

Structural proteins such as muscle protein are abundant in vertebrates and of polar nature (Henneberger et al., 2016a). Analogous to previous work (Endo et al., 2012; Henneberger et al., 2016a), we assumed the experimental sorption data from water to chicken muscle to be a generally valid proxy for the partition coefficient between structural proteins and water, $K_{\text{structural proteins/water}}$, for both the ionic as well as the neutral species. In fact, for 40 neutral chemicals it has been shown in previous work that the differences in $K_{\text{structural proteins/water}}$ between chicken, fish and pig muscle proteins were small (Endo et al., 2012). We used the experimental partitioning data from Endo et al. (2012) and Henneberger et al. (2016a), comprising 63 neutral chemicals, 41 anions and 10 cations (we left out those values that are only given as lower border). In order to be used in our screening model the experimental values had to be converted into volume based partitioning coefficients (multiplied with the density of muscle protein of 1.36 kg/L) (Linden et al., 2017). Note that this is a rather limited data set of chemicals. Increasing predictive errors have to be expected for chemicals that do not fall into the range spanned by the calibration data. Given that there are only ten cations in the data set, a meaningful MLR for cations is not possible (i.e. overfitting is inevitable). This gap needs to be filled by future work. For the time being it might be advisable for the screening to just add a log $K_{\text{structural proteins (cation)}}$ value of 1.5 for any cationic chemical (being the mean value of the exisiting experimental data).

1.2.1.3 Sorption to albumin

The partitioning to blood plasma is dominated by the sorption to the plasma proteins. Among these proteins serum albumin is the major sorption matrix for both neutral and ionic chemicals (Endo and Goss, 2011; Henneberger et al., 2016). We rely on two consistent experimental datasets (Endo and Goss, 2011; Henneberger et al., 2016) for our model development. The experimental data were derived with bovine serum albumin, which is comparable to human serum albumin (Henneberger et al., 2016). Due to the lack of reliable partitioning data for rainbow trout albumin, we use bovine serum albumin as a surrogate. Obviously, this assumption needs to be revised when new experimental values for fish plasma protein come up and as the circumstances require, a new MLR will have to be set up. In order to be used in our screening, the experimental values were converted to volume based partition coefficients (i.e. they were multiplied with the density of serum albumin, being 1.36 kg/L).

1.2.2 Methods for the development of the sorption model

1.2.2.1 Calculation of log $K_{\text{fish/water}}$

The partitioning of a permanently charged ionic chemical between any organism and water can be described as the additive sorption to all the sorption matrices in the body of the organism. For ions this is expressed in the following equation for the partitioning into fish:

$$K_{fish/water}^{ion} = f_{membrane} K_{membrane/water}^{ion} + f_{structural\ proteins} K_{structural\ proteins/water}^{ion} + f_{plasma\ proteins} K_{plasma\ proteins/water}^{ion} + f_{water} \quad (1)$$

with f_x denoting the volume fractions of the respective matrices/phases and the K's describing the partition coefficients between the matrices/phases and water given in the subscripts (trivially, $K_{\text{water/water}}$ equals one and thus only f_{water} needs to be considered). For our screening approach we looked at a 1 kg rainbow trout with the following composition (volume %): storage lipid 11 %, phospholipids 1.0 %, structural proteins 15.8 %, plasma proteins 0.27 %, and water 69.8 % (adapted from Nichols et al.,1990). A side note to the wording used here: a 'phase' is per definition homogeneous like water or hexadecane. Phospholipids and albumin are highly

heterogeneous, while muscle protein is probably a little less heterogeneous (Henneberger et al., 2016b) – therefore we denote these latter sorption media as (sorption) matrices.

When we describe the bioaccumulation potential of acids and bases that are partly neutral at the investigated pH, then the partitioning of both species needs to be assessed. For the neutral species, we also consider storage lipids (triglycerides) as a major sorbing compartment in addition to membranes, structural proteins and albumin (Endo et al., 2013).

$$K_{fish/water}^{neutral} = f_{membrane}K_{membrane/water}^{neutral} + f_{structural\ proteins}K_{structural\ proteins/water}^{neutral} + f_{plasma\ proteins}K_{plasma\ proteins/water}^{neutral} + f_{storage\ lipid}K_{storage\ lipid/water}^{neutral} + f_{water} \quad (2)$$

The total partition coefficients of both species are then combined according to their fractionation in water that depends on the respective pK_a value.

$$K_{fish/water}^{total} = f_{neutral}K_{fish/water}^{neutral} + f_{ion}K_{fish/water}^{ion} \quad (3)$$

Note that this model is purely based on equilibrium partitioning and does not account for any kind of metabolism and kinetics.

1.2.2.2 Predicting $K_{x/water}$ for neutral chemicals with pp-LFERs

The partitioning of neutral chemicals to the different sorption phases/matrices listed in Eq. 2 can be predicted with poly parameter free energy relationships (pp-LFERs) from the literature. In general, pp-LFER models are widely used and accepted as documented by a number of reviews (Abraham et al., 2004; Vitha and Carr, 2006; Endo and Goss, 2014). We used the UFZ-LSER database (Ulrich et al., 2017) in order to get a maximum amount of experimentally determined solute descriptors, L (log of the hexadecane-air partition coefficient), S (dipolarity/polarizability parameter), A (solute H-bond acidity), B (solute H-bond basicity), and V (molar volume). For cases where no experimental solute descriptors were available we used the UFZ-QSPR, available free of charge from the same source. We used these solute descriptors in the following pp-LFERs from the literature to calculate $K_{membrane/water}$(neutral), $K_{storage\ lipid/water}$(neutral), $K_{structural\ proteins/water}$(neutral), and $K_{albumin/water}$(neutral), respectively (Endo and Goss, 2011; Endo et al., 2011; Endo et al., 2012; Geisler et al., 2012):

$$logK_{membrane/water}^{neutral} = -0.93S - 0.18A - 3.75B + 1.73V + 0.49L + 0.53;\ n = 131,\ SE = 0.28,\ T = 37\ °C \quad (4)$$

$$logK_{storage\ lipid/water}^{neutral} = -1.62S - 1.93A - 4.15B + 1.99V + 0.58L + 0.55;\ n = 247,\ SE = 0.20,\ T = 37\ °C \quad (5)$$

$$logK_{structural\ proteins/water}^{neutral} = -0.59S + 0.21A - 3.17B + 2.13V + 0.33L - 0.94;\ n = 46,\ SE = 0.23,\ T = 37\ °C \quad (6)$$

$$logK_{plasma\ proteins/water}^{neutral} = -0.46S + 0.20A - 3.18B + 1.84V + 0.28L + 0.48;\ n = 82,\ SE = 0.41,\ T = 37\ °C \quad (7)$$

In addition to the pp-LFER predictions, the partitioning of neutral chemicals to structural proteins and albumin was also predicted with multi-linear regressions (MLRs) against the sigma moments of the respective chemicals (as outlined in detail below), while the partitioning of neutral chemicals to membrane was also predicted with COSMOmic. Hence, for the neutral chemicals we ended up having two predictive models (based on the same calibration data sets), one using the pp-LFER approach and one using the sigma moments derived from quantum chemical COSMO calculations (see below). We expect that all models have their shortcomings due to the finite calibration set, so we decided to use a consensus model for neutral chemicals,

meaning that $K_{x/water}$ of the respective sorption matrix was finally determined by the average of the two respective model results. For storage lipid we relied solely on the pp-LFER (Eq. 5).

1.2.2.3 Generation of COSMOfiles

Prior to the partitioning calculations with COSMOtherm (including the calculations via COSMOmic or via sigma moments) COSMOfiles of the respective chemicals were generated with quantum mechanical calculations (BP-TZVP level) (Perdew, 1986; Becke, 1988; Schäfer et al., 1994). We used COSMOconfX16 and Turbomole version 7.1 for full energy minimization and conformer generation (Vainio and Johnson, 2007).

1.2.2.4 Predicting $K_{x/water}$ of ionic and neutral chemicals via sigma moments

Analogous to the pp-LFER approach the interaction possibilities of a solute can be described with five descriptors, derived from the COSMOfile of the specific chemical. In fact, it has been demonstrated that the five Abraham solute descriptors for neutral chemicals correlate well with the following five sigma moments Sig0, Sig2, Sig3, Hb_acc3 and Hb_don3 – all of which can be calculated with the commercial software COSMOtherm (Zissimos et al., 2002). Given that a) these five sigma moments are also well-suited for describing partitioning for neutral chemicals via a multi-linear regression (MLR) (Mehler et al., 2002; Zissimos et al., 2002) and b) the partitioning systems of structural protein and plasma protein are not well defined (i.e. no molecular structure of the binding site is known), it is an obvious choice to use the sigma moments to describe the respective partitioning systems with a MLR of the following general form:

$$logK_{x/water} = aSig0 + bSig2 + cSig3 + dHb_{acc3} + eHb_{don3} + const \quad (8)$$

This is done in exact analogy to the calibration of a pp-LFER equation – but unlike the pp-LFERs, sigma moments should per se be able to describe both ionic and neutral chemicals, if we also consider the additional sigma moment Sig1, which describes the charge. A big advantage of sigma moments based MLR's over other QSAR's is, that the sigma moments describe intuitively understandable physicochemical parameters, as outlined in the Appendix A.

1.2.2.5 Sorption to structural (muscle) proteins

For $K_{\text{structural proteins/water}}$ (ion) a tentative pp-LFER had already been set up for monovalent ions by including additional descriptors accounting for the charge (Henneberger et al., 2016b). However, this pp-LFER can only account for the ionic forms of phenols, carboxylic acids, pyridines and amines and is therefore not suited for our screening purpose. Therefore, we modelled $K_{\text{structural proteins/water}}$ via the MLR based on sigma moments as discussed above.

1.2.2.6 Sorption to albumin

The sorption of ions to serum albumin is partly influenced by strong steric effects (Henneberger et al., 2016b), which can only be included in a modelling approach through extensive calibration and calculation effort (Linden et al., 2017). Such a model is not feasible for our screening purpose because a) it requires a very time-consuming and meticulous calculation effort and b) its domain of applicability is rather narrow (Linden et al., 2017). But we can use the existing experimental data for a simplified model (which is expected to have a wider applicability domain while predicting the fitting data set less accurate) that is based on the sigma moments as discussed above. Prior to construction of this sigma-moment based model we excluded those chemicals that are highly influenced by steric effects, which cannot be covered by the sigma moments. Due to our previous 3D-QSAR modelling experience (Linden et al., 2017) we know

that especially anions that have a substitution in direct vicinity to the carboxylic group are strongly influenced by steric effects (they experience a twist of the carboxyl group). Thus, we excluded these anions from the calibration data set (Henneberger et al., 2016), namely 2,6-dichlorobenzoic acid anion, 2-chlorobenzoic acid anion, 2-naphthalenacetic acid anion, 2-naphthoic acid anion, and naphthalene-2-sulphonate anion.

1.2.2.7 Sorption to membrane lipid

$K_{membrane/water}$ (ion) of ionic organic chemicals can be modeled with the COSMOmic application in COSMOtherm (Bittermann et al., 2014) which is currently the most reliable method available for this purpose (Bittermann et al., 2016) and the only prediction method that can be used for screening purposes (Bittermann and Goss, 2017) (in contrary to MD simulations). COSMOmic has been validated with a rather diverse data set, including a few zwitterions and di-cations. For our screening approach, we used exactly the same calculation details as in the original COSMOmic publication: 1401 parametrization of the COSMOtherm software with an offset of 0.32 log units for the prediction of $K_{membrane/water}$ of organic ions, using a pure DMPC membrane (Bittermann et al., 2014).

For neutral chemicals the sorption to membrane lipid, $K_{membrane/water}$ (neutral) was also modelled with COSMOmic (with the same settings as used for ions), and, additionally, with the pp-LFER shown in Eq. 4.

1.2.2.8 Overall Workflow

Once, all predictive models for the required partition coefficients had been set up, we were able to start the screening task. Our overall screening workflow can be summarized as outlined in Fig. 1.

1.2.3 Screening for potentially bioaccumulative chemicals

For our screening for potentially bioaccumulative ions we largely investigated an ECHA data set comprised of more than 70 000 chemicals (personal communication Jane Caley from ECHA). We first filtered the data set for those chemicals with a molecular weight between 100 and 800, having only one pK_a. Chemicals with a pK_a between 3 and 7 were treated as ionizable, i.e. we considered both neutral and anionic species. Here, we relied on the pK_a values given in the ECHA data set, which were predicted with the ChemAxon software package. If the pK_a values were below 3, we only considered the anionic fraction, if the pK_a values were above 11, we only considered the cationic species. Also, we restricted our investigation on chemicals constructed by the atoms H, C, N, S, O, P and halogenates. We further included some chemicals in our screening of known environmental relevance such as perfluorinated chemicals, ionic liquids and quaternary phosphonium cations. If adequate, we predicted the pK_a of these chemicals with JChem for Excel, version 15.10.2600.341 (Copyright 2008-2015 ChemAxon Ltd. https://www.chemaxon.com/) using a SMILES code as input. According to the literature, JChem performs equally well as ACD and the topological method MoK_a on pK_a predictions.

Figure 1: **Workflow for our screening procedure for potentially bioaccumulative chemicals. All models based on MLRs with sigma moments were newly developed in this work.**

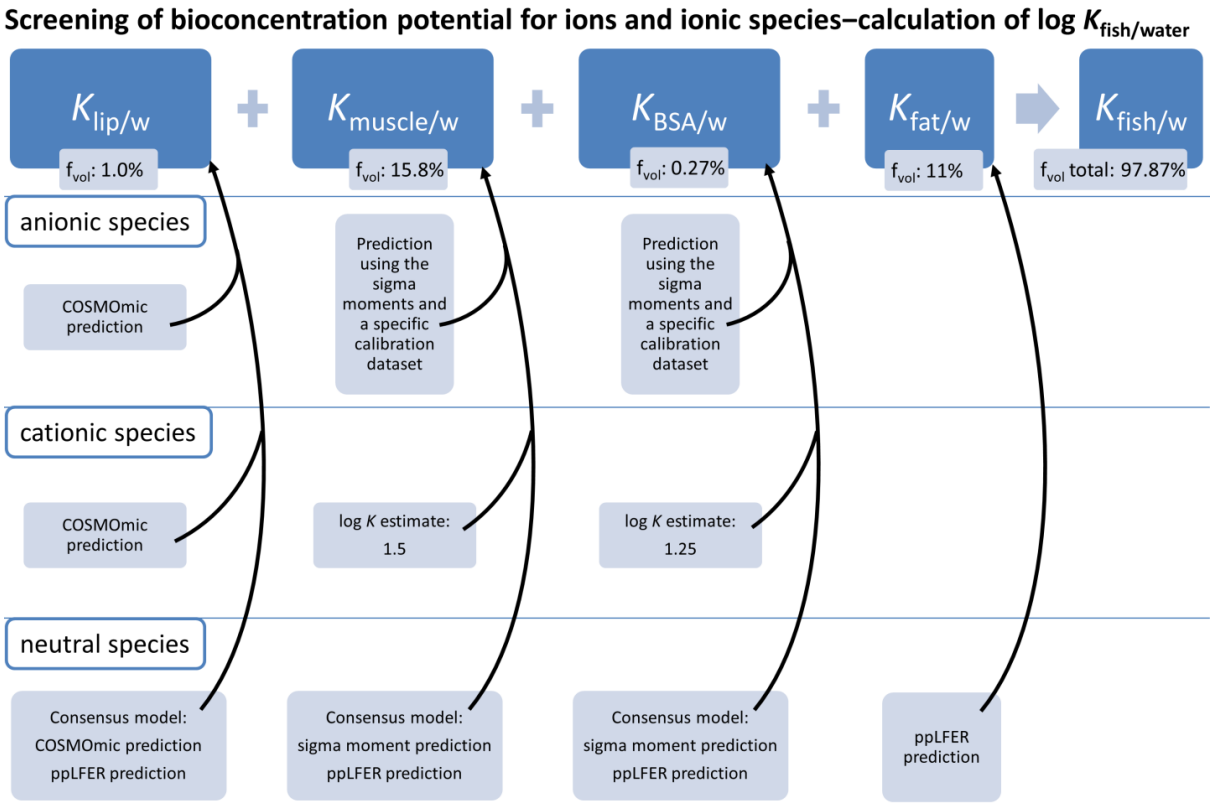

Source: Bittermann et al., 2018.

1.2.4 Results and Discussion

1.2.4.1 Models for the different sorption matrices

1.2.4.1.1 Structural protein

The Abraham solute descriptors are always positive (with the notable exception of perfluorinated chemicals and silicates), which makes the resulting pp-LFER equation instructive and easily understandable (Endo and Goss, 2014). In contrast, Sig1 and Sig3 can also take on negative values. This and the fact that the absolute values of the sigma moments are not normalized prohibit an easy interpretation of MLRs fitted with sigma moments as compared to pp-LFER equations.

In a first attempt, we fitted the experimental data of the 63 neutral chemicals, 41 anions and ten cations altogether with a MLR and obtained already a promising fit (RMSE = 0.46, R^2 = 0.67, Appendix A, Fig. 19). But we also assumed that differently charged chemicals might sorb to different sorption sites within the muscle proteins, so we also fitted the neutral chemicals and anions with MLRs separately. These two fits have less fitting parameters because we excluded those parameters that had a standard deviation larger than the fitted parameters themselves (resulting in three sigma moments and one constant for the anions, and four sigma moments and one constant for neutral chemicals). Additionally, the separate fits had a better statistical outcome (i.e. the RMSE was smaller and R^2 was higher) and are thus our first choice for screening.

$$\log K^{anion}_{structural\ proteins} = 0.072\ (\pm 0.019)\ Hb_{acc3} - 0.034\ (\pm 0.005)\ Sig2 + 0.016\ (\pm 0.002)\ Sig0 + 2.284\ (\pm 0.405);\ R^2 = 0.81,\ RMSE = 0.30,\ F = 53,\ n = 41 \text{ anions} \quad (9)$$

$$\log K^{neutral}_{structural\ proteins} = -0.092\ (\pm 0.051)\ Hb_{don3} - 0.028\ (\pm 0.003)\ Sig3 - 0.024\ (\pm 0.003)\ Sig2 + 0.021\ (\pm 0.002)\ Sig0 - 0.628\ (\pm 0.290);\ R^2 = 0.78,\ RMSE = 0.38,\ F = 52,\ n = 63 \text{ neutral chemicals} \quad (10)$$

Unfortunately, for cationic chemicals, there were only ten data points; we regard this as not enough for a meaningful MLR. Therefore we decided to add the average log $K_{structural\ proteins/water}$ (cation) value of 1.5 for cations for screening purposes as a rough estimate (originating from the ten cations of the data set and their log $K_{albumin/water}$ (cation) range of 0.97 to 2.29).

For neutral chemicals the prediction of $K_{structural\ proteins/water}$ (neutral) is also possible with a pp-LFER equation (Endo et al., 2012). Analogous to the calculation of $K_{membrane/water}$ (neutral) we used a consensus model for the neutral chemicals, averaging the outcomes of Eq.s 6 and 10.

Figure 2: **MLR based on sigma moments for structural protein (chicken muscle), left for anions (3 descriptors + constant), right for neutral chemicals (4 descriptors + constant).**

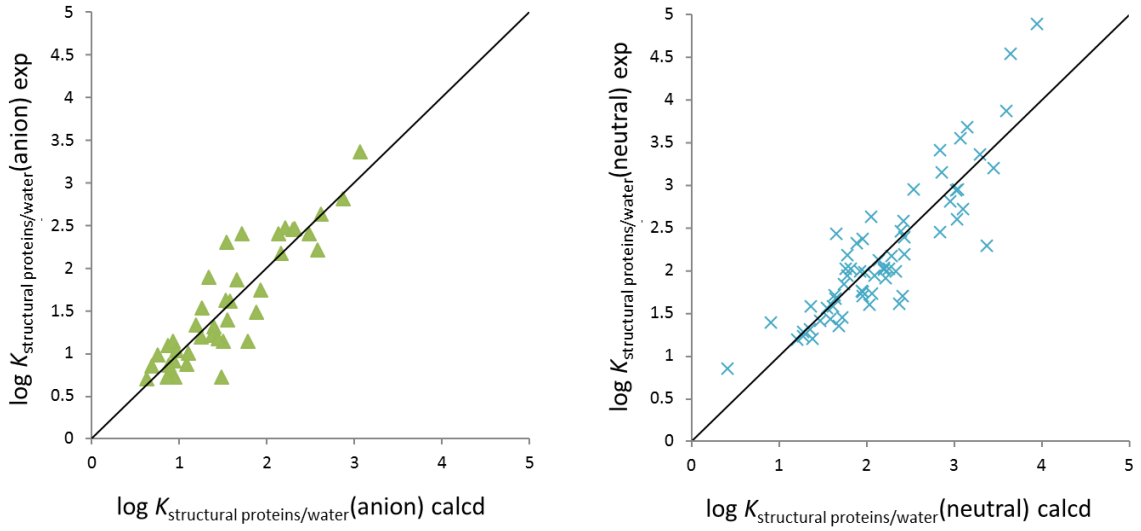

Source: Bittermann et al. 2018.

1.2.4.1.2 Albumin

Analogous to the structural protein, it is plausible to assume that anions and neutral chemicals sorb to different sorption sites within the BSA protein. This can explain the rather poor fit of the data, when the 40 anions and the 83 neutral chemicals are fitted together (Appendix A, Fig. 20). The separated fits of anions and neutral chemicals yield the following system descriptors (again leaving out insignificant descriptors).

$$\log K^{anion}_{plasma\ proteins} = 0.484\ (\pm 0.059)\ Hb_{acc3} - 0.031\ (\pm 0.006)\ Sig3 - 0.049\ (\pm 0.005)\ Sig2 + 0.020\ (\pm 0.002)\ Sig0 + 4.465\ (\pm 0.617);\ R^2 = 0.82,\ RMSE = 0.33,\ F = 39,\ n = 40\ anions \quad (11)$$

Note that this model has to be used with caution for those anionic chemicals that are sterically hindered in vicinity to a carboxyl group, as explained above.

$$\log K^{neutral}_{plasma\ proteins} = -0.257\ (\pm 0.090)\ Hb_{acc3} - 0.010\ (\pm 0.005)\ Sig3 - 0.016\ (\pm 0.004)\ Sig2 + 0.018\ (\pm 0.002)\ Sig0 + 0.225\ (\pm 0.332);\ R^2 = 0.56,\ RMSE = 0.57,\ F = 25,\ n = 83\ neutral\ chemicals \quad (12)$$

Again, we described the partitioning to BSA for neutral chemicals with a consensus model, averaging the results from Eq. 12 and the pp-LFER (Eq. 8).

As before, there are not enough data for cations to establish a MLR, so we used the average log K value of 1.25 (originating from the four cations of the data set and their log $K_{albumin/water}$ (cation) range of 0.97 to 1.58).

Figure 3: MLR based on sigma moments for albumin, left for anions (4 descriptors + constant), right for neutral chemicals (4 descriptors + constant).

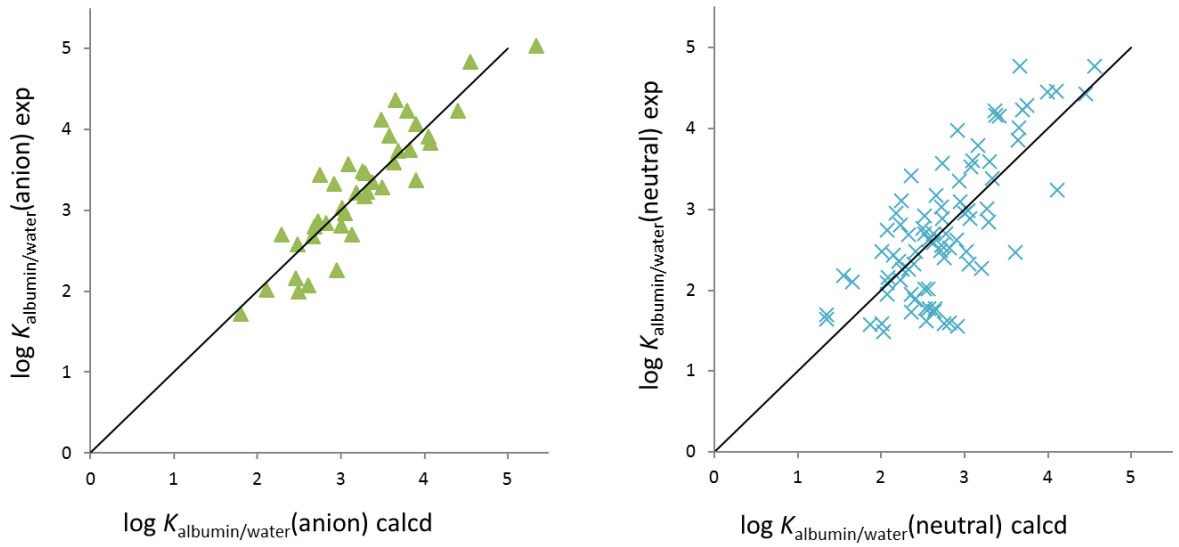

Source: Bittermann et al. 2018.

1.2.4.1.3 Model constraints

In order to facilitate the interpretation of the results and prevent misuse of the model, we repeat the model weaknesses in a bullet point form here:

- It is questionable whether poly- and perfluorinated chemicals are well described with the sigma moment approach, given that van-der-Waals interactions are only depicted via the Sig1 (area). We therefore expect systematic deviations for perfluorinated chemicals, but due to the lack of experimental data this cannot be quantified.
- Unfortunately, also for neutral chemicals there is a lack of experimental data for perfluorinated chemicals. So also the pp-LFER based submodels for neutral chemicals can only be used with great caution for this class of chemicals.
- Sorption of cations to structural proteins and plasma proteins is only roughly estimated by average values due to an insufficient number of calibration data (i.e. the sorption to serum albumin is presumably weak for cations but they sorb stronger to other plasma proteins than albumin which are not included in our screening approach due to the lack of consistent data) (Kremer et al., 1988).
- Complex ions, i.e. ions with several ionizable groups, as well as surfactants were not part of the calibration or validation set of our models and the model performance for these chemicals/species is unknown.
- Chemicals that show a distinct steric effect in their sorption to serum albumin might not be correctly covered by our modelling approach.

1.2.4.2 Screening of potentially bioaccumulative monovalent organic ions

We screened 1839 preselected chemicals for their bioaccumulative potential, 187 (10 %) of them have predicted log $K_{fish/water}$ values larger than 4 (Fig. 4). The molecular weight of these potentially bioaccumulative chemicals ranged between 255 and 756 u thus spanning almost the entire range of the preselected values (see methods).

Log $K_{fish/water}$ correlates reasonably with the molecular surface area as it can be expected (Fig. 5); larger chemicals tend to be more bioaccumulative than smaller ones due to their increased hydrophobicity. For the chemicals that possess a neutral and anionic species at a pH of 7 (acids), the neutral species has generally the higher log $K_{fish/water}$ value compared to the anionic species (Fig. 7). But, we also compared the pH dependent contribution of the two species to $K_{fish/water\ (total)}$ and in most of the cases the anionic species dominated the $K_{fish/water}$ (total) at pH 7 (Fig. 8). The two outliers with a relatively high log $K_{fish/water}$ with a Sig0 of roughly 200 are adamantanes, which are cubic molecules with a relatively small volume.

For the further discussion, we only consider the contribution and the influence of the ionic species on the bioaccumulative potential because this is the most important contribution.

Figure 4: Histogram of calculated log $K_{fish/water}$ according to Eq. 3.

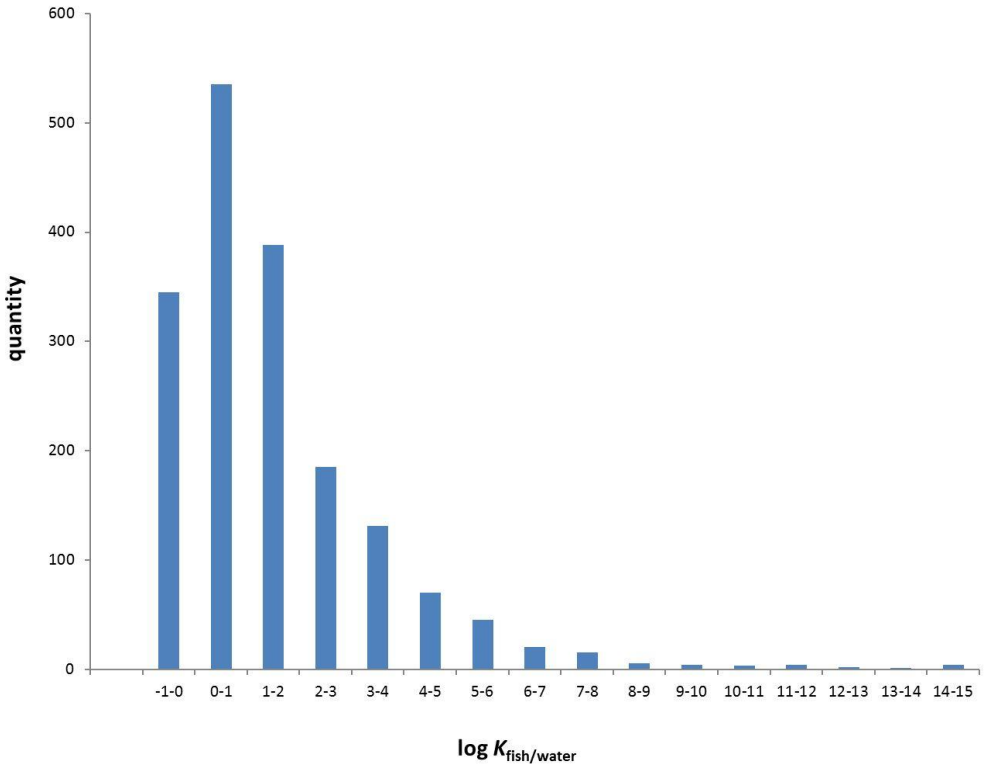

Source: Bittermann et al. 2018.

Figure 5: Calculated log $K_{fish/water}$ against Sig0 (area).

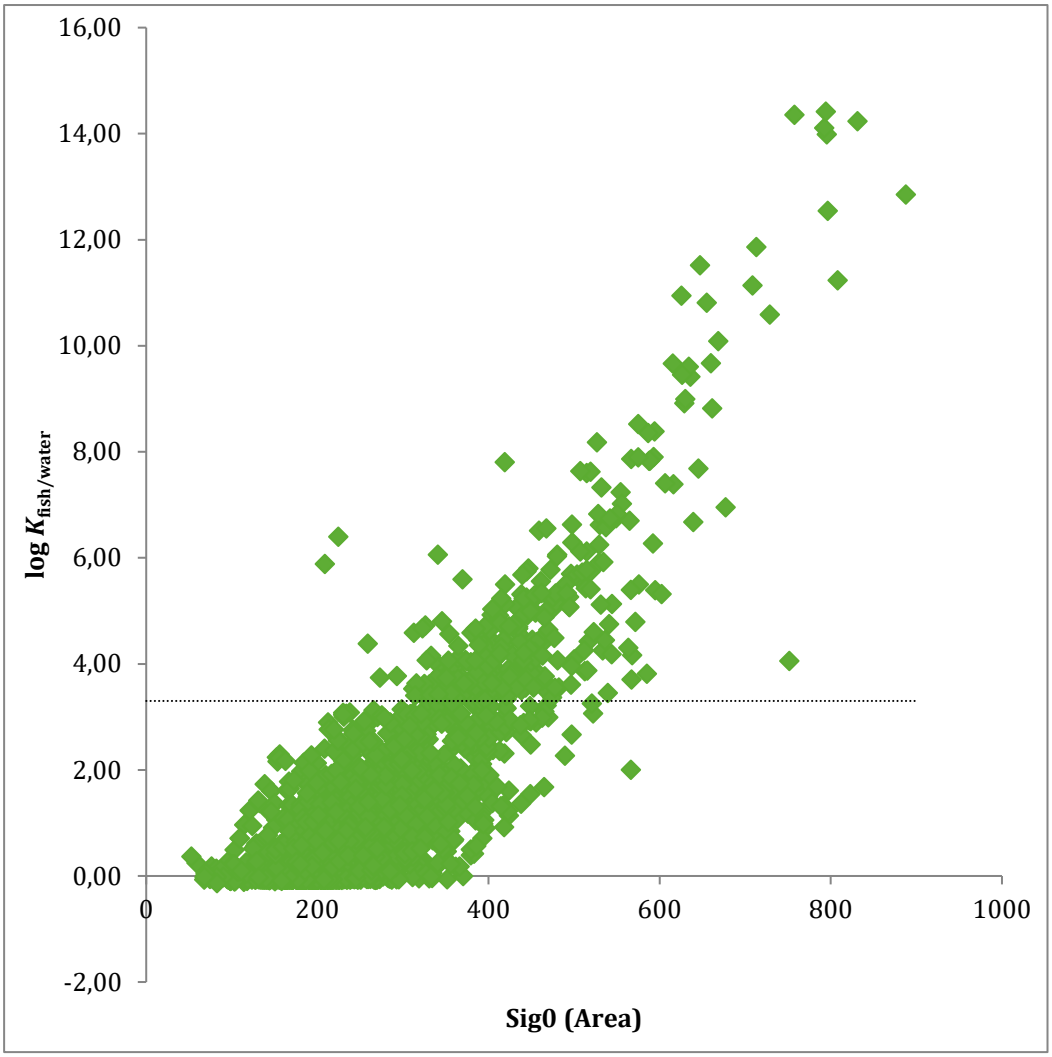

Source: Bittermann et al. 2018.

Analysis of the results indicated the following general trends:

- Aliphatic chemicals tend to be more bioaccumulative than aromatic chemicals (Tab. 1).
- Sorption to albumin is generally dominated by smaller chemicals while bigger molecules tend to sorb stronger to membrane lipids.
- Structural proteins as a dominating sorption matrix (> 60 %) rarely leads to bioconcentration potential (Fig. 6).
- Albumin and membranes dominate the sorption behaviour of bioconcentrating chemicals, membranes especially in the log $K_{fish/water\ (total)}$ range over 9 (Fig. 6).
- Aromatic chemicals preferably sorb to albumin while aliphatic chemicals preferably sorb to membranes (Tab. 1).
- Sorption of S based acids is dominated by plasma proteins while for C based acids sorption can be dominated by both plasma proteins and membranes (Appendix A).
- Sorption to plasma proteins is similar to sorption to structural proteins but higher (Fig. 9).
- Sorption to plasma proteins is considerably different to sorption to membranes but high values correlate (Fig. 10).

Table 1: Overview of screened chemicals. Note that the sum of the sub-groups does not always add up to the total of 1839 chemicals because chemicals fit not always into the shown categories.

			log $K_{fish/water}$ < 4		log $K_{fish/water}$ > 4	
			quantity	%	quantity	%
total		**1839**	**1652**	**89.83**	**187**	**10.17**
aromatic		822	783	95.26	39	4.74
aliphatic		942	794	84.29	148	15.71
S based acid		409	343	83.86	66	16.14
C based acid		606	562	92.74	44	7.26
Sorbing matrix dominated by structural proteins		177	165	93.22	12	6.78
dominated by plasma proteins		408	354	86.76	54	13.24
	S based acid	102	75	73.53	27	26.47
	C based acid	223	207	92.83	16	7.17
	aromatic	250	228	91.20	22	8.80
	aliphatic	158	207	131.01	32	20.25
dominated by membrane lipids		266	171	64.29	95	35.71
	S based acid	34	12	35.29	22	64.71
	C based acid	33	17	51.52	16	48.48
	aromatic	66	59	89.39	7	10.61
	aliphatic	200	112	56.00	88	44.00

Figure 6: **log $K_{fish/water}$ (ionic) against the surface area of the ionic chemical. The color code indicates the dominating sorption matrix that contributes for more than 60 % of the total log K value.**

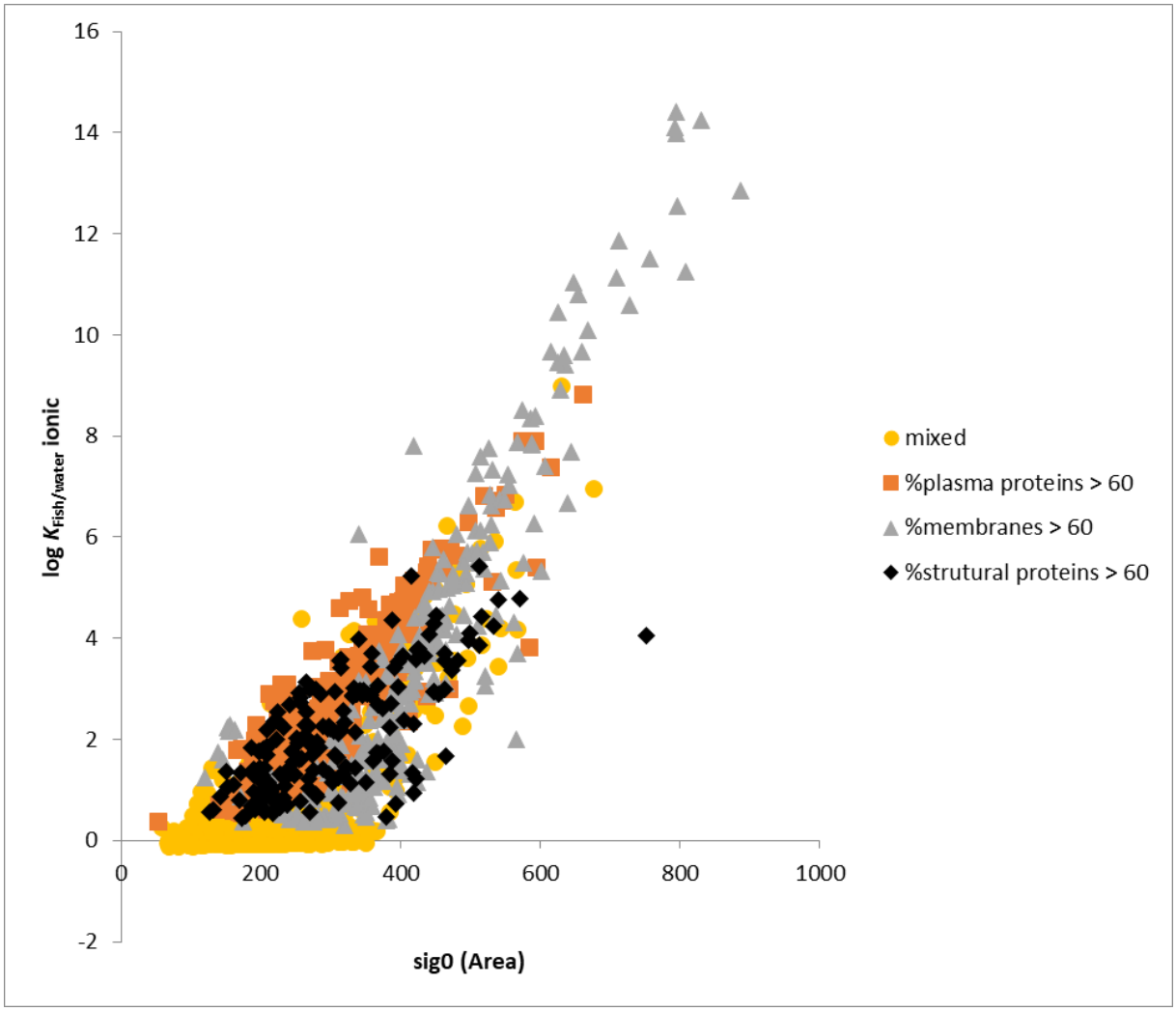

Source: Bittermann et al., 2018.

1.2.4.2.1 Potential Impact of ion trapping mechanism

Here, our assessment was based on the assumption that the exposure pH value is the same as the internal pH of the fish (i.e. pH = 7). If this is not the case then an ion trap effect will occur (Neuwoehner and Escher, 2011). If the pH in the exposure medium is 2 log units smaller (i.e. pH = 5), the BCF increases by a factor 100 for acids with a $pK_a < 5$ due to ion trapping. In a regulatory process this also has to be considered. Many of the chemicals that are not expected to have a BCF potential may still have a substantial bioaccumulation potential in terrestrial organisms. Chemicals that are not volatile (log $K_{oa} > 5$) and that do not metabolize, possess a bioaccumulative potential in terrestrial organisms if their log $K_{organism/water}$ exceeds 1 (Czub and McLachlan, 2004; Armitage and Gobas, 2007; Kelly et al., 2007; Goss et al., 2013). If we take the $K_{fish/water}$ as a proxy for a more general $K_{organism/water}$ for all vertebrates, then a large portion of the ionizable chemicals tested here would be classified as potentially bioaccumulative in air breathing organisms.

For further information on the developing screening tools for the bioaccumulation potential of monovalent organic ions see Appendix A. Note, the content of Chapter 1 was published as Bittermann et al., 2018.

2 Reviewing the screening parameters with existing BCF and BMF values of IOCs

2.1 Introduction

The objectives of the current study were to: (a) review existing literature with respect to dietary bioaccumulation in fish, with reference to OECD guideline 305, and collect biomagnification factor (BMF) data for ionizable substances; (b) identify single- and multi-parameter regressions to predict BMF from molecular descriptors; (c) use regressions to identify candidate ionizable compounds with possibly high dietary bioaccumulation.

This report provides a description of:

- Biomagnification factor (BMF) data collection and screening methodology applied to derive data from published literature.
- Identification and collection of molecular descriptors from software predictions.
- Database of chemicals, molecular descriptors and BMF values from dietary exposure studies.
- Statistical methodology to identify single- and multi-parameter regressions of BMF for strong acids.
- Single-parameter regressions for weak acids and entire data set of ionizable compounds.

2.2 Materials and Methods

2.2.1 Data set definition

A database of BMF values from fish dietary exposure studies was developed by reviewexisting scientific literature and collecting relevant articles published until December 2017. The database was initially developed based on the critical review by Arnot and Quinn (2015), and was completed by including later publications on ionizable compounds. The database compilation focused on BMF measurements from laboratory studies carried out under controlled conditions.

Dietary whole-body BMF data ($g_{food}\ g_{fish}^{-1}$) were first sorted in

steady state BMF (BMF_{SS}),

$$BMF_{SS} = C_{fish}/C_{feed}$$

where C_{fish} ($g\ g_{fish}^{-1}$) and C_{feed} ($g\ g_{food}^{-1}$) denote the chemical concentrations in fish body (wet weight basis) and feed, under the assumption that steady state between uptake and depuration kinetics is reached, and

kinetic BMF (BMF_k),

$$BMF_k = \alpha\ I/k_2$$

where α (-) denotes the chemical absorption efficiency, I ($g_{food}\ g_{fish}^{-1}\ d^{-1}$) the specific fish feeding rate administration, and k_2 the depuration rate (d^{-1}).

Where not explicitly reported, BMF_{ss} and/or BMF_k values were calculated from concentration values measured at the end of the uptake phase, the feeding rate, and estimated α and k_2 values. If possible, BMF_k values were recalculated from α, I and k_2 and compared with reported BMF_k to verify the reliability of presented data. In case the deviation between reported and recalculated BMF_k was significant (≥ 20 %) and not attributable only to numerical approximation of reported α and k_2, recalculated BMF_k values were taken into account for further analysis.

Following a preliminary database compilation, further screening of available data was carried out to select reliable dietary BMF values. Screening was based on quality criteria set by OECD 305 and further extended by Arnot and Quinn (2015), namely: (a) for BMF_{SS}, the assumption of steady state between uptake and depuration kinetics could be verified based on reported time-resolved concentration data or depuration rate (in the latter case, the time to reach 90 % steady state had to be lower than the uptake phase duration; (Martin et al., 2003); (b) fish growth was explicitly accounted in adjusting feeding rate during uptake phase and correctly used to calculate growth-corrected depuration rate (k_{2g}); (c) α had been estimated to be lower than 100 %.

Differently from the recommendations made in OECD TG 305 (OECD, 2012), lipid-normalized BMF values were not considered for the assessment, given that more than half of ionizable chemicals in the database were perfluorinated substances.

2.2.2 Selection of predictors

Molecular descriptors were selected to assess their capability of empirically predicting BMF values for ionizable substances and include: (a) acid dissociation constants (pK_a); (b) molar mass (MM), molar volume (MV) and McGowan's estimation of molar volume (McGV); (c) distribution coefficients K_{ow} (octanol/water), D (octanol/water, pH dependent) and K_{HSA} (human serum albumin-water); (d) solubility (S) at neutral pH; (e) Lipinski''s properties, namely topological polar surface area (TPSA), number of rotable bonds (nRB), number of hydrogen bond donors (nHBD) and acceptors (nHBA) and total number of hydrogen bonds (nHBD+A); (f) volume of distribution (V_d). Predicted values for each descriptor were collected from ACD/Labs by using commercial names or SMILES structures specifying the investigated compounds.

In addition, four additional descriptors estimated using a recently developed approach (Bittermann et al., 2018) were considered, namely the distribution coefficients: (a) between fish and water ($K_{fish/water}$); (b) to muscle protein (K_{MP}); (c) to bovine serum albumin (K_{BSA}); (d) between lipids and water (COSMOmic $K_{lip/water}$).

Based on collected pK_a values, dissociation patterns at typical pH conditions in experiments and fish tissues (2 – 8) were used to subdivide the ionizable compounds into acidic, basic and amphoteric. Furthermore, acidic substances were subdivided into strong acids ($pK_a < 4.0$) and weak acids ($pK_a > 4.0$), and separate regressions were identified for these two groups. If possible, distribution coefficients D were determined at different pH (2.0, 3.0, 7.4, 8.5) representative of specific fish tissues (≤ 3.0: stomach; 7.4: blood; 8.5: intestine; Page et al., 1976).

2.2.3 Statistical analysis

Calculated BMF values and selected molecular descriptors (MM, MV, McGV, K_{ow}, D, K_{HSA}, S, TPSA and V_d) were log-transformed for the identification of regressions. Data treatment and evaluation of single- and multi-parameter regressions were performed using Microsoft Excel® 2010. High quality data, fulfilling all criteria (a) – (c) as defined in section 2.1, were used as calibration data set to identify single- and multi-parameter regressions, while data points not responding to at least one of the criteria were used for validation of identified regressions.

2.2.3.1 Single-parameter regressions

The capability of each molecular descriptor to predict biomagnification in fish was assessed by evaluating single-parameter regressions in the generic form:

$$log\ BMF = a + bX$$

where X denotes the molecular descriptor (log X for log-transformed descriptors). Linear Pearson product-moment and Spearman correlation analysis were used to assess the goodness of single-parameter regressions. Significance levels for a two-tailed test ($p < 0.05$) were used to determine significant correlations.

2.2.3.2 Multi-parameter regressions

The capability of different combinations of molecular descriptors of predicting biomagnification in fish was assessed by evaluating multi-parameter regressions in the generic form:

$$log\ BMF = a + b_1X_1 + \cdots + b_iX_i$$

where X_1, …, X_i denote the molecular descriptors used in the regression (log X_i, for log-transformed descriptors), b_1, …, b_i the respective regression coefficients, and a the intercept of the regression.

A number of criteria were considered to ensure the statistical reliability of tested regressions (Field et al., 2012; Dormann et al., 2013), namely: (a) low correlation ($R < 0.7$, equivalent to R^2 of 50 %) between descriptors in the same regression; (b) significance of identified regression based on F-test ($F < 0.05$); (c) p-values for each descriptor were significant ($p < 0.05$), indicating that the added descriptor could describe ; (d) p-values for the intercept were significant ($p < 0.05$); (e) variance inflation factors (VIF) for each descriptor in a regression were lower than 10. Criteria (a) and (d) were used to verify the collinearity, hence the independence, between descriptors. Criterium (b) was used to verify that the inclusion of a specific descriptor in a regression could provide a significant improvement in describing the output variance.

Based on criterium (a), a number of predictors (log K_{ow}, log D, log K_{HSA}, log MM, log MV, log McGV, log S, nRB) exhibiting high interdependency ($R > 0.7$) based on the collected data set were clustered and separately included in regressions.

2.3 Results and discussion

2.3.1 Data set definition

- Following the review of existing literature, 12 dietary exposure studies providing whole body BMF values for ionizable substances were initially identified. Further screening based on test and data quality criteria lead to the compilation of the final BMF data set for regression identification based on the following studies: Fisk et al. (1998), Martin et al. (2003), Nyholm et al. (2009), Inoue et al. (2012), Lee et al. (2012) and Goeritz et al. (2013). The final data set included 25 dietary BMF values for a total of 21 compounds, of which 1 strong acids: perfluoroalkyl acids (PFOA, perfluorononanoic acid), perfluorinated sulfonic acids (perfluorobutane sulfonic acid, perfluorohexane sulfonic acid, PFOS) perfluoro-phosphonates (C10 PFPA, C6 PFPA, C8 PFPA) and -phosphinates (C6/C6 PFPiA, C6/C8 PFPiA, C8/C8 PFPiA);
- 7 weak acids: isodecanol, isotridecanol, isoundecanol ethoxylate, 2,2,4,6,6-pentamethyl-heptane-4-thiol, 4,4'-methylenebis(2,6-di-tert-butylphenol), 2,4,6-tribromophenol, tris(4-chlorophenyl)methanol;
- 2 bases: Solvent Blue 36, N,N'-di-2-naphthyl-p-phenylenediamine.

A summary of empirical data (BMF_k and BMF_{ss}, α, k_2) describing dietary bioaccumulation of ionizable compounds in fish is presented in Table 2. The summary includes both higher quality data that were used for identification of single- and multi-parameter regressions (n = 25) and lower quality data (n = 14) that were used for validation of identified regressions.

In a number of cases (n = 16), data reported in selected literature studies allowed for the combined determination of BMF_{ss} and BMF_k for the same substance under the same experimental conditions. The comparison of measured BMF_{ss} and BMF_k (Figure 7a) for the higher quality data set, fulfilling all data quality criteria, revealed some deviation between the two factors, especially with increasing biomagnification potential. The same comparison was made for the lower quality data set (Figure 7b), for which the steady state assumption was not verified or BMF_k determination was considered to be biased (e.g. $\alpha > 1$). Not unexpectedly, significant deviation between BMF_k and BMF_{ss} was observed, with BMF_{ss} providing on average for > 35 % underestimation of dietary biomagnification of ionizable substances. This observation further confirms the need of (a) verifying the steady state assumption for dietary bioaccumulation studies; (b) relying on kinetic methods when this verification is not possible. Therefore, further identification of single- and multi-parameter regressions relied solely on measured BMF_k values

Figure 7: Comparison of measured steady state BMF (BMF_{ss}) and kinetic BMF (BMF_k). Each data point represents one determination for the same substance in the same experimental study.

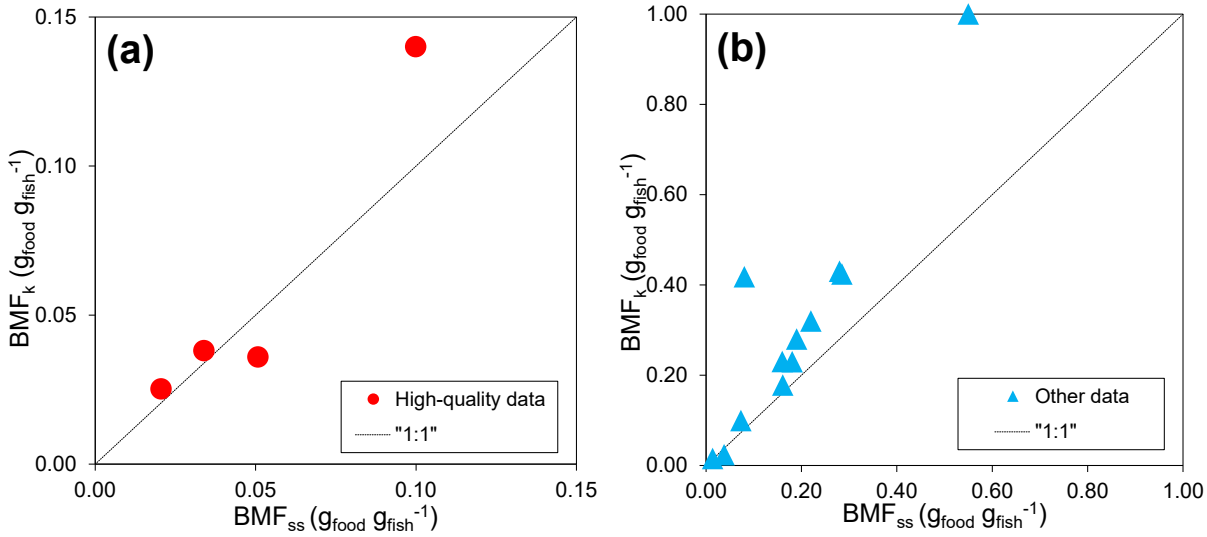

Source: Technical University of Denmark.

Table 2: Overview of ionizable compounds (strong and weak acids, bases), for which dietary biomagnification in fish has been assessed.

In italics, experimental results that were excluded from regression identification due to poor data quality and used for validation purposes.

Chemical	BMF_k ($g_{food}\ g_{fish}^{-1}$)	α (-)	k_2 (d^{-1})	BMF_{ss} ($g_{food}\ g_{fish}^{-1}$)	pK_a	Reference	Rationale for exclusion from calibration data set
Strong acids							
Perfluorooctanoic acid (PFOA)	0.038	0.590	0.230	0.034	0.50	Martin et al. (2003)	
Perfluorooctanoic acid (PFOA)	0.036	0.138	0.097	0.051	0.50	Goeritz et al. (2013)	
Perfluorononanoic acid (PFNA)	0.230	0.522	0.058	0.181*	0.52	Goeritz et al. (2013)	
Perfluorobutane sulfonic acid (PFBS)	0.024	0.0598	0.064	0.038*	-3.57	Goeritz et al. (2013)	
Perfluorohexane sulfonic acid (PFHxS)	0.138	0.700	0.076	0.100	-3.34	Martin et al. (2003)	
Perfluorohexane sulfonic acid (PFHxS)	0.178	0.558	0.079	0.161*	-3.34	Goeritz et al. (2013)	
Perfluooctane sulfonic acid (PFOS)	0.424	0.721	0.043	0.285*	-3.27	Goeritz et al. (2013)	
C6 perfluorophosphonate (C6 PFPA)	0.004	0.053	0.190		0.74, 5.29	Lee et al. (2012)	
C8 perfluorophosphonate (C8 PFPA)	0.007	0.070	0.160		0.78, 5.34	Lee et al. (2012)	
C10 perfluorophosphonate (C10 PFPA)	0.018	0.160	0.130		0.78, 5.35	Lee et al. (2012)	

Chemical	BMF_k ($g_{food}\ g_{fish}^{-1}$)	α (-)	k_2 (d^{-1})	BMF_{ss} ($g_{food}\ g_{fish}^{-1}$)	pK_a	Reference	Rationale for exclusion from calibration data set
C6/C6 perfluorophosphinate (C6/C6 PFPiA)	0.041	0.340	0.130		0.24	Lee et al. (2012)	
C6/C8 perfluorophosphinate (C6/C8 PFPiA)	0.106	0.240	0.030		0.26	Lee et al. (2012)	
C8/C8 perfluorophosphinate (C8/C8 PFPiA)	0.189	0.170	0.020		0.29	Lee et al. (2012)	
Perfluorodecanoic acid (PFDA)	*0.236*	*1.100*	*0.070*	*0.160*	*0.52*	*Martin et al. (2003)*	*α > 1*
Perfluoroundecanoic acid (PFUnA)	*0.280*	*1.100*	*0.061*	*0.190**	*0.52*	*Martin et al. (2003)*	*α > 1*
Perfluorododecanoic acid (PFDoA)	*0.430*	*1.300*	*0.047*	*0.280**	*0.52*	*Martin et al. (2003)*	*α > 1*
Perfluorotetradecanoic acid (PFTeA)	*1.000*	*1.300*	*0.020*	*0.550**	*0.52*	*Martin et al. (2003)*	*α > 1*
Perfluorooctane sulfonic acid (PFOS)	*0.320*	*1.200*	*0.054*	*0.220**	*-3.27*	*Martin et al. (2003)*	*α > 1*
Weak acids							
Tris(4-chlorophenyl) methanol	0.105, 0.133	0.230, 0.330	0.033, 0.036		12.1	Fisk et al. (1998)**	
Isodecanol	0.0025, 0.0031	0.200, 0.340	4.08, 3.30		15.02	EMBSI (2008)***	
Isotridecanol	0.0020, 0.0033	0.120, 0.130	1.78, 1.20		15.20	EMBSI (2008)***	

Chemical	BMF_k ($g_{food}\ g_{fish}^{-1}$)	α (-)	k_2 (d^{-1})	BMF_{ss} ($g_{food}\ g_{fish}^{-1}$)	pK_a	Reference	Rationale for exclusion from calibration data set
Isoundecanol ethoxylate	0.0020	0.230	3.47		14.36	EMBSI (2008)***	
2,4,6-Tribromophenol	0.017	0.450	0.540		6.34	Nyholm et al. (2009)	
2,2,4,6,6-pentamethylheptane-4-thiol	0.01		0.317		11.34	ECHA (2009)***	
4,4'-methylenebis(2,6-di-*tert*-butylphenol)	0.418	0.336	0.024	0.080*	12.03, 12.71	Inoue et al. (2012)	
Pigment Orange 73	*0.015*	*1.250*	*2.46*	*0.014*	*8.90, 13.15*	*ECHA (2012)****	*α > 1*
Pentachlorophenol	*0.224*	*0.943*	*0.253*		*4.68*	*Xiao et al. (2013)*	*Single instantaneous feeding; Depuration rate extrapolated from previous water exposure studies and software predictions*
Bases							
Solvent Blue 36	0.099	0.564	0.170	0.073*	-0.07, 6.13	Inoue et al. (2012)	
N,N'-di-2-naphthyl-*p*-phenylenediamine	0.025	0.190	0.226	0.021	0.30, 3.10	Inoue et al. (2012)	
Azithromycin				*0.016–0.026*	*8.16, 8.59*	*Fairgrieve et al. (2005)*	*Assumption of steady state at the end of uptake phase cannot be verified*
Erythromycin				*0.0012–0.0018*	*8.16*	*Fairgrieve et al. (2005)*	*Assumption of steady state at the end of uptake phase cannot be verified*

Chemical	BMF_k ($g_{food}\ g_{fish}^{-1}$)	α (-)	k_2 (d^{-1})	BMF_{ss} ($g_{food}\ g_{fish}^{-1}$)	pK_a	Reference	Rationale for exclusion from calibration data set
Oxazepam				*0.08*	*1.17*	*Heynen et al. (2016)*	*Assumption of steady state at the end of uptake phase cannot be verified*

*Steady state assumption not verified, time to reach 90 % steady state = $t_{ss} = \ln(0.1)/-k_2$ > uptake phase duration.

**Revised BMF_k data presented in Arnot and Quinn (2015).

***Study description, test and data treatment quality and empirical data presented by Arnot and Quinn (2015).

2.3.2 Strong acids

All compounds identified here as strong acids were perfluorinated compounds (perfluoroalkyl substances, perfluorosulfonates, -phosphonates and -phosphinates), of which several were estimated to be permanently ionized at the pH range under consideration (Table 2).

A preliminary assessment of factors influencing the biomagnification of these substances revealed a strong, positive and consistent relationship between log BMF and the number of perfluorinated carbon atoms for each sub-category (Figure 8).

Figure 8: Dietary biomagnification factors (log BMF) as a function of the number of perfluorinated carbon atoms for different categories of perfluorinated substances: perfluoroalkyl carboxylic acids (PFCAs, red), perfluorinated sulfonic acids (PFSAs, blue).

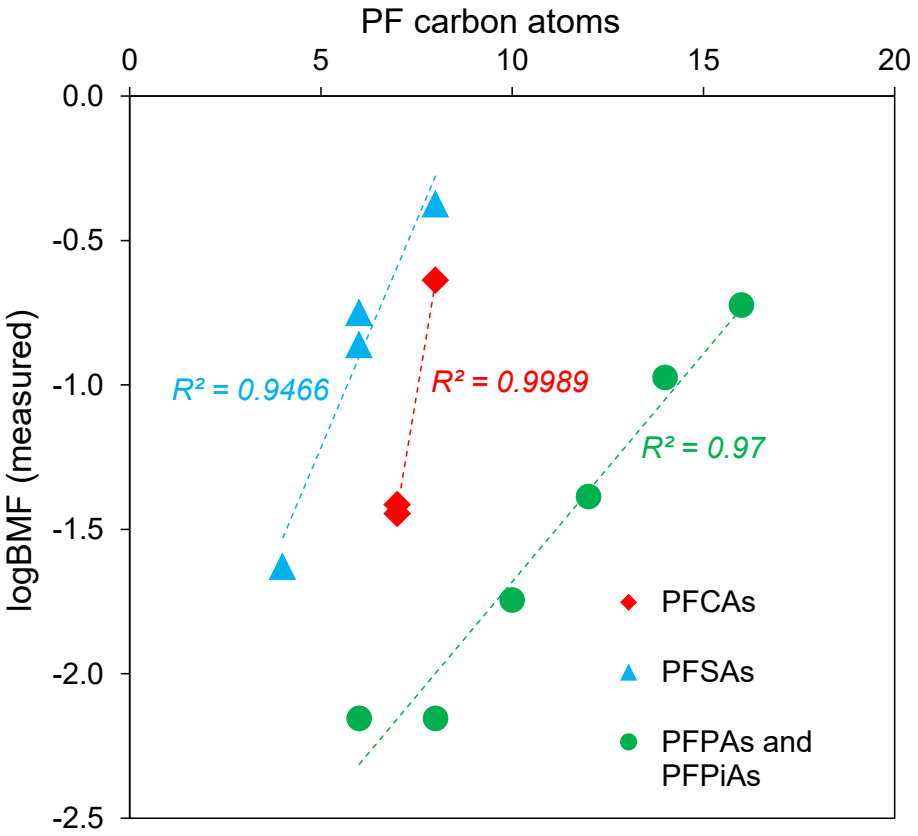

Source: Technical University of Denmark.

2.3.2.1 Single-parameter regressions

Correlations between log BMF and each separate molecular descriptor were evaluated using Pearson and Spearman analysis. An overview of the results of the correlation analysis is provided in Table 3. A significant correlation based on both Pearson and Spearman analysis was found only for nHBD, with a log BMF being negatively influenced by the number of hydrogen bond donors. No distribution descriptor was found to be a significant predictor of dietary biomagnification, with the exception of log $K_{fish/water}$ (only Spearman). A positive, but not significant correlation was also found with log K_{HSA}, possibly as a result of the influence of sorption to proteins on the biomagnification of perfluorinated substances (Ng and Hungerbühler, 2013).

Table 3: Results of Pearson and Spearman correlation between log BMF (n = 10) and selected descriptors for strong acids.

Asterisks (*) indicate significant correlation (two-tailed test, $p < 0.05$).

Molecular descriptor	Pearson R	Spearman R
log $K_{fish/water}$	0.515	0.645 (*)
log K_{HSA}	0.456	0.523
log D (pH = 8.5)	0.350	0.408
log D (pH = 7.4)	0.335	0.408
nRB	0.267	0.275
log K_{ow}	0.259	0.253
log MV	0.253	0.171
log MM	0.246	0.325
log McGV	0.211	0.171
log K_{MP}	0.206	0.421
COSMOmic log $K_{lip/water}$	0.161	-0.011
log K_{BSA}	0.093	0.226
log D (pH = 3)	0.073	0.187
log D (pH = 2)	0.021	0.187
log S	-0.224	-0.165
nHBA	-0.266	-0.289
log V_d	-0.271	-0.209
log TPSA	-0.303	-0.470
nHBD+A	-0.573 (*)	-0.517
nHBD	-0.772 (*)	-0.732 (*)

Figure 9 presents plots of the best correlations between log BMF and single molecular descriptors, i.e. nHBD (a), log K_{HSA} (b) and log $K_{fish/water}$ (c-d). An overall reduction of dietary biomagnification is clearly observed with an increase of the number of hydrogen bond donors from 1 to 2 (Figure 9a). Biomagnification of strong acids is also shown to increase with log K_{HSA} and log $K_{fish/water}$ (Figure 9b-c). Notably, a major improvement in the correlation with log $K_{fish/water}$ is shown when excluding PFPiAs (with estimated log $K_{fish/water} > 6$), with possible implications on the applicability range of this descriptor.

Figure 9: **Correlation between dietary biomagnification factors (log BMF) of strong acids and (a) number of H-bond donors (nHBD); (b) log K_{HSA}; (c-d) log $K_{fish/water}$ with (c) and without (d) considering PFPiAs in the evaluation.**

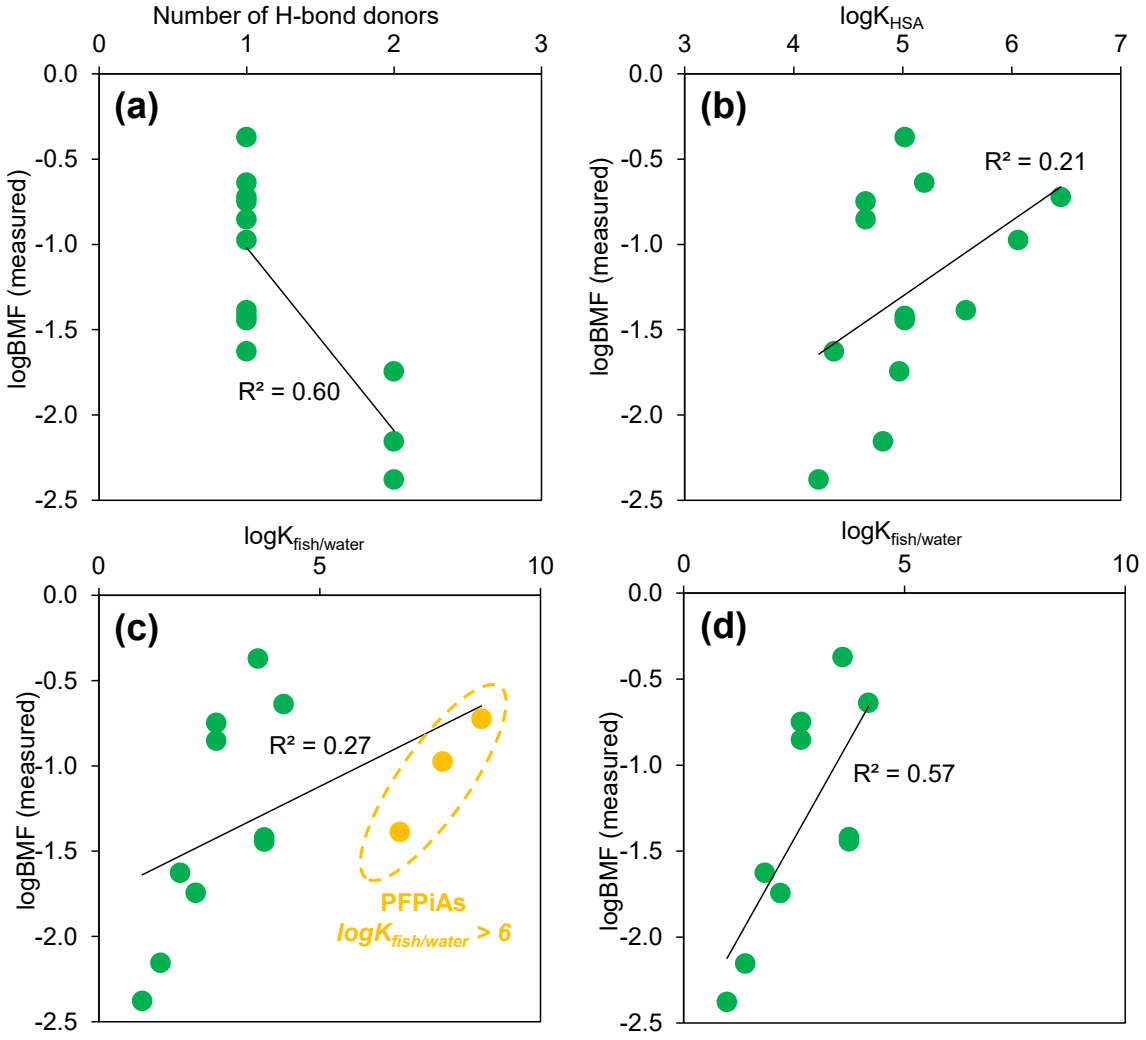

Source: Technical University of Denmark.

When considering correlation significance, it is clear that single-parameter regressions are not sufficient to predict BMF of strong acids. Therefore, multi-parameter regressions between log BMF and combinations of molecular descriptors were investigated.

2.3.2.2 Multi-parameter regressions

Multi-parameter regressions describing log BMF as a function of a combination of molecular descriptors were identified based on the calibration data set (high quality data). Considering the size of the data set, only 2- and 3-parameter regressions were investigated.

A further assessment of the molecular descriptors for the targeted compounds revealed strong intercorrelation ($R > 0.7$) among distribution coefficients (log K_{ow}, log D, log K_{HSA}, log $K_{fish/water}$, COSMOmic log $K_{lip/water}$) and other hydrophobicity (log S, log MM, log MV, log McGV) and bioavailability (nRB) descriptors. Therefore, clustering of these descriptors was considered, and each combination of tested parameters included only one of these descriptors at a time.

An overview of identified 2- and 3-parameter regressions, ranked based on adjusted R^2 and with additional information on the fulfilment of statistical criteria, is given inTable 4. A comparison

with predictive capability of single-parameter regressions revealed that no improvement was shown by the inclusion of one additional parameter, as further highlighted by p-values of regression coefficients. Nevertheless, the two best regressions (with log MM-nHBD and log MV-nHBD) exhibited rather good capability of predicting the validation data set.

A major improvement in the prediction of log BMF of strong acids was found for 3-parameter regressions, with adjusted R^2 up to 0.89 (Table 4). Both two best regressions included one distribution descriptor (log $K_{fish/water}$ or log D (pH = 3)) and a combination of two other descriptors (nHBA-logT PSA or nHBD-nHBA).

Table 4: Summary of multi-parameter regressions between log BMF and selected descriptors for strong acids, with respective goodness of fit to calibration data set (adjusted R^2) and validation data set (validation R^2) and fulfilment of criteria for regression identification.

Molecular descriptors	Adjusted R^2	Intercorrelation R < 0.7	F-test significance (F < 0.05)	Regression coeff. p < 0.05	VIF < 10	Validation R^2
1-parameter						
nHBD	0.596					/
log $K_{fish/water}$	0.270					
2-parameters						
log MM, nHBD	0.579	Yes	Yes	No	Yes	0.780
log MV, nHBD	0.573	Yes	Yes	No	Yes	0.751
log V_d, nHBD	0.564	Yes	Yes	No	Yes	0.036
log K_{HSA}, nHBD	0.529	No	Yes	No	Yes	
log K_{HSA}, log S	0.483	No	Yes	Yes	No	
log K_{HSA}, log K_{ow}	0.474	No	Yes	Yes	No	
3-parameters						
log $K_{fish/water}$, nHBA, log TPSA	0.888	No	Yes	Yes	No	0.981
log D(pH = 3), nHBD, nHBA	0.763	No	Yes	Yes	No	0.647
log V_d, nHBD, nHBA	0.696	Yes	Yes	No	Yes	/
log K_{HSA}, log K_{ow}, P	0.684	No	Yes	Yes	No	
log K_{HSA}, nHBD, nHBA	0.679	No	Yes	No	No	
log D (pH = 3), log V_d, nHBD	0.610	Yes	Yes	No	Yes	/
log K_{HSA}, nRB, nHBA	0.563	No	Yes	Yes	No	

The 3-parameter regression with the highest predictive capability is summarized by the equation:

$$log\ BMF = 16.22\ (\pm 2.45) + 0.54\ (\pm 0.06) log\ K_{fish/water} + 5.24\ (\pm 0.63)\ nHBA - 19.07\ (\pm 2.36) log\ TPSA$$

where numbers in parenthesis indicate the estimated standard errors of each regression coefficient. The small relative error (≤ 15 %) provides a first indication of the goodness of this regression, as further confirmed by significance of F tests (F < 0.0001) and of p-values of regression coefficients (p < 0.0001). Nevertheless, the high intercorrelation of nHBA with log $K_{fish/water}$ (R = -0.77) and log TPSA (R = 0.93) challenges further evaluation of the statistical reliability of the above regression.

Figure 10 presents a comparison of measured log BMF and predicted log BMF using the 3-parameter regression above for the calibration data set (a) and the validation data set (b). As also shown in Table 4, the regression provides the best description (R^2 > 0.90) of both data sets, although with major deviation from the 1:1 line for the validation data set.

Figure 10: Comparison of measured and predicted log BMF with the 3-parameter regression with log $K_{fish/water}$, nHBA and log TPSA for (a) calibration data set; (b) validation data set.

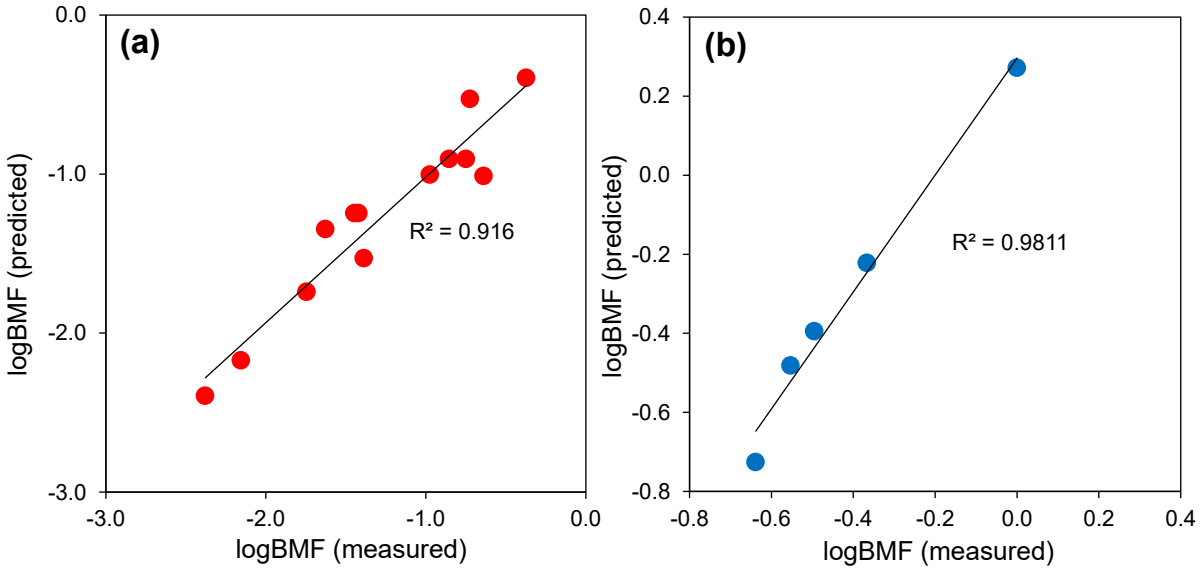

Source: Technical University of Denmark.

2.3.3 Weak acids

2.3.3.1 Single-parameter regressions

Table 5 presents results of the Pearson and Spearman correlation analysis for molecular descriptors in single-parameter log BMF regressions for weak acids. Mechanistic partitioning descriptors were not included in this correlation analysis due to the limited number of available data (n = 2). Differently from strong acids, a high correlation was shown for partitioning descriptors (log K_{HSA}, log K_{ow}, log D) and other hydrophobicity descriptors (i.e. solubility, molar mass). For these descriptors, significant correlation was confirmed by both Pearson and Spearman analysis.

These results are in agreement with previous observations for neutral substances. Accordingly, only 2,4,6-Tribromophenol exhibits relevant ionization (> 90 % at pH ≥ 7) and can be therefore considered as truly ionizable in the considered pH range.

Table 5: Results of Pearson and Spearman correlation between log BMF (n = 10) and selected descriptors for weak acids.

Asterisks (*) indicate significant correlation (two-tailed test, $p < 0.05$).

Molecular descriptor	Pearson R	Spearman R
log K_{HSA}	0.947 (*)	0.911 (*)
log K_{ow}	0.870 (*)	0.850 (*)
log D (pH = 2)	0.870 (*)	0.850 (*)
log D (pH = 3)	0.870 (*)	0.850 (*)
log MM	0.827 (*)	0.829 (*)
log D (pH = 7.4)	0.801 (*)	0.679 (*)
log D (pH = 8.5)	0.725 (*)	0.679 (*)
log V_d	0.682 (*)	0.679 (*)
log McGV	0.595	0.373
log MV	0.448	0.373
nHBD	0.431	0.311
log TPSA	0.122	0.052
nHBD+A	0.085	-0.022
nHBA	-0.084	-0.022
nRB	-0.478	-0.532
log S	-0.956 (*)	-0.850 (*)

2.3.4 All ionizable compounds

2.3.4.1 Single-parameter regressions

Table 6 presents results of the Pearson and Spearman correlation analysis for molecular descriptors in single-parameter log BMF regressions for the entire set of ionizable substances (n = 25). Significant correlations based on both Pearson and Spearman analysis were shown only for four parameters, namely log K_{HSA}, log MM and log $K_{fish/water}$ (positive) and log S (negative). The best distribution descriptor was log K_{HSA}, indicating that partitioning to proteins plays a major role in the biomagnification in fish. Nevertheless, this finding should be evaluated under the consideration that 23 out of 25 observations in the data set referred to acidic substances.

Table 6: Results of Pearson and Spearman correlation between log BMF (n = 25) and selected descriptors for ionizable compounds.

Asterisks (*) indicate significant correlation (two-tailed test, $p < 0.05$).

Molecular descriptor	Pearson R	Spearman R
log K_{HSA}	0.769 (*)	0.746 (*)
log MM	0.643 (*)	0.671 (*)
log $K_{fish/water}$	0.564 (*)	0.755 (*)
log K_{MP}	0.438	0.660 (*)
log MV	0.388	0.362
log K_{BSA}	0.322	0.526
log TPSA	0.322	0.225
logK_{ow}	0.316	0.308
log McGV	0.299	0.200
COSMOmic log $K_{lip/water}$	0.224	0.061
nHBA	0.205	0.221
nHBD+A	0.171	0.174
log D (pH = 3)	0.045	0.214
log D (pH = 2)	0.045	0.257
nHBD	0.044	0.011
log D(pH=8.5)	0.028	0.065
logD (pH = 7.4)	0.021	0.060
nRB	-0.028	0.012
log V_d	-0.181	-0.213
log S	-0.554 (*)	-0.535 (*)

2.4 Conclusions

- A database of biomagnification factors (BMF) measured in fish as part of controlled laboratory-scale dietary exposure studies was compiled for ionizable compounds. In total, 39 data entries for 29 ionizable compounds (15 strong acids, $pK_a < 4$; 9 weak acids, $pK_a > 4$; 5 bases) were available. The database was further screened and a data set of high quality BMF data (n = 25) was compiled and further used for regression identification.
- Molecular descriptors (distribution coefficients, molar mass and volume, Lipinski's properties) were evaluated for their capability of predicting dietary biomagnification of ionizable compounds. Empirical single- and multi-parameter regressions were assessed for different sub-categories of ionizable compounds:
- Strong acids: BMF were found to be significantly correlated only to the number of hydrogen bond donors (nHBD) and the fish-water partitioning coefficient (log $K_{fish/water}$). A 3-parameter regression, with log BMF as a function of log $K_{fish/water}$, nHBA and log TPSA, successfully predicted dietary biomagnification ($R^2 = 0.89$) and could be validated against additional BMF measurements.
- Weak acids: highest correlation (|Pearson R| > 0.90) was found with log K_{HSA} (positive) and log S (negative). Other commonly used distribution coefficients (log K_{ow}, log D) were good BMF predictors, indicating hydrophobicity as a relevant driver for biomagnification in fish.

3 Biomagnification studies with IOCs

3.1 Methods

3.1.1 Preparation of the experimental diets for pre and main study

For preparation of enriched test feed for the preliminary study commercially available fish feed pellets (Inicio Plus® BioMar, Denmark) with a size of 2 mm were spiked according to the method described by Goeritz et al. (2013). Feed batches prepared for the pre-study were spiked with one test substance each. The spiking procedure applied for the cationic substance TMOA is described below. The same spiking procedure was applied for all test substances unless otherwise stated. Specific informations related to the preparation of the test diets are summarized in Table 7.

An application solution of TMOA was prepared taking the purity and the reduced molecular weight of the ion into account (see Table 8). Therefore, 23.5 mg TMOA were dissolved in 20 mL methanol, corresponding to a concentration of 1 mg/mL. For spiking, 100 g fish feed were placed in a 2 L pear-shaped flask connected to a rotary evaporator equipped with a stainless steel capillary to apply the test solution via a solvent-inlet tube to the pellets under vacuum. 3.44 mL application solution were applied to the feed particles by spray application, while the feed was thoroughly mixed by rotation to ensure a homogenous distribution of the test item on the pellets. During the spiking procedure, a low pressure of approximately 700 mbar was applied. After administration of the application solution 0.5 – 1.0 mL pure solvent was utilized to rinse the beaker of the application solution which was also applied via the spray-apparatus to ensure transfer of the whole amount of test item. Afterwards, a vacuum of 350 mbar was set to evaporate the solvent in the flask. In order to remove potential solvent residues, spiked pellets were dispersed in an aluminium tray and left in the fume hood overnight.

Subsequently, spiked feed pellets were coated with sodium alginate and calcium chloride to avoid test item loss through leaching into test water. For this, a 2 % sodium alginate solution (w/w) was prepared by dissolving 3 g of sodium alginate in 150 g distilled ultra-pure water (UHQ). The suspension was heated to 100 °C and stirred until a homogenous viscous solution was obtained. 3.90 g of this solution were applied in a heated 1 L glass bottle and after even distribution of the sodium alginate solution on the inner walls of the bottle by gentle shaking, 100 g of the spiked feed pellets were added. The bottle was shaken thoroughly until no feed pellets were sticking to the wall anymore. In a last step, 0.89 g calcium chloride per 100 g feed were added and the bottle was mixed until no visual inhomogeneity could be observed.

Table 7: Overview of substance-specific data and amounts for preparation of application solution for test diets in preliminary study.

Each feed batch (100 g) was spiked with one test substance.

	$MW_{molecule}$ [g/mol]	MW_{ion} [g/mol]	Purity [%]	Mass [mg]	Solvent (V_T = 20 mL)	Conc. of AS [mg/mL]	V_u [mL]
TMOA	348	313	95.0	23.5	Methanol	1.000	3.44
TBP	339	259	98.0	26.1	Acetone	0.976	3.53
Benzotriazol	339	---	95.0	20.4	Acetone	0.969	3.56
Tecloftalam	448	447	95.0	19.5	Acetone	0.924	3.74
Pentachlorophenol	266	---	97.0	20.0	Acetone	0.968	3.56
MEE-Phosphonate	306	---	95.0	28.8	Acetone	1.130	3.05

AS = application solution, V_T = total volume, V_u = used volume for application, MW = molecular weight.

During the main study, ionic compounds were applied in pairs. The co-exposure of two test items reduced the number of separate studies and thus the required number of fish. The experimental diets were prepared and treated the same way as described above. Here, 250 g feed with a pellet size of 1.1 mm were prepared by solvent spiking. The application solution volumes of the ion pairs (TBP and TMOA, Benzotriazol and Tecloftalam, Pentachlorophenol and MEE-Phosphonate) were mixed beforehand and applied concurrently (Table 8). For alginate coating, two batches of 100 g and one batch of 50 g feed were handled. The amount of sodium alginate and calcium chloride dihydrate applied to each batch were adjusted according to the protocol.

The control diet used during the uptake phase for feeding control fish, was prepared in exactly the same way, but without the IOCs in the spiking solvent.

Homogeneity and content IOCs in the spiked test diets were analysed directly after preparation in five replicates.

Table 8: Overview of substance-specific data and amounts for preparation of application solution for test diets in main study.

Each feed batch (200 g) was spiked with two test substances.

	$MW_{molecule}$ [g/mol]	MW_{ion} [g/mol]	Purity [%]	Mass [mg]	Solvent (V_T = 20 mL)	Conc. of AS [mg/mL]	V_u of AS [mL]
TMOA	348	313	95.0	36.9	Methanol	1.57	4.38
TBP	339	259	98.0	36.1	Acetone	1.35	5.10
Benzotriazol	339	---	95.0	28.9	Acetone	1.37	5.03
Tecloftalam	448	447	95.0	26.9	Acetone	1.28	5.40
Pentachlorophenol	266	---	97.0	26.9	Acetone	1.30	5.29
MEE-Phosphonate	306	---	95.0	30.3	Acetone	1.44	4.80

AS = application solution, V_T = total volume, V_u = used volume for application, MW = molecular weight.

3.1.2 Design of biomagnification studies with ionic test substances

The biomagnification studies were carried out following the principles of OECD TG 305 and were performed in accordance with the German animal welfare act under the Landesamt für Naturschutz, Umwelt und Verbraucherschutz Nordrhein-Westfalen, Germany (permit 81-02.04.2018.A023).

Juvenile rainbow trout were purchased from Fischzucht Störk (Bad Saulgau, Germany) and maintained in a flow-through system in 200 to 250 L tanks filled with copper ion reduced tap water. Animals were kept under constant aeration at 14 ± 2 °C and under a 16:8 light-dark cycle until the start of the study for acclimatization purposes. The fish were fed with a commercially available food for fish breeding (Inicio Plus®, BioMar, Denmark).

A preliminary test was carried out before the main study to test the palatability and potential toxic effects of each experimental diet spiked with one of the six test substances. Each substance was tested separately. Thus, six treatments and one control group, each consisting of 8 fishes, were tested during an uptake phase lasting 14 days. The feeding rate was increased from 2.0 to 2.5 % in the second week of the uptake phase. Experimental conditions during the pre-test were similar to the main study as described below. A single sampling was carried out at the end of the uptake phase. Two of the eight animals were shock frozen in whole and stored at -20 °C until chemical analysis. The other six animals were dissected and liver, GIT, filet and carcass of three animals were pooled to one replicate. The two pooled replicates per compartment were shock frozen and stored at -20 °C until analysis.

For the main study rainbow trout with an average weight of 5.42 ± 1.14 g (n = 160) were fed per treatment one of three test diets enriched with two different ionic organic compounds, each. The first experimental diet was enriched with two cations (TBP and TMOA). The further diets were spiked with two groups of two anions each, consisting of Benzotriazol and Tecloftalam and Pentachlorophenol and MEE-Phosphonate, respectively. The resulting treatments and one control group (each 40 animals) were tested simultaneously. 80 L glass tanks were used as experimental tanks filled with 75 L of copper reduced tap water with a flow rate of 15.6 L/h resulting in a 5-fold water exchange per day.

The condition of the test animals was examined with the aid of score sheets at least once per day. The water temperature, oxygen content (saturation in % and mg/L) and pH were checked every second day. Concentrations of nitrite, nitrate and ammonia were determined on day one, day seven and at the end of the tests.

The uptake phase of 14 days was followed by a depuration phase lasting 14 days. All animals were fed the non-spiked feed during the depuration phase. A feeding rate equivalent to 2 % of the body wet weight of the test animals per day was applied in compliance with the recommendation given by the feed manufacturer. Feces which may result in uptake via aqueous exposure, feces were removed at least three times per day to reduce the risk of a secondary exposure pathway via the water due to the release of freely dissolved test substance from feed residues and fecal matter.

In the main study five animals of each group were sampled randomized on day 7 and day 14 of the uptake phase and after 10 h, 24 h, 2 days, 3 days, 7 days and 14 days of depuration. Samplings were done before feeding of the animals. After each sampling the remaining biomass of each group was determined by weighing the complete group of fishes to adjust the daily feed ration.

The sampled animals were anesthetized in a water bath containing 150 mg/L MS 222 (Sigma Aldrich) and euthanized by a deep cut through the neck. Animals were weighed, blotted and the

compartments (liver, gastrointestinal tract (GIT) and carcass) were dissected. In addition, the GIT was rinsed with ultra-pure water to remove remaining feed or feces presumably containing the test items. After weighing all compartments, the samples were shock frozen and stored at -20 °C until further sample processing for chemical analysis.

The experimental diet was analysed before and after the exposure phase to verify the stability of the test items during the uptake phase.

3.1.3 Chemical analysis of fish feed and fish samples

Chemical analysis of the test substances was performed by liquid chromatography with coupled mass spectrometry (LC-MS/MS). Concentrations of the test substances were calculated based on the recorded sample weight. All feed and fish samples collected during the pre and main study, were processed by solid liquid extraction. The extracts were measured with LC-MS/MS after appropriate dilution. All instrumental and chromatographical settings are described in Appendix B. Analyses of samples collected during the main study were carried out in the multiple reaction monitoring (MRM) mode. During the preliminary study Benzotriazol and Pentachlorophenol were analysed with single ion recording mode (SIM) while the other ions were analysed with MRM. Quantification of analytes was performed externally using a matrix-matched-calibration, as no isotope-labelled analytical standards were available. Here, the dilution of the sample extracts is equal to the amount of matrix contained in the calibration solutions. All sample measurements were performed simultaneously with a calibration allowing to compensate for potential matrix effects.

3.1.3.1 Determination of content, homogeneity and stability of IOCs in experimental diets

For the determination of substance concentrations in fish feed approximately 1 g feed was weighed into a 15 mL PP-vial. 4 mL MeOH were added, homogenized for 30 seconds and then treated in an ultrasonic bath for 10 min. The samples were centrifuged for 5 min at 5 000 rpm and the supernatants transferred into a volumetric flask. After homogenization, the dispersing tool was washed with 3 mL MeOH. This solution was then used for the second extraction step which is similar to the first one. A third extraction step (using the methanol for washing the dispersing tool) was performed and the combined supernatants were filled up with methanol to a volume of 10 mL.

The extracts of the feed samples were diluted by a factor of 1000 in two steps yielding a concentration within the calibration range. For external calibration, calibration ranges of 0.1 - 20 µg/L for the cations, 0.25 - 50 µg/L for Benzotriazol and Tecloftalam and 0.5 - 50 µg/L for Pentachlorophenol and MEE-Phosphonate were used. Here, at least 6 different calibration points containing blank matrix, test substance and MeOH were mixed. The amount of matrix in the calibration samples was equal to the amount of matrix in the samples. The specific concentrations measured in each sample were calculated based on the recorded weight.

The homogeneity of spiked feed was determined by measuring substance concentrations in five replicates. The stability of spiked feed was measured in triplicates after specific time points. For the preliminary study, the substance concentrations in the experimental diets were presented as the mean concentration measured at test start and test end. For the main study, the average feed concentration during the study was calculated by taking the mean of the concentrations measured at test start and at the end of the uptake phase.

3.1.3.2 Determination of IOC content in fish samples

The concentrations of the test substances in fish samples were determined by chemical analysis and all tissue concentrations were calculated based on a wet weight basis. For analysis, all tissue samples, except for liver and GIT, were homogenized first. Afterwards, approximately 1 g of homogenate was weighed into a 15 mL PP-vial and after addition of 4 mL MeOH mixed with a dispersing tool for 30 seconds. The whole liver and GIT samples were homogenized using a dispersing tool following addition of 4 mL MeOH. After mixing, samples were treated in an ultrasonic bath for 10 min, centrifuged for 5 min at 5,000 rpm and the supernatants were transferred into a volumetric flask. The dispersing tool was rinsed with 3 mL MeOH, which was then used to repeat the extraction step followed by a further rinse. Supernatants obtained from the three extraction steps were combined and filled up to a total volume of 10 mL.

The extraction efficiency of the used extraction protocols was assessed. Therefore, blank matrices (GIT, liver and carcass) were spiked with a known amount of test substance:

- GIT: 1 µg/L for cations
  5 µg/L for Tecloftalam and Benzotriazol
  1 µg/L for Pentachlorophenol and MEE-Phosphonate
- Liver: 2 µg/L for cations
  1 µg/L for anions
- Carcass: 5 µg/L for cations and anions

The extraction was performed as described above. For assessment, recovery rates were calculated.

The matrix-matched calibrations with at least 6 points ranged between 0.05 - 20 µg/L for the cations and between 0.25 - 50 µg/L, 0.5 - 50 µg/L, 0.25 - 50 µg/L and 1 - 50 µg/L for Benzotriazol, Tecloftalam, Pentachlorophenol and MEE-Phosphonate, respectively. The extracts of the different matrices were diluted depending on the substance concentrations to yield a concentration within the calibration range. For the main study, TBP GIT samples from the uptake phase and 10 h and 24 h depuration phase were measured with a 1:5 dilution. Time points 48 h, 72 h, 7 d and 14 d of depuration of TBP GIT samples and all TBP liver and carcass samples were diluted 1:1. All TMOA GIT samples were diluted 1:80 and all liver and all carcass samples 1:1. For Benzotriazol, GIT samples were diluted 1:10, liver samples 1:5 and carcass 1:4. All Tecloftalam, all MEE-Phosphonate and Pentachlorophenol liver and carcass samples were diluted 1:1. Pentachlorophenol GIT samples were diluted 1:10. The organic content in each measured solution was between 50 - 55 %. For the calibration solutions, depending on the end volume (200 -1000 µL), 10 to 50 µL of the substance stock solutions were diluted with blank matrix, UHQ and MeOH leading to the approximate ratio of 1:1 (v:v) of organic solvent and UHQ. Importantly, depending on the dilution of the samples the amount of the matrix in the calibration solutions was adjusted.

3.1.4 Calculations of biomagnification and tissue distribution factors

Biomagnification and distribution factors were calculated based on the tissue concentrations measured at the end of the uptake phase. For calculation of steady-state biomagnification factors (BMF_{ss}) the substance concentration in the whole fish measured at the end of the uptake phase was divided by the concentration of the enriched feed. In case of the main study, the sum of the compartment concentrations was used to derive 'whole fish' concentrations. Individual tissue distribution factors of the different substances were calculated from the compartment-specific tissue concentration divided by the concentration in the whole fish.

3.1.4.1 Calculation of kinetic biomagnification factors of different matrices and of the whole fish (main study)

Assimilation efficiency

The assimilation efficiency (α, absorption of the test item across the gut) was calculated as:

$$\alpha = \frac{c_{0,d} * k_2}{I * c_{feed}} * \left[\frac{1}{1-e^{(-k_2 * t)}}\right]$$

with

$c_{0,d}$ derived concentration in fish at time zero of the depuration phase [mg/kg]

k_2 overall (not growth-corrected) depuration rate constant [1/day]

I feed ingestion rate constant [g_{feed}/g_{fish}*day]

c_{feed} concentration in feed [mg/kg]

t duration of the uptake phase [day]

Feeding rate

The feeding rate (I) used in the calculation was adjusted for fish growth to give an accurate assimilation efficiency (α). The growth-corrected feeding rate I_g was calculated as:

$$I_g = \frac{I * W_{f,0}}{W_{f,end\ uptake}}$$

with

$W_{f,0}$ mean fish weight at start of the experiment [g]

$W_{f,\ end\ of\ uptake}$ mean fish weight on the last day of exposure [g]

Kinetic BMF

The kinetic BMF (BMF_k) was calculated by multiplying the assimilation efficiency (α) with the feeding rate constant (I), divided by the product of the overall depuration rate constant (k_2):

$$BMF_k = \frac{I * \alpha}{k_2}$$

Depuration rate constant

The depuration rate constant (k_2) was calculated by performing a linear regression of ln(concentration in fish) versus time [day]:

$$k_2 = -m$$

The growth-rate constant k_g was calculated by linear correlation of plotting ln(fish weight) versus time [day] with the slope of the regression line m = k_g.

The calculated growth rate constant (k_g expressed as [1/day]) was subtracted from the overall depuration rate constant (k_2) to give a growth-corrected depuration rate constant (k_{2g}).

From the corrected depuration rate constant, the substance-specific half-life was determined by calculating:

$$t_{1/2} = \frac{ln2}{k_{2g}}$$

Growth-corrected BMF

The growth-corrected biomagnification factor was calculated using the growth corrected depuration rate constant:

$$BMF_{kg} = \frac{I*\alpha}{k_{2g}}$$

3.2 Results

3.2.1 Determination of homogeneity, content and stability of IOCs on diet

For all test substances a linear relationship between the peak area of the quantifier mass trace and the concentration in the matrix-matched calibrations was found (see Appendix B).

The homogenous distribution of the IOCs on feed was confirmed by the analysis of the test substance concentrations in five individually processed replicates. These measurements also represented the starting point of the stability measurement. Table 9 shows the results of the homogeneity test of the two feed batches spiked with the two cations TBP and TMOA. The relative standard deviations (RSD) were < 10 % for both ions. Thus, a homogenous distribution of the test substances in the feed can be assumed.

Table 9: Determination of homogeneity of cationic substances in fish feed used in pre and main study.

Substance	Preliminary study			Main study		
	Content in feed samples [mg/kg]	Mean [mg/kg]	RSD [%]	Content in feed samples [mg/kg]	Mean [mg/kg]	RSD [%]
TBP	20.72	20.1	6.7	22.59	23.8	5.8
	19.86			25.27		
	22.14			24.90		
	18.14			22.03		
	19.41			23.56		
TMOA	20.96	22.5	4.3	25.16	25.9	4.4
	23.62			26.98		
	23.46			27.35		
	22.04			24.26		
	22.36			25.81		

The results of the investigations on the homogeneity of the anions in the experimental diets are shown in Table 10. With RSD values of 2.1 %, to 10.6 % the feed batches enriched with Benzotriazol (pre and main study), Tecloftalam (main study), Pentachlorophenol (pre and main study) and MEE-Phosphonate (pre study) can be considered homogenous. Concentrations of Tecloftalam in the enriched feed applied in the preliminary study had an RSD value of 24.8 %. However, the following stability measurements in triplicate showed RSD values of 7.6 % and 7.7 % leading to the conclusion that the feed applied during the pre study can also be assumed to be homogenous. Investigations on the homogeneity of MEE-Phosphonate in the experimental diet applied during the main study revealed a RSD of 24.3 %. As MEE-Phosphonate was spiked collectively with Pentachlorophenol which had a RSD of 5.6 % and the subsequent stability measurements after 14 days and after the uptake phase showed RSD values of 6.3 % and 8.5 %, the test diet was also assumed to be homogenous.

Table 10: Determination of homogeneity of anionic substances in fish feed used in pre and main study.

Substances	Preliminary study			Main study		
	Content in feed samples [mg/kg]	Mean [mg/kg]	RSD [%]	Content in feed samples [mg/kg]	Mean [mg/kg]	RSD [%]
Benzotriazol	25.96	27.3	5.70	32.53	31.9	2.1
	27.86			31.56		
	27.21			32.64		
	29.83			30.83		
	25.41			31.97		
Tecloftalam	27.14	21.2	24.8	28.95	27.5	5.8
	26.01			28.04		
	22.81			28.98		
	14.82			24.66		
	15.76			27.07		
Pentachlorophenol	19.76	19.3	3.6	18.58	20.3	5.6
	20.21			20.10		
	18.61			21.56		
	18.43			20.16		
	19.61			21.02		
MEE-Phosphonate	25.20	23.4	10.6	22.84	29.6	24.3
	27.11			21.82		
	22.78			36.95		
	21.76			27.09		
	20.16			39.11		

Conclusively, all feed batches showed a homogenous distribution of the test substances. The stability measurements were performed to confirm stable concentrations during the whole uptake phase. Table 11 summarizes the results of the investigations to confirm the stability of the test substances during the pre and main study (see Appendix B for raw data). Stability was defined as the recovery of a test substance in the spiked diet in comparison to the feed concentration measured immediately after feed preparation. In the preliminary test, recoveries of 96.1 – 136 % in comparison to the day of feed preparation were determined. During the main test the stability of the dietary concentrations of the test substances were assessed twice. First, 14 days after diet preparation (96.1 – 123% recovery) and second, at the end of the uptake phase, where recoveries of 86.2 – 109 % relative to the original concentrations were ascertained.

Table 11: Results of stability investigations of feed batches for pre and main study.

		Preliminary study			Main study		
		t_{start}	$t_{14\ d}$	t_{end}	t_{start}	$t_{14\ d}$	t_{end}
TBP	mean conc. [mg/kg]	20.1		21.1	23.8	23.5	25.9
	SD [mg/kg]	1.34		2.08	1.38	0.88	0.18
	RSD [%]	6.66		9.85	5.8	3.75	0.69
	mean recovery [%]			**105**		**99.0**	**109**
TMOA	mean conc. [mg/kg]	22.5		23.0	25.9	24.9	22.3
	SD [mg/kg]	0.976		1.71	1.14	0.63	1.07
	RSD [%]	4.34		7.43	4.41	2.54	4.81
	mean recovery [%]			**102**		**96.1**	**86.2**
Benzotriazol	mean conc. [mg/kg]	27.3	29.1	28.5	31.9	34.7	28.3
	SD [mg/kg]	1.55	1.14	1.26	0.66	1.34	1.22
	RSD [%]	5.70	3.92	4.44	2.08	3.87	4.31
	mean recovery [%]		**107**	**104**		**109**	**88.7**
Tecloftalam	mean conc. [mg/kg]	21.2	21.0	20.4	27.5	27.0	26.5
	SD [mg/kg]	5.26	1.61	0.94	1.60	2.36	1.98
	RSD [%]	24.8	7.67	4.61	5.83	8.72	7.47
	mean recovery [%]		**99.1**	**96.1**		**98.2**	**96.3**
Pentachloro-phenol	mean conc. [mg/kg]	19.3	21.9	23.5	20.3	23.0	18.6
	SD [mg/kg]	0.69	0.53	1.62	1.13	1.82	0.66
	RSD [%]	3.56	2.44	6.91	5.58	7.91	3.55
	mean recovery [%]		**113**	**112**		**114**	**91.7**
MEE-Phosphonate	mean conc. [mg/kg]	23.4	34.7	31.9	29.6	36.3	26.9
	SD [mg/kg]	2.47	5.02	0.55	7.17	2.30	2.28
	RSD [%]	10.6	14.5	1.73	24.3	6.34	8.46
	mean recovery [%]		**148**	**136**		**123**	**91**

With t_{start} = day of preparation (here n = 5), t_{14} d = after 14 days (here n = 3), t_{end} = end of the uptake phase (here n = 3), SD = standard deviation, RSD = relative standard deviations.

Based on the results of the stability measurements the dietary concentrations were calculated (see Appendix B for single values). The test diets had mean concentrations of 20.6 ± 0.54 mg/kg and 22.8 ± 0.27 mg/kg for the preliminary study and 24.7 ± 1.21 mg/kg and 23.6 ± 1.28 mg/kg during the main study for the cationic substances TBP and TMOA, respectively. The concentrations of the anionic substances during the preliminary study were 28.8 ± 0.30 mg/kg for Benzotriazol, 20.7 ± 0.32 mg/kg for Tecloftalam, 22.7 ± 0.79 mg/kg for Pentachlorophenol and 33.3 ± 1.42 mg/kg for MEE-Phosphonate (Table 12). During the main study concentrations of 31.5 ± 3.21 mg/kg, 26.8 ± 0.26 mg/kg, 20.8 ± 2.22 mg/kg and 31.6 ± 4.66 mg/kg for the anions were determined.

Table 12: Overview of dietary concentrations in fish feed used in pre and main study.

	Preliminary study: Mean conc. in feed [mg/kg]	Main study: Mean conc. in feed [mg/kg]
TBP	20.6 ± 0.54	24.7 ± 1.21
TMOA	22.8 ± 0.27	23.6 ± 1.28
Benzotriazol	28.8 ± 0.30	31.5 ± 3.21
Tecloftalam	20.7 ± 0.32	26.8 ± 0.26
Pentachlorophenol	22.7 ± 0.79	20.8 ± 2.22
MEE-Phosphonate	33.3 ± 1.42	31.6 ± 4.66

3.2.2 Biological Observation

No mortality or abnormal behaviour of the test animals were observed during the main study. The experimental diets were accepted by the test animals and showed a decent digestibility as confirmed by the texture and appearance of the feces. One fish in the “cation” was euthanized at day 25 due to injuries.

The animals' average weight ranged from 4.70 ± 0.93 g (Control) to 6.27 ± 1.16 g (Pentachlorophenol/MEE-Phosphonate) at the beginning of the test and increased to average weights from 6.18 ± 0.92 g (Control) to 9.79 ± 1.09 g (Pentachlorophenol/MEE-Phosphonate) until the end of the uptake phase after 14 days of exposure. At the end of the depuration phase and the experiment, the average weight ranged from 9.24 ± 2.03 g (Control) to 13.28 ± 2.47 g (Pentachlorophenol/MEE-Phosphonate) (Table 13).

The specific growth rates of the animals ranged from 2.22 (Benzotriazol/Tecloftalam) to 2.68 %/d (Pentachlorophenol/MEE-Phosphonate) over the entire experiment. During the study, the feed conversion ratio (FCR) was very similar in all treatments (0.82 to 0.86), only for the Pentachlorophenol/MEE-Phosphonate treatment a lower FCR of 0.71 was calculated (Table 13).

Table 13: Feed conversion ratio (FCR) and specific growth rate (SGR) of experimental animals during the feeding study.

		Uptake phase (days 1 - 14)	Depuration phase (days 15 - 28)	Total experiment (days 1 - 28)
Control	Average body weight gain (g/fish)	1.48	3.06	4.54
	Average feed intake (g/fish)	1.56	2.22	3.78
	FCR	1.05	0.72	0.83
	W_{t1} (g)	4.70	6.18	4.70
	W_{t2} (g)	6.18	9.24	9.24
	t_2-t_1 (d)	14	14	28
	SGR (%/d)	1.96	2.87	2.41
TBP/TMOA	Average body weight gain (g/fish)	2.39	2.37	4.76
	Average feed intake (g/fish)	1.66	2.25	3.90
	FCR	0.69	0.95	0.82
	W_{t1} (g)	5.18	7.57	5.18
	W_{t2} (g)	7.57	9.94	9.94
	t_2-t_1 (d)[a]	14	14	28
	SGR(%/d)	2.71	1.95	2.33
Benzotriazol/Tecloftalam	Average body weight gain (g/fish)	3.03	1.72	4.74
	Average feed intake (g/fish)	1.76	2.31	4.07
	FCR	0.58	1.34	0.86
	W_{t1} (g)	5.52	8.55	5.52
	W_{t2} (g)	8.55	10.27	10.27
	t_2-t_1 (d)[a]	14	14	28
	SGR (%/d)	3.13	1.31	2.22
Pentachlorophenol/MEE-	Average body weight gain (g/fish)	3.52	3.49	7.01
	Average feed intake (g/fish)	2.02	2.98	5.00
	FCR	0.57	0.85	0.71
	W_{t1} (g)	6.27	9.79	6.27
	W_{t2} (g)	9.79	13.28	13.28
	t_2-t_1 (d)[a]	14	14	28
	SGR (%/d)	3.18	2.18	2.68

For accumulation: t_1 = day 0 and t_2 = day 14; for the depuration, t_1 = day 14 and t_2 = day 28, for the total experiment, t_1 = day 0 and t_2 = day 14. W_{t1} = average body weight at t_1; W_{t2} = average body weight at t_2.

3.2.3 Growth correction

Fish were measured and weighed at the beginning of the experiment as well as at respective sampling time points to monitor growth and associated growth-dilution effects during the feeding study. Growth of the test animals is also an important measure to detect potential adverse effects that may occur following dietary exposure. Growth rate constants were determined separately for the uptake and depuration phases, for the treatments and the control group, using the ln-transformed weights of the fish. A subsequent parallel line analysis (PLA, as suggested by the OECD Guideline) resulted in no statistical differences between the uptake and the depuration phase among the treated groups with P = 0.7784, P = 0.1116 and P = 0.5802 for TBP/TMOA, Benzotriazol/Tecloftalam and Pentachlorophenol/MEE-Phosphonate, respectively. No statistically significant difference was detected with regard to the growth of the treated groups (P = 0.7162). Hence it was deduced that neither adverse nor toxic effects were caused by the enriched diets. Weight data of the three groups could be pooled deriving the overall fish growth rate constant k_g. The value determined for k_g of 0.021 1/d, based on ln-transformed weight data of all fish, was then used for growth correction of the depuration constants.

3.2.4 Analysis of test item content in fish samples

During the main study the extraction efficiency of the used extraction protocol was assessed by spiking samples with a known concentration in five replicates. Subsequently, tissue samples were extracted with the same protocol and recovery rates regarding the applied amount of test substance were determined (Table 14). The estimated recovery rates were in a range of 80 - 120 % confirming the suitability of the applied extraction procedure. Note, standard deviations ranged from 5.0 - 28.0 %.

Table 14: Overview of extraction efficiencies of ionic pairs.

	Compartment	Recovery		Compartment	Recovery
TBP	GIT	85.1 ± 5.69 %	**TMOA**	GIT	83.2 ± 7.67 %
	liver	85.9 ± 7.94 %		liver	102 ± 20.5 %
	carcass	99.4 ± 7.79 %		carcass	115 ± 8.61 %
Benzotriazol	GIT	81.4 ± 28.0 %	**Tecloftalam**	GIT	104 ± 8.97 %
	liver (n = 4)	98.7 ± 20.4 %		liver	107 ± 18.9 %
	carcass	105 ± 5.61 %		carcass	83.8 ± 10.2 %
Pentachlorophenol	GIT	85.0 ± 16.4 %	**MEE-Phosphonate**	GIT	86.7 ± 9.19 %
	liver	87.3 ± 6.77 %		liver	96.6 ± 22.0 %
	carcass	110 ± 4.99 %		carcass	103 ± 20.2 %

Concentrations in whole fish at day 14 (pre and main study- end of uptake) and specific tissue concentrations can be found in Table 15 (for values of all time points of main study see Appendix B).

Table 15: IOC concentrations in fish samples collected at end of uptake (pre and main study)

		Preliminary study: Conc. ± SD [mg/kg]	Main study: Conc. ± SD [mg/kg]
TBP	(calc.) whole fish	0.274 ± 0.036	0.0338
	filet	0.064 ± 0.004	---
	GIT	0.912 ± 0.091	0.3620 ± 0.122
	liver	0.271 ± 0.038	0.0769 ± 0.038
	carcass	0.123 ± 0.018	0.0094 ± 0.005
TMOA	(calc.) whole fish	0.633 ± 0.042	0.6399
	filet	0.206 ± 0.081	---
	GIT	2.324 ± 0.799	8.2331 ± 1.661
	liver	1.632 ± 0.389	1.0178 ± 0.190
	carcass	1.218 ± 0.094	0.0862 ± 0.020
Benzotriazol	(calc.) whole fish	0.491 ± 0.052	1.2460
	filet	0.208 ± 0.011	---
	GIT	0.534 ± 0.081	3.6064 ± 2.605
	liver	0.294 ± 0.160	3.2658 ± 1.027
	carcass	0.267 ± 0.036	1.0198 ± 0.363
Tecloftalam	(calc.) whole fish	0.537 ± 0.168	0.0454
	filet	< LOQ	---
	GIT	0.677 ± 0.116	0.4950 ± 0.072
	liver	< LOQ	0.1274 ± 0.030
	carcass	< LOQ	0.0076 ± 0.004
Pentachlorophenol	(calc.) whole fish	0.575 ± 0.243	0.1870
	filet	< LOQ	---
	GIT	0.669 ± 0.090	1.3363 ± 0.119
	liver	0.558 ± 0.066	0.8322 ± 0.217
	carcass	0.170 ± 0.014	0.0736 ± 0.030
MEE-Phosphonate	(calc.) whole fish	0.684 ± 0.114	0.2931
	filet	< LOQ	---
	GIT	0.628 ± 0.190	2.6627 ± 0.355
	liver	< LOQ	0.4808 ± 0.188
	carcass	< LOQ	0.0820 ± 0.044

3.2.5 Calculation of substance specific tissue distribution and biomagnification factors in preliminary study

Based on the tisuue concentrations measured in fish collected on day 14 of the uptake phase (preliminary study), tissue distribution and magnification factors were calculated. The biomagnification factors for the cationic substances were determined to be 0.014 and 0.028 for TBA and TMOA, respectively. The biomagnification factors of the anionic substances were in the same range. Here, BMF values of 0.017 and 0.026 for Benzotriazol and Tecloftalam and 0.026 and 0.020 for Pentachlorophenol and MEE-Phosphonate were determined. The tissue specific distribution factors for the test substances applied during the preliminary study are shown in Figure 11.

Figure 11: Tissue distribution factors of ionic compounds (preliminary study).

Concentrations in different compartments divided by the concentration in the whole fish.

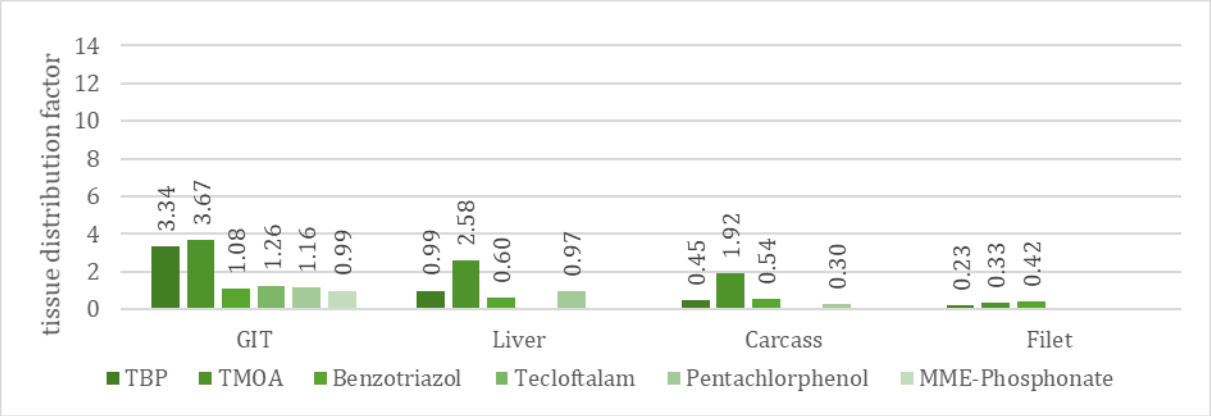

Source: Fh IME, own diagram.

3.2.6 Calculation of biomagnification factors (main study)

For the main study, the tissue specific distribution of IOCs measured at the end of the uptake phase are summarized in Figure 12. As steady state seemed to be reached after 14 days of exposure, steady state biomagnification factors (BMF_{ss}) could be calculated (Figure 13 - Figure 18).

Tissue concentrations measured during the uptake and depuration phase were used to calculate BMF_k and BMF_{kg} values for the different compartments and for the 'whole fish'. All derived kinetic BMF values are based on at least three time points measured during depuration, starting at day 0 of the depuration phase (day 14 of uptake phase). The calculated BMF values show that none of the IOCs tested in this study seems to biomagnify after dietary exposure (Table 17). The lowest BMF_k and BMF_{kg} were calculated for the anionic Tecloftalam (both values = 0.001), whereas the highest BMF_k and BMF_{kg} were calculated for the cationic TMOA (0.040 and 0.046, respectively). For all ions the highest tissue specific BMF_k and BMF_{kg} were calculated for the GIT (Table 16). The tissue distribution factors of the ions are given in the Figure 11 (preliminary study) and Figure 12 (main study). The highest single values for the BMF_k and BMF_{kg} were 0.489 and 0.542 for TMOA in the GIT. In general, the GIT and the liver showed the highest values for the BMF_k and BMF_{kg}. All calculated BMF values are presented inTable 17. Growth corrected depuration rate constants k_{2g}, were used to calculate BMF values. The absolute tissue concentrations during the uptake and depuration phase and all parameters that were used for the calculation of the BMF values are described in Appendix B.

Figure 12: Tissue distribution factors of ionic compounds (main study).

Concentrations in different compartments divided by the concentration in the whole fish.

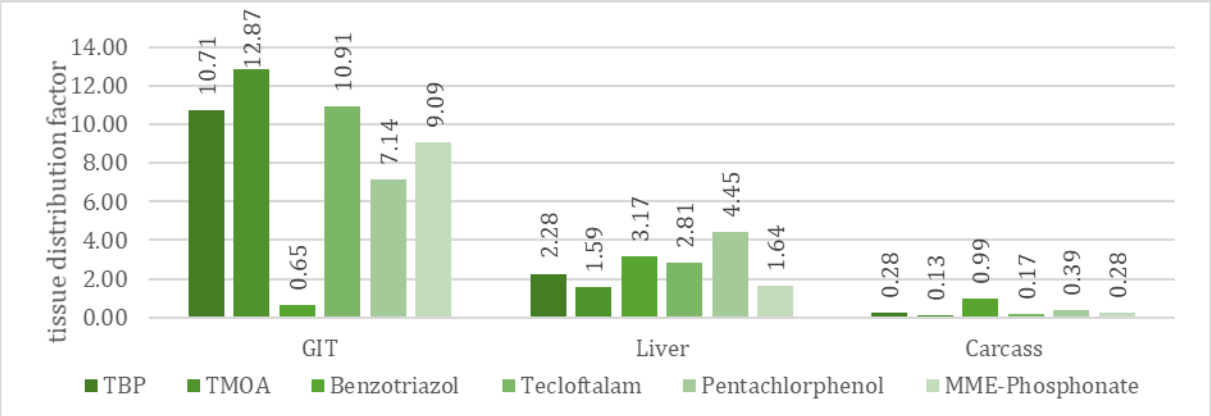

Source: Fh IME, own diagram.

Figure 13: Absolute tissue concentrations of TBP in the 'whole fish' (main study).

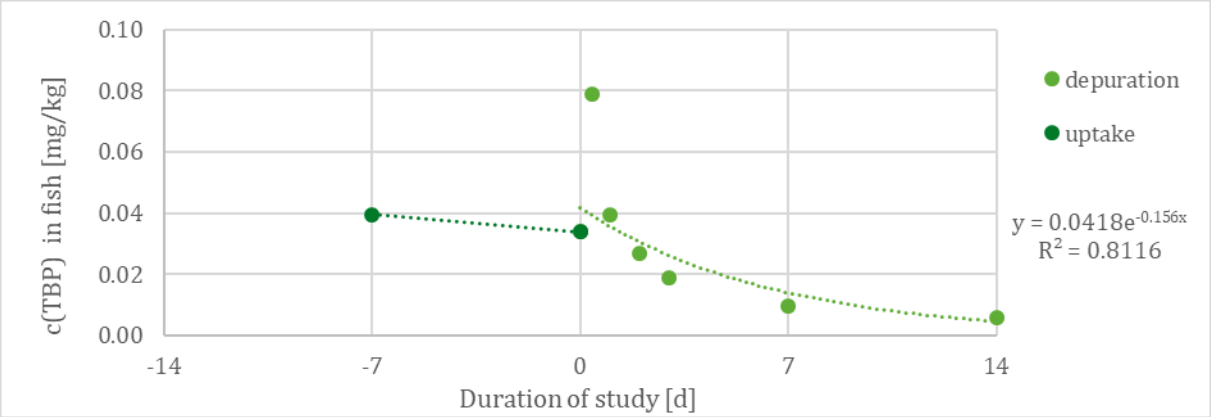

Source: Fh IME, own diagram.

Figure 14: Absolute tissue concentrations of TMOA in the 'whole fish' (main study).

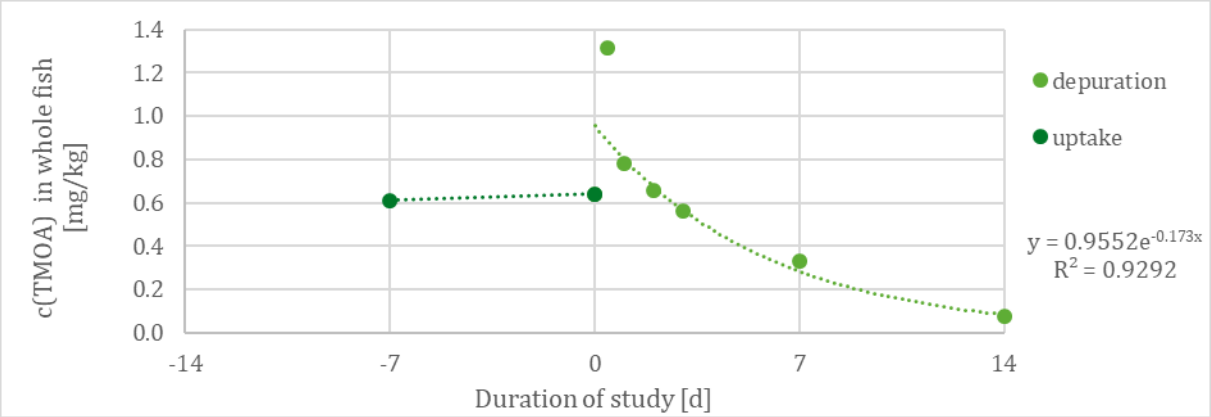

Source: Fh IME, own diagram.

Figure 15: Absolute tissue concentrations of Benzotriazol in the 'whole fish' (main study).

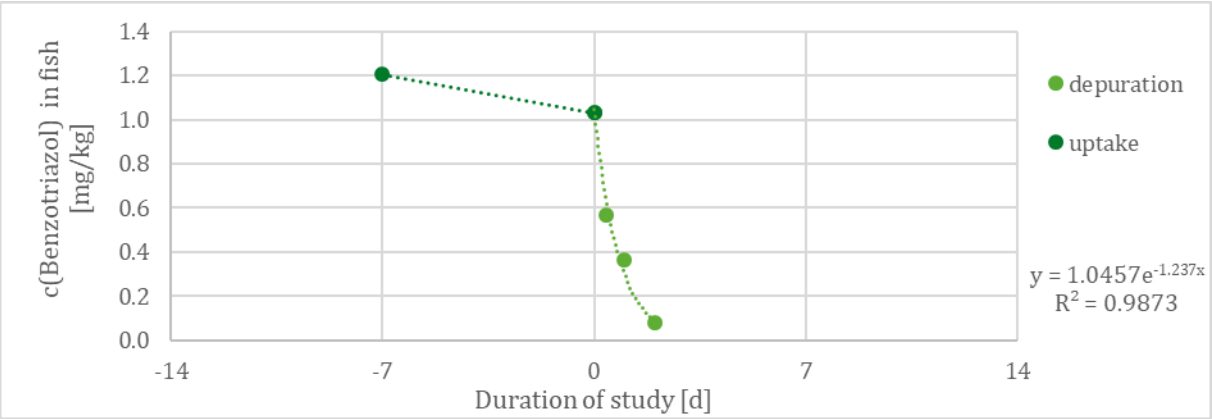

Source: Fh IME, own diagram.

Figure 16: Absolute tissue concentrations of Tecloftalam in the 'whole fish' (main study).

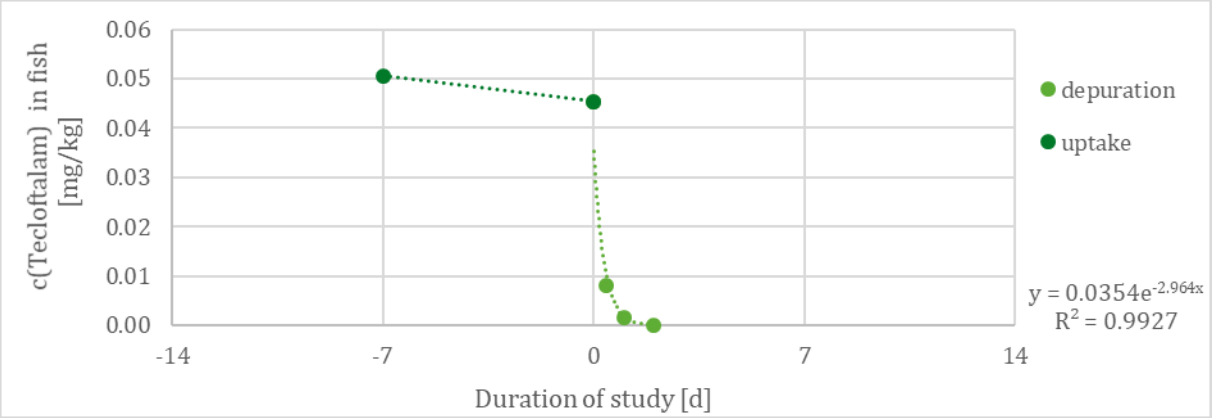

Source: Fh IME, own diagram.

Figure 17: Absolute tissue concentrations of Pentachlorophenol in the 'whole fish' (main study).

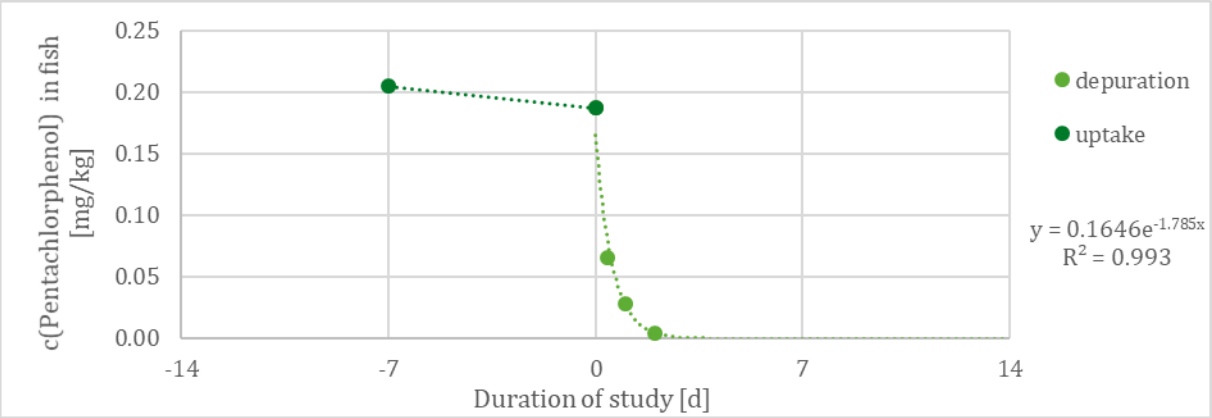

Source: Fh IME, own diagram.

Figure 18: Absolute tissue concentrations of MEE-Phosphonate in the 'whole fish' (main study).

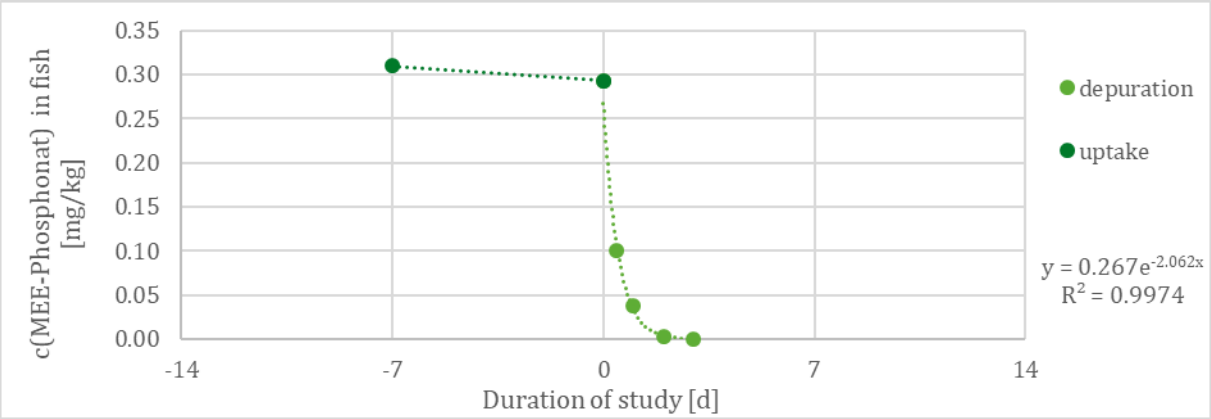

Source: Fh IME, own diagram.

Table 16: Overview of determined tissue specific BMF_k and BMF_{kg} of IOCs.

	GIT		Liver		Carcass	
	BMF_k	BMF_{kg}	BMF_k	BMF_{kg}	BMF_k	BMF_{kg}
TBP	0.0225	0.0264	0.000906	0.00100	0.000275	0.000278
TMOA	0.489	0.542	0.0621	0.0833	0.00450	0.00742
Benzotriazol	---	---	0.0779	0.0797	0.0308	0.0314
Tecloftalam	0.00982	0.00992	---	---	---	---
Pentachlorophenol	0.0554	0.0561	0.0351	0.0356	0.00291	0.00294
MEE-Phosphonate	0.0938	0.0948	---	---	---	---

Table 17: Summary of 'whole fish' BMF_{ss}, BMF_k and BMF_{kg} of IOCs.

	TBP	TMOA	Benzotriazol	Tecloftalam	Penta-chlorophenol	MEE-Phosphonate
BMF_{ss}	0.00137	0.02709	0.03952	0.00169	0.00898	0.00928
BMF_k	0.00198	0.04044	0.03657	0.00128	0.00812	0.00903
BMF_{kg}	0.00231	0.04629	0.03712	0.00129	0.00822	0.00913

3.3 Evaluation

The spiking procedure used for the enrichment of the experimental diets was suitable and led to stable and homogenous concentrations of the IOCs.

The BMF values were determined as BMF_{ss}, BMF_{k} and BMF_{kg}. For the anions, comparable or nearly similar BMF_{ss} and BMF_{kg} values were determined. For the cations (TBP and TMOA) the values of the BMF_{kg} were 1.7 times higher than the values of the $BMF_{ss.}$ indicating that the steady-state conditions were not reached for the cation tissue concentrations at the end of the uptake phase. Neither the BMF values determined for the whole fish nor for any compartment indicate a significant biomagnification potential of the tested compounds in fish. Nevertheless, differences in the biomagnification potential of the different compounds were observed. Benzotriazol and TMOA led to BMF values that were 5 to 10 times higher than those of the other ions. The Tecloftalam and MEE-Phosphonate concentrations were only detected in the GIT, which may be the result of ions adsorbed to the GIT mucous membran/proteins indicating a lack of bioavailability of these compounds.

In addition, a clear pattern of compartment or tissue specific magnification was observed. For all compounds the highest BMF values were determined for the GIT (except Benzotriazol) followed by the liver and finally the carcass. This might be explained by the location of the GIT and the transport of the compounds by blood via the vena portae from the GIT to the liver.

4 General discussion

4.1 Interpretation of results

Overall, the measured BMF-values are low. The median of the six experimental BMF is at 0.0087 g/g, while it was at 0.178 g/g for the data set of existing BMFs (Chapter 2, strong acids plus Pentachlorophenol, PCP). The largest BMF is 0.0463 g/g (TMOA), while the kinetic BMF of perfluorotetradecanoic acid was 1.00 g/g, and that of PFOS was 0.42 g/g (Table 2). This is surprising, since the test compounds were selected in order to achieve high BMF values. What could be the reasons for the low bioaccumulation?

Two of the compounds, Tecloftalam and MEE-Phosphonate, were only detected in the GIT. This is a strong indication for a slow or inhibited uptake into the organism. Similarly, TBP has a very low α (assimilation efficiency) and subsequently also a low BMF in liver, carcass and whole fish. However, the median of alpha-values of the six test compounds is at 0.54 and thus very similar to that of the literature data (0.56, Table 2, strong acids plus PCP). Benzotriazol even shows an α of 2.39, which is much higher than expected (typically ≤ 1).

A second reason for low BMF are the rather high loss rates. Tecloftalam, Benzotriazol, PCP and MEE-Phosphonate (i.e. the four acids) have clearly higher loss rates than the two cations TBP and TMOA. The median of loss rates is 1.5 d^{-1}, while the literature data (strong acids plus PCP) had a median k_2 of only 0.07 d^{-1} (Table 2).

The only compound for which data are available from earlier studies is PCP. While in our study the BMF was at 0.008 g/g, it was 0.22 g/g there. Alpha is similar (0.73 g/g versus 0.94 g/g), but the loss rate k_2 is much higher in our study (1.76 d^{-1} versus 0.25 d^{-1}). It should be mentioned that the depuration rate of PCP in the literature data was not directly measured but extrapolated.

Overall, it can be concluded that the experimental BMF are low due to slow uptake and rapid depuration. Possible reasons for this will be discussed below.

4.2 Screening parameter of the test substances

ACD-screening parameters that were collected for the six test substances are shown in Table 18 (compare chapter 2). For the data set of existing BMF data, a positive correlation to the fish BMF was found for log D (r = 0.335), log KHSA (r = 0.456), number of rotating bonds RB (r = 0.267). A negative correlation was found with the number of hydrogen bond donors HBD (r = -0.772) and acceptors HBA (-0.266), total polar surface area TPSA (r = -0.303) and solubility (r = -0.224). Except HBD, none of these relations was significant (Table 3). Similarly, the correlations between the screening parameters and the measured BMF of this study are weak, none is significant. The highest correlation shows RB (+0.417) followed by log D at pH 7.4 (+0.366).

Lipinski et al. (2001) presented the 'rule of 5' which predicts that poor absorption or permeation of orally applied drugs is more likely when there are more than 5 H-bond donors, 10 H-bond acceptors, the molecular weight is greater than 500 g/mol and the log D (log K_{ow}) is greater than 5. With regard to the six test chemicals, none has more than 5 H-bond donors or > 10 HBA, none has a molar mass > 500 g/mol and none has a log D > 5 at a neutral pH. Tecloftalam and PCP have, however, a log D > 5 at pH 3 (which may occur in the GIT).

Veber et al. (2002) did not fully corroborate the findings of Lipinksi et al. (2001). Instead they found, using a data set of 1100 oral studies that compounds which meet only the two criteria of (a) 10 or fewer rotatable bonds and (b) polar surface area equal to or less than 140 $Å^2$ or 12 or fewer H-bond donors and acceptors, will have a high probability of good oral bioavailability (in

the rat). Applied to the experimental data here, all compounds have a TSPA < 140 Å^2, but TBP (17), TMOA (12) and MEE-Phosphonate (12) have more than 10 rotatable bonds and would accordingly show limited oral bioavailability. Veber et al. (2002) studied also data sets for the artificial membrane permeation rate. Reduced polar surface area correlated better with increased permeation rate than did lipophilicity, and increased rotatable bond number had a negative effect on the permeation rate. Taking the criteria of Lipinski and Veber together, only Benzotriazol does not violate any of the criteria for good oral uptake.

The sorption parameters are shown in

Table 19. The $K_{fish/water}$ was determined with the methods described in Chapter 1 (no data available for TBP and TMOA). The BCF_{Fu} is the BCF calculated with the regressions in Fu et al. (2009), and the BCF_{Meylan} is a rule-based estimation method (Meylan et al., 1999), both using the log D as predictor. All three distribution parameters ($K_{fish/water}$, BCF_{Fu} and BCF_{Meylan}) show a negative but insignificant correlation to the BMF values measured in fish.

Brief, Lipinski's rule of five did not indicate reduced BMF; Veber's rules indicated low BMF for TBA, TMOA and MEE-Phosphonate but not for the other three compounds, the $K_{fish/water}$ predicted the highest BMF for MEE-Phosphonate and the lowest for Benzotriazol (which had a four-times higher experimental BMF than predicted). The methods of Meylan and Fu predicted the highest bioaccumulation for Tecloftalam, which had a measurable uptake only in the GIT. In conclusion, none of these screening parameters or methods was of real value when applied to the experimental results of the six test substances. Also the rule of five of Lipinski and the modification made by Veber et al. (2002) do not hold, as all ionised chemicals show limited accumulation. This can be both due to a low permeability and to a low bioavailability of ions in the gut, but also due to a rapid metabolism, e.g., conjugation.

All ionic compounds have at least one reactive groupthe charged moietyand it is well known that living organisms form conjugates or complexes with such compounds (Polesel et al., 2016). Moreover, cells can possess enzymes acting as extrusion pumps (Eytan et al., 1997).

Table 18: Screening parameters of the test substances. Source: ACD/i-Lab.

	Molar mass	HBD	HBA	TPSA	RB	log D pH 7.4	log D pH 3	charge	Solubility	log K HSA
	g/mol	#	#	Å²	#	(-)	(-)	#	mg/L	(-)
TBP	259.4	0	0	0	12	1.6	1.6	1	1800	3.12
TMOA	312.6	0	1	0	17	4.08	4.08	1	120	3.9
Benzotriazol	339.4	2	6	87.7	5	0.78	3.5	-1	54	5.03
Tecloftalam	447.9	2	4	66.4	3	2.29	5.5	-1	64	6.18
PCP	266.3	1	1	20.2	0	2.41	5.12	-1	23	5.35
MEE-Phosphonate	292.4	1	3	56.3	12	0.01	3	-1	2.6	3.77

Table 19: Sorption parameters of the test substances.

	$K_{fish/water}$	log $K_{fish/water}$	BCF_{Fu}	BCF_{Meylan}	$BMF_{kg\ fish}$
TBP	nb		17.9	3.2	0.0023
TMOA	nb		70.7	3.2	0.0463
Benzotriazol	398	2.6 ionic or 3.3 neutral	11.5	3.2	0.0371
Tecloftalam	3162	3.50	85.6	56.2	0.0013
PCP	1995	3.30	46.3	5.6	0.0082
MEE-Phosphonate	35481	4.55	32.7	5.6	0.0091

Unit L/kg, except fish BCF with g/g.

4.3 Comparison to earlier results

Nendza et al. (2018) screened data sources for aquatic bioaccumulation and collected experimental and physico-chemical data of 998 (training set) plus 181 (validation set) compounds. In the training set were seven acids that were classified as "B" (bioconcentration factor > 2000 L/kg) and six bases. However, of the acids in the training set, only two were more than 10 % ionised at neutral pH, both polyfluorinated compounds, and their names were perfluorooctane sulfonate (PFOS) and perfluorohexane sulfonic acid. None of the bases in the training set with B property showed significant ionization at test conditions (neutral pH). In the validation set, two acids showed B property, namely potassium heptadecafluorooctane-1-sulfonate (also a fluorocompound) and Pentachlorophenol, plus two amphoteric compounds named 2-(2H-benzotriazol -2-YL)-4,6-di-tert-pentylphenol and a methylpyridine carboxamide (CAS 835621-07-3). The ionization status of the latter is unknown but their log D values indicates little ionization. PCP has a pK_a of 4.6, i.e. it depends on the test pH whether it is ionized or not (usually it is), and the sulfonate is a strong acid. Summarized, all acids and bases that are labelled B in this large, selected data set are either mostly non-ionized or are polyfluorinated sulfonic acids, with the exception of PCP which was listed in this data set with an experimental BCF-value of 4898 L/kg. All compounds in the data set of Nendza et al. (2018) that showed high bioaccumulation were "not readily biodegradable", and there was a strong relation between BCF and degradation half time. All acids and bases that showed a high BCF had also a high log D (> 3), but as mentioned this includes also non-ionized electrolytes. Polyfluorinated compounds are an exception from this rule.

Fu et al. (2009) also studied the fish BCF values of ionizable substances. In their database, the experimental value for the BCF of PCP is only 10 L/kg, and none of the anions or cations showed any bioaccumulation above the criterion for B (> 2000 L/kg). The highest BCF of acids (n = 74) were for tefluthrin, cyhalothrin (not ionized at test pH) and 2,4,5-trichlorophenol (BCF 1800 L/kg, pK_a at 7.10 and thus about half neutral half ionized at test conditions). Mostly ionized acids, like 2,3,4,6-tetrachlorophenol (pK_a 5.64) or the mentioned PCP had BCF values clearly < 2000 L/kg. Similarly, out of the 65 data sets for bases, only one named azocyclotin had a BCF > 2000 L/kg, but that compound has a pK_a of 2.74 and is thus completely non-ionized at neutral pH. Among the mostly ionized bases (pK_a > 9), fenpropidin showed the highest experimental BCF with 160 L/kg.

Fu et al. (2009) made correlations between BCF and log D. Interestingly, acids with high pK_a (mostly neutral) showed an excellent correlation between the two parameters (R^2 was 0.91) and

the regression had a high slope and a low y-axis intercept. Also for mostly neutral bases, the correlation of log D to BCF was high (R^2 was 0.80), and like before a regression line with a high slope and a low y-axis intercept was observed.

For the mostly ionized acids as well as for the mostly ionized bases, the correlation of log D to BCF was weak (R^2 of 0.34 and 0.38), the slopes of the regression lines were low and the y-axis intercept high. This clearly shows that log D (or log K_{ow}) is a good predictor for the bioaccumulation of the neutral molecule fraction of ionizable substances, but a weak predictor (if at all) for the ionized fraction. It also shows that if a compound is only partly ionized, the neutral fraction will dominate the BCF. This was confirmed by the studies of Rendal et al. (2011 a, b), where acids and bases in neutral form showed both higher toxicity and higher uptake into organisms.

Subsequently, Armitage et al. (2017) recommend to consider only the neutral fraction if the ionization is < 90 %. These authors also "expect" that biotransformation plays "a crucial role" for compounds with a high adsorption, i.e. a high log K_{ow}.

Arnot and Quinn (2015) show, for a data set with mostly neutral compounds, that the BMF follows an optimum curve, due to the growth dilution for very highly adsorbing compounds. The maximum BMF is at 10 g/g for the range from log K_{ow} 5 to 8. It is likely that such a BMF optimum also could be found for ionic compounds, if the database for such a study would exist. Importantly, that optimum BMF would be lower than that for neutral compounds, due to the slower permeability of ionic compounds across membranes (Bittermann and Goss, 2017).

The uptake of permanent phosphonium cations into cells was determined by Ross et al. (2008). Investigated substances were MitoQ (mitoquinone), DecylTPP and TPMP (methyltriphenylphosphonium), which is hydrophilic. Both MitoQ and DecylTPP were taken up very rapidly into cells, reaching a steady state within 15 min, compared with approximately 8 h for TPMP. The uptake of MitoQ by mitochondria and cells was described by the Nernst equation and was approximately 5-fold greater than that for TPMP, as a result of its greater binding within the mitochondrial matrix. DecylTPP was also taken up extensively by cells, indicating that an increased hydrophobicity enhanced the uptake. This far faster uptake was the result of the increased rate of passage of hydrophobic TPP molecules through the plasma membrane. These findings show that lipophilic permanent cations (similar to TBP and TMOA) can principally cross membranes rapidly, while more hydrophilic cations permeate very slowly.

4.4 Conclusions for the assessment of ionic substances

The bioaccumulation of six ionized organic compounds (IOCs) was tested in an OECD 305 dietary uptake study. None of the tested IOCs showed a distinct biomagnification (BMF_{kg} < 0.1 g/g) and the highest tissue concentrations of most IOCs were found in the GIT. The low concentrations in the other tissues might be explained by the absent or limited transport into other tissues, and/or by rapid biotransformation. The only exception was Benzotriazol, for which a rapid elimination from GIT and transfer into liver and carcass were observed. Hence, the hypothesis that IOCs show a higher bioaccumulation potential by uptake through the gastrointestinal tract (GIT) could not be confirmed. Overall, the four anions showed a considerably higher depuration rate than the two cations.

None of the more than twenty screening parameters showed a particular high correlation to the test results nor to the BMF values collected from literature. The best correlation to the literature BMF values was obtained with the $K_{fish/water}$, which considers adsorption to proteins, storage lipids and membranes and thus predicts adsorption to cell tissue. However, this screening parameter showed to be of no relevance for predicting BMF values experimentally determined

in this study. The results of this study showed that the uptake and elimination kinetics are decisive for the dietary BMF of the investigated IOCs. The tissue analysis indicated that the low BMF of the investigated organic cations was due to a slow uptake from the GIT into the blood. This was also seen for some of the organic anions, but for those, the main reason for the low BMF was a rapid elimination, i.e. a high depuration rate. Hence, screening parameters primarily predicting adsorption, like $K_{fish/water}$, log K_{ow}, log D_{ow}, or the K_{HSA}, may not be well suited to indicate high biomagnification following dietary uptake.

Overall, it can be concluded from the screening that ionization lowers the tendency of a chemical to bioaccumulate, compared to non-ionized chemicals. This is also the conclusion of several reviews on bioaccumulation of IOCs. Aside of the well-known lipophobicity of ionized groups, fast depuration seems to be a major reason for the observed low biomagnification of ionic compounds, in particular anions. Fast depuration may happen due to rapid metabolism or conjugation of charged compounds, and future studies should test this hypothesis.

Appendix A: Supporting information: Developing screening tools for the bioaccumulation potential of monovalent organic ions

A.1 Meaning of the different sigma moments

Overall, COSMOtherm outputs 22 different sigma moments, most of which have no easily understandable physicochemical meaning, but can be seen rather as a refinement of the decisive six sigma moments Sig0 to Sig3, Hb_{acc3} and Hb_{don3}, which can be interpreted as follows:

Sig0 = area, describing van-der Waals interactions.

Sig1 = total charge. This sigma moment is obviously only necessary when differently charged chemicals are fitted together within one MLR, but it can be neglected when the partitioning of chemicals carrying the same charge is characterized via a MLR. Note that long ranging Coulomb interactions are not described in COSMO-RS.

Sig2 = polarity.

Sig3 = asymmetry of positive and negative partial surface charges, indicating whether or not polarities match each other.

Hb_{acc3} and Hb_{don3} = given in the COSMOtherm output for each of these properties. Hb_{acc3} and Hb_{don3} have been chosen empirically just as the COSMOtherm internal H-bond threshold of 0.1 e/Å² on the TZVP level.

It has been shown that the use of higher sigma moments does not yield higher prediction accuracies for the description of $K_{x/water}$ (COSMOlogic, personal communication), but implicates the danger of over-fitting the training data.

In this work only the conformer with the lowest energy with regard to the perfect conductor was used for calculating the sigma moments (i.e. the COSMOtherm "c0" conformer), as it was done in the initial work that showed the inherent similarity between sigma moments and Abraham solute descriptors (Zissimos et al., 2002). The perfect conductor seems to be a good choice when comparing different partitioning systems as long as all the partitioning systems are slightly polar. Note however, that neglecting higher energy state conformers inevitably results in a loss of information.

A.2 Sorption to membrane lipid

As outlined in the manuscript, we used exactly the same calculation details as in the original COSMOmic publication (Bittermann et al., 2014). Note, however, that there is also an updated, yet unpublished, version available that rotates the most polar surface segment in each membrane layer ("centersig2"-option) instead of the center of mass (which was done in the original publication (Bittermann et al., 2014) and is still the default). The calculation of $K_{membrane/water}$ with the center of rotation according to polarity instead of mass has only a negligible influence on the calculated $K_{membrane/water}$: for calculations with the 1401 parametrization, the maximal difference between the two methods is 0.022 log units in the updated calibration data set. The centersig2 option appears to be physically more sound and gives a more realistic picture of the actual energy barrier in the membrane center (publication in progress). But given that it hardly has an influence on $K_{membrane/water}$ we stick to the previous calculation details (Bittermann et al., 2014).

Tentatively, we also investigated whether the originally published offset value of 0.32 log units is still valid for the updated experimental data set used here, mainly based on the extended $K_{membrane/water}$ data (Endo et al., 2011; Bittermann et al., 2016), published after the implementation of the membrane dipole potential (Bittermann et al., 2014) (n = 86(ions), n = 217(neutrals)). The offset value describes the 'volume' work missing in the COSMOmic model (see Bittermann et al., 2014; Bittermann et al., 2016 for detailed discussion). Using this extended data set we determined a new offset value of 0.28 log units results, which is slightly and negligible smaller than the originally determined offset value of 0.32 log units. In this work we still use the originally published offset value because the difference was insignificant. Note, that the offset is not implemented as default in the current version of COSMOmic (i.e. we manually subtracted 0.32 log units from our COSMOmic results). We get an overall RMSE for all 217 neutral chemicals, 53 anions, 29 cations, 2 zwitterions and 2 dications of 0.73 log units.

Figure 19: Calculation of 217 neutral chemicals, 53 anions, 29 cations, 2 zwitterions and 2 dications with COSMOmic using the 1401 parametrization (which was used in the original publication to optimize the membrane dipole potential), a polarity based center of rotation and a newly determined offset value of 0.28 log units.

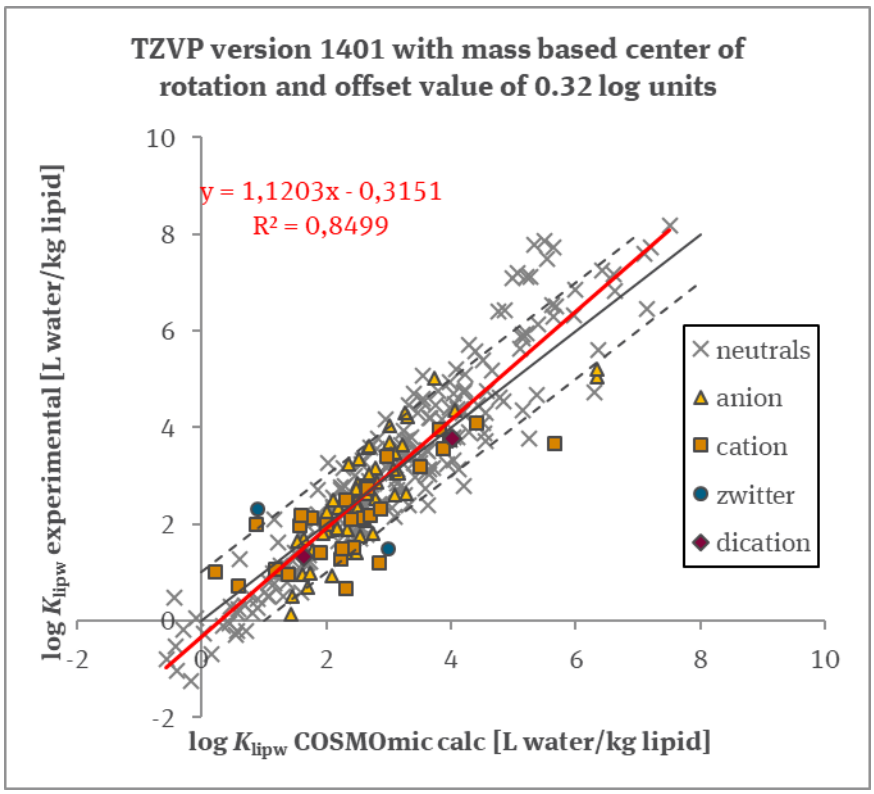

Source: UFZ, Leipzig.

COSMOlogic is working on a new membrane potential that is optimized for the TZVPD-FINE parametrization (Bittermann et al. 2018), which is announced to become implemented in the upcoming COSMOthermX distribution. According to COSMOlogic the TZVPD-FINE parametrization will become the most accurate parametrization for COSMOtherm predictions in the future.

A.3 Sorption to structural (muscle) protein

If differently charged chemicals (i.e. neutral chemicals, anions and cations) are fitted together, it is necessary to include Sig1 (charge). Sig1 can be left out, when neutral chemicals, anions and cations are fitted separately.

Table 20: The minima and maxima of the six relevant sigma moments (TZVP level) for the description of a partition coefficient.

	Area	Sig1	Sig2	Sig3	Hb_acc3	Hb_don3
63 neutral chemicals	138.9 - 341.2	0	6.2 - 118.0	-47.9 - 70.1	0-5.2	0 - 6.9
41 anions	170.2 - 337.0	100	105.0 - 233.7	147.6 - 392.0	8. 5 - 36.4	0 - 0.014
10 cations	258.8 - 468.6	-100	81.4 - 207.9	-232.3 - 45.5	0 - 3.9	- 14.4

Figure 20: Fit for the calculation of log $K_{MP/water}$ with TZVP sigma moments and a constant using the complete data set.

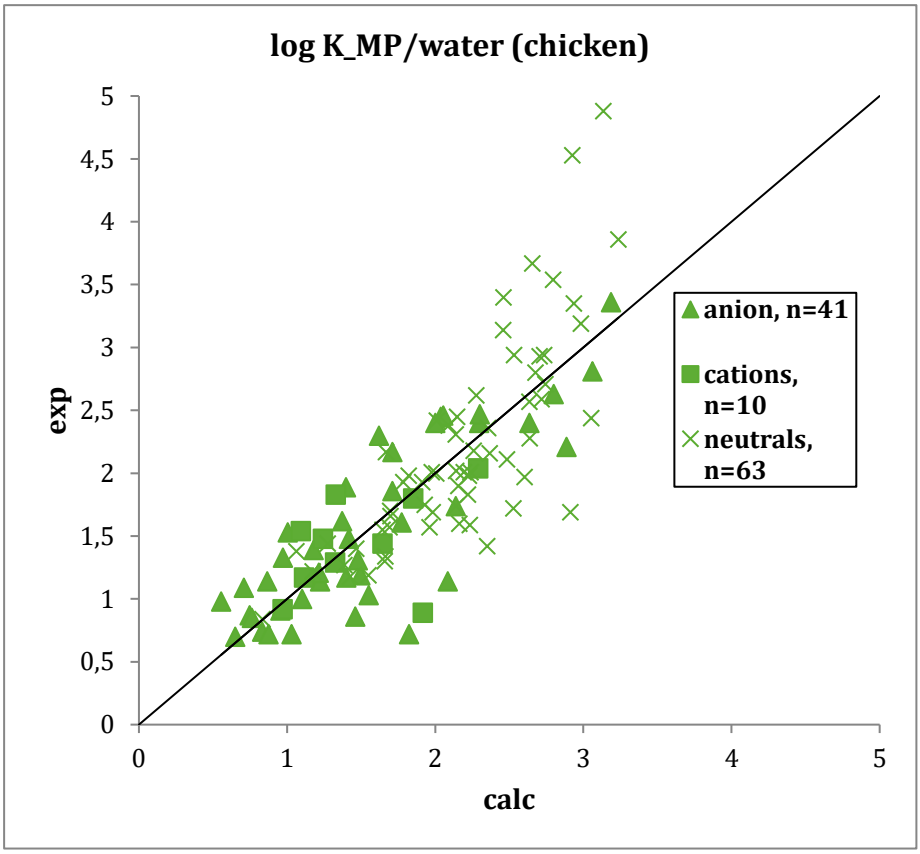

Source: UFZ, Leipzig.

A.4 Sorption to albumin

$\log K_{albumin} = -0.232\ (\pm 0.097)\ Hb_{don3} + 0.387\ (\pm 0.074)\ Hb_{acc3} - 0.033\ (\pm 0.007)\ Sig3 - 0.022\ (\pm 0.005)\ Sig2 + 0.014\ (\pm 0.002)\ Sig1 + 0.026\ (\pm 0.006)\ Sig0 + 0.977 (\pm 0.284)$; $R^2 = 0.45$, RMSE = 0.64, F = 42, n = 83 neutrals and 40 anions.

Figure 21: Sigma moments based fit of 40 anions and 83 neutral chemicals together.

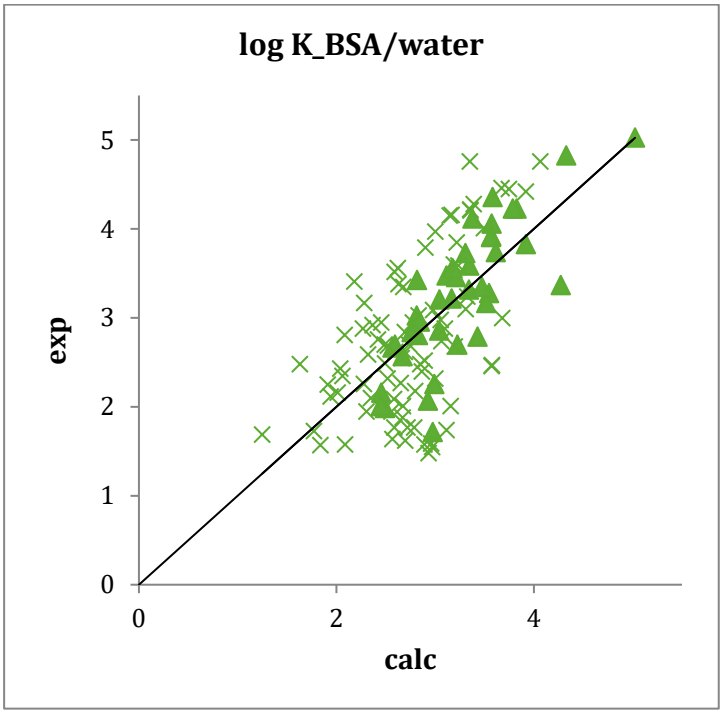

Source: UFZ, Leipzig.

Figure 22: pp-LFER based fit of 83 neutral chemicals.

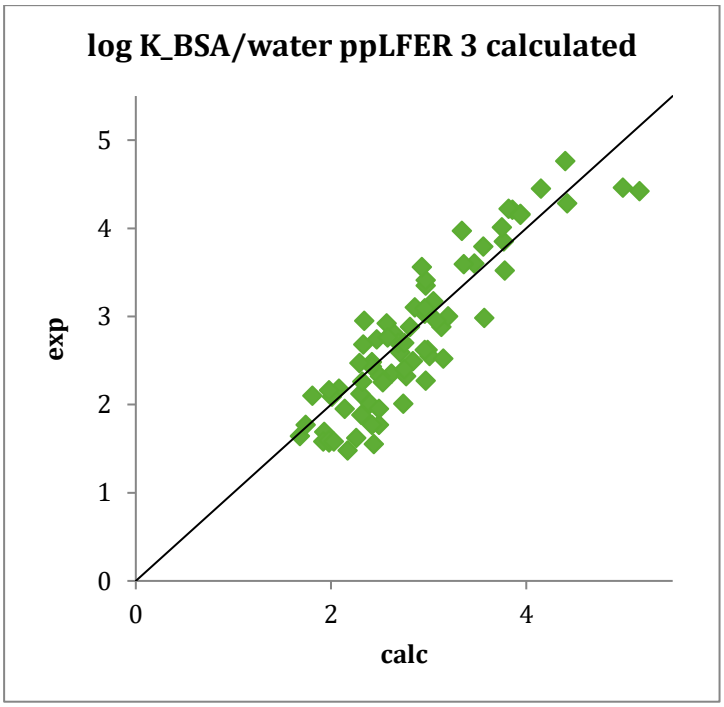

Source: UFZ, Leipzig.

A.5 Consensus model for neutrals

Table 21: Comparison of sigma moments based models and pp-LFER. Note that the pp-LFER is only for neutral chemicals, while the sigma moments based models are for both anions and neutral chemicals.

model	RMSE	R^2
SigmaMoments all	0.64	0.45
SigmaMoments anions	0.33	0.82
SigmaMoments neutral	0.57	0.56
pp-LFER (eq. 3)	0.40	0.82

The prediction based on the sigma moments performed inferior for the neutral chemicals than the pp-LFER prediction (RMSE 0.57 vs 0.395 log units). It is worth noting that the pp-LFER fit described in the literature (Endo et al., 2013) shows an influence of size exclusion for large chemicals and thus problems with the prediction of high log $K_{BSA/water}$ values. This is not the case for the fit with the sigma moments, which could be advantageous for our screening purpose of a large, divers data set.

Figure 23: Comparison of the prediction of log $K_{muscle\ protein/water}$ based on the TZVP sigma moments versus the prediction using pp-LFER. Green dots indicate calculated pp-LFER descriptors with the warning level 2c and black squares indicate calculated pp-LFER descriptors with the warning level 3.

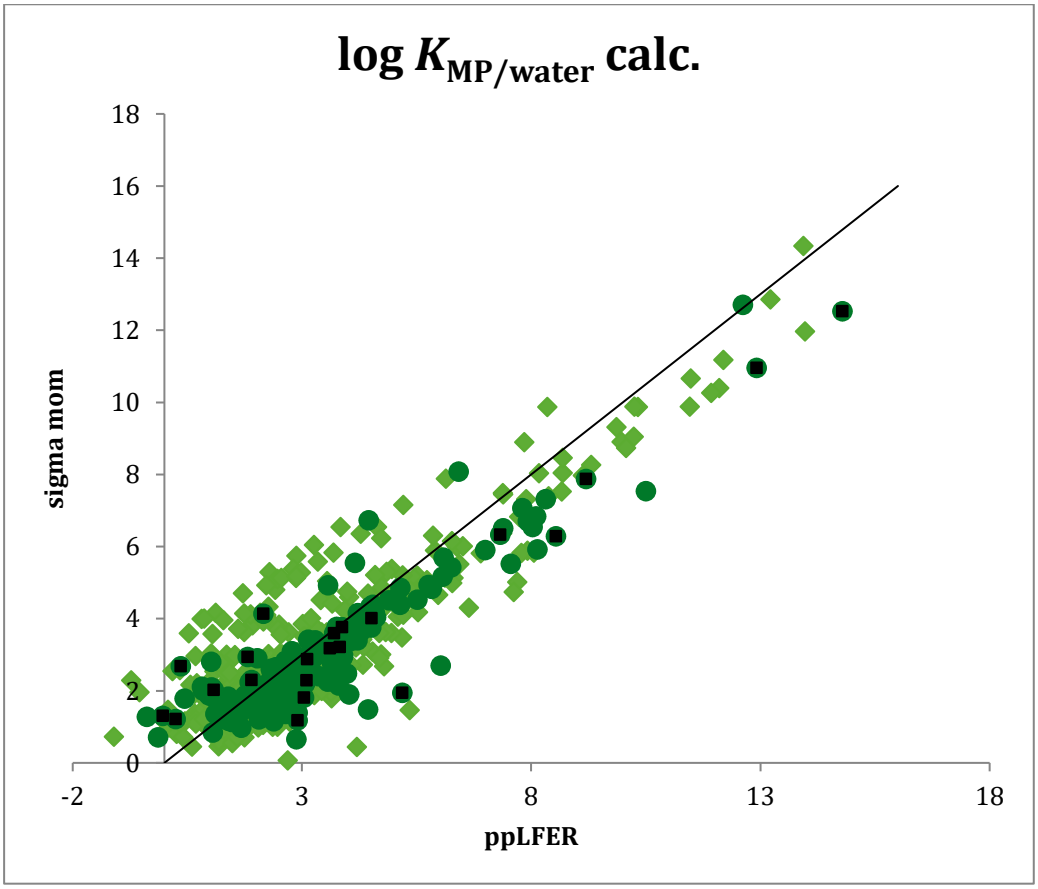

Source: UFZ, Leipzig.

Figure 24: **Comparison of the predictions of log $K_{BSA/water}$ based on the TZVP sigma moments versus the prediction using pp-LFER. Bluedots indicate calculated pp-LFER descriptors with the warning level 2c and black squares indicate calculated pp-LFER descriptors with the warning level 3.**

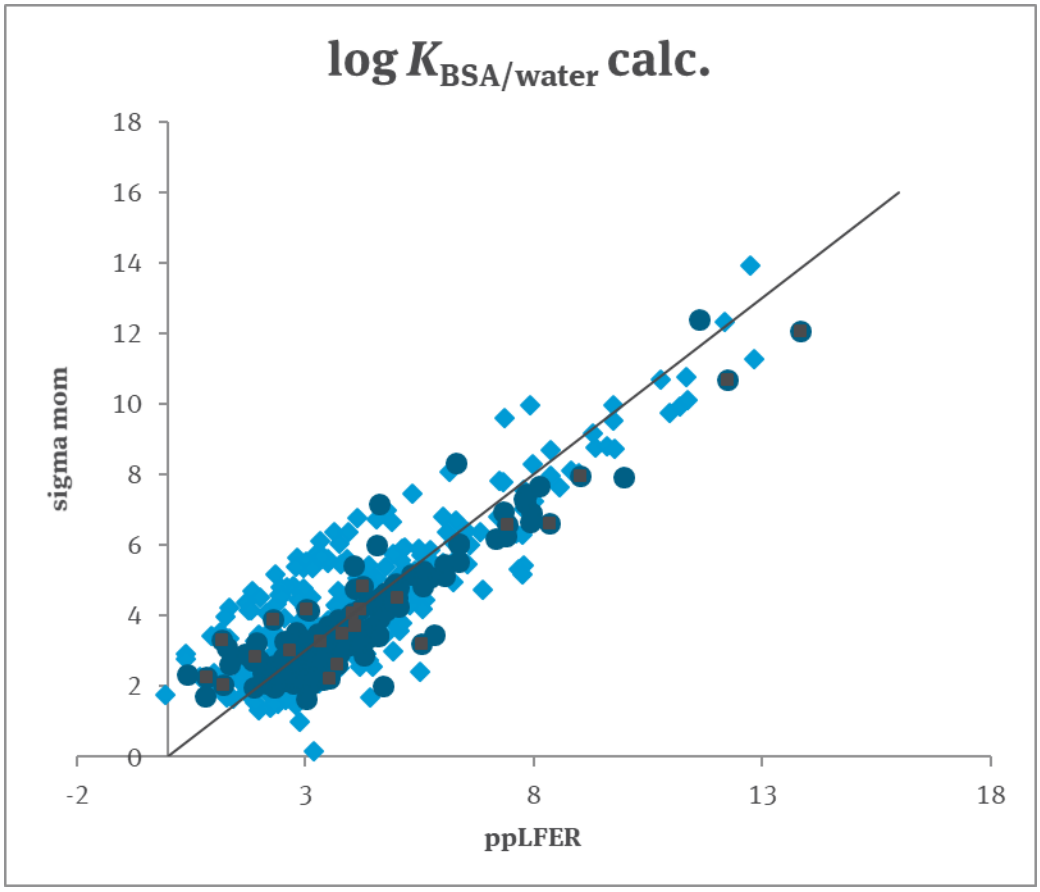

Source: UFZ, Leipzig.

Both figures clearly show a correlation between both models with log K values ranging from -1.1 to 14.79 and -0.06 and 13.82, respectively. Interestingly, the chemicals that have at least one highly unreliable calculated pp-LFER descriptor (warning levels 2c or 3, indicated in blue and black, respectively) show no clear trend in both figures, meaning that they are equally distributed around the 1:1 line and that they disappear in the overall scatter of the correlation. This overall scatter is markedly large; the difference between the predictions of both models can be three log units in extreme cases. This situation is somewhat unsatisfying because we cannot determine which model is closer to the true partition coefficients or which model is better for a specific set of chemicals (e.g., unfortunately, we suspect that both models have problems with fluorinated chemicals). Hence, it is difficult to decide which model should be used for our screening purpose. Thus, it has to be kept in mind for the further interpretation of the screening results that: a) some of the predicted values might be clearly over or under predicted, which can lead to undetected bioaccumulative chemicals in the screening and vice versa to false alarms, b) this situation can only be improved with more experimental data regarding the sorption to proteins and other biological important sorption matrices. Finally, for neutral chemicals we suggest to use a consensus modelling approach based on both the pp-LFER prediction as well as the MLR modelling approach based on sigma moments derived on the TZVP level (if only pp-LFER descriptors were available, the pp-LFER model was used alone).

A.6 Screening results

Figure 25: Comparison of log $K_{fish/water}$ for neutral and ionic spezies of each ionizable chemical (without considering the pH dependent fraction).

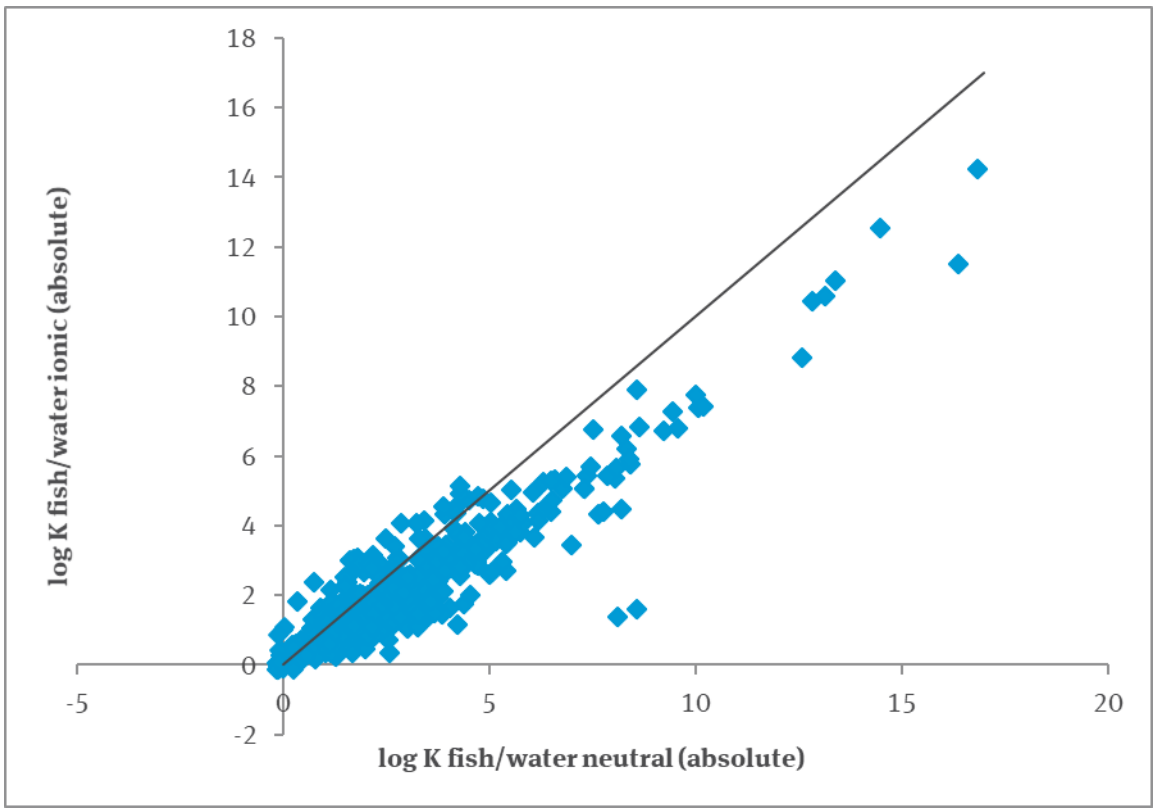

Source: UFZ, Leipzig.

Figure 26: Comparison of log $K_{fish/water}$ for neutral and ionic spezies of each ionizable chemical considering the pH dependent fraction at pH 7.

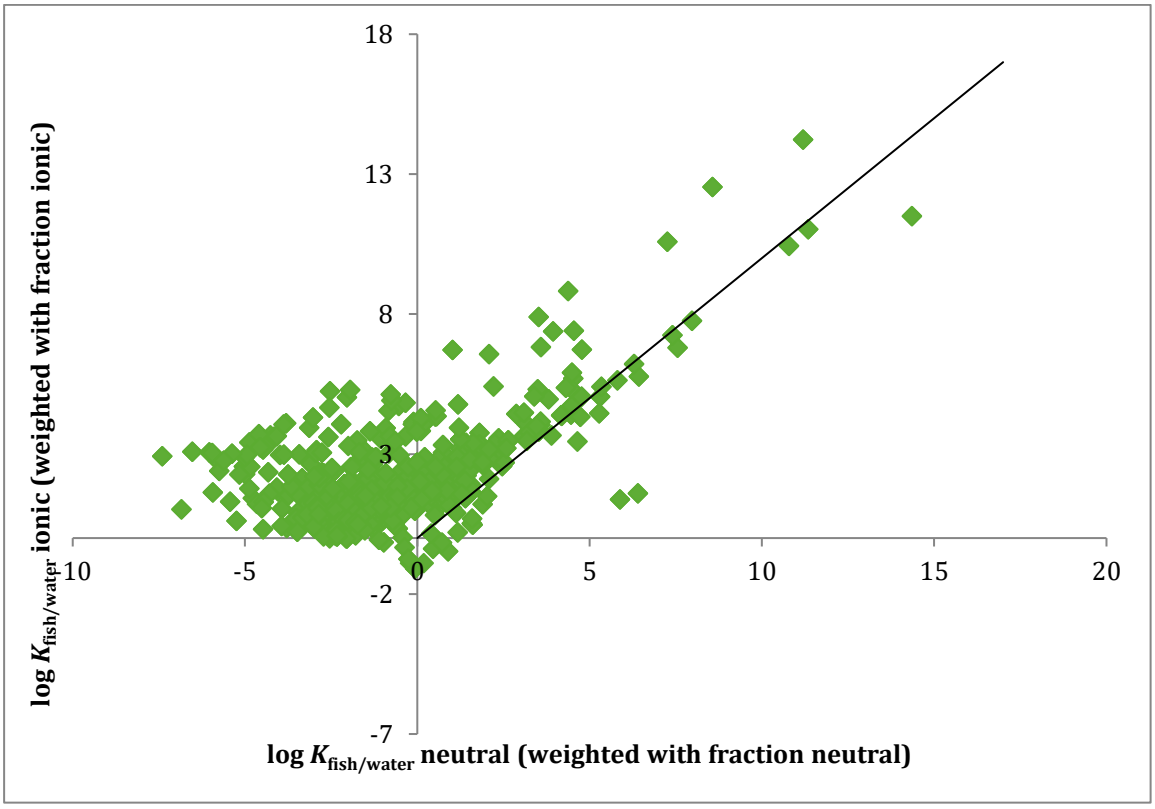

Source: UFZ, Leipzig.

Figure 27: log $K_{plasma\ proteins/water}$ values of anions versus log $K_{structural\ proteins/water}$ values of anions.

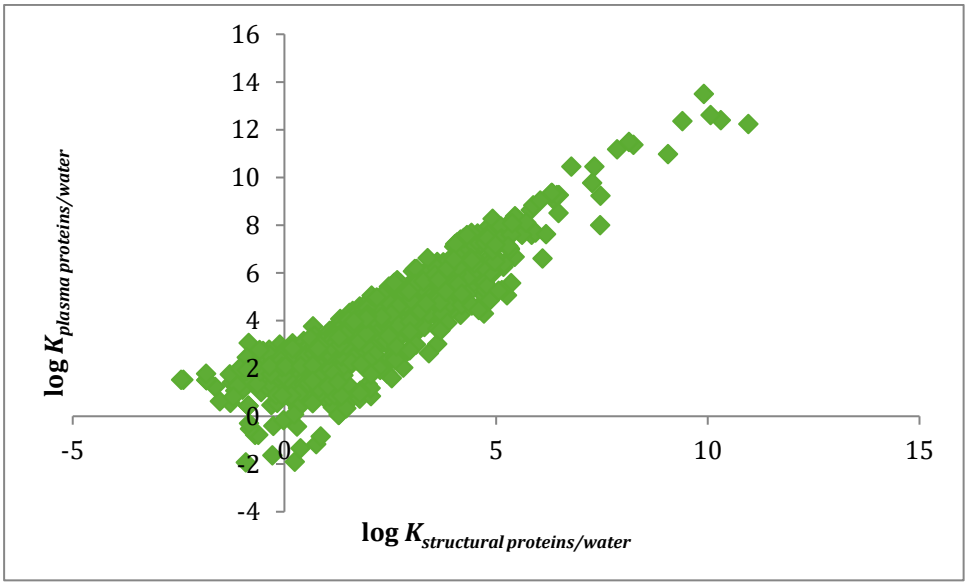

Source: UFZ, Leipzig.

Figure 28: log $K_{plasma\ proteins/water}$ values of anions versus log $K_{membranes/water}$ values of anions.

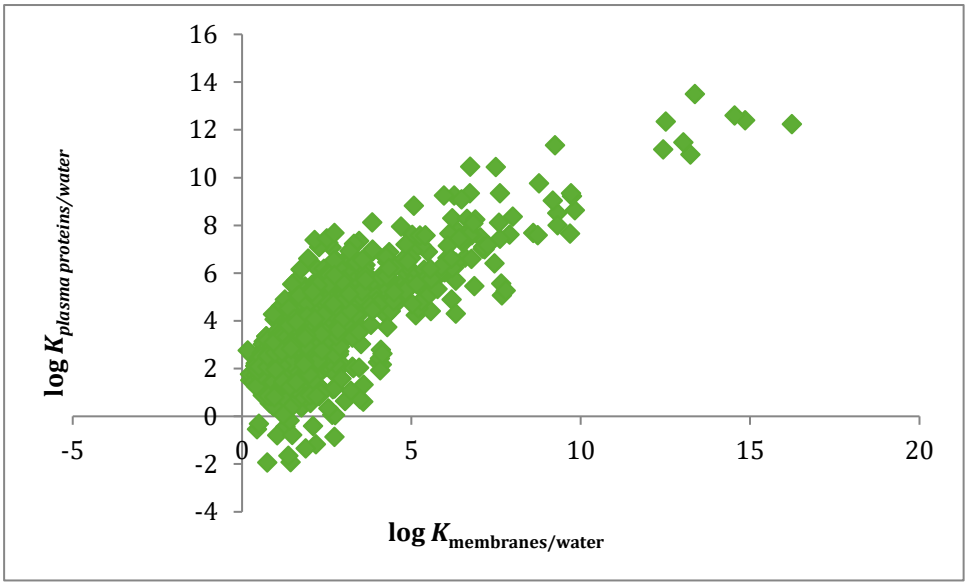

Source: UFZ, Leipzig.

Table 22: Summary of screening results.

	log $K_{fish/water}$ < 4		log $K_{fish/water}$ > 4	
n	1652		187	
Dominated structural proteins	169	10.23 %	12	6.42 %
Dominated plasma proteins	358	21.67 %	54	28.88 %
Dominated membranes	171	10.35 %	95	50.80 %

Table 23: Comparison between domination of plasma proteins and membranes and the chemical functional groups.

	log $K_{fish/water}$ < 4		log $K_{fish/water}$ > 4	
Sorption dominated by plasma proteins	358		54	
S based acid	78	21.79 %	27	50.00 %
C based acid	207	57.82 %	16	29.63 %
Aromatic	232	64.80 %	22	40.74 %
Aliphatic	207	57.82 %	32	59.26 %
Sorption dominated by membranes	171		95	
S based acid	12	7.02 %	22	23.16 %
C based acid	17	9.94 %	16	16.84 %
Aromatic	59	34.50 %	7	7.37 %
Aliphatic	112	65.50 %	88	92.63 %

B Appendix B: Supporting Information: Biomagnification Studies with IOCs

B.1 Instrumental Parameter for LC-MS/MS analyses of ionic compounds in biomagnification studies

B.1.1 Instrumental parameters

All measurements of the analysis of the ionic compounds where performed on a LC-MS/MS system operated in tandem MS/MS mode. Two different MS systems were used:

HPLC system (WATERS): Acquity UHPLC System

Mass spectrometer (WATERS):

- Benzotriazol:
  LC-MS/MS Xevo TQ-S Detector
- TBP, TMOA, Tecloftalam, Pentachlorophenol and MEE-Phosphonate:
  LC-MS/MS TQ-D Detector
- Software (WATERS): MICROMASS MassLynx
- Quantification software (WATERS): MICROMASS TargetLynx

Table 24: Overview of chromatographical conditions for analysis of TBP and TMOA in fish feed and fish samples in pre and main study.

	TBP and TMOA
Stationary phase	Preliminary study: ACUITY UPLCr BEH C18, 1,7 µm (Ser. no.: 03103734015120) Main study: ACUITY UPLCr BEH C8, 1,7 µm (Ser. no.: 01523901418385)
Mobile phases	Solvent A: preliminary study: 95 vol % H_2O, 5 vol % MeOH, 0.1 vol % formic acid main study: 95 vol % H_2O, 5 vol % MeOH, 2 mm ammonium acetate Solvent B: preliminary study: methanol, 0.1 vol% formic acid(v/v) main study: methanol, 2 mm ammonium acetate
Injection volume	10 µL
Column temperature	55 °C
Flow rate	250 µL/min
Gradient	Preliminary study: initial: 100 % A – 0 % B 0.50 min – 100 % A – 0 % B (curve 6) 7.00 min – 0 % A – 100 % B (curve 6) 8.00 min – 0 % A – 100 % B (curve 6) 8.10 min – 100 % A – 0 % B (curve 6) 10.0 min – 100 % A – 0 % B (curve 6) Main study: initial: 100 % A – 0 % B 0.50 min – 100 % A – 0 % B (curve 6) 10.0 min – 0 % A – 100 % B (curve 6) 12.0 min – 0 % A – 100 % B (curve 6) 15.0 min – 100 % A – 0 % B (curve 1)

Table 25: Overview of chromatographical conditions for analysis of Benzotriazol in fish feed and fish samples in pre and main study.

	Benzotriazol
Stationary phase	Preliminary study: ACUITY UPLCr BEH C18, 1.7 µm (Ser. no.: 03103734015122) Main study: ACUITY UPLCr BEH C8, 1.7 µm (Ser. no.: 01533910218301)
Mobile phases	Solvent A: 95 vol % H_2O, 5 vol % MeOH, 0.1 vol % formic acid Solvent B: preliminary study: methanol, 0.1 vol % formic acid (v/v)
Injection volume	Preliminary study: 20 µL Main study: 10 µL
Column temperature	55 °C
Flow rate	Preliminary study: 250 µL/min Main study: 150 µL/min
Gradient	Preliminary study: initial: 30 % A – 70 % B 0.50 min – 30 % A – 70 % B (curve 6) 10.0 min – 30 % A – 70 % B (curve 6) 13.0 min – 0 % A – 100 % B (curve 6) 14.0 min – 0 % A – 100 % B (curve 6) 14.1 min – 30 % A – 70 % B (curve 6) Main study: initial: 95 % A – 5 % B 0.50 min – 95 % A – 5 % B (curve 6) 1.00 min – 40 % A – 60 % B (curve 6) 8.00 min – 0 % A – 100 % B (curve 6) 10.0 min – 0 % A – 100 % B (curve 6) 10.1 min – 95 % A – 5 % B (curve 6) 12.0 min – 95 % A – 5 % B (curve 1)

Table 26: Overview of chromatographical conditions for analysis of Tecloftalam in fish feed and fish samples in pre and main study.

	Tecloftalam
Stationary phase	Preliminary study: ACUITY UPLCr BEH C18, 1.7 µm (Ser. no.: 02153301515703) Main study: ACUITY UPLCr BEH C18, 1.7 µm (Ser. no.: 03323904525133)
Mobile phases	Solvent A: 95 vol % H_2O, 5 vol % MeOH, 2 mm ammonium acetate Solvent B: methanol, 2 mm ammonium acetate
Injection volume	20 µL
Column temperature	55 °C
Flow rate	250 µL/min
Gradient	Preliminary study: initial: 100 % A – 0 % B 0.50 min – 100 % A – 0 % B (curve 6) 7.00 min – 0 % A – 100 % B (curve 6) 8.00 min – 0 % A – 100 % B (curve 6) 8.10 min – 100 % A – 0 % B (curve 6) 10.0 min – 100 % A – 0 % B (curve 6) Main study: initial: 80 % A – 20 % B 0.50 min – 80 % A – 20 % B (curve 6) 6.00 min – 0 % A – 100 % B (curve 6) 8.00 min – 0 % A – 100 % B (curve 6) 10.0 min – 80 % A – 20 % B (curve 1)

Table 27: Overview of chromatographical conditions for analysis of Pentachlorophenol in fish feed and fish samples in pre and main study.

	Pentachlorophenol
Stationary phase	Preliminary study: ACUITY UPLCr BEH C18, 1.7 µm (Ser. no.: 02153301515703) Main study: ACUITY UPLCr BEH C18, 1.7 µm (Ser. no.: 03323904525133)
Mobile phases	Solvent A: 95 vol % H_2O, 5 vol % MeOH, 2 mm ammonium acetate Solvent B: methanol, 2 mm ammonium acetate
Injection volume	20 µL
Column temperature	55 °C
Flow rate	250 µL/min
Gradient	Preliminary study: initial: 60 % A – 40 % B 0.50 min – 60 % A – 40 % B (curve 6) 7.00 min – 0 % A – 100 % B (curve 6) 8.00 min – 0 % A – 100 % B (curve 6) 8.10 min – 60 % A – 40 % B (curve 6) 10.0 min – 60 % A – 40 % B (curve 6) Main study: initial: 100 % A – 0 % B 0.50 min – 100 % A – 0 % B (curve 6) 10.0 min – 0 % A – 100 % B (curve 6) 12.0 min – 0 % A – 100 % B (curve 6) 15.0 min – 100 % A – 0 % B (curve 1)

Table 28: Overview of chromatographical conditions for analysis of MEE-Phosphonate in fish feed and fish samples in pre and main study.

	MEE-Phosphonate
Stationary phase	Preliminary study: ACUITY UPLCr BEH C18, 1.7 µm (Ser. no.: 02153301515703) Main study: ACUITY UPLCr BEH C18,1.7 µm (Ser. no.: 03323904525133)
Mobile phases	Solvent A: 95 vol % H_2O, 5 vol % MeOH, 2 mm ammonium acetate Solvent B: methanol, 2 mm ammonium acetate
Injection volume	20 µL
Column temperature	55 °C
Flow rate	250 µL/min
Gradient	Preliminary study: initial: 100 % A – 0 % B 0.50 min – 100 % A – 0 % B (curve 6) 2.00 min – 0 % A – 100 % B (curve 6) 8.00 min – 0 % A – 100 % B (curve 6) 8.10 min – 100 % A – 0 % B (curve 6) 10.0 min – 100 % A – 0 % B (curve 6) Main study: initial: 100 % A – 0 % B 0.50 min – 100 % A – 0 % B (curve 6) 10.0 min – 0 % A – 100 % B (curve 6) 12.0 min – 0 % A – 100 % B (curve 6) 15.0 min – 100 % A – 0 % B (curve 1)

Table 29: MS parameter for ionic compounds.

With SIM = single ion recording mode, MRM = multiple reaction monitoring mode, Temp. = temperature, Delv. = desolvation, LM = low mass, HM = high mass.

c	TBP/TMOA	Benzotriazol	Tecloftalam	Pentachlorophenol	MEE-Phosphonate
Type	MRM	Preliminary study: SIM Main study: MRM	MRM	preliminary study: SIM main study: MRM	MRM
Span [Da]	0.2	0.0	0.2	0.0	0.2
Ion mode	ES+	ES-	ES-	ES-	ES-
Capillary [kV]	0.6	2.4	0.2	0.5	2.8
Cone [V]	45.0	60.0	39.0	50.0	35.0
Source temp. [°C]	120	150	150	150	120
Desolv. temp. [°C]	350	200	350	350	350
Cone gas flow [L h^{-1}]	50.0	150	10	50	100
Desolv. gas flow [L h^{-1}]	500	550	650	650	500
LM 1/HM 1 resolution	15.0/15.0	3.0/15.0	15.0/15.0	15.0/15.0	8.0/12.0
Ion energy 1	0.5	0.9	1.0	1.0	0.2
LM 2/HM 2 resolution	15.0/15.0	3.0/15.3	15.0/15.0	15.0/15.0	8.0/10.0
Ion energy 2	0.5	0.2	1.0	1.0	8.0
Multiplier gain	1.0	0.1	1.0	1.0	2.0

Table 30: Mass transitions for ionic compounds.

With quan. = quantifier, qual. = qualifier, SIM = single ion recording mode, MRM = multiple reaction monitoring mode.

c	Parent ion [m z-1]	Daughter ion [m z-1]	Dwell time [sec]	Collision energy [eV]
TBP (quan.)	259.26	75.85	0.20	35.0
TBP (qual.)	259.26	89.91	0.20	35.0
TMOA (quant.)	312.36	59.80	0.20	30.0
TMOA (qual.)	312.36	70.84	0.20	30.0
Benzotriazol (SIM) Benzotriazol (MRM)	338.14 338.14	--- 338.14	0.33 0.33	--- 20.0
Tecloftalam	399.81	213.01	0.20	19
Pentachlorophenol (SIM) Pentachlorophenol (MRM)	262.84 262.84	--- 262.84	0.50 0.50	--- 20
MEE-Phosphonate (quant.)	305.22	174.86	0.20	35
MEE-Phosphonate (qual.)	305.22	193.06	0.20	35

B.1.2 Raw data for fish feed concentrations

Table 31: Content on fish feed for stability measurements during preliminary study.

Substances	14 days			End of uptake		
	Content in feed samples [mg/kg]	Mean [mg/kg]	RSD [%]	Content in feed samples [mg/kg]	Mean [mg/kg]	RSD [%]
TBP	---	---	---	18.39		
	---	---	---	23.44	21.1	9.85
	---	---	---	21.55		
TMOA	---	---	---	24.20		
	---	---	---	24.26	23.0	7.43
	---	---	---	20.60		
Benzotriazol	27.62	29.1	3.92	27.11	28.5	4.44
	30.40			30.15		
	29.16			28.15		
Tecloftalam	20.98	21.0	7.67	19.28	20.4	4.61
	23.00			21.58		
	19.05			20.26		
Pentachlorophenol	22.44	21.9	2.44	21.26	23.5	6.91
	22.15			25.02		
	21.19			24.27		
MEE-Phosphonate	34.74	34.7	14.5	31.15	31.9	1.73
	28.55			31.97		
	40.85			32.49		

Table 32: Content on fish feed for stability measurements during main study.

Substances	14 days			End of uptake		
	Content in feed samples [mg/kg]	Mean [mg/kg]	RSD [%]	Content in feed samples [mg/kg]	Mean [mg/kg]	RSD [%]
TBP	24.31	23.5	3.75	26.09	25.9	0.69
	23.94			26.02		
	22.28			25.68		
TMOA	25.25	24.9	2.54	23.86	22.3	4.81
	25.43			21.71		
	24.01			21.47		
Benzotriazol	34.52	34.7	3.87	26.87	28.3	4.31
	36.48			28.21		
	33.21			29.85		
Tecloftalam	27.61	27.04	8.72	23.86	26.5	7.47
	29.61			27.10		
	23.91			28.61		
Pentachlorophenol	21.00	23.0	7.91	18.19	18.61	3.55
	23.62			18.26		
	24.51			19.37		
MEE-Phosphonate	34.06	36.3	6.34	30.11	26.9	8.46
	35.28			25.81		
	39.43			24.88		

B.1.3 Biological raw data in main study

Table 33: Sample weights of TBP and TMOA treated group in main study.

	No.	Total body [g]	GIT [g]	Liver [g]	Carcass [g]
	1	7.001	0.6437	0.1082	5.884
uptake	2	7.851	0.6163	0.0849	6.803
7 d	3	6.580	0.5910	0.0985	5.616
	4	6.309	0.5784	0.0882	5.340
	5	5.990	0.5262	0.0961	5.077
mean		**6.746**	**0.5911**	**0.0952**	**5.744**
	1	7.593	0.5311	0.1312	6.530
uptake	2	9.565	0.5979	0.1597	8.458
14 d	3	5.524	0.3725	0.0872	4.796
	4	6.227	0.3836	0.1209	5.406
	5	8.963	0.4877	0.1363	7.783
mean		**7.574**	**0.4746**	**0.1270**	**6.595**
	1	8.652	0.6583	0.0944	7.062
depuration	2	8.889	0.5904	0.1283	7.443
10 h	3	7.217	0.5756	0.1010	5.850
	4	9.469	0.7830	0.1526	7.489
	5	9.577	0.7243	0.1192	7.912
mean		**8.761**	**0.6663**	**0.1191**	**7.151**
	1	7.090	0.6221	0.1257	8.951
depuration	2	6.746	0.4630	0.0652	5.928
24 h	3	5.926	0.4602	0.0792	5.240
	4	8.546	0.6455	0.1021	7.379
	5	10.200	0.7730	0.1826	8.526
mean		**7.701**	**0.5928**	**0.1109**	**7.205**
	1	7.265	0.6135	0.1101	6.211
depuration	2	7.670	0.4410	0.1100	6.759
48 h	3	5.508	0.3255	0.0531	4.943

	No.	Total body [g]	GIT [g]	Liver [g]	Carcass [g]
	4	6.596	0.4536	0.0803	5.784
	5	7.450	0.5359	0.0747	6.467
mean		**6.898**	**0.4739**	**0.0856**	**6.033**
	1	6.789	0.4600	0.1155	5.870
depuration	2	8.146	0.5998	0.1326	7.110
72 h	3	9.507	0.7172	0.1182	8.000
	4	10.415	0.6301	0.1616	8.989
	5	13.124	0.9005	0.2404	11.176
mean		**9.596**	**0.6615**	**0.1537**	**8.229**
	1	8.126	0.4869	0.1173	7.189
depuration	2	10.123	0.7483	0.1454	8.874
168 h	3	8.873	0.6231	0.1068	7.542
	4	9.584	0.7733	0.1393	8.294
	5	10.850	0.7188	0.1562	9.379
mean		**9.511**	**0.6701**	**0.1330**	**8.256**
	1	9.309	0.7654	0.1418	7.963
depuration	2	9.276	0.7015	0.1456	8.141
336 h	3	10.211	0.8321	0.1724	8.810
	4	11.027	0.8837	0.1849	9.293
	5	9.860	0.7191	0.1557	8.455
mean		**9.936**	**0.7803**	**0.1601**	**8.532**

Table 34: Sample weights of Benzotriazol and Tecloftalam treated group in main study.

	No.	Total body [g]	GIT [g]	Liver [g]	Carcass [g]
	1	6.359	0.6266	0.1026	5.397
uptake	2	5.977	0.4576	0.1182	5.050
7 d	3	7.626	0.4917	0.1250	6.593
	4	5.904	0.4274	0.0684	5.178
	5	7.733	0.5899	0.0942	6.649
mean		**6.720**	**0.5186**	**0.10168**	**5.773**
	1	6.348	0.4603	0.1085	5.383
uptake	2	8.395	0.6239	0.1403	7.290
14 d	3	8.878	0.6153	0.1217	7.541
	4	10.867	0.7198	0.1668	9.449
	5	8.286	0.5671	0.1080	7.272
mean		**8.555**	**0.5973**	**0.1291**	**7.387**
	1	10.218	0.7081	0.1390	8.771
depuration	2	9.113	0.6856	0.1175	7.695
10 h	3	8.773	0.6077	0.1405	7.207
	4	10.777	0.7753	0.1579	9.372
	5	8.611	0.7085	0.0887	6.975
mean		**9.498**	**0.6970**	**0.1287**	**8.004**
	1	9.666	0.7154	0.1262	8.279
depuration	2	9.882	0.6587	0.1418	8.504
24 h	3	10.040	0.7316	0.1565	8.523
	4	8.582	0.5716	0.1574	7.386
	5	7.152	0.5613	0.1153	5.988
mean		**9.065**	**0.6477**	**0.1394**	**7.736**
	1	5.592	0.3937	0.0730	4.931
depuration	2	11.429	0.7793	0.1980	9.819
48 h	3	7.933	0.4234	0.1214	7.070
	4	10.303	0.7212	0.1553	8.681

	No.	Total body [g]	GIT [g]	Liver [g]	Carcass [g]
	5	15.968	0.8229	0.1688	9.679
mean		**10.245**	**0.6281**	**0.1433**	**8.036**
	1	7.600	0.6400	0.1126	6.435
depuration	2	9.161	0.6925	0.1150	7.937
72 h	3	9.905	0.7031	0.1364	8.503
	4	8.331	0.5900	0.1212	7.073
	5	12.866	0.7294	0.1512	11.267
mean		**9.572**	**0.6710**	**0.1273**	**8.243**
	1	8.155	0.6939	0.0965	7.009
depuration	2	9.350	0.7236	0.0977	8.053
168 h	3	9.665	0.6337	0.0919	8.552
	4	12.865	1.0046	0.2022	10.950
	5	11.980	0.7864	0.1622	10.423
mean		**10.403**	**0.7684**	**0.1301**	**8.997**
	1	9.504	0.6906	0.1436	8.242
depuration	2	9.633	0.8652	0.1474	8.360
336 h	3	9.826	0.8449	0.1354	8.387
	4	12.099	0.9194	0.1773	10.127
	5	---	---	---	---
mean		**10.265**	**0.8300**	**0.1509**	**8.779**

Table 35: Sample weights of Pentachlorophenol and MEE-Phosphonate treated group in main study.

	No.	Total body [g]	GIT [g]	Liver [g]	Carcass [g]
	1	10.903	0.7464	0.1592	9.564
uptake	2	6.564	0.4459	0.0843	5.724
7 d	3	8.052	0.6020	0.1163	6.799
	4	7.152	0.5845	0.1030	6.180
	5	7.624	0.5266	0.0851	6.364
mean		**8.059**	**0.5811**	**0.1096**	**6.926**
	1	10.240	0.8238	0.1803	8.693
uptake	2	11.115	0.7714	0.2140	9.403
14 d	3	8.293	0.5626	0.1250	7.119
	4	8.720	0.6237	0.1823	7.389
	5	10.587	0.8710	0.1319	9.144
mean		**9.791**	**0.7305**	**0.1667**	**8.349**
	1	9.041	0.6027	0.1014	7.606
depuration	2	10.812	0.8221	0.1422	8.820
10 h	3	11.426	0.6348	0.1602	9.753
	4	11.508	0.8727	0.1770	9.274
	5	8.650	0.5516	0.1249	7.078
mean		**10.287**	**0.6968**	**0.1411**	**8.506**
	1	8.388	0.4509	0.0962	7.617
depuration	2	8.134	0.5456	0.1412	7.022
24 h	3	8.048	0.5863	0.1270	6.961
	4	10.316	0.7231	0.1737	8.711
	5	13.321	0.9045	0.2185	11.241
mean		**9.641**	**0.6421**	**0.1513**	**8.310**
	1	12.905	0.9306	0.2323	11.084
depuration	2	9.627	0.6871	0.1270	8.447
48 h	3	8.535	0.5214	0.1718	7.383
	4	9.361	0.7671	0.1362	8.048

	No.	Total body [g]	GIT [g]	Liver [g]	Carcass [g]
	5	13.529	0.9125	0.2231	11.705
mean		**10.791**	**0.7637**	**0.1781**	**9.333**
	1	8.984	0.6354	0.1945	7.668
depuration	2	9.766	0.8365	0.1336	8.163
72 h	3	11.009	0.7369	0.1529	9.792
	4	13.204	0.8052	0.2117	11.637
	5	13.370	0.8211	0.1965	11.656
mean		**11.267**	**0.7670**	**0.1779**	**9.783**
	1	12.389	0.9318	0.1626	10.771
depuration	2	13.251	0.9918	0.1813	11.615
168 h	3	11.613	0.6127	0.1461	9.995
	4	13.398	1.0974	0.1972	11.361
	5	13.318	1.2278	0.1918	11.261
mean		**12.794**	**0.9723**	**0.1758**	**11.001**
	1	10.668	0.8163	0.1421	9.040
depuration	2	10.233	0.8513	0.1677	8.695
336 h	3	14.800	1.2622	0.2486	12.313
	4	14.014	1.3249	0.2102	12.053
	5	16.694	1.4807	0.2980	13.978
mean		**13.282**	**1.1471**	**0.2133**	**11.216**

B.1.4 Raw data of test item concentrations in analyzed fish samples (main study)

Table 36: Analytical results of TBP in fish matrices in the main study.

* = ½ LOQ (with LOQ = 0.050 µg/L).

With LOQ = 0.050 µg/L corresponding to 0.01 mg/kg for GIT, 0.01 mg/kg for liver and 0.002 mg/kg for carcass

Phase	Sampling	Compartment	Ext. mass [g]	Content [mg/kg]	Mean [mg/kg]	RSD [%]
			0.6437	0.3657		
			0.6163	0.3318		
		GIT	0.5910	0.5897	0.4037	24.7
			0.5784	0.3124		
			0.5262	0.4191		
			0.1082	0.0311		
			0.0849	0.0360		
uptake	7 d	liver	0.0985	0.0305	0.0362	24.1
			0.0882	0.0531		
			0.0961	0.0302		
			0.5321	0.0023		
			0.5247	0.0025		
		carcass	0.5693	0.0026	0.0022	28.6
			0.5221	0.0010*		
			0.5469	0.0026		
				whole fish	**0.0396**	
			0.53108	0.2277		
			0.59788	0.3251		
		GIT	0.37253	0.5621	0.3620	33.8
			0.38364	0.4341		
			0.48767	0.2609		
			0.13119	0.1287		
			0.15966	0.1154		
uptake	14 d	liver	0.08716	0.0503	0.0769	49.0
			0.12094	0.0557		
			0.13626	0.0346		

Phase	Sampling	Compartment	Ext. mass [g]	Content [mg/kg]	Mean [mg/kg]	RSD [%]
			0.5110	0.0043		
			0.4974	0.0182		
		carcass	0.5449	0.0117	0.0093	54.3
			0.5431	0.0066		
			0.5507	0.0060		
				whole fish	**0.0338**	
			0.65834	0.4081		
			0.59037	0.7970		
		GIT	0.57556	0.9327	0.9062	37.1
			0.78300	1.6042		
			0.72428	0.7891		
			0.09438	0.0053*		
			0.12829	0.0477		
depuration	10 h	liver	0.10098	0.0182	0.0347	64.8
			0.15255	0.0326		
			0.11920	0.0696		
			0.4984	0.0010*		
			0.4843	0.0010*		
		carcass	0.5269	0.0026	0.0024	56.5
			0.5164	0.0025		
			0.5576	0.0046		
				whole fish	**0.0787**	
			0.62210	0.3503		
			0.46299	0.3389		
		GIT	0.46018	1.3759	0.5093	85.7
			0.64550	0.2786		
			0.77303	0.2027		
			0.12571	0.0040*		
			0.06524	0.0077*		

Phase	Sampling	Compartment	Ext. mass [g]	Content [mg/kg]	Mean [mg/kg]	RSD [%]
depuration	24 h	liver	0.07915	0.0152	0.0077	51.8
			0.10209	0.0049*		
			0.18255	0.0066		
			0.5206	0.0010*		
			0.5307	0.0009*		
		carcass	0.5043	0.0020	0.0011	36.4
			0.5516	0.0009*		
			0.5261	0.0010*		
				whole fish	**0.0393**	
			0.61353	0.3004		
			0.44099	0.2900		
		GIT	0.32548	0.5198	0.3733	22.1
			0.45355	0.3862		
			0.53592	0.3698		
			0.11011	0.0045*		
			0.10998	0.0045*		
depuration	48 h	liver	0.05311	0.0094*	0.0110	60.1
			0.08025	0.0147		
			0.07466	0.0220		
		carcass			< LOQ	
				whole fish	**0.0270**	
			0.45996	0.2307		
			0.59983	0.2842		
		GIT	0.71718	0.1546	0.2556	30.3
			0.63008	0.3867		
			0.90046	0.2215		
			0.11553	0.0043*		
			0.13264	0.0038*		
depuration	72 h	liver	0.11819	0.0042*	0.0052	53.2

Phase	Sampling	Compartment	Ext. mass [g]	Content [mg/kg]	Mean [mg/kg]	RSD [%]
			0.16160	0.0031*		
			0.24037	0.0107		
		carcass			< LOQ	
				whole fish	**0.0188**	
			0.48685	0.1687		
			0.74834	0.0951		
		GIT	0.6231	0.1965	0.1296	34.6
			0.77326	0.0810		
			0.7188	0.1069		
			0.11734	0.01398		
			0.14543	0.01183		
depuration	168 h	liver	0.10682	0.00468*	0.0087	47.6
			0.13926	0.00962		
			0.15616	0.00320*		
		carcass			< LOQ	
				whole fish	**0.0097**	
			0.76535	0.0540		
			0.70148	0.0963		
		GIT	0.83205	0.0876	0.0727	22.4
			0.88373	0.0652		
			0.7191	0.0606		
depuration	336 h	liver			< LOQ	
		carcass			< LOQ	
				whole fish	**0.0060**	

Table 37: Analytical results of TMOA in fish matrices in the main study.

With LOQ = 0.025 µg/L corresponding to 0.02 mg/kg for GIT, 0.007 mg/kg for liver and 0.002 mg/kg for carcass

Phase	Sampling	Compartment	Ext. mass [g]	Content [mg/kg]	Mean [mg/kg]	RSD [%]
			0.6437	8,6947		
			0.6163	4.3901		
		GIT	0.5910	6.6315	6.3379	23.9
			0.5784	6.9212		
			0.5262	5.0521		
			0.1082	0.4993		
			0.0849	0.4888		
uptake	7 d	liver	0.0985	0.4323	0.5595	32.4
			0.0882	0.9186		
			0.0961	0.4585		
			0.5321	0.0196		
			0.5247	0.0222		
		carcass	0.5693	0.0310	0.0230	18.7
			0.5221	0.0189		
			0.5469	0.0232		
				whole fish	**0.6114**	
			0.53108	9.2174		
			0.59788	9.2139		
		GIT	0.37253	9.2385	8.2331	20.2
			0.38364	8.5434		
			0.48767	4.9525		
			0.13119	1.2996		
			0.15966	1.1647		
uptake	14 d	liver	0.08716	0.8176	1.0178	18.7
			0.12094	0.9851		
			0.13626	0.8220		
			0.5110	0.0570		
			0.4974	0.0913		

Phase	Sampling	Compartment	Ext. mass [g]	Content [mg/kg]	Mean [mg/kg]	RSD [%]
		carcass	0.5449	0.1131	0.0862	23.7
			0.5431	0.1003		
			0.5507	0.0694		
				whole fish	**1.3148**	
			0.65834	11.0800		
			0.59037	12.4437		
		GIT	0.57556	12.9710	14.8504	22.6
			0.783	18.6554		
			0.72428	19.1020		
			0.09438	0.8898		
			0.12829	2.1364		
depuration	10 h	liver	0.10098	1.1208	1.3474	31.4
			0.15255	1.2454		
			0.11920	1.3448		
			0.4984	0.0543		
			0.4843	0.0517		
		carcass	0.5269	0.0559	0.0531	6.4
			0.5164	0.0472		
			0.5576	0.0563		
				whole fish	**1.3148**	
			0.62210	8.9979		
			0.46299	7.5008		
		GIT	0.46018	8.1307	9.5158	30.9
			0.6455	15.2998		
			0.77303	7.6499		
			0.12571	0.7629		
			0.06524	1.0432		
depuration	24 h	liver	0.07915	0.8440	0.8723	12.6
			0.10209	0.7619		

Phase	Sampling	Compartment	Ext. mass [g]	Content [mg/kg]	Mean [mg/kg]	RSD [%]
			0.18255	0.9495		
			0.5206	0.0655		
			0.5307	0.0643		
		carcass	0.5043	0.0635	0.0598	11.4
			0.5516	0.0471		
			0.5261	0.0584		
				whole fish	**0.7799**	
			0.61353	11.0990		
			0.44099	8.4138		
		GIT	0.32548	5.0461	8.3214	24.4
			0.45355	7.5017		
			0.53592	9.5462		
			0.11011	1.2070		
			0.10998	0.9444		
depuration	48 h	liver	0.05311	0.8778	0.9719	16.0
			0.08025	1.0734		
			0.16882	0.7569		
			0.4930	0.0540		
			0.5028	0.0459		
		carcass	0.5581	0.0379	0.0513	22.8
			0.5312	0.0463		
			0.5334	0.0723		
				whole fish	**0.6577**	
			0.45996	4.5621		
			0.59983	12.6703		
		GIT	0.71718	6.1385	6.7589	45.4
			0.63008	4.1734		
			0.90046	6.2501		
			0.11553	0.7325		

Phase	Sampling	Compartment	Ext. mass [g]	Content [mg/kg]	Mean [mg/kg]	RSD [%]
			0.13264	1.1377		
depuration	72 h	liver	0.11819	0.9449	0.9127	14.7
			0.16160	0.9120		
			0.24037	0.8365		
			0.5331	0.0533		
			0.5391	0.0925		
		carcass	0.4907	0.0404	0.0574	31.5
			0.4930	0.0516		
			0.5299	0.0492		
				whole fish	**0.5621**	
			0.48685	3.6251		
			0.74834	2.7625		
		GIT	0.6231	4.3770	3.8663	38.2
			0.77326	6.4050		
			0.7188	2.1619		
			0.11734	0.5911		
			0.14543	0.5977		
depuration	168 h	liver	0.10682	0.9873	0.7512	22.5
			0.13926	0.9224		
			0.15616	0.6574		
			0.11734	0.0372		
			0.14543	0.0333		
		carcass	0.10682	0.0403	0.0391	8.9
			0.13926	0.0431		
			0.15616	0.0415		
				whole fish	**0.3326**	
			0.76535	0.3234		
			0.70148	1.0982		
		GIT	0.83205	0.3144	0.5339	60.3

Phase	Sampling	Compartment	Ext. mass [g]	Content [mg/kg]	Mean [mg/kg]	RSD [%]
			0.88373	0.6891		
			0.7191	0.2445		
			0.14175	0.4545		
			0.1456	0.3231		
depuration	336 h	liver	0.17235	0.2349	0.3184	24.5
			0.18491	0.3303		
			0.1557	0.2495		
			0.5132	0.0420		
			0.4759	0.0369		
		carcass	0.5042	0.0274	0.0315	21.6
			0.4982	0.0274		
			0.5149	0.0239		
				whole fish	**0.0778**	

Table 38: Analytical results of Benzotriazol in fish matrices in the main study.

* = ½ LOQ

with LOQ = 1.00 µg/L corresponding to 0.17 mg/kg for GIT, 0.25 mg/kg for liver and 0.07 mg/kg for carcass

Phase	Sampling	Compartment	Ext. mass [g]	Content [mg/kg]	Mean [mg/kg]	RSD [%]
			0.6266	0.52617		
			0.4576	1.00852		
		GIT	0.4917	0.72219	0.6178	49.8
			0.4274	0.74754		
			0.5899	0.08476*		
			0.1026	0.76365		
			0.1182	3.77369		
uptake	7 d	liver	0.1250	1.65960	2.7557	48.7
			0.0684	3.21857		
			0.0942	4.36306		
			0.4949	1.18254		
			0.5035	1.47480		
		carcass	0.5053	1.29903	1.2307	17.1
			0.5503	0.85343		
			0.5031	1.34391		
				whole fish	**1.2053**	
			0.46029	1.78800		
			0.62389	0.44880		
		GIT	0.61527	0.69059	0.6657	89.3
			0.71983	0.31299		
			0.56705	0.08818*		
			0.10848	3.97907		
			0.14032	1.73995		
uptake	14 d	liver	0.12174	4.70963	3.2658	31.4
			0.16680	3.22542		
			0.10803	2.67472		
			0.51250	1.41588		

Phase	Sampling	Compartment	Ext. mass [g]	Content [mg/kg]	Mean [mg/kg]	RSD [%]
			0.55120	1.05290		
		carcass	0.53550	1.40011	1.0198	35.6
			0.53380	0.49239		
			0.51230	0.73761		
				whole fish	**1.0294**	
		GIT			< LOQ	
			0.13900	2.35360		
			0.11749	3.11686		
depuration	10 h	liver	0.14049	0.67443	1.8334	65.1
			0.15790	0.15833*		
			0.08868	2.86367		
			0.5069	0.68495		
			0.4966	0.72388		
		carcass	0.5436	0.18389	0.5994	34.9
			0.5331	0.73630		
			0.5128	0.66786		
				whole fish	**0.5700**	
		GIT			< LOQ	
			0.12619	0.61693		
			0.14177	1.83889		
depuration	24 h	liver	0.15654	1.32905	1.0791	42.2
			0.15736	0.67330		
			0.11530	0.93755		
			0.54580	0.19597		
			0.50830	0.46382		
		carcass	0.50500	0.47794	0.3796	26.8
			0.49250	0.40317		
			0.53890	0.35688		
				whole fish	**0.3622**	

Phase	Sampling	Compartment	Ext. mass [g]	Content [mg/kg]	Mean [mg/kg]	RSD [%]
		GIT			< LOQ	
			0.07300	0.34247		
			0.19701	0.28323		
depuration	48 h	liver	0.12139	0.20595*	0.3564	29.9
			0.15525	0.49082		
			0.16882	0.45937		
			0.5497	0.03638*		
			0.5069	0.08609		
		carcass	0.5097	0.10532	0.0838	34.1
			0.5290	0.11894		
			0.5572	0.07243		
				whole fish	**0.0823**	

Table 39: Analytical results of Tecloftalam in fish matrices in the main study.

* = ½ LOQ

with LOQ = 0.25 µg/L corresponding to 0.007 mg/kg for GIT, 0.04 mg/kg for liver and 0.01 mg/kg for carcass

Phase	Sampling	Compartment	Ext. mass [g]	Content [mg/kg]	Mean [mg/kg]	RSD [%]
			0.6266	0.3737		
			0.4576	0.9700		
		GIT	0.4917	0.7248	0.5974	37.3
			0.4274	0.4120		
			0.5899	0.5067		
			0.1026	0.0772		
			0.1182	0.1068		
uptake	7 d	liver	0.1250	0.1022	0.1309	34.3
			0.0684	0.1915		
			0.0942	0.1769		
		carcass			< LOQ	
				whole fish	**0.0505**	
			0.46029	0.5252		
			0.62389	0.6180		
		GIT	0.61527	0.4078	0.4950	14.5
			0.71983	0.4594		
			0.56705	0.4644		
			0.10848	0.1597		
			0.14032	0.1088		
uptake	14 d	liver	0.12174	0.1525	0.1274	23.5
			0.16680	0.0789		
			0.10803	0.1374		
			0.5125	0.004878*		
			0.5512	0.004536*		
		carcass	0.5355	0.004669*	0.00758	46.9
			0.5338	0.012552		
			0.5123	0.011243		

Phase	Sampling	Compartment	Ext. mass [g]	Content [mg/kg]	Mean [mg/kg]	RSD [%]
				whole fish	**0.0454**	
			0.70808	0.07299		
			0.68562	0.06476		
		GIT	0.60769	0.05210	0.0903	46.3
			0.77528	0.16993		
			0.70847	0.09192		
			0.13900	0.04201		
			0.11749	0.02128*		
depuration	10 h	liver	0.14049	0.01779*	0.0586	108
			0.15790	0.18379		
			0.08868	0.02819*		
		carcass			< LOQ	
				whole fish	**0.0080**	
			0.71538	0.014622		
			0.65867	0.072874		
		GIT	0.73156	0.007245	0.0218	118
			0.57158	0.004374*		
			0.56128	0.009977		
depuration	24 h	liver			< LOQ	
		carcass			< LOQ	
				whole fish	**0.0017**	
			0.39373	0.00635*		
			0.77926	0.00321*		
		GIT	0.42339	0.00590*	0.0049	29.9
			0.72116	0.00607		
			0.82285	0.00304*		
depuration	48 h	liver			< LOQ	
		carcass			< LOQ	
				whole fish	**0.0001**	

Table 40: Analytical results of Pentachlorophenol in fish matrices in the main study.

* = ½ LOQ

with LOQ = 0.25 µg/L corresponding to 0.02 mg/kg for GIT, 0.03 mg/kg for liver and 0.01 mg/kg for carcass

Phase	Sampling	Compartment	Ext. mass [g]	Content [mg/kg]	Mean [mg/kg]	RSD [%]
			0.74640	1.3939		
			0.44590	0.9818		
		GIT	0.60200	2.3837	1.8702	38.9
			0.58450	1.5851		
			0.52660	3.0065		
			0.1592	0.23317		
			0.0843	0.35469		
uptake	7 d	liver	0.1163	0.74910	0.5806	41.0
			0.1030	0.75981		
			0.0851	0.80611		
			0.5108	0.015818		
			0.5026	0.050298		
		carcass	0.5010	0.104910	0.0591	48.3
			0.5032	0.061924		
			0.5197	0.062459		
				whole fish	**0.2048**	
			0.82378	1.56692		
			0.77143	1.29616		
		GIT	0.56263	1.30885	1.3363	8.9
			0.62371	1.28569		
			0.87096	1.22405		
			0.18034	0.81746		
			0.21399	0.56330		
uptake	14 d	liver	0.12501	1.19238	0.8322	26.0
			0.18231	0.67226		
			0.13191	0.91578		
			0.54090	0.03683		

Phase	Sampling	Compartment	Ext. mass [g]	Content [mg/kg]	Mean [mg/kg]	RSD [%]
			0.49710	0.10626		
		carcass	0.53550	0.07268	0.0736	40.3
			0.52540	0.10742		
			0.50520	0.04481		
				whole fish	**0.1870**	
			0.60267	0.26947		
			0.82207	0.64630		
		GIT	0.63484	0.46957	0.5507	34.1
			0.87265	0.83642		
			0.55157	0.53157		
			0.10135	0.09038		
			0.14222	0.43201		
depuration	10 h	liver	0.16020	0.28327	0.3147	40.0
			0.17700	0.33571		
			0.12485	0.43220		
			0.5338	0.01311		
			0.5207	0.01390		
		carcass	0.5131	0.02027	0.0214	34.4
			0.5119	0.02821		
			0.5085	0.03127		
				whole fish	**0.0653**	
			0.45087	0.49948		
			0.54563	0.15872		
		GIT	0.58634	0.22444	0.2493	57.4
			0.72312	0.07744		
			0.90448	0.28624		
			0.09623	0.40320		
			0.14121	0.07379		
depuration	24 h	liver	0.12698	0.15499	0.1628	80.6

Phase	Sampling	Compartment	Ext. mass [g]	Content [mg/kg]	Mean [mg/kg]	RSD [%]
			0.1737	0.01992		
			0.21850	0.16220		
			0.5381	0.01319		
			0.5241	0.00477*		
		carcass	0.5272	0.01074	0.0090	38.9
			0.5091	0.00491*		
			0.5448	0.01160		
				whole fish	**0.0285**	
			0.93062	0.02751		
			0.68707	0.06593		
		GIT	0.52137	0.04776	0.05933	33.3
			0.76710	0.08434		
			0.91253	0.07112		
			0.23231	0.01076*		
			0.12704	0.01968*		
depuration	48 h	liver	0.17184	0.01455*	0.01873	52.8
			0.13618	0.03745		
			0.22314	0.01120*		
		carcass			< LOQ	
				whole fish	**0.0047**	

Table 41: Analytical results of MEE-Phosphonate in fish matrices in the main study.

* = ½ LOQ (with LOQ = 2.0 µg/L); # = ½ LOQ (with LOQ = 1.0 µg/L).

With LOQ corresponding to 0.01 mg/kg for GIT, 0.16 mg/kg for liver and 0.08 mg/kg for carcass

Phase	Sampling	Compartment	Ext. mass [g]	Content [mg/kg]	Mean [mg/kg]	RSD [%]
			0.74640	2.76675		
			0.44590	1.58309		
		GIT	0.60200	1.17259	3.1734	68.5
			0.58450	3.28469		
			0.52660	7.06001		
			0.1592	1.61646		
			0.0843	0.31056		
uptake	7 d	liver	0.1163	0.76715	0.9008	46.6
			0.1030	0.94388		
			0.0851	0.86580		
			0.5108	0.03915*		
			0.5026	0.03979*		
		carcass	0.5010	0.14164	0.0598	68.5
			0.5032	0.03975*		
			0.5197	0.03848*		
				whole fish	**0.3094**	
			0.82378	3.02180		
			0.77143	2.96670		
		GIT	0.56263	2.10245	2.6627	13.3
			0.62371	2.39807		
			0.87096	2.82470		
			0.18034	0.71010		
			0.21399	0.39880		
uptake	14 d	liver	0.12501	0.21678	0.4808	39.0
			0.18231	0.39778		
			0.13191	0.68062		
			0.5409	0.03698*		

Phase	Sampling	Compartment	Ext. mass [g]	Content [mg/kg]	Mean [mg/kg]	RSD [%]
			0.4971	0.15711		
		carcass	0.5355	0.08000	0.0820	53.7
			0.5254	0.09623		
			0.5052	0.03959*		
				whole fish	**0.2931**	
			0.60267	0.78119		
			0.82207	1.39684		
		GIT	0.63484	0.88085	1.2968	48.2
			0.87265	2.47270		
			0.55157	0.95219		
			0.10135	0.0987#		
			0.14222	0.2924		
depuration	10 h	liver	0.16020	0.1981	0.2159	57.1
			0.17700	0.4102		
			0.12485	0.0801#		
		carcass			< LOQ	
				whole fish	**0.1000**	
			0.45087	0.861224		
			0.54563	0.320913		
		GIT	0.58634	0.473104	0.5314	41.5
			0.72312	0.295387		
			0.90448	0.706152		
depuration	24 h	liver			< LOQ	
		carcass			< LOQ	
				whole fish	**0.0375**	
			0.93062	0.04300		
			0.68707	0.02375		
		GIT	0.52137	0.00959	0.0497	66
			0.76710	0.10038		

Phase	Sampling	Compartment	Ext. mass [g]	Content [mg/kg]	Mean [mg/kg]	RSD [%]
			0.91253	0.07178		
depuration	48 h	liver			< LOQ	
		carcass			< LOQ	
				whole fish	**0.0037**	
			0.63536	0.00787		
			0.83653	0.00598		
		GIT	0.73688	0.01585	0.0084	45.1
			0.80516	0.00621		
			0.82114	0.00609		
depuration	72 h	liver			< LOQ	
		carcass			< LOQ	
				whole fish	**0.0006**	

B.1.5 ln-linear fits of the whole fish concentrations of all substances during depuration phase of main study

Figure 29: ln-linear fit of the whole fish concentrations of TBP during depuration phase.

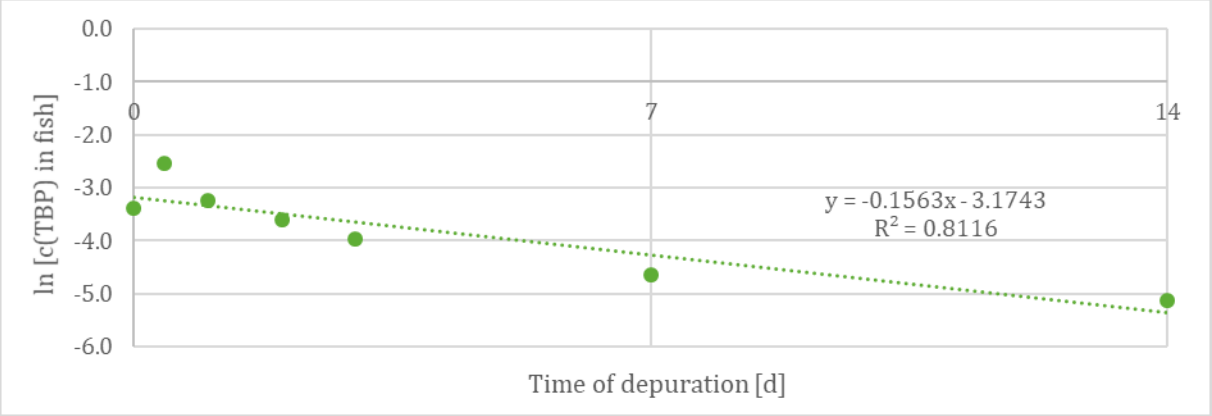

Source: Fh IME, own diagram.

Figure 30: ln-linear fit of the whole fish concentrations of TMOA during depuration phase.

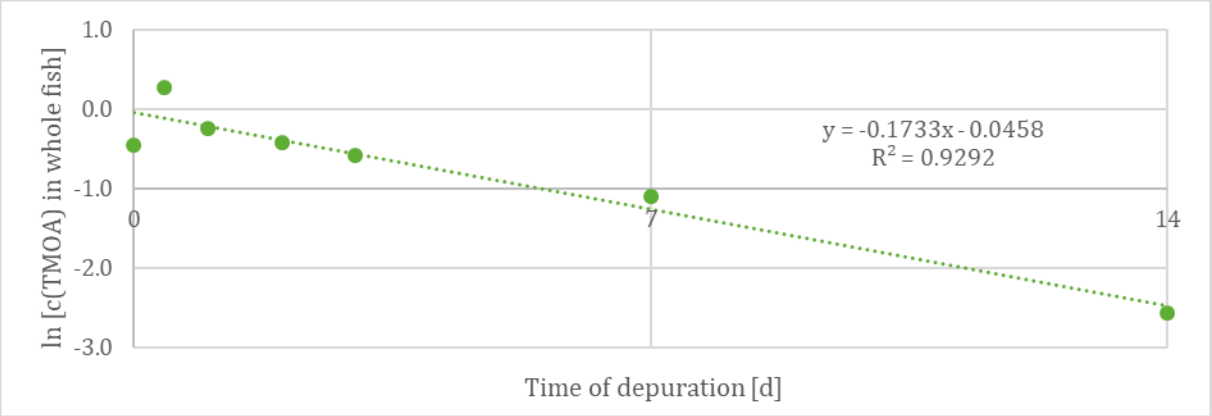

Source: Fh IME, own diagram.

Figure 31: ln-linear fit of the whole fish concentrations of Benzotriazol during depuration phase.

Source: Fh IME, own diagram.

Figure 32: ln-linear fit of the whole fish concentrations of Tecloftalam during depuration phase.

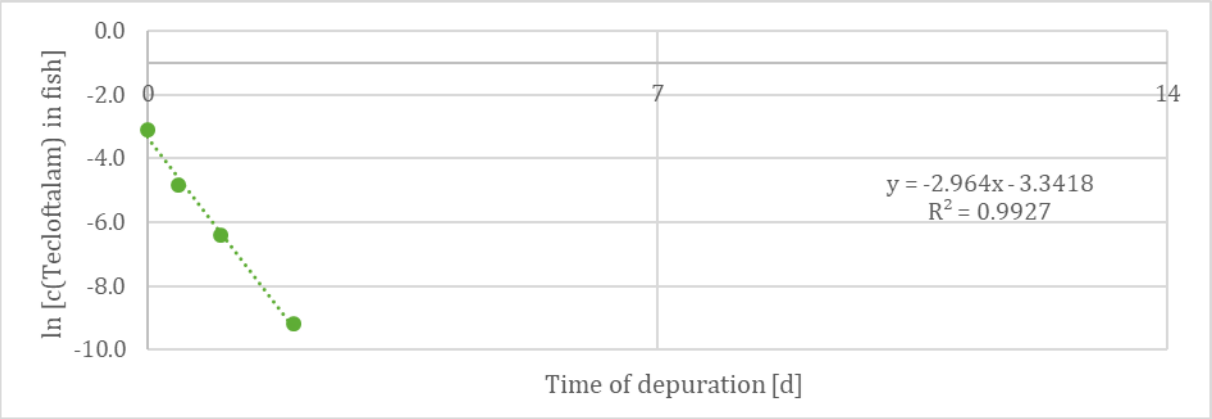

Source: Fh IME, own diagram.

Figure 33: ln-linear fit of the whole fish concentrations of Pentachlorophenol during depuration phase.

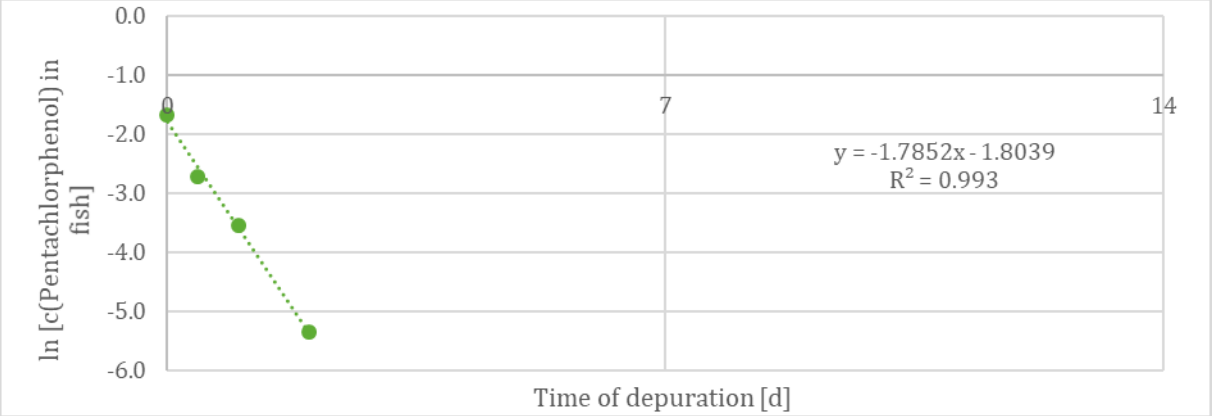

Source: Fh IME, own diagram.

Figure 34: ln-linear fit of the whole fish concentrations of MEE-Phosphonate during depuration phase.

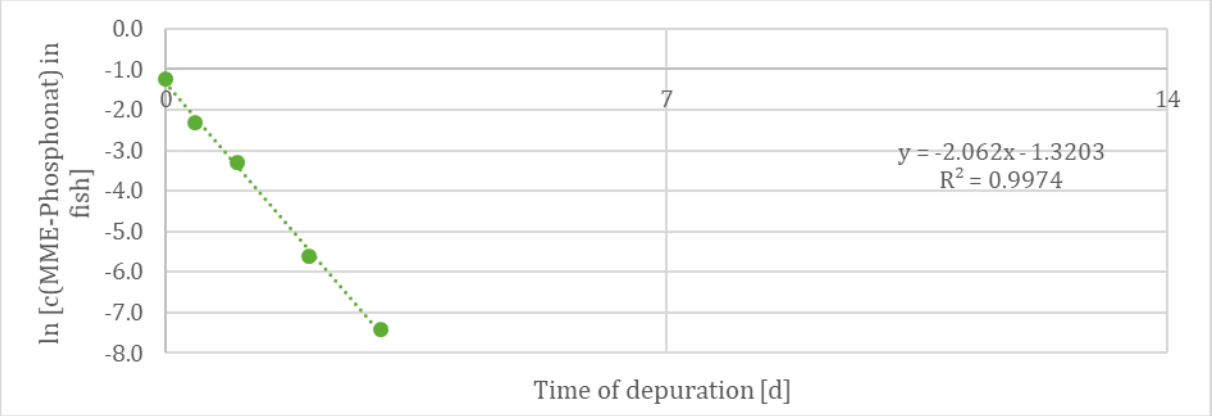

Source: Fh IME, own diagram.

B.1.6 Test item concentration in fish compartments (main study)

Figure 35: Absolute tissue concentrations of TBP in fish GIT.

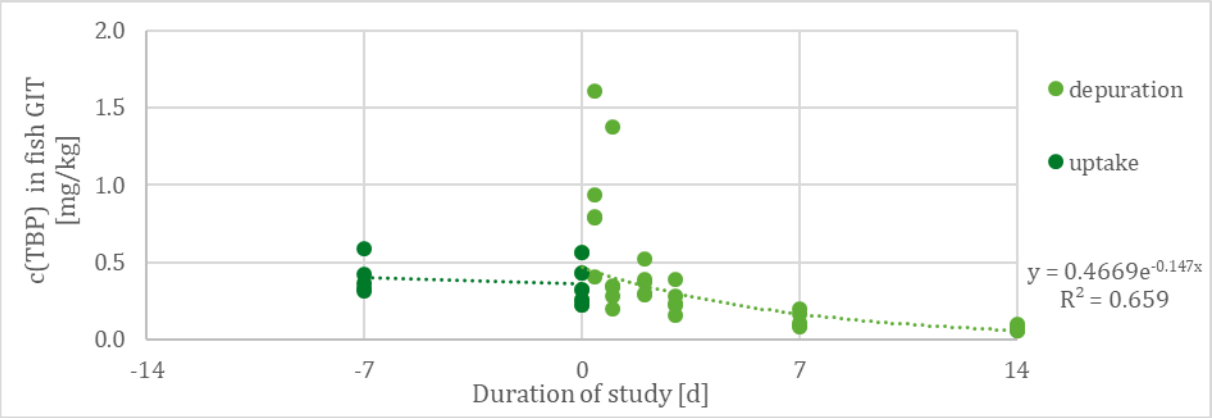

Source: Fh IME, own diagram.

Figure 36: ln-linear fit of the fish GIT concentrations of TBP during depuration phase.

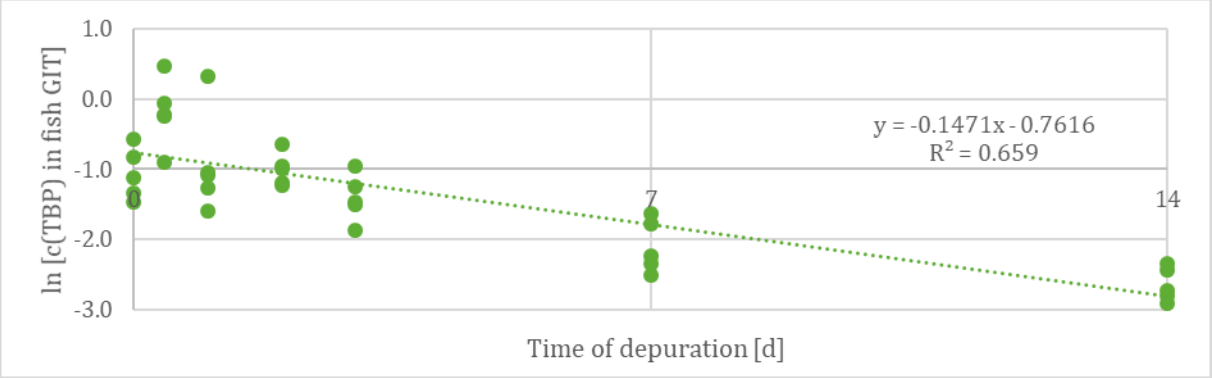

Source: Fh IME, own diagram.

Figure 37: Absolute tissue concentrations of TBP in fish liver.

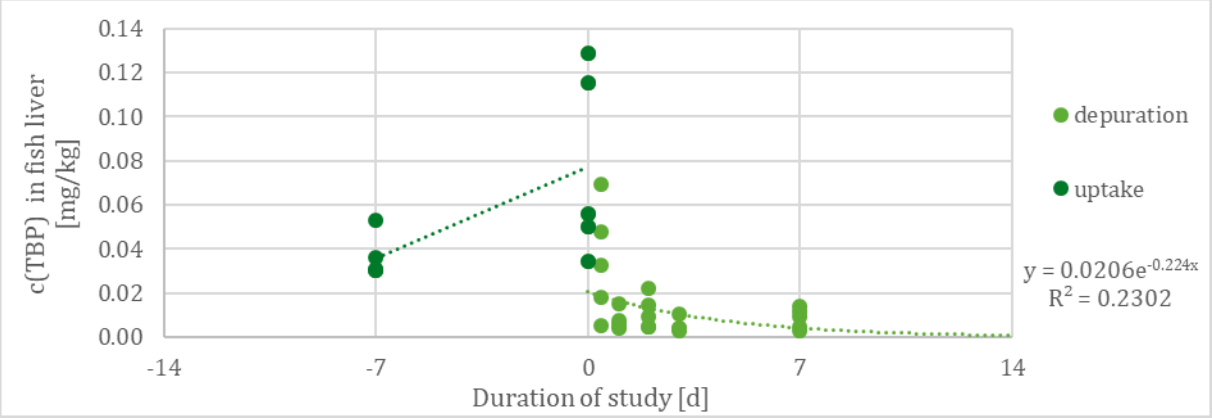

Source: Fh IME, own diagram.

Figure 38: ln-linear fit of the fish liver concentrations of TBP during depuration phase.

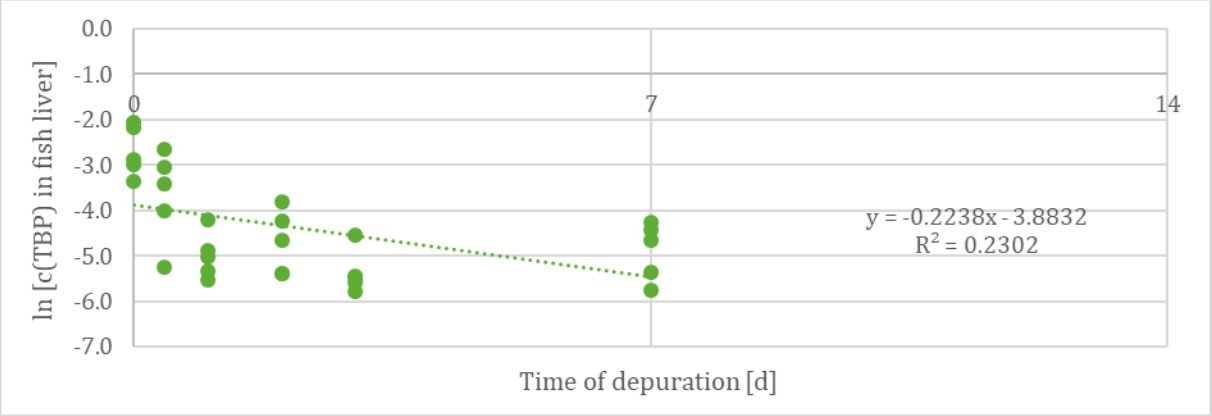

Source: Fh IME, own diagram.

Figure 39: Absolute tissue concentrations of TBP in fish carcass.

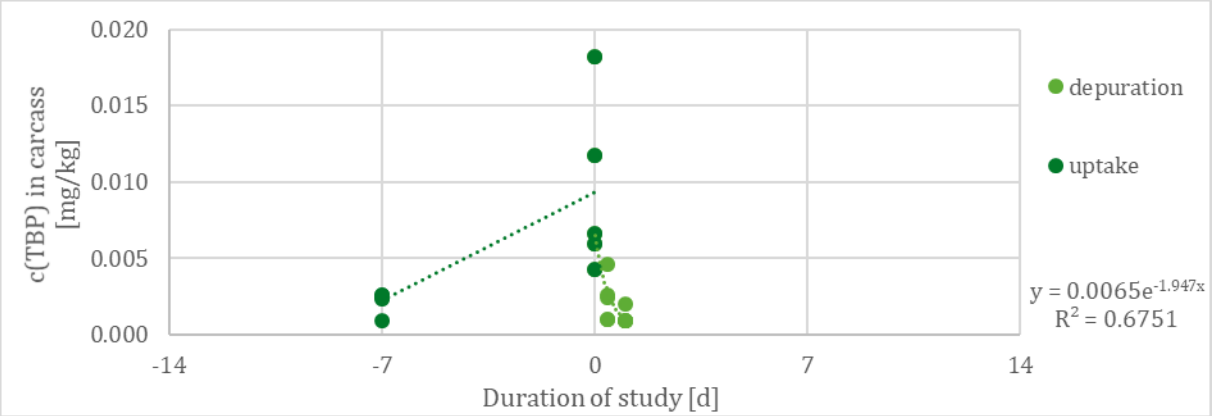

Source: Fh IME, own diagram.

Figure 40: ln-linear fit of the fish carcass concentrations of TBP during depuration phase.

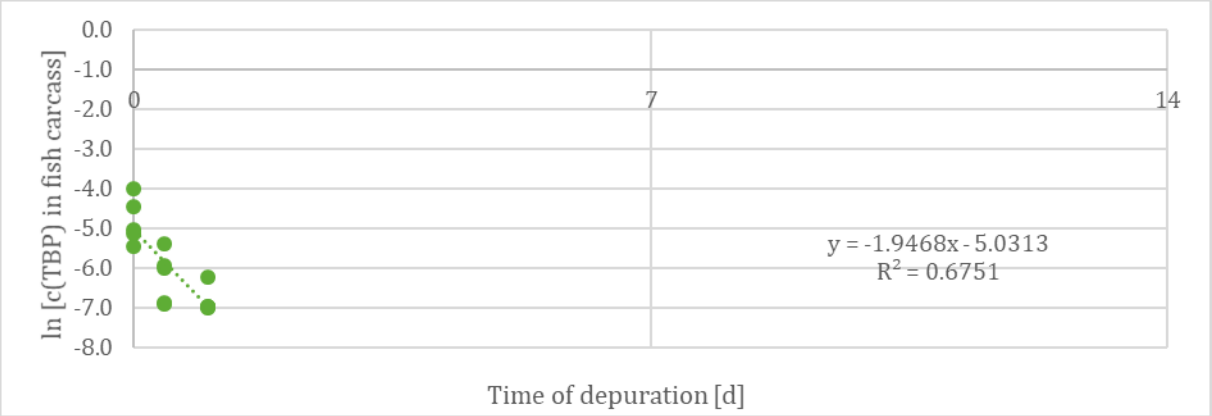

Source: Fh IME, own diagram.

Figure 41: Absolute tissue concentrations of TMOA in fish GIT.

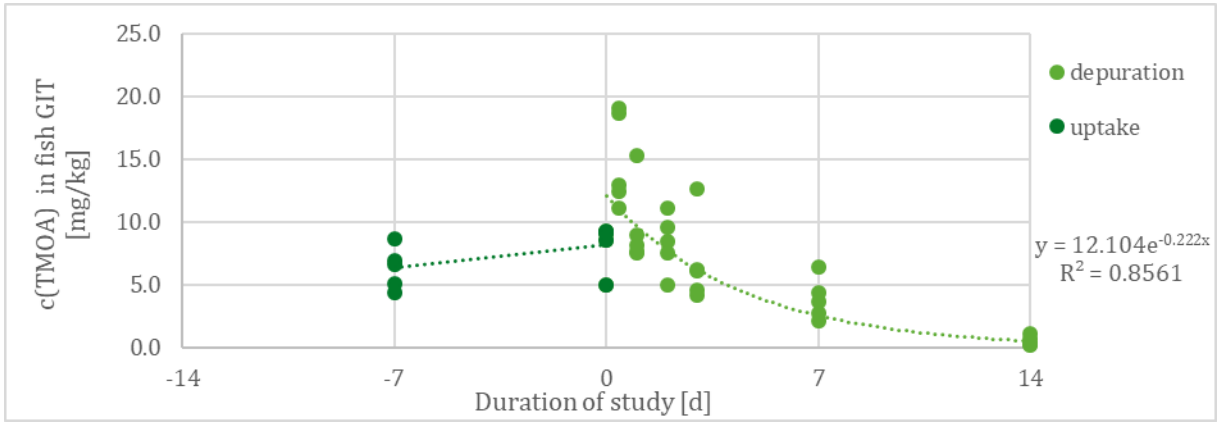

Source: Fh IME, own diagram.

Figure 42: ln-linear fit of the fish GIT concentrations of TMOA during depuration phase.

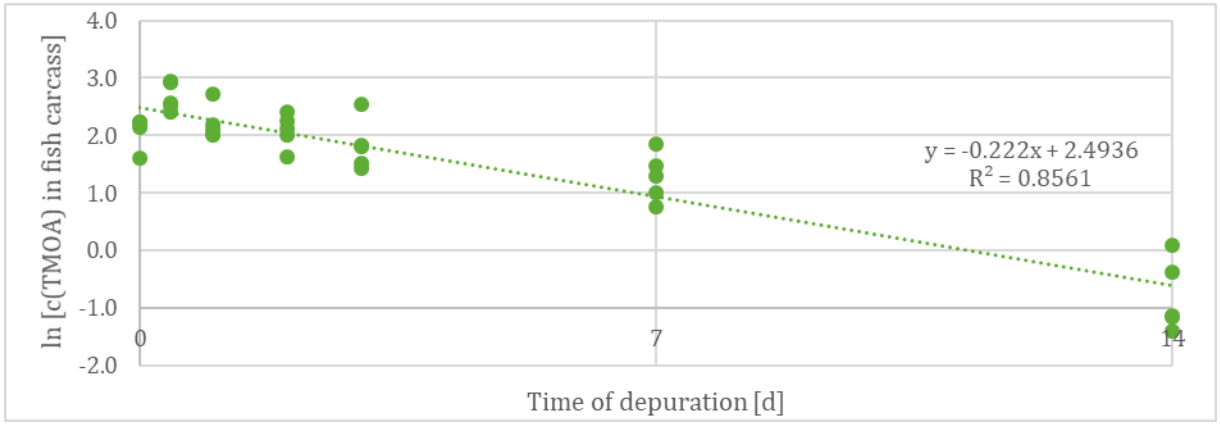

Source: Fh IME, own diagram.

Figure 43: Absolute tissue concentrations of TMOA in fish liver.

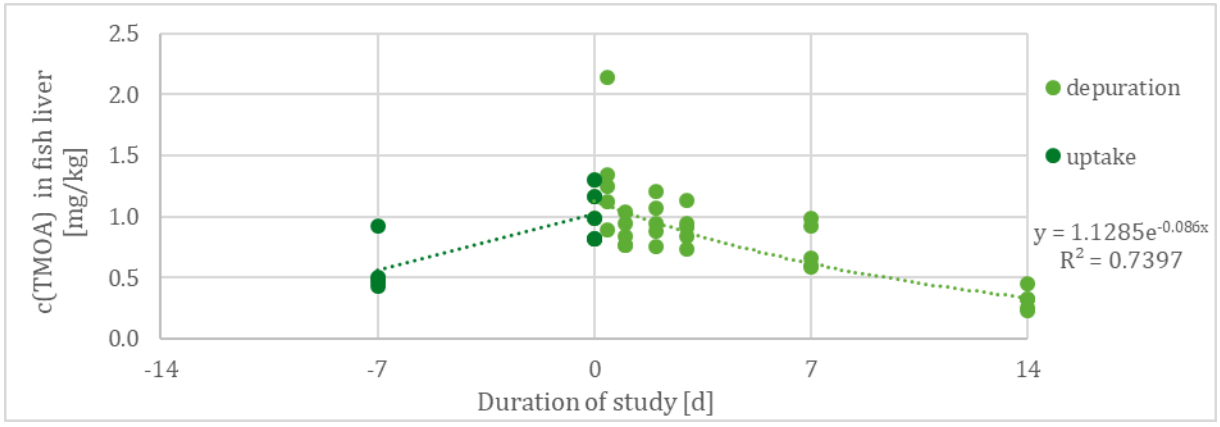

Source: Fh IME, own diagram.

Figure 44: ln-linear fit of the fish liver concentrations of TMOA during depuration phase.

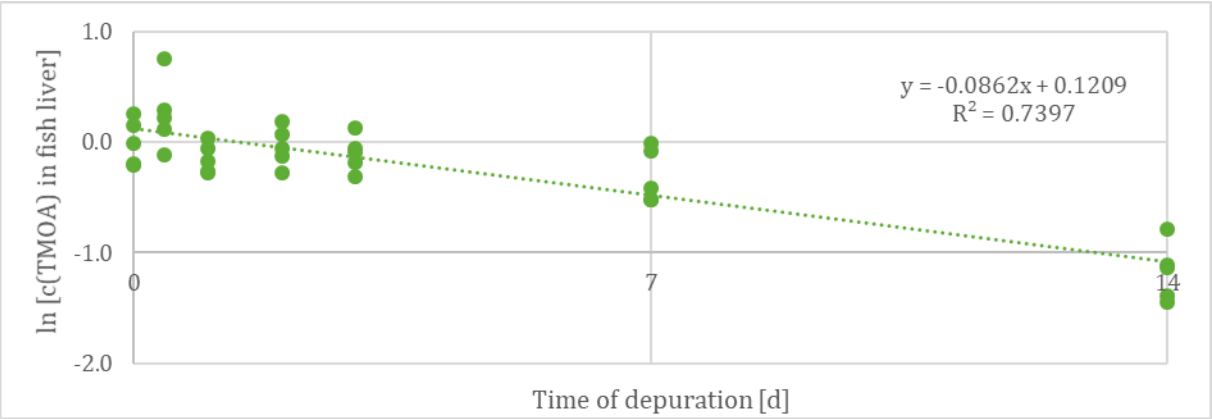

Source: Fh IME, own diagram.

Figure 45: Absolute tissue concentrations of TMOA in fish carcass.

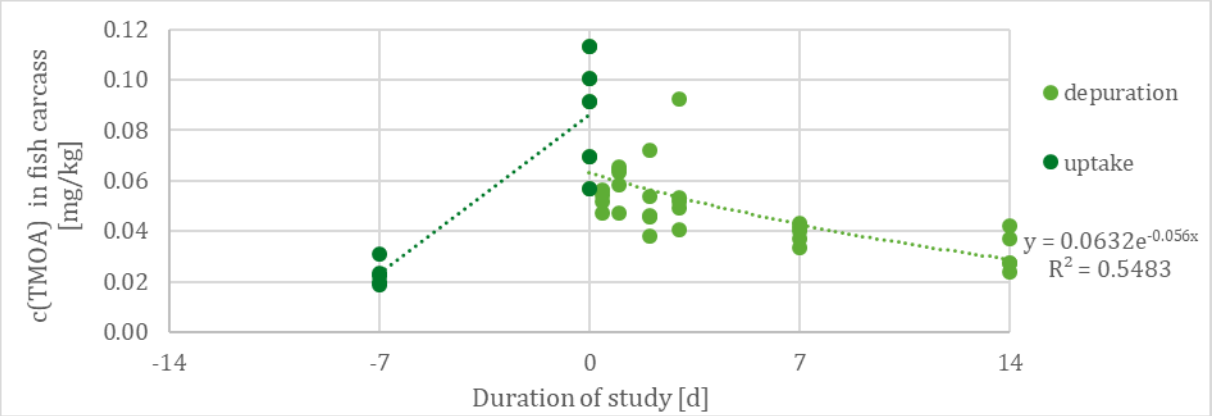

Source: Fh IME, own diagram.

Figure 46: ln-linear fit of the fish carcass concentrations of TMOA during depuration phase.

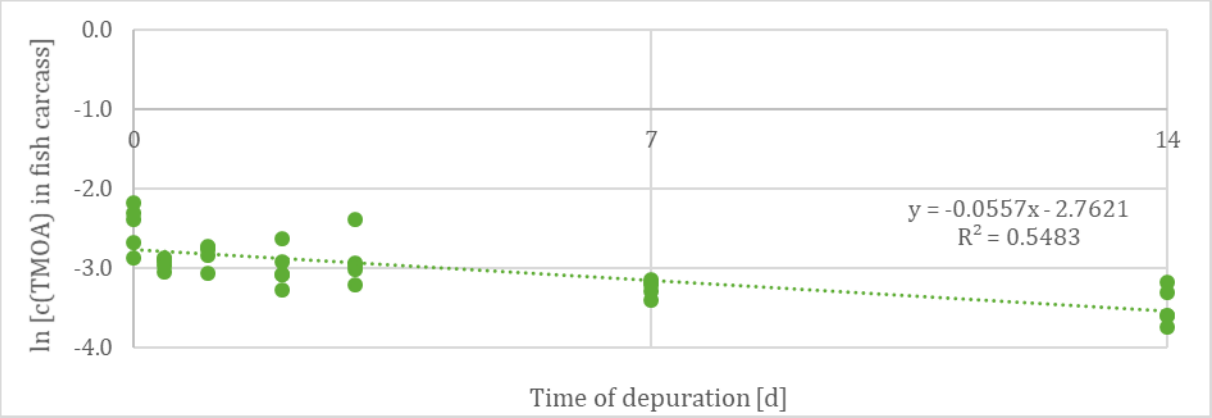

Source: Fh IME, own diagram.

Figure 47: Absolute tissue concentrations of Benzotriazol in fish liver.

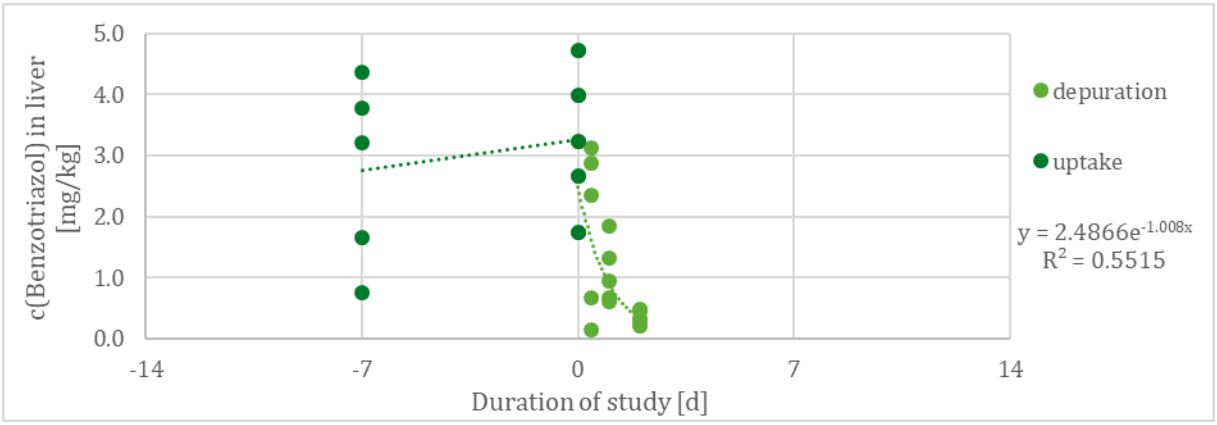

Source: Fh IME, own diagram.

Figure 48: In-linear fit of the fish liver concentrations of Benzotriazol during depuration phase.

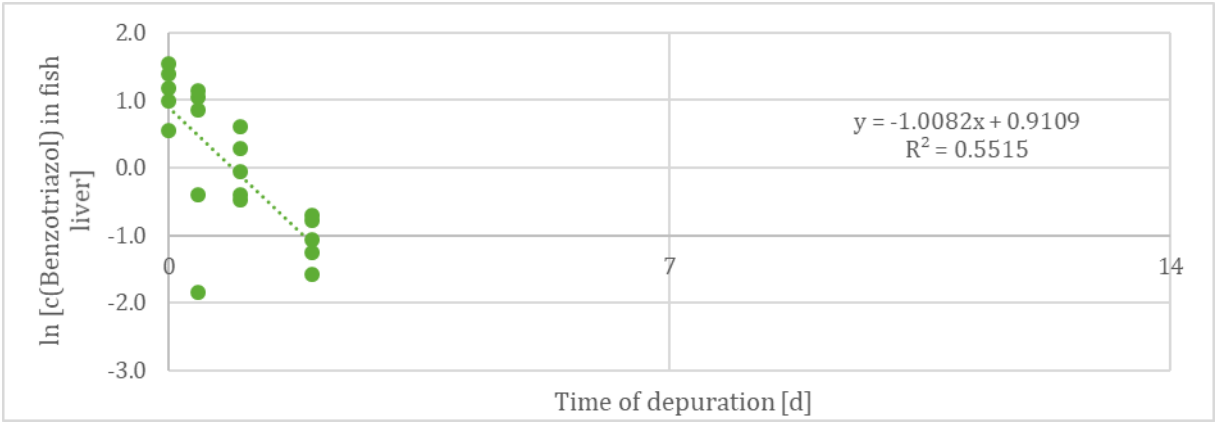

Source: Fh IME, own diagram.

Figure 49: Absolute tissue concentrations of Benzotriazol in fish carcass.

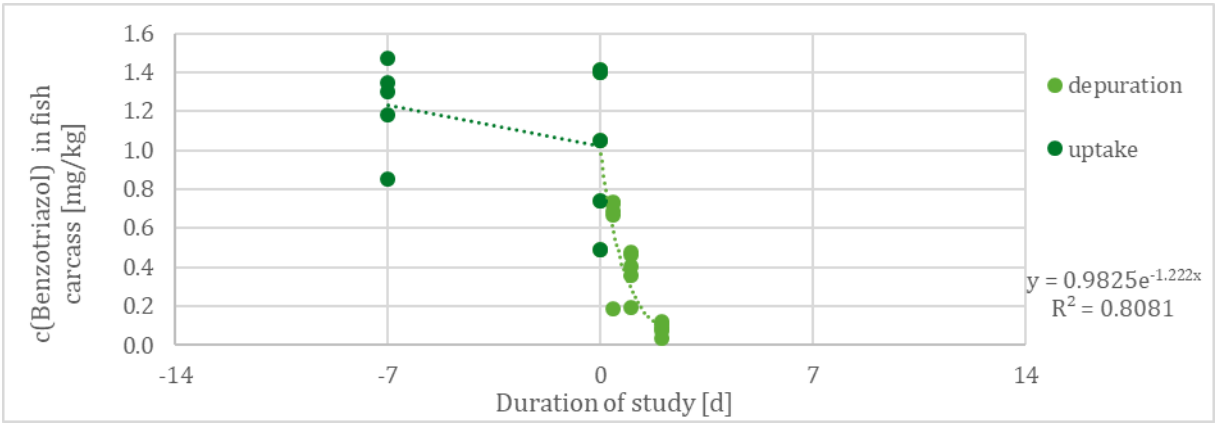

Source: Fh IME, own diagram.

Figure 50: ln-linear fit of the fish carcass concentrations of Benzotriazol during depuration phase.

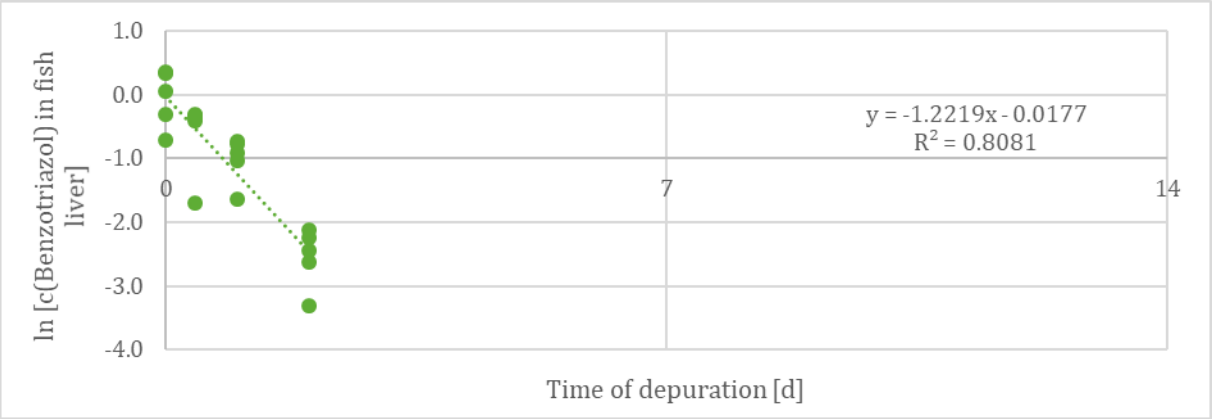

Source: Fh IME, own diagram.

Figure 51: Absolute tissue concentrations of Tecloftalam in fish GIT.

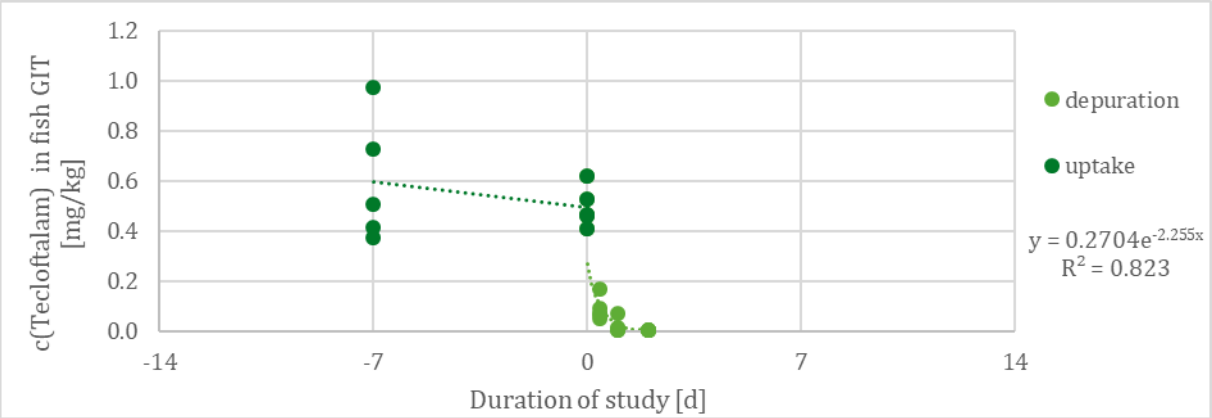

Source: Fh IME, own diagram.

Figure 52: ln-linear fit of the fish GIT concentrations of Tecloftalam during depuration phase.

Source: Fh IME, own diagram.

Figure 53: Absolute tissue concentrations of Pentachlorophenol in fish GIT.

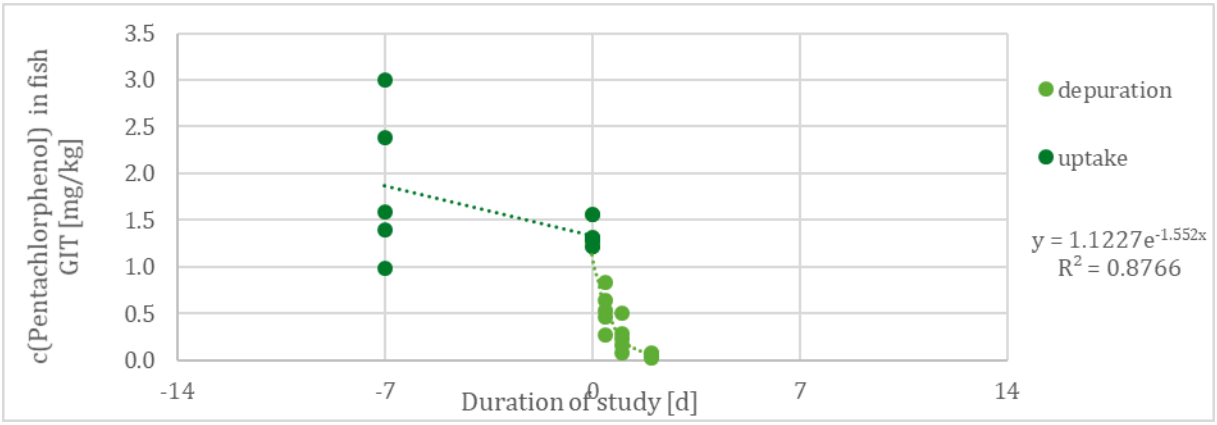

Source: Fh IME, own diagram.

Figure 54: ln-linear fit of the fish GIT concentrations of Pentachlorophenol during depuration phase.

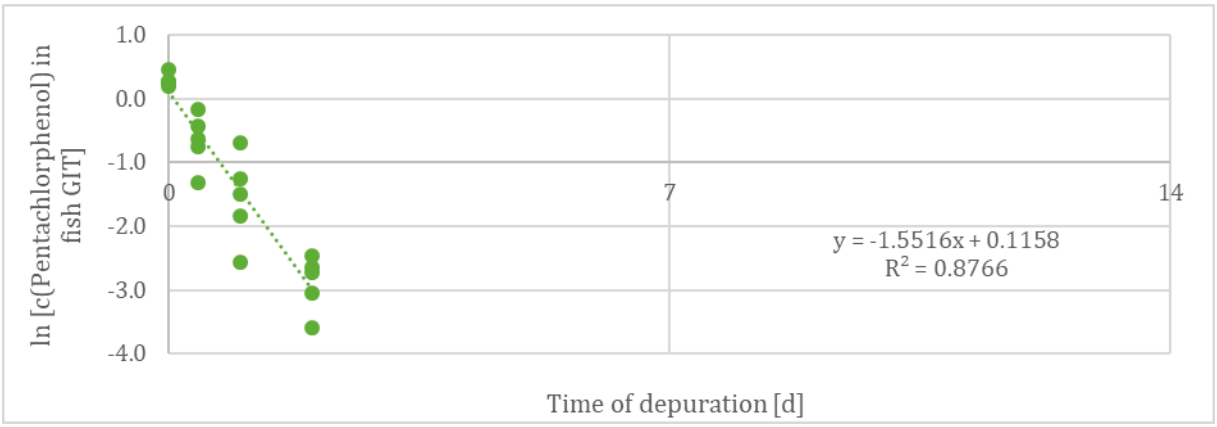

Source: Fh IME, own diagram.

Figure 55: Absolute tissue concentrations of Pentachlorophenol in fish liver.

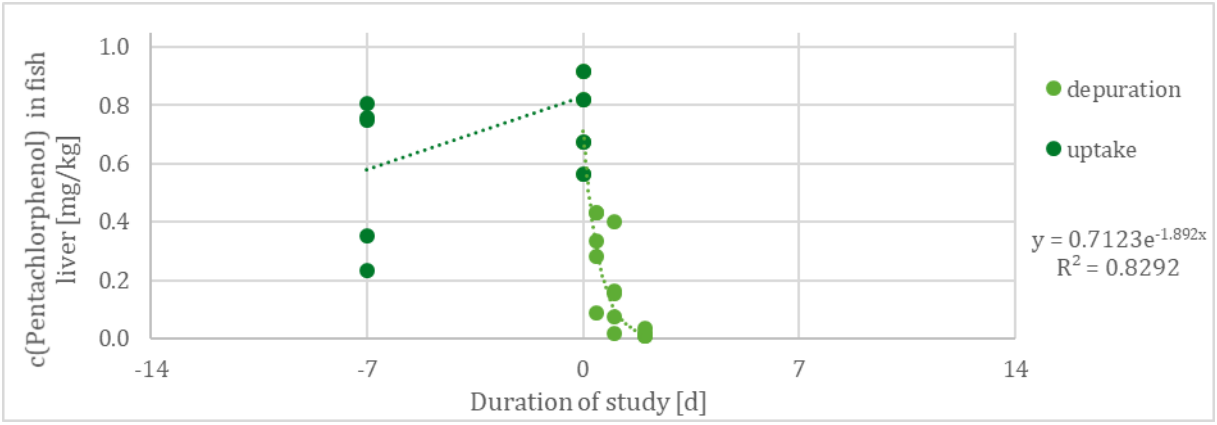

Source: Fh IME, own diagram.

Figure 56: ln-linear fit of the fish liver concentrations of Pentachlorophenol during depuration phase.

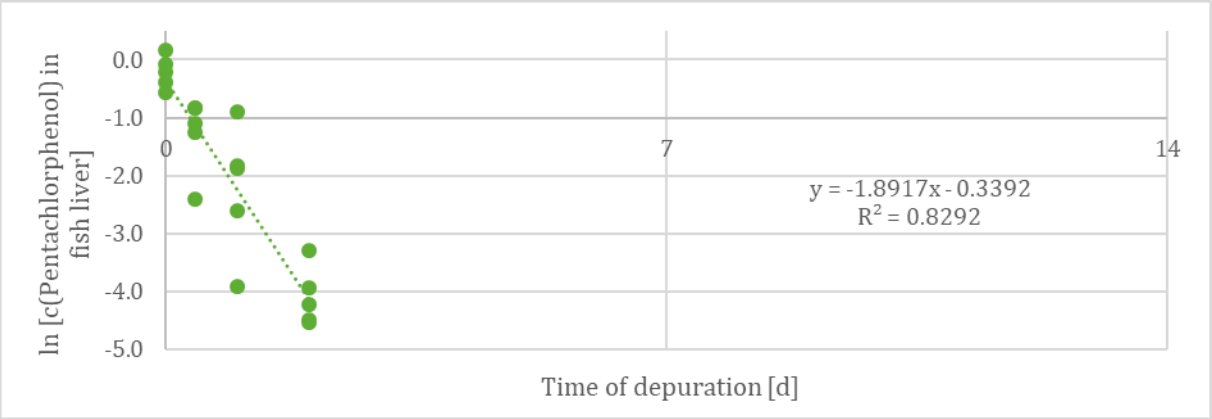

Source: Fh IME, own diagram.

Figure 57: Absolute tissue concentrations of Pentachlorophenol in fish carcass.

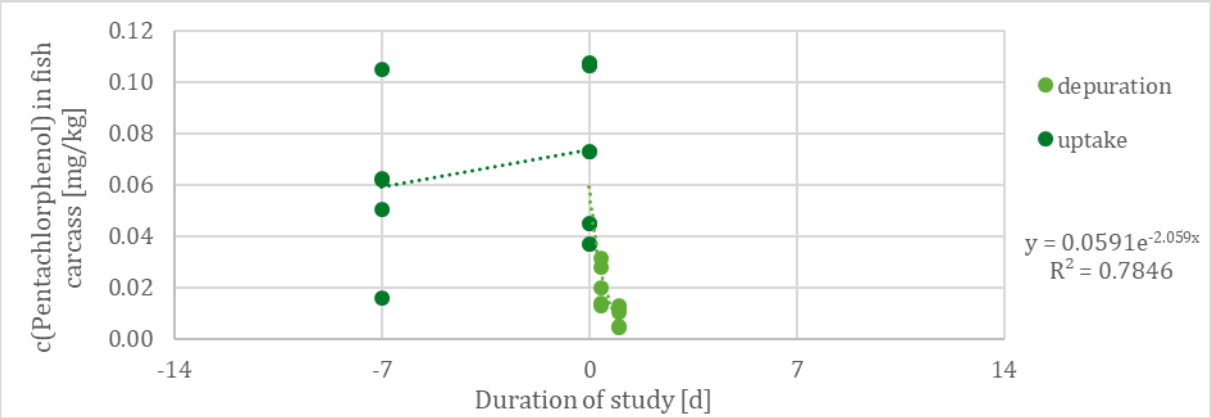

Source: Fh IME, own diagram.

Figure 58: ln-linear fit of the fish carcass concentrations of Pentachlorophenol during depuration phase.

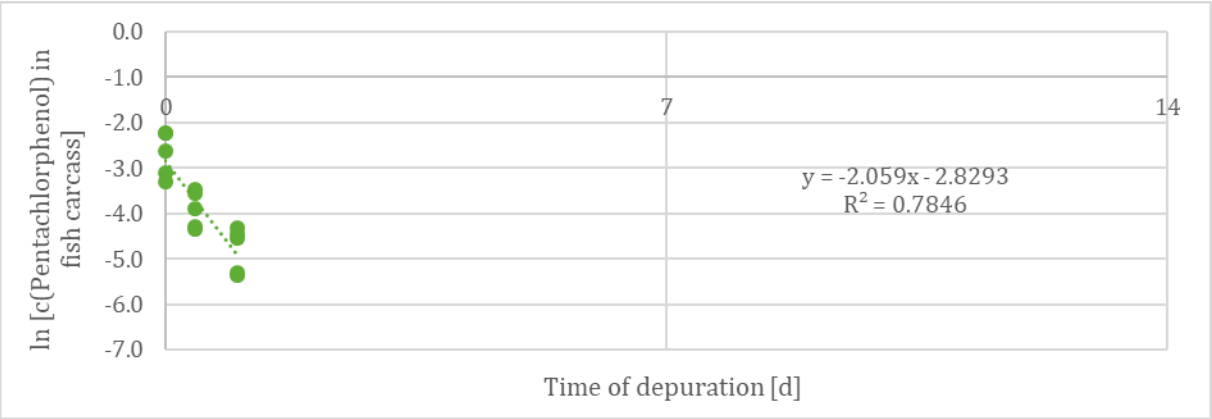

Source: Fh IME, own diagram.

Figure 59: Absolute tissue concentrations of MEE-Phosphonate in fish GIT.

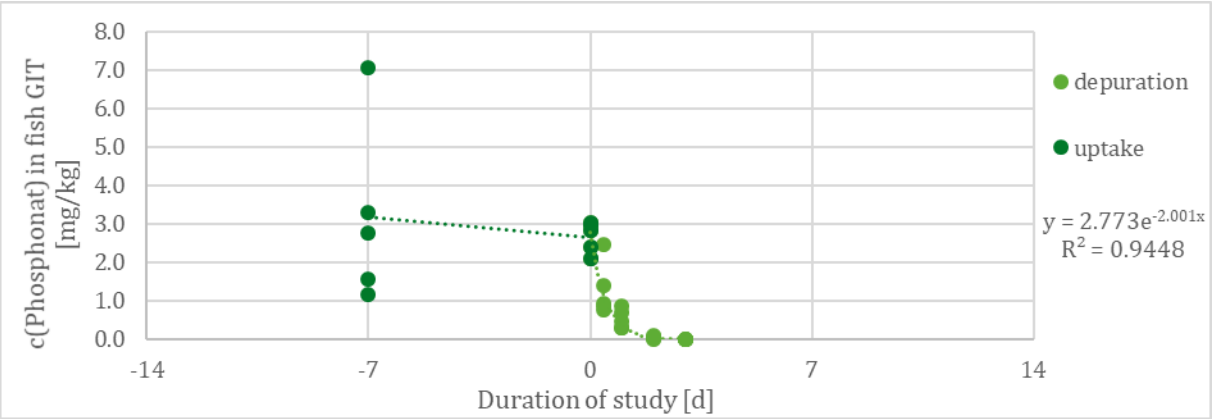

Source: Fh IME, own diagram.

Figure 60: ln-linear fit of the fish GIT concentrations of MEE-Phosphonate during depuration phase.

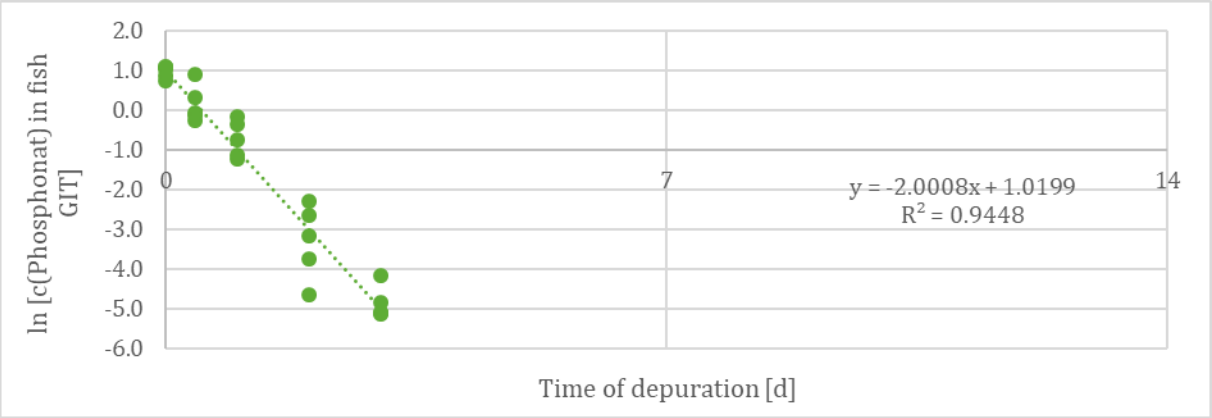

Source: Fh IME, own diagram.

B.1.7 Parameter for BMF calculations

Table 42: Parameter for BMF calculation of TBP in compartments and 'whole fish'.

	Unit		GIT	Liver	Carcass	Fish
$C_{0,d}$	mg/kg	conc. at start of dep.	0.467	0.021	0.00653	**0.0418**
k_2	1/day	dep. rate constant	0.147	0.224	1.95	**0.156**
t	day	duration uptake	14	14	14	**14**
I	g_{feed}/g_{fish} * day	feed ingestion rate	0.02	0.02	0.02	**0.02**
C_{feed}	mg/kg_{feed}	conc. in feed	23.8	23.8	23.8	**23.8**
α		**assimilation efficiency**	**0.166**	**0.0101**	**0.0268**	**0.0155**
k_g	1/d	growth rate constant	0.0219	0.0219	0.0219	**0.0219**
k_{2g}	1/d	growth rate corrected k_2	0.125	0.202	1.925	**0.134**
$t_{1/2}$ (uncorrected)	days	substance-specific half life (based on uncorr. k_2)	4.71	3.10	0.356	**4.436**
$t_{1/2}$ (corrected)	days	substance-specific half life (based on growth-corr. k_2)	5.53	3.43	0.360	**5.16**
BMF_k		**kinetic BMF**	**0.0225**	**0.000906**	**0.000275**	**0.00198**
BMF_{kg}		**growth-corrected BMF**	**0.0264**	**0.00100**	**0.000278**	**0.00231**

Table 43: Parameter for BMF calculation of TMOA in compartments and 'whole fish'.

	Unit		GIT	Liver	Carcass	Fish
$C_{0,d}$	mg/kg	conc. at start of dep.	12.104	1.129	0.0632	**0.955**
k_2	1/day	dep. rate constant	0.222	0.0862	0.0557	**0.173**
t	day	duration uptake	14	14	14	**14**
I	g_{feed}/g_{fish} * day	feed ingestion rate	0.02	0.02	0.02	**0.02**
C_{feed}	mg/kg_{feed}	conc. in feed	25.9	25.9	25.9	**25.9**
α		**assimilation efficiency**	**5.43**	**0.268**	**0.0125**	**0.350**
k_g	1/d	growth rate constant	0.0219	0.0219	0.0219	**0.0219**
k_{2g}	1/d	growth rate corrected k_2	0.200	0.0643	0.0338	**0.151**
$t_{1/2}$ (uncorrected)	days	substance-specific half life (based on uncorr. k_2)	3.12	8.04	12.4	**4.00**
$t_{1/2}$ (corrected)	days	substance-specific half life (based on growth-corr. k_2)	3.46	10.8	20.5	**4.58**
BMF_k		**kinetic BMF**	**0.489**	**0.0621**	**0.00450**	**0.0404**
BMF_{kg}		**growth-corrected BMF**	**0.542**	**0.0833**	**0.00742**	**0.0463**

Table 44: Parameter for BMF calculation of Benzotriazol in compartments and 'whole fish'.

	Unit		Liver	Carcass	Fish
$C_{0,d}$	mg/kg	conc. at start of dep.	2.487	0.983	**1.046**
k_2	1/day	dep. rate constant	1.00	1.22	**1.24**
t	day	duration uptake	14	14	**14**
I	g_{feed}/g_{fish} * day	feed ingestion rate	0.02	0.02	**0.02**
C_{feed}	mg/kg_{feed}	conc. in feed	31.9	31.9	**31.9**
α		**assimilation efficiency**	**3.93**	**1.88**	**2.03**
k_g	1/d	growth rate constant	0.0219	0.0219	**0.0219**
k_{2g}	1/d	growth rate corrected k_2	0.986	1.200	**1.215**
$t_{1/2}$ (uncorrected)	days	substance-specific half life (based on uncorr. k_2)	0.688	0.567	**0.561**
$t_{1/2}$ (corrected)	days	substance-specific half life (based on growth-corr. k_2)	0.703	0.578	**0.571**
BMF_k		**kinetic BMF**	**0.0779**	**0.0308**	**0.0328**
BMF_{kg}		**growth-corrected BMF**	**0.0797**	**0.0314**	**0.0334**

Table 45: Parameter for BMF calculation of Tecloftalam in compartments and 'whole fish'.

	Unit		GIT	Fish
$C_{0,d}$	mg/kg	conc. at start of dep.	0.270	**0.035**
k_2	1/day	dep. rate constant	2.25	**2.96**
t	day	duration uptake	14	**14**
I	g_{feed}/g_{fish} * day	feed ingestion rate	0.02	**0.02**
C_{feed}	mg/kg_{feed}	conc. in feed	27.5	**27.5**
α		**assimilation efficiency**	**1.11**	**0.190**
k_g	1/d	growth rate constant	0.0219	**0.0219**
k_{2g}	1/d	growth rate corrected k_2	2.23	**2.94**
$t_{1/2}$ (uncorrected)	days	substance-specific half life (based on uncorr. k_2)	0.307	**0.234**
$t_{1/2}$ (corrected)	days	substance-specific half life (based on growth-corr. k_2)	0.310	**0.236**
BMF_k		**kinetic BMF**	**0.00982**	**0.00128**
BMF_{kg}		**growth-corrected BMF**	**0.00992**	**0.00129**

Table 46: Parameter for BMF calculation of Pentachlorophenol in compartments and ' whole fish'.

	Unit		GIT	Liver	Carcass	Fish
$C_{0,d}$	mg/kg	conc. at start of dep.	1.12	0.712	0.05906	**0.165**
k_2	1/day	dep. rate constant	1.55	1.89	2.06	**1.79**
t	day	duration uptake	14	14	14	**14**
I	g_{feed}/g_{fish} * day	feed ingestion rate	0.2	0.2	0.2	**0.02**
C_{feed}	mg/kg_{feed}	conc. in feed	20.3	20.3	20.3	**20.3**
α		**assimilation efficiency**	**4.29**	**3.32**	**0.300**	**0.725**
k_g	1/d	growth rate constant	0.0219	0.0219	0.0219	**0.0219**
k_{2g}	1/d	growth rate corrected k_2	1.53	1.87	2.04	**1.76**
$t_{1/2}$ (uncorrected)	days	substance-specific half life (based on uncorr. k_2)	0.447	0.366	0.337	**0.388**
$t_{1/2}$ (corrected)	days	substance-specific half life (based on growth-corr. k_2)	0.453	0.371	0.340	**0.393**
BMF_k		**kinetic BMF**	0.0554	0.0351	0.00291	**0.00812**
BMF_{kg}		**growth-corrected BMF**	0.0561	0.0356	0.00294	**0.00822**

Table 47: Parameter for BMF calculation of MEE-Phosphonate in compartments and 'whole fish'.

	Unit		GIT	Fish
$C_{0,d}$	mg/kg	conc. at start of dep.	2.77	**0.267**
k_2	1/day	dep. rate constant	2.00	**2.06**
t	day	duration uptake	14	**14**
I	g_{feed}/g_{fish} * day	feed ingestion rate	0.02	**0.02**
C_{feed}	mg/kg_{feed}	conc. in feed	29.6	**29.6**
α		**assimilation efficiency**	**9.3**	**0.931**
k_g	1/d	growth rate constant	0.0219	**0.0219**
k_{2g}	1/d	growth rate corrected k_2	1.98	**2.04**
$t_{1/2}$ (uncorrected)	days	substance-specific half life (based on uncorr. k_2)	0.346	**0.336**
$t_{1/2}$ (corrected)	days	substance-specific half life (based on growth-corr. k_2)	0.350	**0.340**
BMF_k		**kinetic BMF**	**0.0938**	**0.00903**
BMF_{kg}		**growth-corrected BMF**	**0.0948**	**0.00913**

B.1.8 Exemplary chromatograms and calibration curves of main study

Figure 61: Exemplary calibration curve of matrix-matched calibration for TBP in fish GIT.

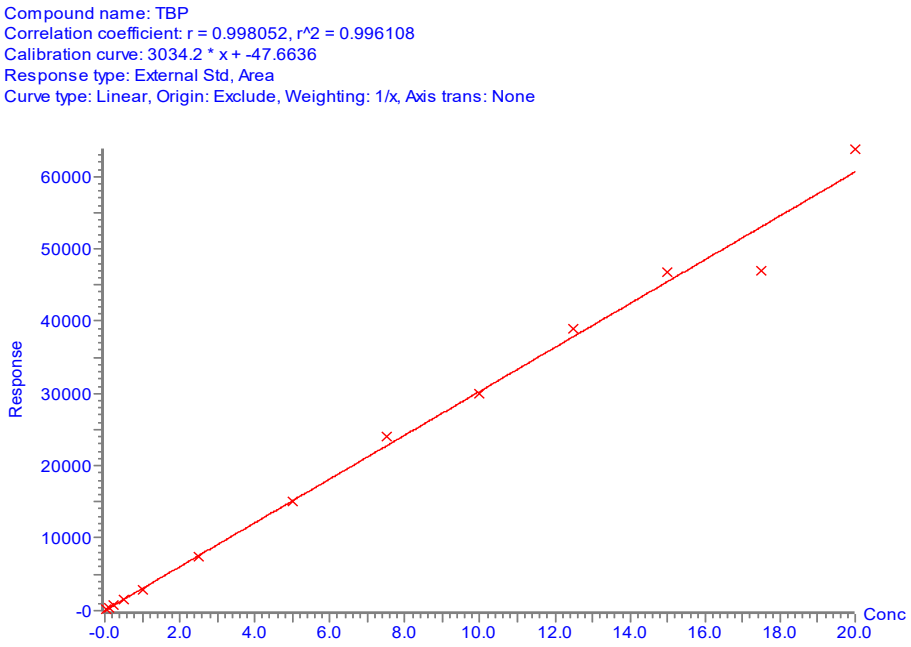

Source: Fh IME.

Figure 62: Exemplary chromatogram of TBP standard (5 µg/L) of matrix-matched calibration with fish GIT.

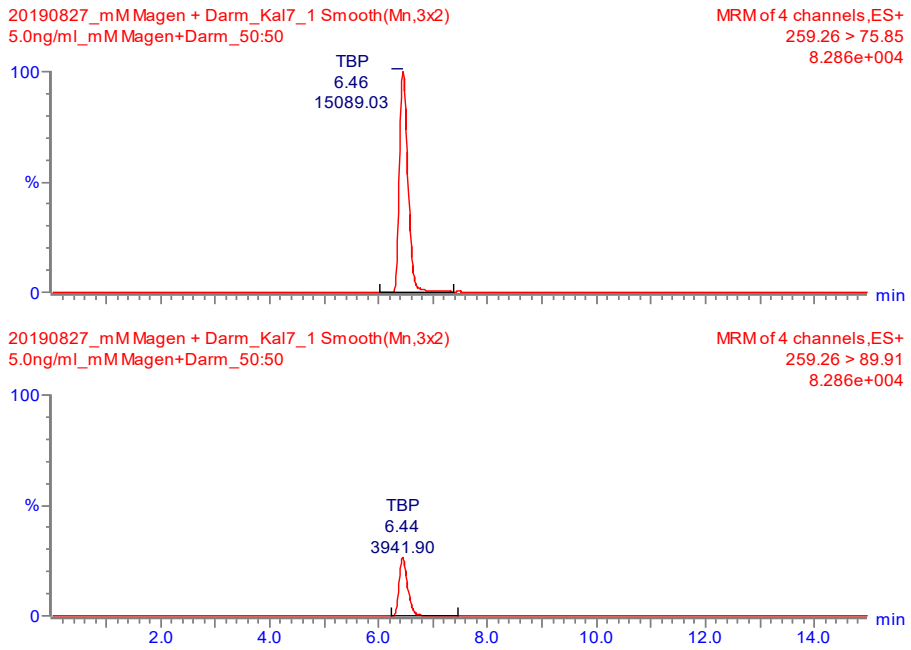

Source: Fh IME.

Figure 63: Exemplary calibration curve of matrix-matched calibration for TBP in fish liver.

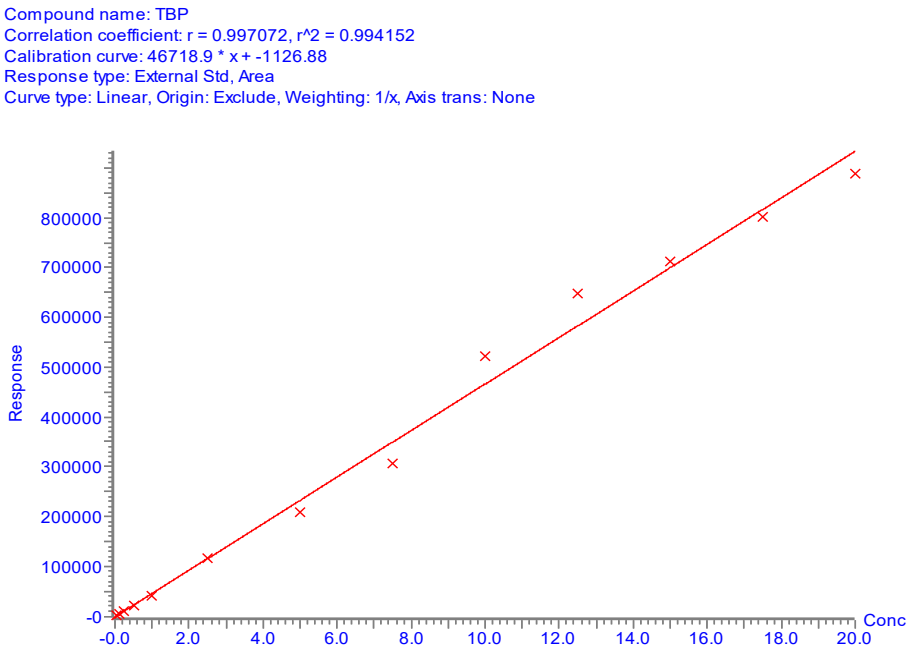

Source: Fh IME.

Figure 64: Exemplary chromatogram of TBP standard (5 µg/L) of matrix-matched calibration with fish liver.

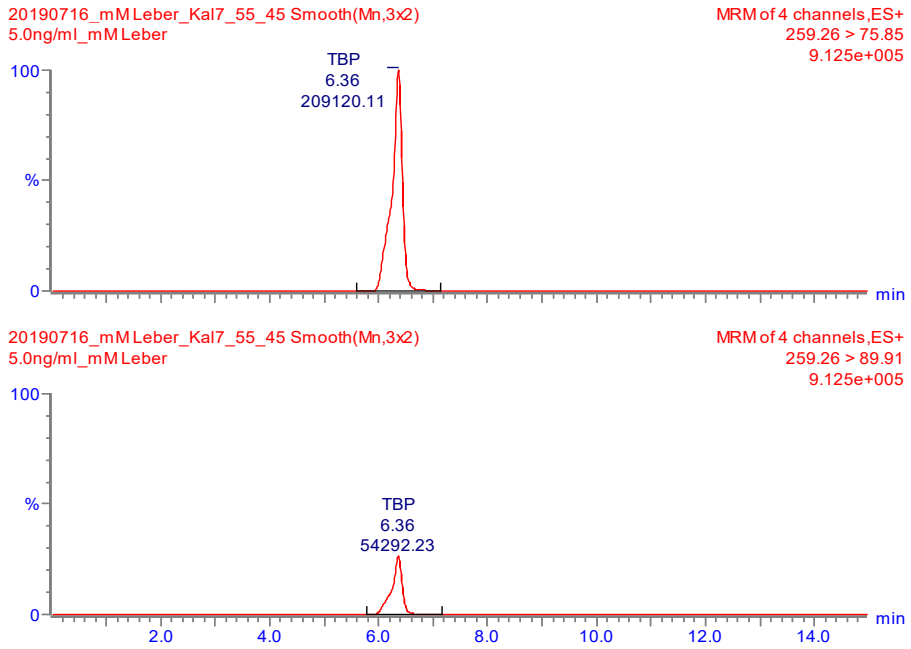

Source: Fh IME.

Figure 65: Exemplary calibration curve of matrix-matched calibration for TBP in fish carcass.

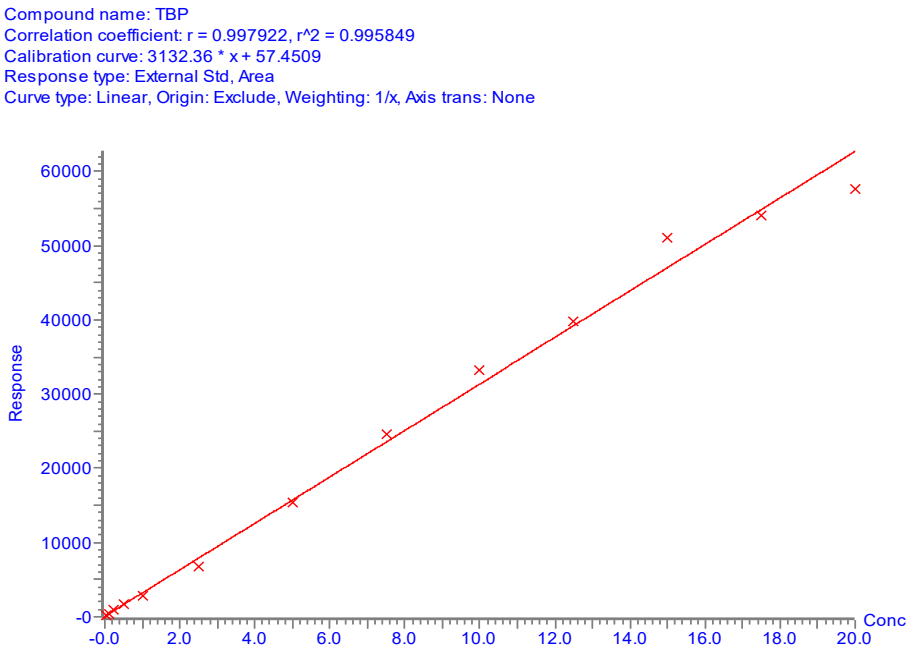

Source: Fh IME.

Figure 66: Exemplary chromatogram of TBP standard (5 µg/L) of matrix-matched calibration with fish carcass.

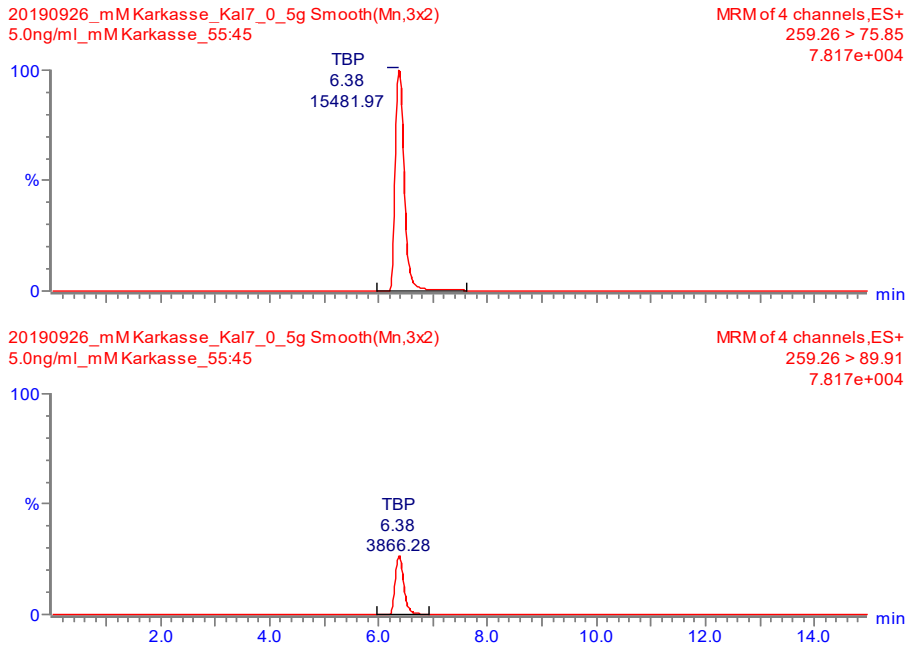

Source: Fh IME.

Figure 67: Exemplary calibration curve of matrix-matched calibration for TMOA in fish GIT.

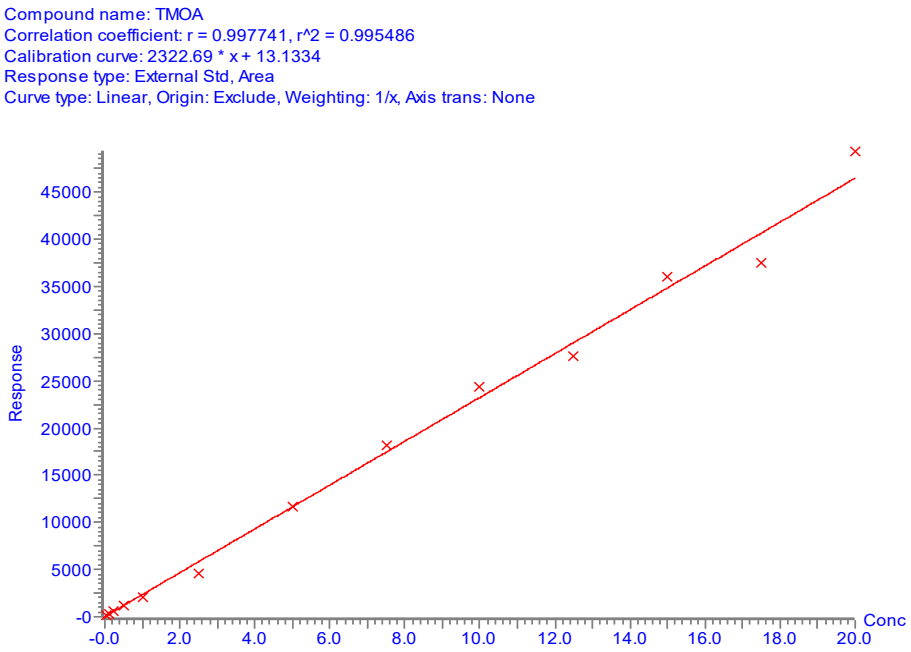

Source: Fh IME.

Figure 68: Exemplary chromatogram of TMOA standard (5 µg/L) of matrix-matched calibration with fish GIT.

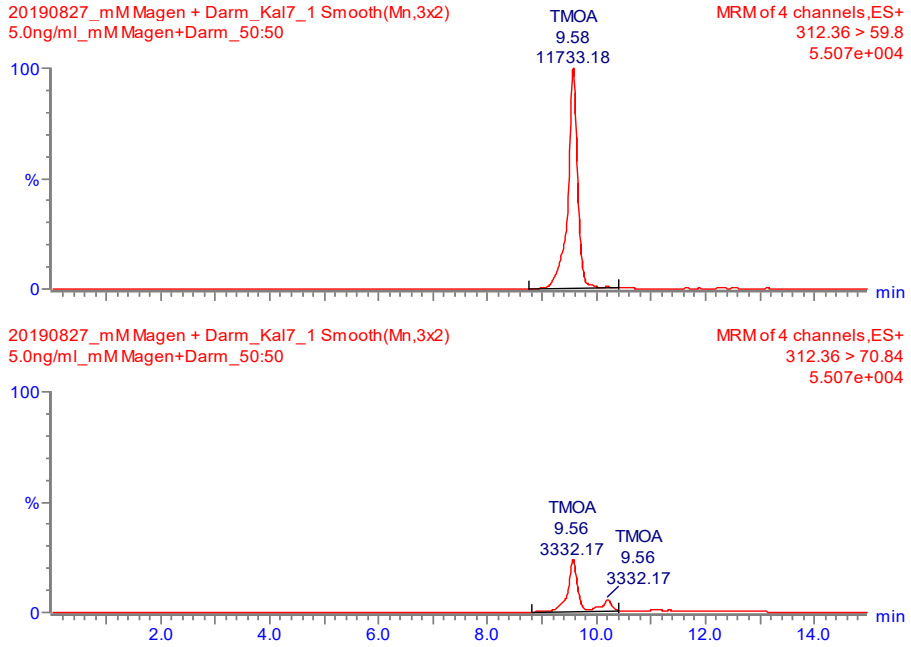

Source: Fh IME.

Figure 69: Exemplary calibration curve of matrix-matched calibration for TMOA in fish liver.

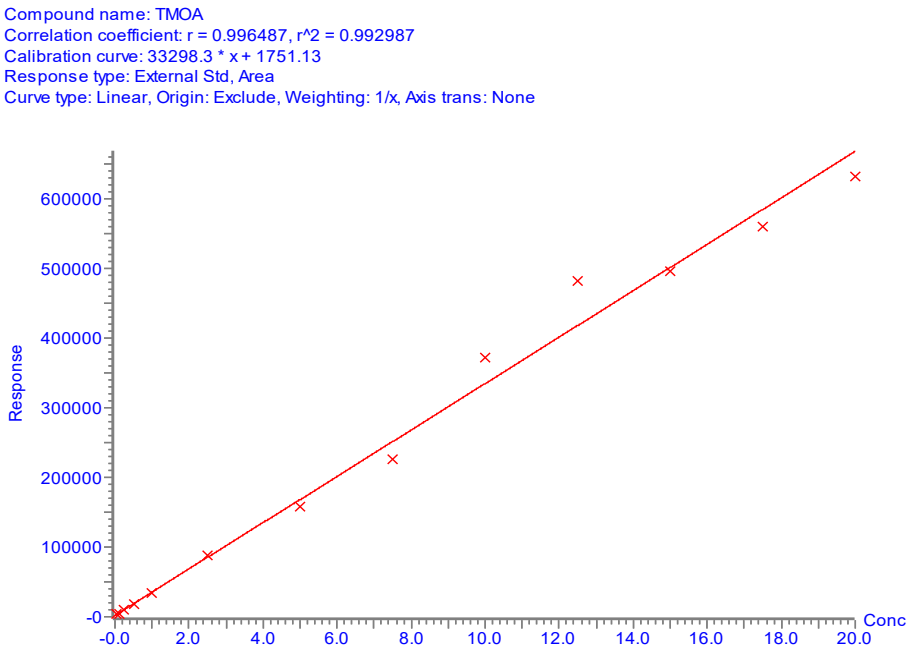

Source: Fh IME.

Figure 70: Exemplary chromatogram of TMOA standard (5 µg/L) of matrix-matched calibration with fish liver.

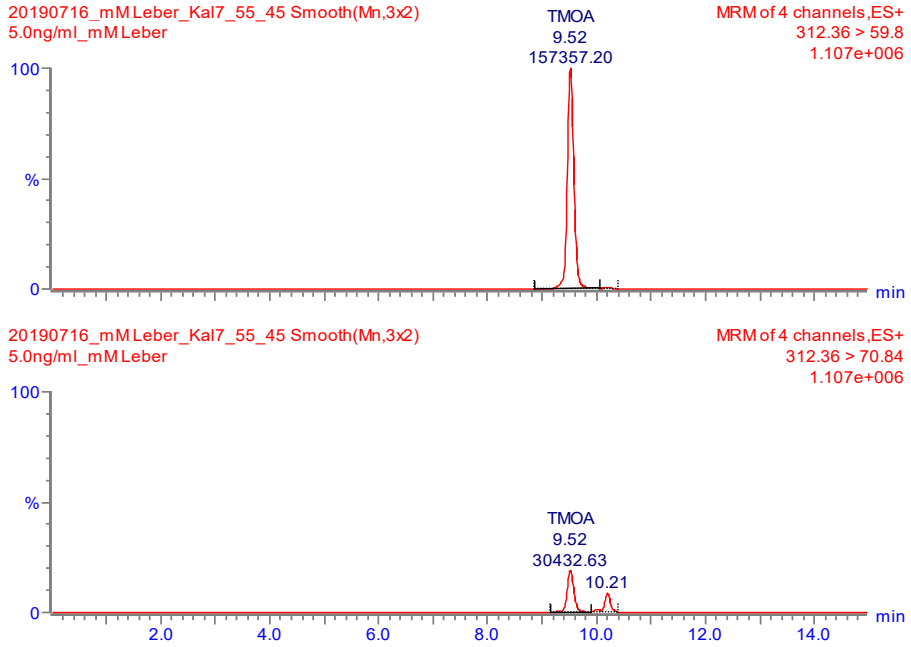

Source: Fh IME.

Figure 71: Exemplary calibration curve of matrix-matched calibration for TMOA in fish carcass.

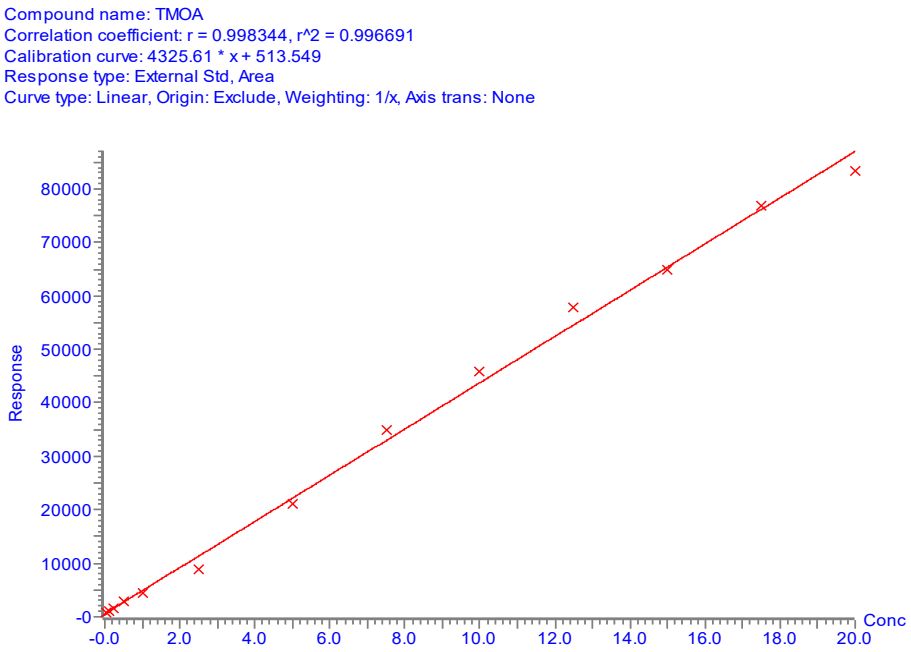

Source: Fh IME.

Figure 72: Exemplary chromatogram of TMOA standard (5 µg/L) of matrix-matched calibration with fish carcass.

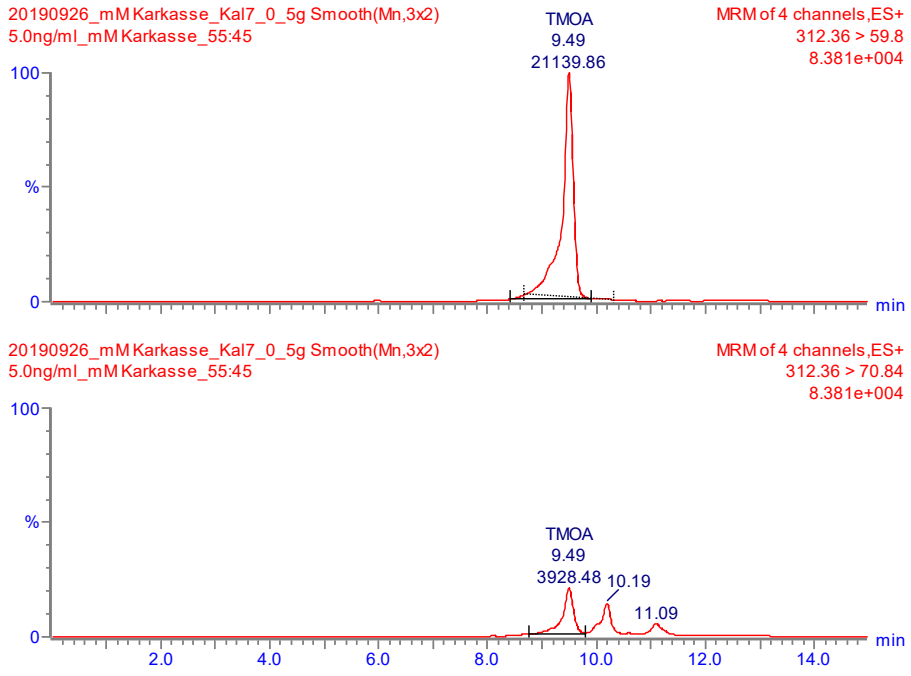

Source: Fh IME.

Figure 73: Exemplary calibration curve of matrix-matched calibration for Benzotriazol in fish GIT.

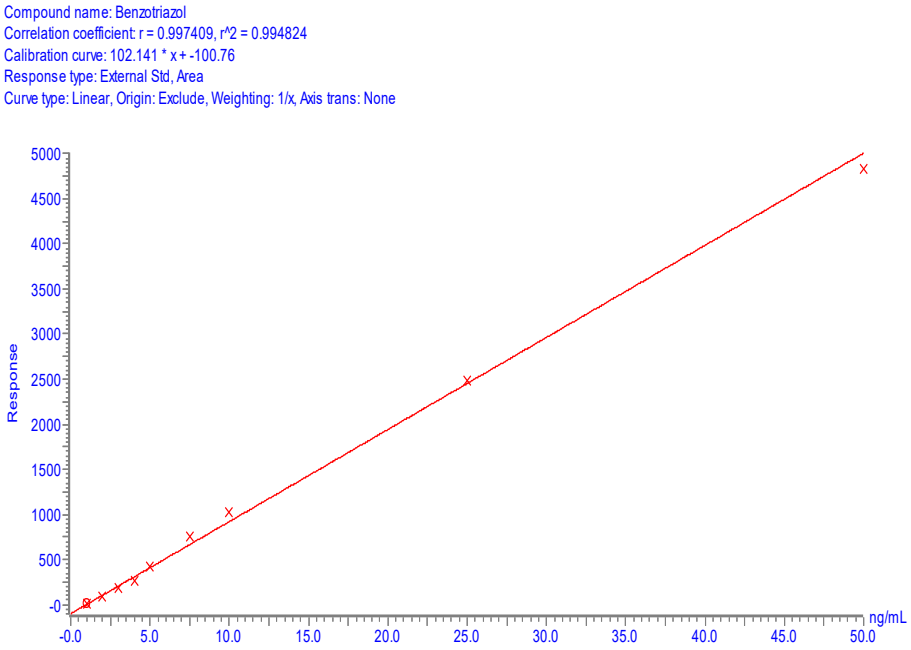

Source: Fh IME.

Figure 74: Exemplary chromatogram of Benzotriazol standard (5 µg/L) of matrix-matched calibration with fish GIT.

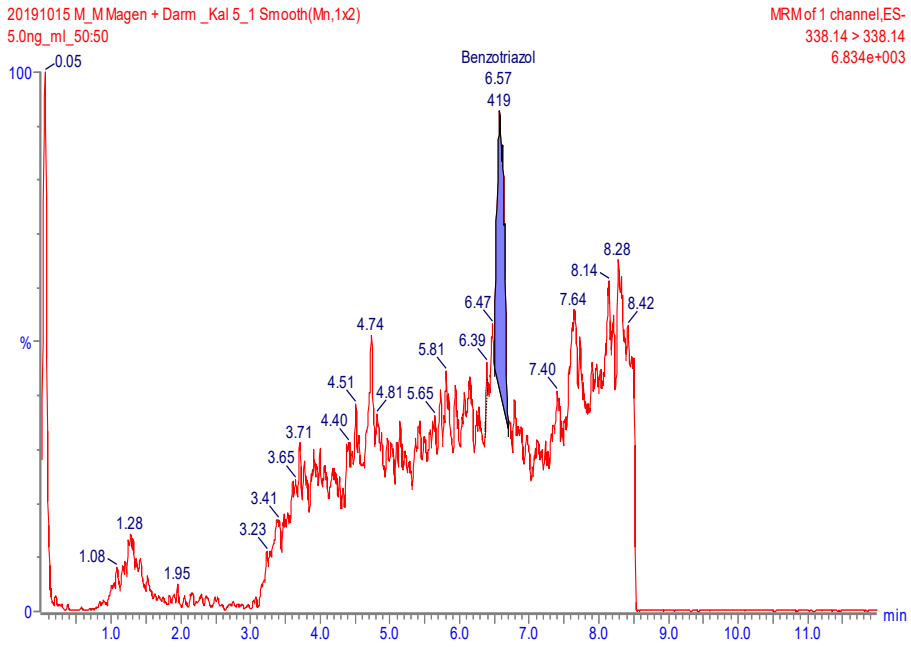

Source: Fh IME.

Figure 75: Exemplary calibration curve of matrix-matched calibration for Benzotriazol in fish liver.

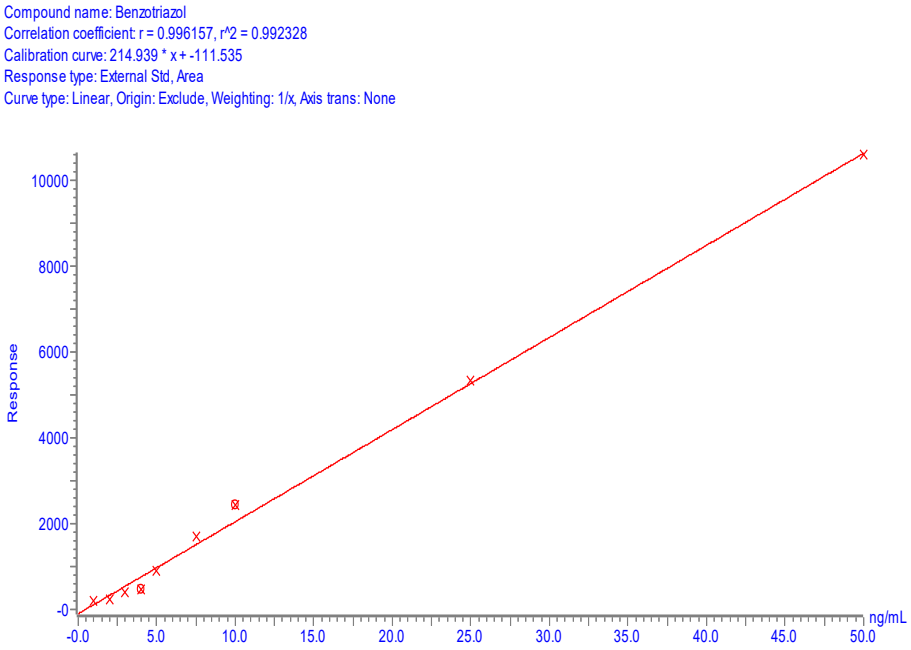

Source: Fh IME.

Figure 76: Exemplary chromatogram of Benzotriazol standard (5 µg/L) of matrix-matched calibration with fish liver.

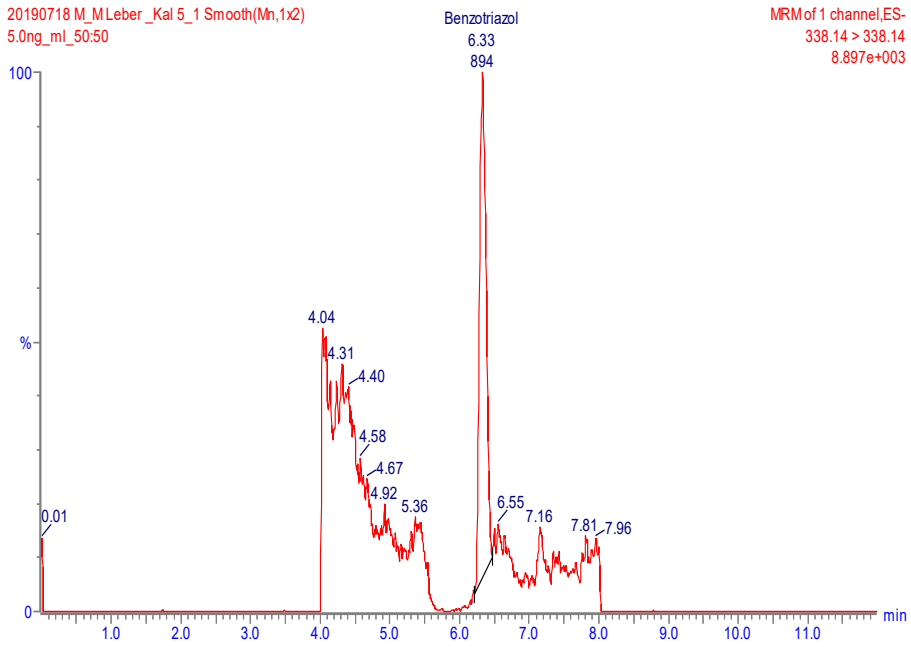

Source: Fh IME.

Figure 77: Exemplary calibration curve of matrix-matched calibration for Benzotriazol in fish carcass.

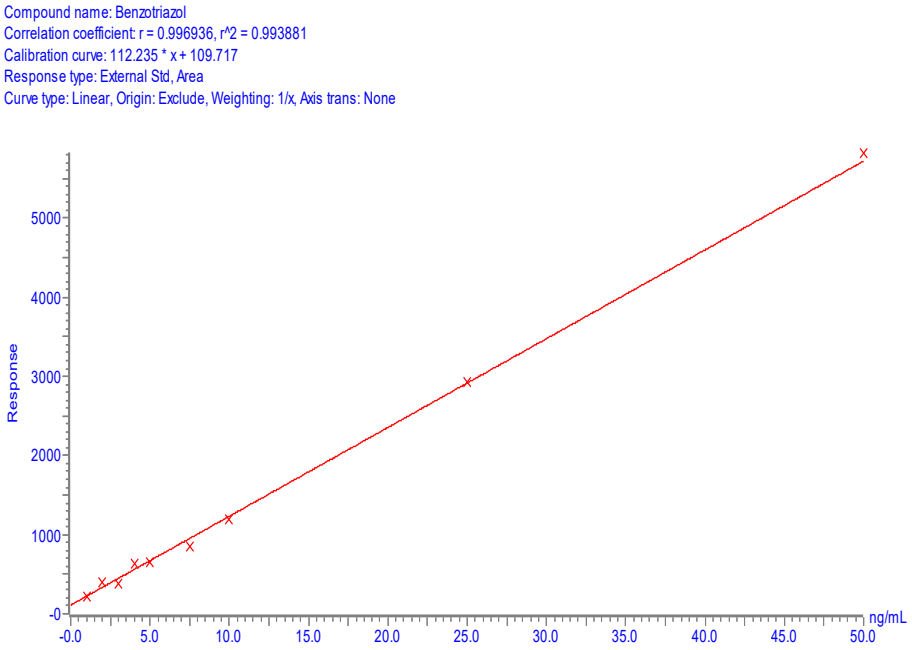

Source: Fh IME.

Figure 78: Exemplary chromatogram of Benzotriazol standard (5 µg/L) of matrix-matched calibration with fish carcass.

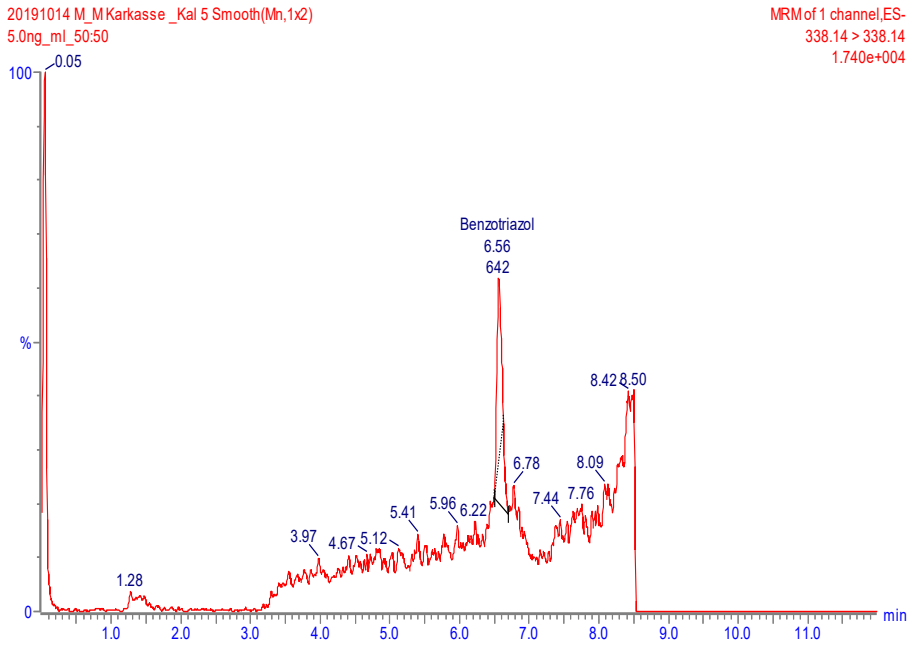

Source: Fh IME.

Figure 79: Exemplary calibration curve of matrix-matched calibration for Tecloftalam in fish GIT.

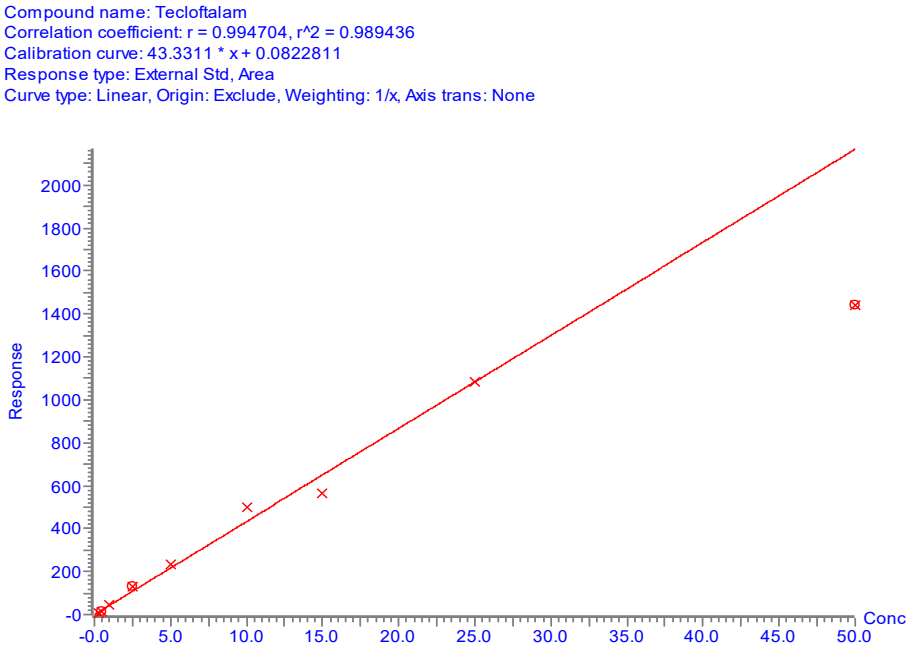

Source: Fh IME.

Figure 80: Exemplary chromatogram of Tecloftalam standard (5 µg/L) of matrix-matched calibration with fish GIT.

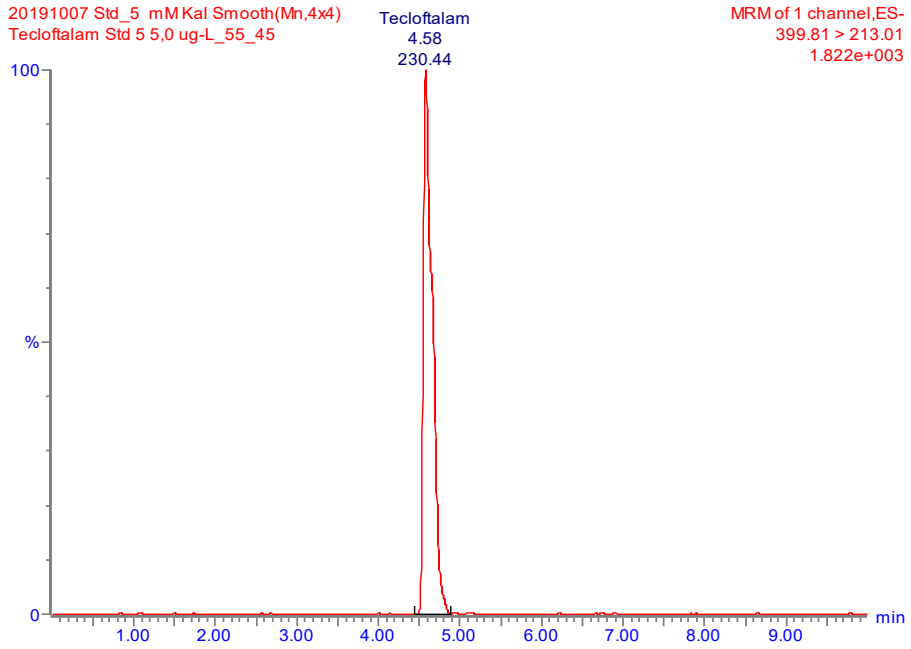

Source: Fh IME.

Figure 81: Exemplary calibration curve of matrix-matched calibration for Tecloftalam in fish liver.

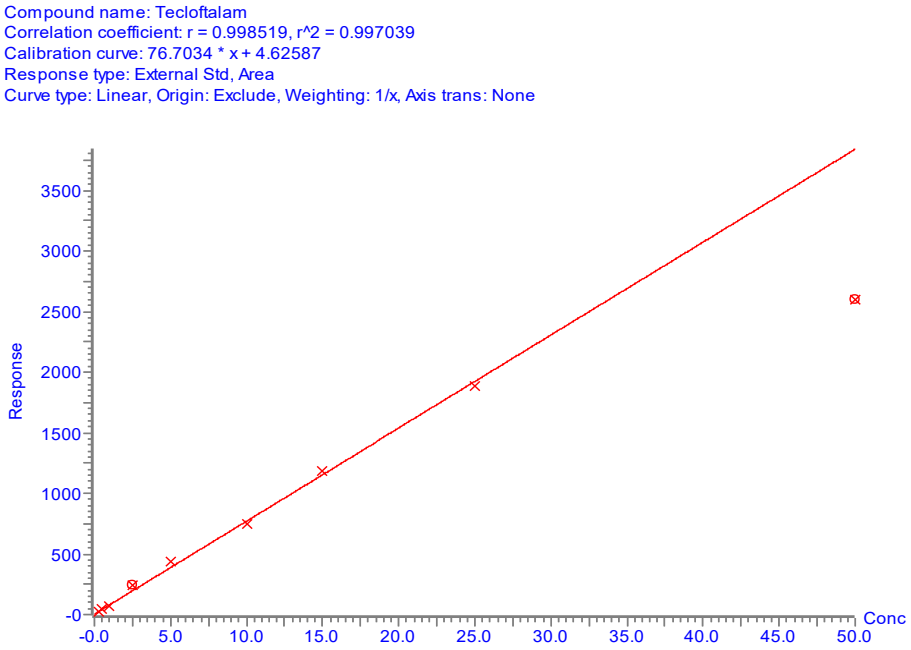

Source: Fh IME.

Figure 82: Exemplary chromatogram of Tecloftalam standard (5 µg/L) of matrix-matched calibration with fish liver.

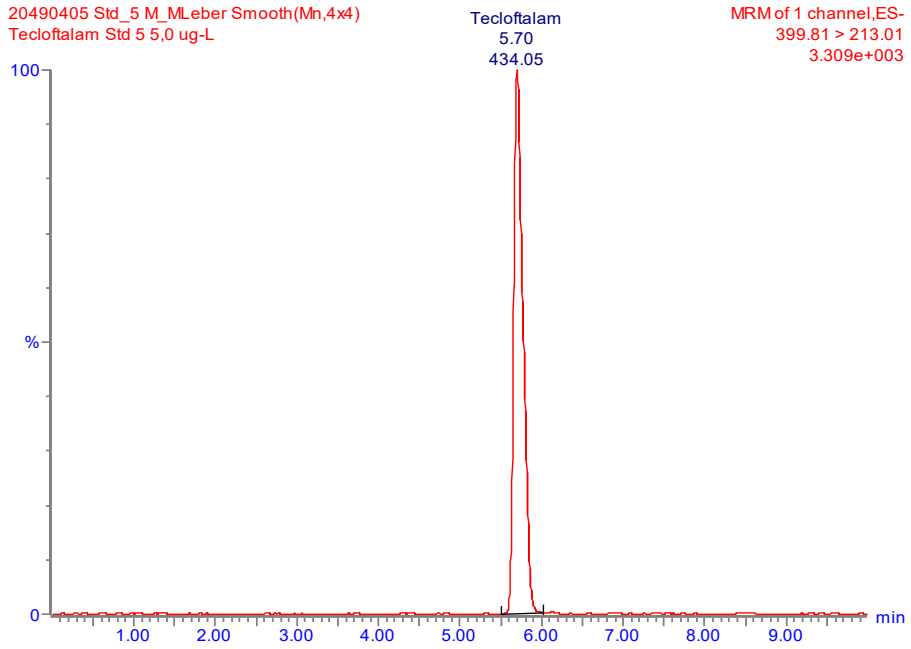

Source: Fh IME.

Figure 83: Exemplary calibration curve of matrix-matched calibration for Tecloftalam in fish carcass.

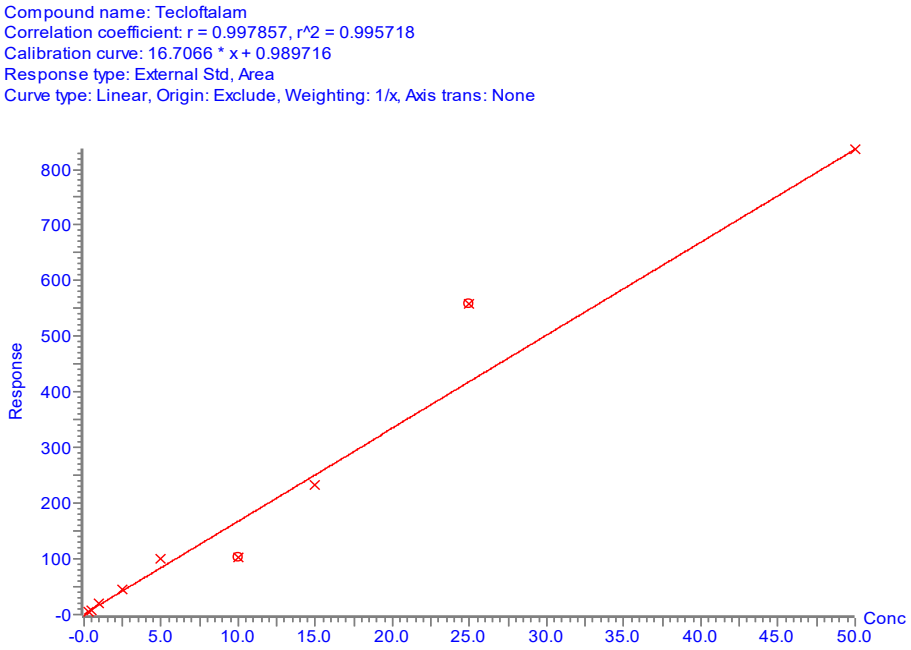

Source: Fh IME.

Figure 84: Exemplary chromatogram of Tecloftalam standard (5 µg/L) of matrix-matched calibration with fish carcass.

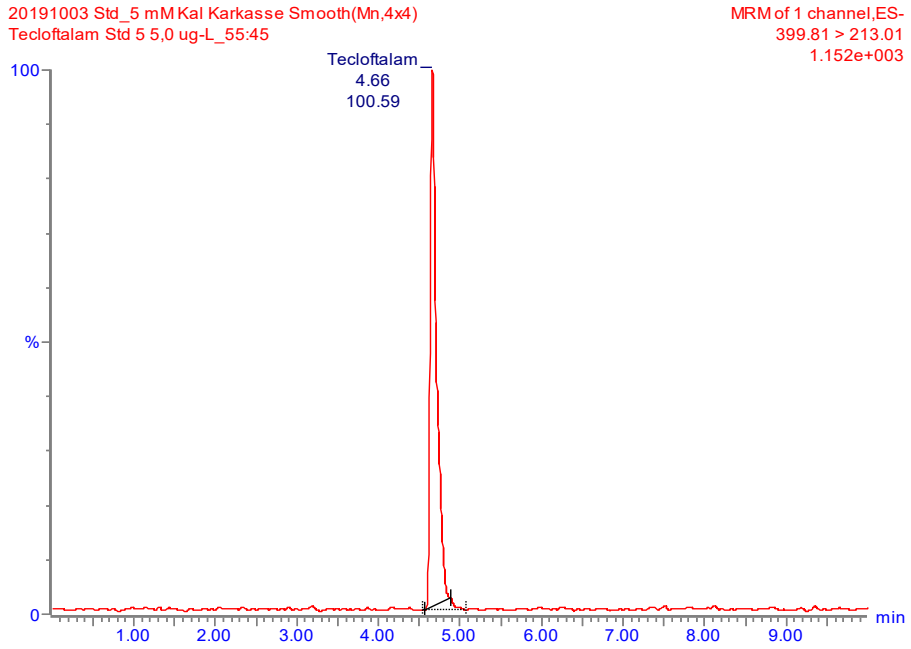

Source: Fh IME.

Figure 85: Exemplary calibration curve of matrix-matched calibration for Pentachlorophenol in fish GIT.

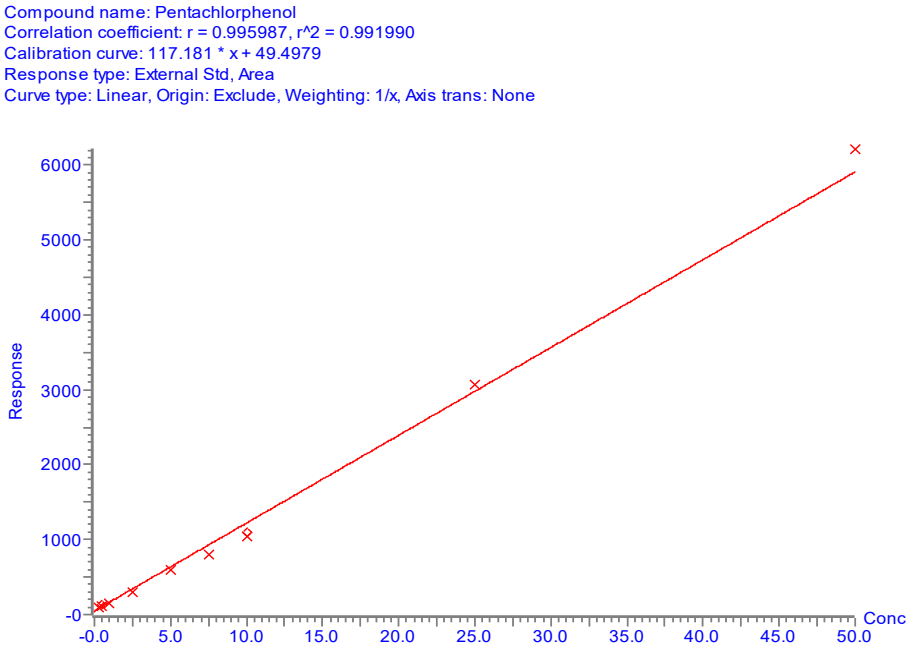

Source: Fh IME.

Figure 86: Exemplary chromatogram of Pentachlorophenol standard (5 µg/L) of matrix-matched calibration with fish GIT.

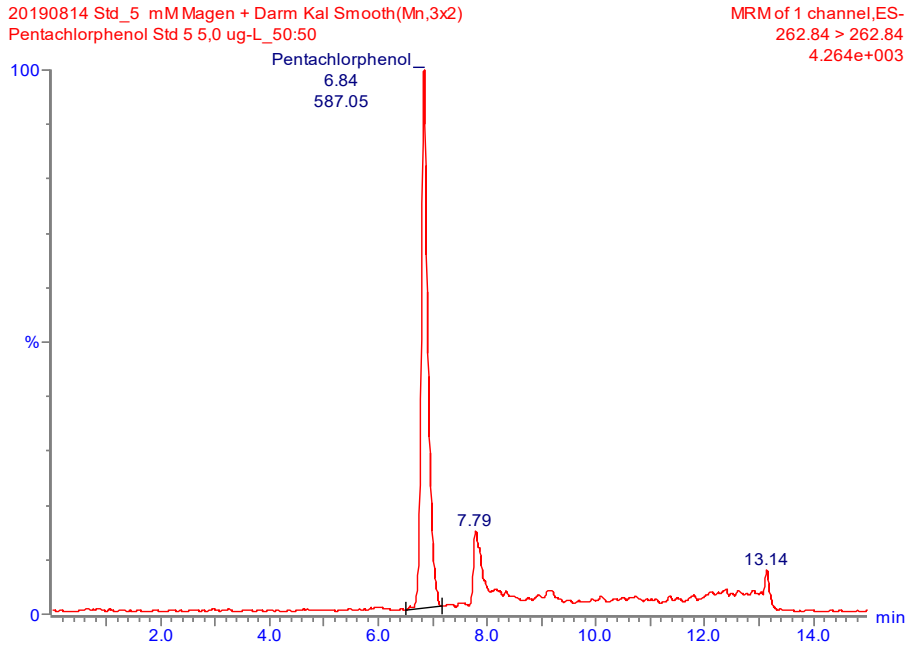

Source: Fh IME.

Figure 87: Exemplary calibration curve of matrix-matched calibration for Pentachlorophenol in fish liver.

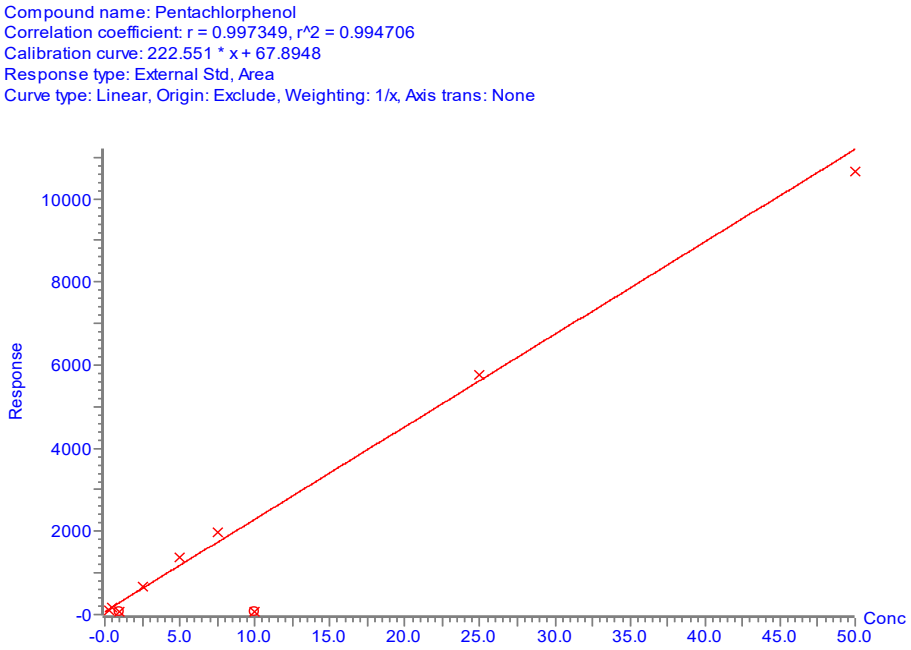

Source: Fh IME.

Figure 88: Exemplary chromatogram of Pentachlorophenol standard (5 µg/L) of matrix-matched calibration with fish liver.

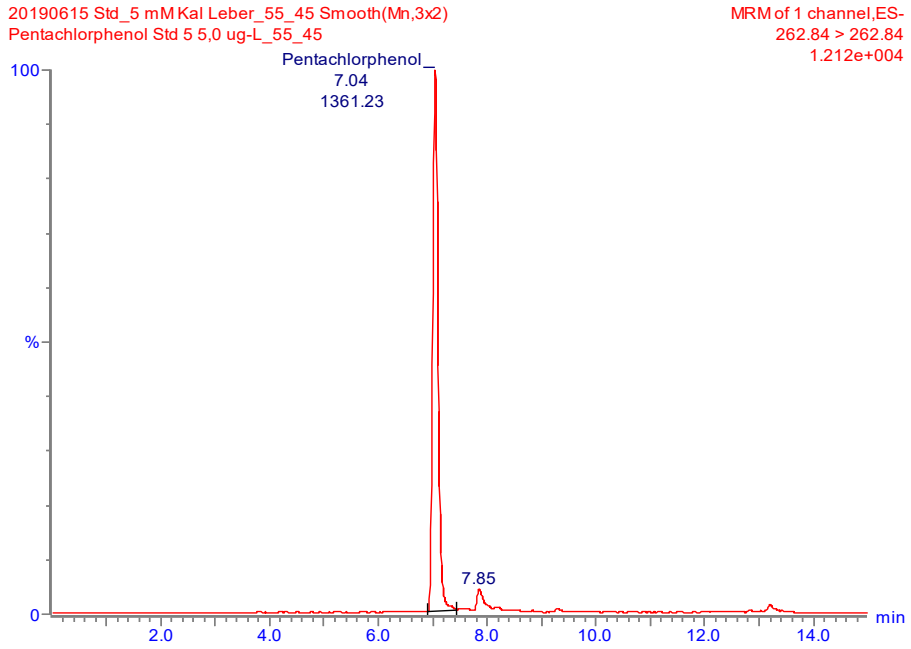

Source: Fh IME.

Figure 89: Exemplary calibration curve of matrix-matched calibration for Pentachlorophenol in fish carcass.

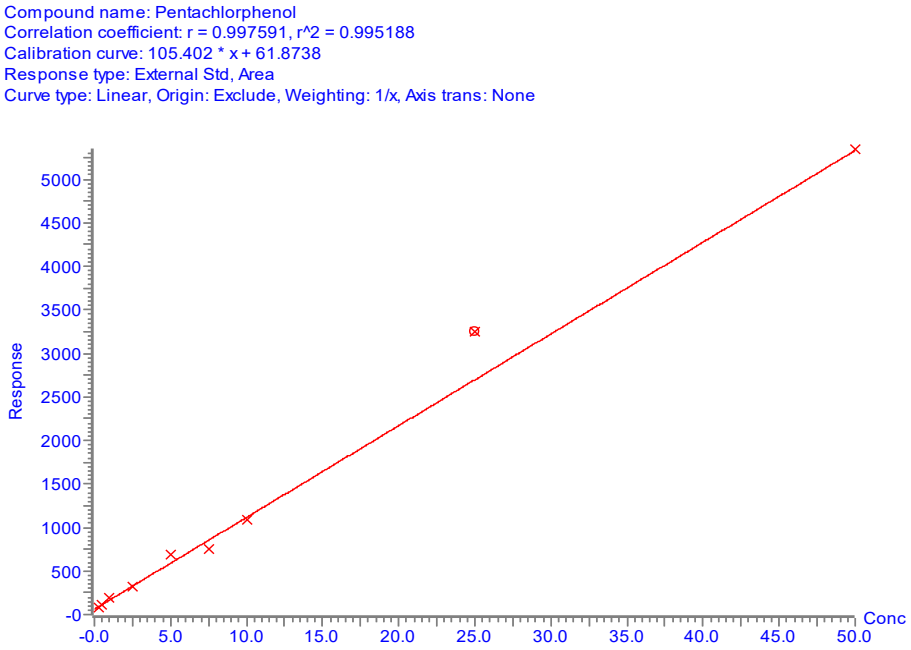

Source: Fh IME.

Figure 90: Exemplary chromatogram of Pentachlorophenol standard (5 µg/L) of matrix-matched calibration with fish carcass.

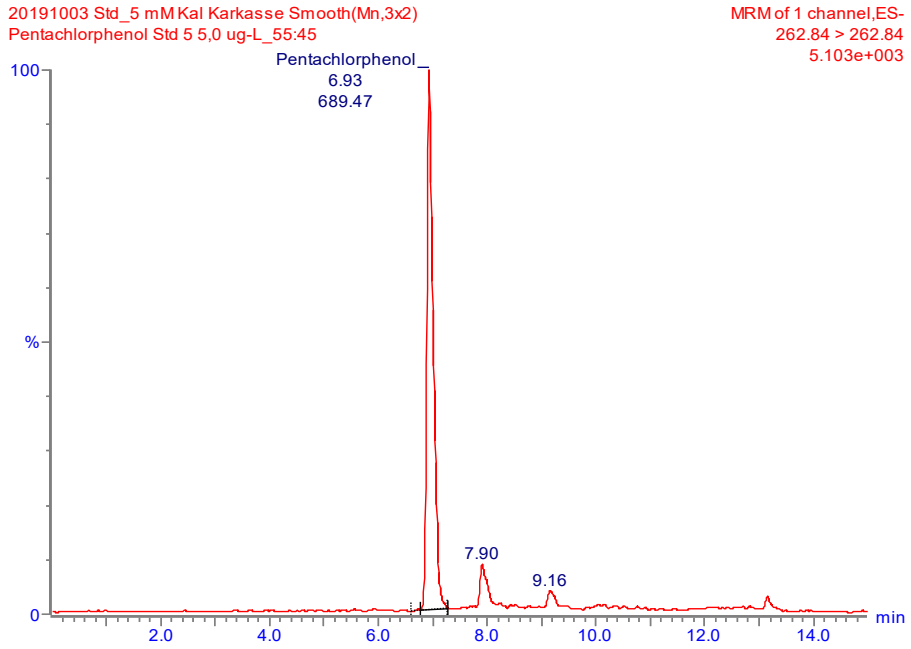

Source: Fh IME.

Figure 91: Exemplary calibration curve of matrix-matched calibration for MEE-Phosphonate in fish GIT.

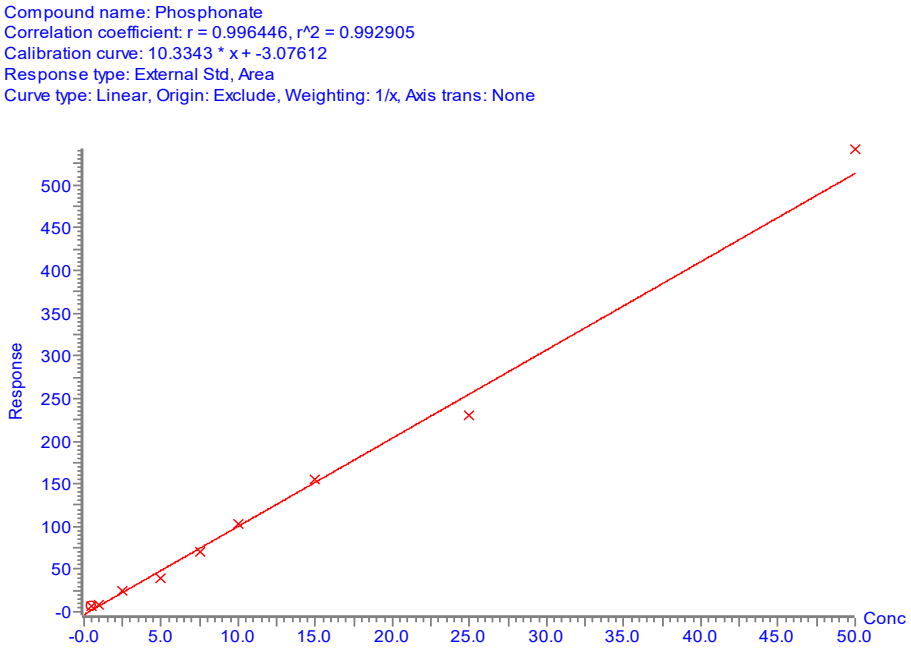

Source: Fh IME.

Figure 92: Exemplary chromatogram of MEE-Phosphonate standard (5 µg/L) of matrix-matched calibration with fish GIT.

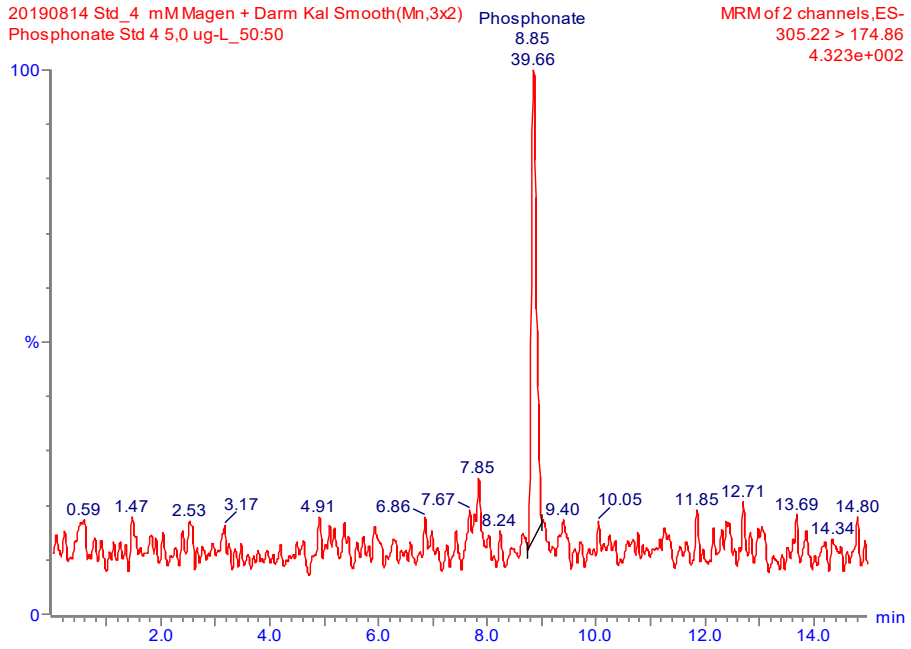

Source: Fh IME.

Figure 93: Exemplary calibration curve of matrix-matched calibration for MEE-Phosphonate in fish liver.

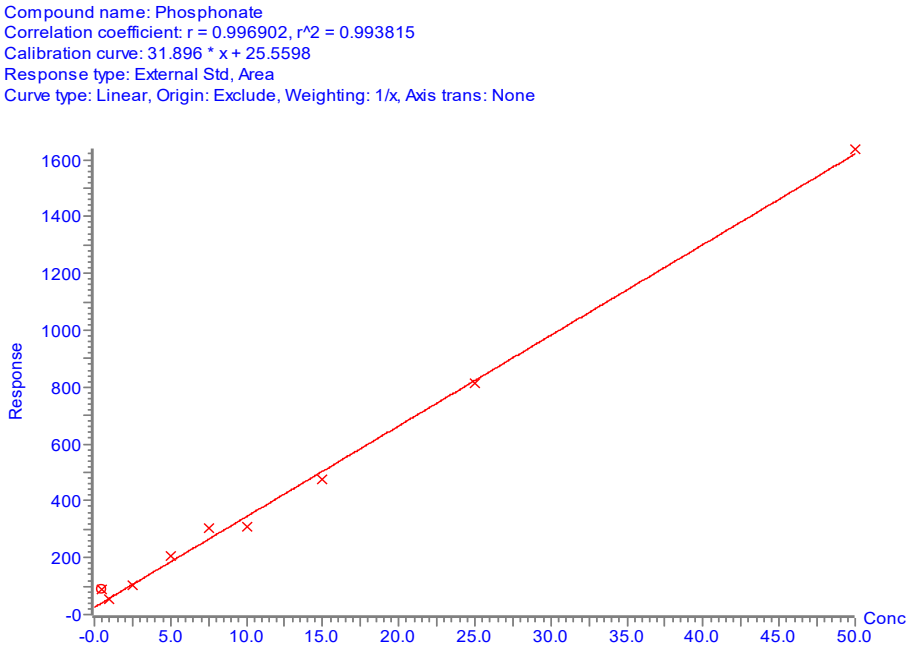

Source: Fh IME.

Figure 94: Exemplary chromatogram of MEE-Phosphonate standard (5 µg/L) of matrix-matched calibration with fish liver.

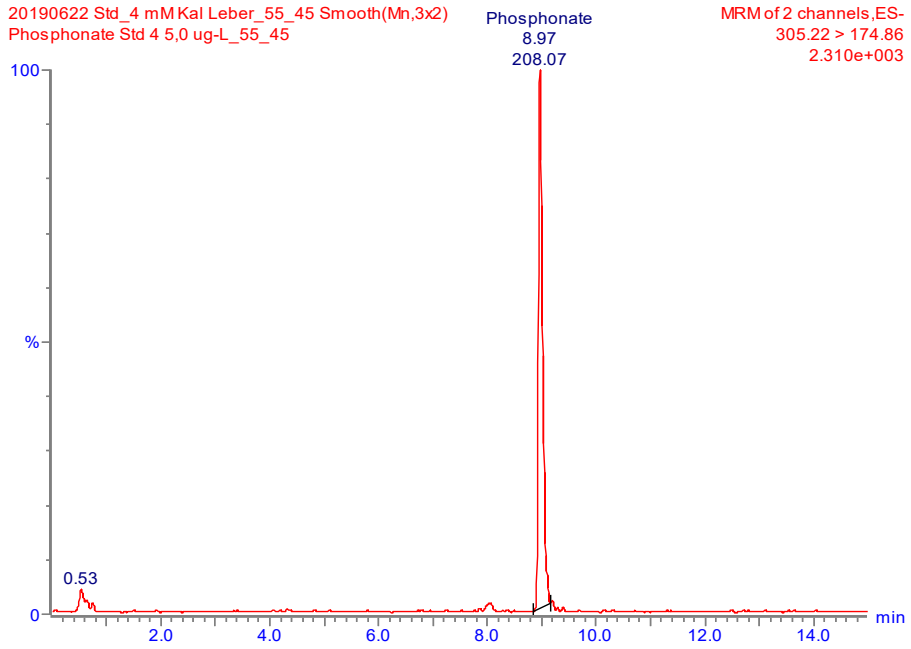

Source: Fh IME.

Figure 95: Exemplary calibration curve of matrix-matched calibration for MEE-Phosphonate in fish carcass.

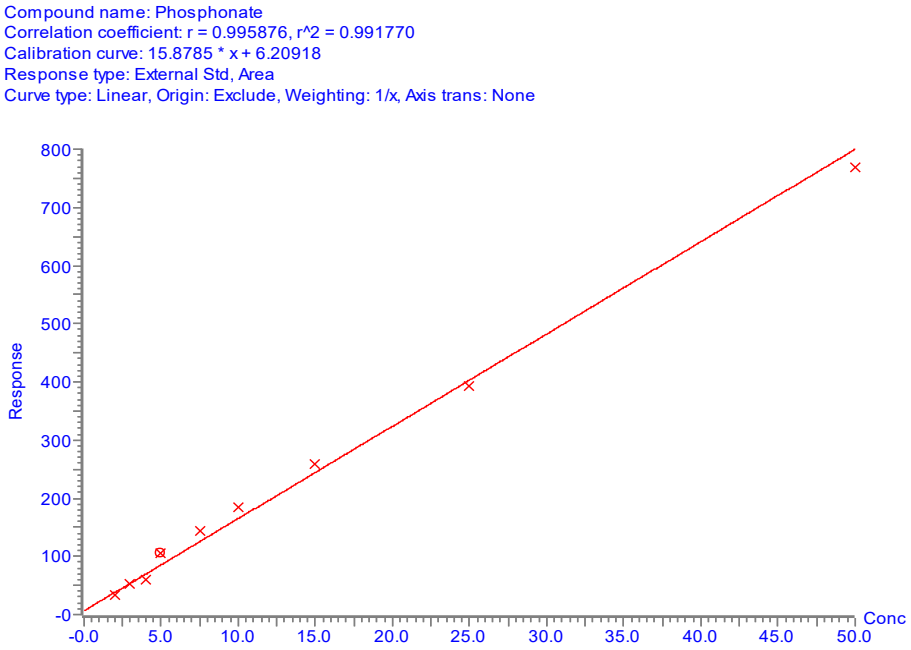

Source: Fh IME.

Figure 96: Exemplary chromatogram of MEE-Phosphonate standard (5 µg/L) of matrix-matched calibration with fish carcass.

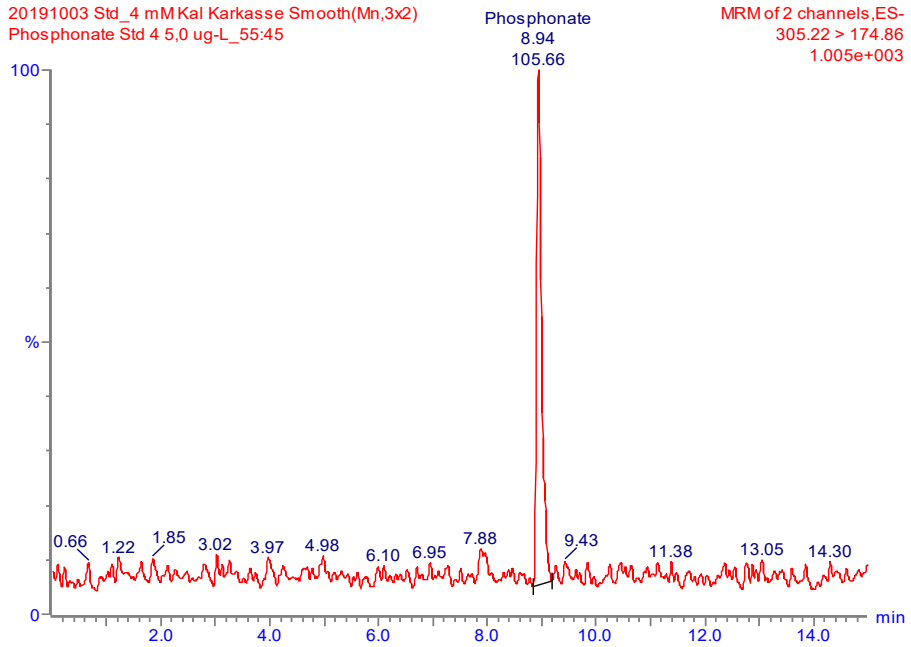

Source: Fh IME.

5 References

Abraham, M. H.; Acree, W. E. (2016): Descriptors for ions and ion-pairs for use in linear free energy relationships. In: Journal of Chromatography A., Elsevier, 1430, pp. 2 – 14. doi: 10.1016/J.CHROMA.2015.07.023.

Abraham, M. H.; Ibrahim, A.; Zissimos, A. M. (2004): Determination of sets of solute descriptors from chromatographic measurements. In: Journal of Chromatography A., Elsevier, 1037(1–2), pp. 29 – 47. doi: 10.1016/J.CHROMA.2003.12.004.

Anskjær, G. G.; Rendal, C.; Kusk, K. O. (2013): Effect of pH on the toxicity and bioconcentration of sulfadiazine on Daphnia magna. In: Chemosphere, Pergamon, 91(8), pp. 1183 – 1188. doi: 10.1016/J.CHEMOSPHERE.2013.01.029.

Armitage, J. M.; Arnot, J. A.; Wania, F.; Mackay, D. (2013): Development and evaluation of a mechanistic bioconcentration model for ionogenic organic chemicals in fish. In: Environmental Toxicology and Chemistry, John Wiley & Sons, Ltd, 32(1), pp. 115 – 128. doi: 10.1002/etc.2020.

Armitage, J. M.; Erickson, R. J.; Luckenbach, T.; Ng, C. A.; Prosser, R. S.; Arnot, J. A.; Schirmer, K.; Nichols, J. W. (2017): Assessing the bioaccumulation potential of ionizable organic compounds: Current knowledge and research priorities. In: Environmental Toxicology and Chemistry, John Wiley & Sons, Ltd, 36(4), pp. 882 – 897. doi: 10.1002/etc.3680.

Armitage, J. M. and Gobas, F. A. P. C. (2007): A Terrestrial Food-Chain Bioaccumulation Model for POPs. In: Environmental Science & Technology, American Chemical Society, 41(11), pp. 4019 – 4025. doi: 10.1021/es0700597.

Arnot, J. A. and Quinn, C. L. (2015): Development and Evaluation of a Database of Dietary Bioaccumulation Test Data for Organic Chemicals in Fish. In: Environmental Science & Technology, American Chemical Society, 49(8), pp. 4783 – 4796. doi: 10.1021/es506251q.

Becke, A. D. (1988): Density-functional exchange-energy approximation with correct asymptotic behavior. In: Physical Review A, American Physical Society 38(6), pp. 3098 – 3100. doi: 10.1103/PhysRevA.38.3098.

Bittermann, K. and Goss, K.-U. (2017a): Assessing the toxicity of ionic liquids – Application of the critical membrane concentration approach. In: Chemosphere, Pergamon, 183, pp. 410 – 418. doi: 10.1016/j.chemosphere.2017.05.097.

Bittermann, K. and Goss, K.-U. (2017b): Predicting apparent passive permeability of Caco-2 and MDCK cell-monolayers: A mechanistic model. In: PLoS ONE 12(12): e0190319. doi.org/10.1371/journal.pone.0190319.

Bittermann, K., Linden, L. and Goss, K.-U. (2018): Screening Tools for the Bioconcentration Potential of monovalent 1 organic ions in fish. In: Environmental Science: Processes & Impacts, Royal Society of Chemistry, 20 (5). DOI: 10.1039/C8EM00084K.

Bittermann, K.; Spycher, S.; Endo, S.; Pohler, L.; Huniar, U.; Goss, K.-U.; Klamt, A. (2014): Prediction of Phospholipid – Water Partition Coefficients of Ionic Organic Chemicals Using the Mechanistic Model COSMOmic. In: The Journal of Physical Chemistry B., American Chemical Society, 118(51), pp. 14833 –14842. doi: 10.1021/jp509348a.

Bittermann, K.; Spycher, S.; Goss, K.-U. (2016): Comparison of different models predicting the phospholipid-membrane water partition coefficients of charged compounds In: Chemosphere, Pergamon, 144, pp. 382 – 391. doi: 10.1016/J.CHEMOSPHERE.2015.08.065.

Czub, G. and McLachlan, M. S. (2004): Bioaccumulation Potential of Persistent Organic Chemicals in Humans. In:Environmental Science and Technology, American Chemical Society, 38(8), pp. 2406 – 2412. doi: 10.1021/es034871v.

Diedenhofen, M. and Klamt, A. (2010): COSMO-RS as a tool for property prediction of IL mixtures — A review. In: Fluid Phase Equilibria, Elsevier, 294(1–2), pp. 31 – 38. doi: 10.1016/J.FLUID.2010.02.002.

Dormann, C. F.; Elith, J.; Bacher, S.; Buchmann, C.; Carl, G.; Carré, G.; Marquéz, J. R. G.; Gruber, B.; Lafourcade, B.; Leitão, P. J.; Münkemüller, T.; McClean, C.; Osborne, P. E.; Reineking, B.; Schröder, B.; Skidmore, A. K.; Zurell, D.; Lautenbach, S. (2013): Collinearity: a review of methods to deal with it and a simulation study evaluating their performance. In: Ecography, John Wiley & Sons, Ltd (10.1111), 36(1), pp. 27 – 46. doi: 10.1111/j.1600-0587.2012.07348.x.

Endo, S.; Bauerfeind, J.; Goss, K.-U. (2012): Partitioning of Neutral Organic Compounds to Structural Proteins. In: Environmental Science & Technology, American Chemical Society, 46(22), pp. 12697 – 12703. doi: 10.1021/es303379y.

Endo, S.; Brown, T. N.; Goss, K.-U. (2013): General Model for Estimating Partition Coefficients to Organisms and Their Tissues Using the Biological Compositions and Polyparameter Linear Free Energy Relationships. In: Environmental Science & Technology, American Chemical Society, 47(12), pp. 6630 – 6639. doi: 10.1021/es401772m.

Endo, S.; Escher, B. I.; Goss, K.-U. (2011): Capacities of Membrane Lipids to Accumulate Neutral Organic Chemicals. In: Environmental Science & Technology, American Chemical Society, 45(14), pp. 5912 – 5921. doi: 10.1021/es200855w.

Endo, S. and Goss, K. (2014): Applications of Polyparameter Linear Free Energy Relationships in Environmental Chemistry. In: Environmental Science & Technology, American Chemical Society, 48(21), pp. 12477 – 12491. doi: 10.1021/es503369t.

Endo, S. and Goss, K.-U. (2011): Serum Albumin Binding of Structurally Diverse Neutral Organic Compounds: Data and Models. In: Chemical Research in Toxicology, ACS Publications, 24(12), pp. 2293–2301. doi: 10.1021/tx200431b.

Ertl, P. (2008): Polar Surface Area. In: Molecular Drug Properties, John Wiley & Sons, Ltd, pp. 111 – 126. doi: 10.1002/9783527621286.ch5.

Escher, B. I. and Schwarzenbach, R. P. (1996): Partitioning of Substituted Phenols in Liposome−Water, Biomembrane−Water, and Octanol−Water Systems. In: Environmental Science & Technology, American Chemical Society, 30(1), pp. 260 – 270. doi: 10.1021/es9503084.

Escher, B. I. and Sigg, L. (2004): Physicochemical Kinetics and Transport at Biointerfaces. In: Leeuwen, H. P. van; Köster, W. (eds): Physicochemical Kinetics and Transport at Biointerfaces, 9th edition, John Wiley & Sons, Ltd., Chichester, UK:, pp. 205 – 269. doi: 10.1002/0470094044.

Eytan, G.D.; Regev, R.; Hurwitz, C.D.; Assaraf, Y.G. (1997): Efficiency of P-glycoprotein-mediated exclusion of rhodamin dyes from multidrug-resistant cells is determined by their passive transmembrane movement rate. In: European Journal of Biochemistry, John Wiley & Sons, Ltd, 248, pp. 104 – 112.

Fairgrieve, W.; Masada, C.; McAuley, W.; Peterson, M.; Myers, M.; Strom, M. (2005): Accumulation and clearance of orally administered erythromycin and its derivative, azithromycin, in juvenile fall Chinook salmon *Oncorhynchus tshawytscha*. In: Diseases of Aquatic Organisms, Inter-Research Science Publisher, 64(2), pp. 99 – 106. doi: 10.3354/dao064099.

Field, A.; Miles, J.; Field, Z. (2012): Discovering statistics using R. Sage publications.

Fisk, A. T.; Norstrom, R. J.; Cymbalisty, C. D.; Muir, D. C. G. (1998): Dietary accumulation and depuration of hydrophobic organochlorines: Bioaccumulation parameters and their relationship with the octanol/water partition coefficient. In: Environmental Toxicology and Chemistry, John Wiley & Sons, Ltd, 17(5), pp. 951 – 961. doi: 10.1002/etc.5620170526.

Franco, A.; Ferranti, A.; Davidsen, C.; Trapp, S. (2010): An unexpected challenge: ionizable compounds in the REACH chemical space. In: The International Journal of Life Cycle Assessment, Springer-Verlag, 15(4), pp. 321 – 325. doi: 10.1007/s11367-010-0165-6.

Fu, W.; Franco, A.; Trapp, S. (2009): Methods for estimating the bioconcentration factor of ionizable organic chemicals. In: Environmental Toxicology and Chemistry, John Wiley & Sons, Ltd, 28(7), p. 1372. doi: 10.1897/08-233.1.

Geisler, A.; Endo, S.; Goss, K.-U. (2012): Partitioning of Organic Chemicals to Storage Lipids: Elucidating the Dependence on Fatty Acid Composition and Temperature. In: Environmental Science & Technology, American Chemical Society, 46(17), pp. 9519 – 9524. doi: 10.1021/es301921w.

Goeritz, I.; Falk, S.; Stahl, T.; Schäfers, C.; Schlechtriem, C. (2013): Biomagnification and tissue distribution of perfluoroalkyl substances (PFASs) in market-size rainbow trout (*Oncorhynchus mykiss*). In: Environmental Toxicology and Chemistry, John Wiley & Sons, Ltd, 32(9), pp. 2078 – 2088. doi: 10.1002/etc.2279.

Goss, K.-U.; Bittermann, K.; Henneberger, L.; Linden, L. (2018): Equilibrium biopartitioning of organic anions – A case study for humans and fish. In: Chemosphere, Pergamon, 199, pp. 174 – 181. doi: 10.1016/J.CHEMOSPHERE.2018.02.026.

Goss, K.-U.; Brown, T. N.; Endo, S. (2013): Elimination half-life as a metric for the bioaccumulation potential of chemicals in aquatic and terrestrial food chains. In: Environmental Toxicology and Chemistry, John Wiley & Sons, Ltd, 32(7), p. 1663-71doi: 10.1002/etc.2229.

van der Heijden, S. A. and Jonker, M. T. O. (2009): Evaluation of Liposome − Water Partitioning for Predicting Bioaccumulation Potential of Hydrophobic Organic Chemicals. In: Environmental Science & Technology, American Chemical Society, 43(23), pp. 8854 – 8859. doi: 10.1021/es902278x.

Henneberger, L.; Goss, K.-U.; Endo, S. (2016a): Equilibrium Sorption of Structurally Diverse Organic Ions to Bovine Serum Albumin. In: Environmental Science & Technology, American Chemical Society, 50(10), pp. 5119 – 5126. doi: 10.1021/acs.est.5b06176.

Henneberger, L.; Goss, K.-U.; Endo, S. (2016b): Partitioning of Organic Ions to Muscle Protein: Experimental Data, Modeling, and Implications for in Vivo Distribution of Organic Ions. In: Environmental Science & Technology, American Chemical Society, 50(13), pp. 7029 – 7036. doi: 10.1021/acs.est.6b01417.

Henneberger, L.; Goss, K. U.; Endo, S. (2016c): Equilibrium Sorption of Structurally Diverse Organic Ions to Bovine Serum Albumin. In: Environmental Science & Technology, American Chemical Society, 50(10), pp. 5119 – 5126. doi: 10.1021/acs.est.5b06176.

Heynen, M.; Fick, J.; Jonsson, M.; Klaminder, J.; Brodin, T. (2016): Effect of bioconcentration and trophic transfer on realized exposure to oxazepam in 2 predators, the dragonfly larvae (*Aeshna grandis*) and the Eurasian perch (*Perca fluviatilis*). In: Environmental Toxicology and Chemistry, John Wiley & Sons, Ltd, 35(4), pp. 930 – 937. doi: 10.1002/etc.3368.

Inoue, Y.; Hashizume, N.; Yoshida, T.; Murakami, H.; Suzuki, Y.; Koga, Y.; Takeshige, R.; Kikushima, E.; Yakata, N.; Otsuka, M. (2012): Comparison of Bioconcentration and Biomagnification Factors for Poorly Water-Soluble Chemicals Using Common Carp (*Cyprinus carpio* L.). In: Archives of Environmental Contamination and Toxicology, Springer-Verlag, 63(2), pp. 241 – 248. doi: 10.1007/s00244-012-9761-8.

Kelly, B. C.; Gobas, F. A. P. C.; McLachlan, M. S. (2004): Intestinal absorption and biomagnification of organic contaminants in fish, wildlife, and humans. In: Environmental Toxicology and Chemistry, Wiley Online Library, 23(10), pp. 2324 – 2336.

Kelly, B. C.; Ikonomou, M. G.; Blair, J. D.; Morin, A. E.; Gobas, F. A. P. C. (2007): Food Web-Specific Biomagnification of Persistent Organic Pollutants. In: Science, AAAS, 317(5835), pp. 236 – 239. doi: 10.1126/science.1138275.

Klamt, A. (1995): Conductor-like Screening Model for Real Solvents: A New Approach to the Quantitative Calculation of Solvation Phenomena. In: The Journal of Physical Chemistry, American Chemical Society, 99(7), pp. 2224 – 2235. doi: 10.1021/j100007a062.

Klamt, A. (2016): COSMO-RS for aqueous solvation and interfaces. In: Fluid Phase Equilibria, Elsevier, 407, pp. 152 – 158. doi: 10.1016/J.FLUID.2015.05.027.

Klamt, A.; Huniar, U.; Spycher, S;. Keldenich, J. (2008): COSMOmic: A Mechanistic Approach to the Calculation of Membrane − Water Partition Coefficients and Internal Distributions within Membranes and Micelles. In: The Journal of Physical Chemistry B., American Chemical Society, 112(38), pp. 12148 – 12157. doi: 10.1021/jp801736k.

Klamt, A. and Schüürmann, G. (1993): COSMO: a new approach to dielectric screening in solvents with explicit expressions for the screening energy and its gradient. In: Journal of the Chemical Society, Royal Society of Chemistry, 0(5), pp. 799 – 805. doi: 10.1039/P29930000799.

Kremer, J. M.; Wilting, J.; Janssen, L. H. (1988): Drug binding to human alpha-1-acid glycoprotein in health and disease. In: Pharmacological Reviews, American Society for Pharmacology and Experimental Therapeutics, 40(1):1-47.

Lee, H.; De Silva, A. O.; Mabury, S. A. (2012): Dietary Bioaccumulation of Perfluorophosphonates and Perfluorophosphinates in Juvenile Rainbow Trout: Evidence of Metabolism of Perfluorophosphinates. In: Environmental Science & Technology, American Chemical Society, 46(6), pp. 3489 – 3497. doi: 10.1021/es204533m.

Linden, L.; Goss, K.-U.; Endo, S. (2017): 3D-QSAR predictions for bovine serum albumin–water partition coefficients of organic anions using quantum mechanically based descriptors. In: Environmental Science: Processes & Impacts, Royal Society of Chemistry, 19(3), pp. 261 – 269. doi: 10.1039/C6EM00555A.

Lipinski, C.A.; Lombardo, F.; Dominy, B.W.; Feeney, P.J. (2001): Experimental and computational approaches to estimate solubility and permeability in drug discovery and development settings. In: Advanced Drug Delivery Reviews, Elsevier, 46, pp. 3 – 26.

Martin, J. W.; Mabury, S. A.; Solomon, K. R.; Muir, D. C. G. (2003): Dietary accumulation of perfluorinated acids in juvenile rainbow trout (*Oncorhynchus mykiss*). In: Environmental Toxicology and Chemistry, John Wiley & Sons, Ltd, 22(1), pp. 189 – 195. doi: 10.1002/etc.5620220125.

Mehler, C.; Klamt, A.; Peukert, W. (2002): Use of COSMO-RS for the prediction of adsorption equilibria. In: AIChE Journal, John Wiley & Sons, Ltd, 48(5), pp. 1093 – 1099. doi: 10.1002/aic.690480518.

Meylan, W. M.; Howard, P. H.; Boethling, R. S.; Aronson, D.; Printup, H.; Gouchie, S. (1999): Improved method for estimating bioconcentration/bioaccumulation factor from octanol/water partition coefficient. In: Environmental Toxicology and Chemistry, John Wiley & Sons, Ltd, 18(4), pp. 664 – 672. doi: 10.1002/etc.5620180412.

Müller, M. T.; Zehnder, A. J. B.; Escher, B. I. (1999): Liposome-water and octanol-water partitioning of alcohol ethoxylates. In: Environmental Toxicology and Chemistry, John Wiley & Sons, Ltd, 18(10), pp. 2191 – 2198. doi: 10.1002/etc.5620181011.

Nakamura, Y.; Yamamoto, H.; Sekizawa, J.; Kondo, T.; Hirai, N.; Tatarazako, N. (2008): The effects of pH on fluoxetine in Japanese medaka (Oryzias latipes): Acute toxicity in fish larvae and bioaccumulation in juvenile fish. In: Chemosphere, Pergamon, 70(5), pp. 865 – 873. doi: 10.1016/J.CHEMOSPHERE.2007.06.089.

Nendza, M.; Kühne, R.; Lombardo, A.; Strempel, S.; Schüürmann, G. (2018): PBT assessment under REACH: Screening for low aquatic bioaccumulation with QSAR classifications based on physicochemical properties to replace BCF in vivo testing on fish. In: Science of the Total Environment, Elsevier, 616–617, pp. 97 – 106.

Neuwoehner, J. and Escher, B. I. (2011): The pH-dependent toxicity of basic pharmaceuticals in the green algae Scenedesmus vacuolatus can be explained with a toxicokinetic ion-trapping model. In: Aquatic Toxicology, Elsevier, 101(1), pp. 266 – 275. doi: 10.1016/J.AQUATOX.2010.10.008.

Ng, C. A. and Hungerbühler, K. (2013): Bioconcentration of perfluorinated alkyl acids: how important is specific binding?. In: Environmental science & technology, ACS Publications, 47(13), pp. 7214 – 7223.

Nichols, J. W.; McKim, J. M.; Andersen, M. E.; Gargas, M. L.; Clewell, H. J.; Erickson, R. J. (1990): A physiologically based toxicokinetic model for the uptake and disposition of waterborne organic chemicals in fish. In: Toxicology and Applied Pharmacology, Academic Press, 106(3), pp. 433 – 447. doi: 10.1016/0041-008X(90)90338-U.

Nyholm, J. R.; Norman, A.; Norrgren, L.; Haglund, P.; Andersson, P. L. (2009): Uptake and biotransformation of structurally diverse brominated flame retardants in zebrafish (*danio rerio*) after dietary exposure. In: Environmental Toxicology and Chemistry, John Wiley & Sons, Ltd, 28(5), p. 1035. doi: 10.1897/08-302.1.

O'Connor, I. A.; Huijbregts, M. A. J.; Ragas, A. M. J.; Hendriks, A. J. (2013): Predicting the oral uptake efficiency of chemicals in mammals: Combining the hydrophilic and lipophilic range. In: Toxicology and applied pharmacology, Elsevier, 266(1), pp. 150 – 156.

OECD, Organisation for Economic Co-operation and Develpement (2008): Test No. 316: Phototransformation of Chemicals in Water – Direct Photolysis. In: OECD Guidelines for the Testing of Chemicals, Section 3. doi: 10.1787/9789264067585-en.

OECD, Organisation for Economic Co-operation and Develpement (2012): Test No. 305: Bioaccumulation in fish: aqueous and dietary exposure. In: OECD Guidelines for the Testing of Chemicals. Paris. OECD Publishing.

Ottiger, C. and Wunderli-Allenspach, H. (1997): Partition behaviour of acids and bases in a phosphatidylcholine liposome – buffer equilibrium dialysis system. In: European Journal of Pharmaceutical Sciences, Elsevier, 5(4), pp. 223 – 231. doi: 10.1016/S0928-0987(97)00278-9.

Page, J.E.; Andreas, J.W.; Murai, T.; Murray, M.M. (1976): Hydrogen ion concentration in the gastrointestinal tract of channel catfish. Journal of Fish Biology, John Wiley & Sons, Ltd, 8, 225-228.

Palm, K.; Luthman, K.; Unge, A.-L.; Strandlund, G.; Artursson, P. (1996): Correlation of Drug Absorption with Molecular Surface Properties. In: Journal of Pharmaceutical Sciences, Elsevier, 85(1), pp. 32 – 39. doi: 10.1021/JS950285R.

Perdew, J. (1986): Density-functional approximation for the correlation energy of the inhomogeneous electron gas. In: Physical Review B, American Physical Society, 33(12), pp. 8822 – 8824. doi: 10.1103/PhysRevB.33.8822.

Polesel, F., Andersen, H.R.; Trapp S.; Plósz, N.G. (2016): Removal of antibiotics in biological wastewater treatment systems – A critical assessment using the Activated Sludge Modelling framework for Xenobiotics (ASM-X).In: Environmental Science & Technology, ACS Publications, 50(19), 10316 – 10334, DOI: 10.1021/acs.est.6b01899.

Poulin, P. and Theil, F. (2000): A Priori Prediction of Tissue:Plasma Partition Coefficients of Drugs to Facilitate the Use of Physiologically-Based Pharmacokinetic Models in Drug Discovery. In: Journal of Pharmaceutical Sciences, Elsevier, 89(1), pp. 16 – 35. doi: 10.1002/(SICI)1520-6017(200001)89:1<16::AID-JPS3>3.0.CO;2-E.

Rendal, C. (2013): The effect of pH on the bioconcentration and toxicity of weak organic electrolytes. In: DTU Environment. Available at: https://orbit.dtu.dk/en/publications/the-effect-of-ph-on-the-bioconcentration-and-toxicity-of-weak-organic-electrolytes(1d8fff56-fe39-4bd9-b25a-adc236750233).html (Accessed: 25 October 2019).

Rendal, C.; Kusk, O.; Trapp, S. (2011a): The effect of pH on the uptake and toxicity of the bivalent weak base chloroquine tested on Salix viminalis and Daphnia magna. In: Environmental Toxicology and Chemistry, John Wiley & Sons, Ltd, 30(2), pp. 354 – 359.

Rendal, C.; Kusk, K. O.; Trapp, S. (2011b): Optimal choice of pH for toxicity and bioaccumulation studies of ionizing organic chemicals. In: Environmental Toxicology and Chemistry, John Wiley & Sons, Ltd, 30(11), pp. 2395 – 2406. doi: 10.1002/etc.641.

Rodgers, T. and Rowland, M. (2006): Physiologically based pharmacokinetic modelling 2: predicting the tissue distribution of acids, very weak bases, neutrals and zwitterions. In: Journal of pharmaceutical *sciences*, Wiley Online Library, 95(6), pp. 1238 – 1257.

Ross, M.F.; Prime, T.A.; Abakumova, .I; James, A.M.; Porteous, C.M.; Smith, R.A.J.; Murphy, M.P. (2008): Rapid and extensive uptake and activation of hydrophobic triphenylphosphonium cations within cells. In: Biochemical Journal, Portland Press, 411,pp. 633 – 645.

Schäfer, A.; Huber, C.; Ahlrichs, R. (1994): Fully optimized contracted Gaussian basis sets of triple zeta valence quality for atoms Li to Kr. In: The Journal of Chemical Physics, American Institute of Physics (AIP), 100(8), p. 5829. doi: 10.1063/1.467146.

Schmitt, W. (2008): General approach for the calculation of tissue to plasma partition coefficients. In: Toxicology in Vitro, Pergamon, 22(2), pp. 457 – 467. doi: 10.1016/J.TIV.2007.09.010.

Smejtek, P. and Wang, S. (1993): Distribution of hydrophobic ionizable xenobiotics between water and lipid membranes: Pentachlorophenol and pentachlorophenate. A comparison with octanol-water partition. In: Archives of Environmental Contamination and Toxicology, Springer-Verlag, 25(3), pp. 394 – 404. doi: 10.1007/BF00210732.

Thuy Pham, T. P.; Cho, C.-W.; Yun, Y.-S. (2010): Environmental fate and toxicity of ionic liquids: A review. In: Water Research, Pergamon, 44(2), pp. 352 – 372. doi: 10.1016/J.WATRES.2009.09.030.

Trapp, S. and Legind, C. (2011): Prediction of uptake into food crops /accumulation in fish, as part of the human exposure assessment. Deliverable 1.5 Pharmas project, EU FP 7, Contract n° 265346.

Treu, G.; Drost, W.; Jöhncke, U.; Rauert, C.; Schlechtriem, C. (2015): The Dessau workshop on bioaccumulation: state of the art, challenges and regulatory implications. In: Environmental Sciences Europe, Springer Berlin Heidelberg, 27(1), p. 34. doi: 10.1186/s12302-015-0067-0.

Ulrich S.; Brown, T.N.; Watanabe, N.; Bronner, G.; Abraham, M.H.; Goss, K.-U. 2017): UFZ-LSER database v 3.2 [Internet]. Leipzig, Deutschland, Helmholtz Zentrum für Umweltforschung - UFZ.

Vainio, M. J. and Johnson, M. S. (2007): Generating Conformer Ensembles Using a Multiobjective Genetic Algorithm. In: Journal of Chemical Information and Modeling, ACS Publications, 47(6), pp. 2462 – 2474. doi: 10.1021/ci6005646.

Veber, D.F.; Johnson, S.R.; Cheng, H.-Y.; Smith, B.R.; Ward, K.W.; Kopple, K.D. (2002): Molecular properties that influence the oral bioavailability of drug candidates. In: Journal of Medicinal Chemistry, ACS Publications, 45, pp. 2615 – 2623

Vitha, M. and Carr, P. W. (2006): The chemical interpretation and practice of linear solvation energy relationships in chromatography. In: Journal of Chromatography A., Elsevier, 1126(1–2), pp. 143 – 194. doi: 10.1016/J.CHROMA.2006.06.074.

Xiao, R.; Adolfsson-Erici, M.; Åkerman, G.; McLachlan, M. S.; MacLeod, M. (2013): A benchmarking method to measure dietary absorption efficiency of chemicals by fish. In: Environmental Toxicology and Chemistry, John Wiley & Sons, Ltd, 32(12), pp. 2695 – 2700. doi: 10.1002/etc.2361.

Yamamoto, H. and Liljestrand, H. M. (2004): Partitioning of Selected Estrogenic Compounds between Synthetic Membrane Vesicles and Water: Effects of Lipid Components. American Chemical Society. doi: 10.1021/ES034311W.

Zissimos, A. M.; Abraham, M. H.; Klamt, A.; Eckert, F.; Wood, J. (2002): A Comparison between the Two General Sets of Linear Free Energy Descriptors of Abraham and Klamt. American Chemical Society. doi: 10.1021/CI025530O.